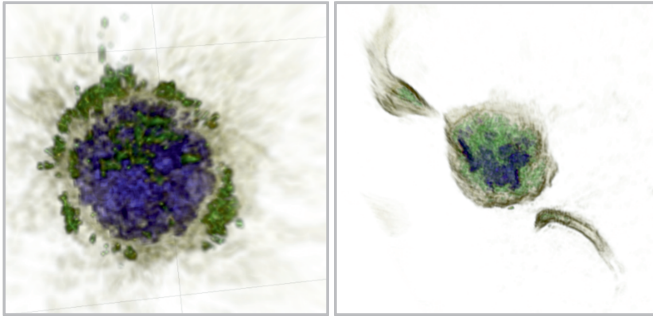


DANIELA PAZ GROB GUERRA

---

NET formation as innate effector mechanism against  
*Trypanosoma brucei brucei* stages and new insights  
on activated PMN by metazoan parasites



Inaugural-Dissertation zur Erlangung des Grades eines

**Dr. med. vet.**

beim Fachbereich Veterinärmedizin der Justus-Liebig-Universität Gießen



*édition scientifique*  
VVB LAUFERSWEILER VERLAG

**Das Werk ist in allen seinen Teilen urheberrechtlich geschützt.**

**Die rechtliche Verantwortung für den gesamten Inhalt dieses Buches liegt ausschließlich bei dem Autoren dieses Werkes.**

Jede Verwertung ist ohne schriftliche Zustimmung der Autoren oder des Verlages unzulässig. Das gilt insbesondere für Vervielfältigungen, Übersetzungen, Mikroverfilmungen und die Einspeicherung in und Verarbeitung durch elektronische Systeme.

1. Auflage 2023

All rights reserved. No part of this publication may be reproduced, stored in a retrieval system, or transmitted, in any form or by any means, electronic, mechanical, photocopying, recording, or otherwise, without the prior written permission of the Authors or the Publisher.

1<sup>st</sup> Edition 2023

© 2023 by VVB LAUFERSWEILER VERLAG, Giessen  
Printed in Germany



*édition scientifique*  
**VVB LAUFERSWEILER VERLAG**

STAUFBENBERGRING 15, 35396 GIESSEN, GERMANY  
Tel: 0641-5599888 Fax: 0641-5599890  
email: [redaktion@doktorverlag.de](mailto:redaktion@doktorverlag.de)

[www.doktorverlag.de](http://www.doktorverlag.de)

Aus dem Institut für Parasitologie, Justus-Liebig-Universität Gießen

**NET formation as innate effector mechanism against  
*Trypanosoma brucei brucei* stages and new insights  
on activated PMN by metazoan parasites**

Inaugural-Dissertation zur Erlangung des Grades eines  
Dr. med. vet.  
beim Fachbereich Veterinärmedizin der  
Justus-Liebig-Universität Gießen

eingereicht von

**Daniela Paz Grob Guerra**

Tierärztin aus Valdivia, Chile

Gießen 2023

Mit Genehmigung des Fachbereichs Veterinärmedizin  
der Justus-Liebig-Universität Gießen

Dekan: Prof. Dr. Dr. Stefan Arnhold

Gutachter: Prof. Dr. Carlos Hermosilla

Gutachter: Prof. Dr. Martin Diener

Prüfer: Prof. Dr. Walter Grünberg

Tag der Disputation: 14.02.2023

To my parents, sister, friends and beloved husband

## LIST OF PUBLICATIONS, MANUSCRIPTS IN PREPARATION AND CONFERENCE CONTRIBUTIONS

### Original articles

Conejeros I, Velásquez ZD, **Grob D**, Zhou E, Salecker H, Hermosilla C, Taubert A. Histone H2A and Bovine Neutrophil Extracellular Traps Induce Damage of *Besnoitia besnoiti*-Infected Host Endothelial Cells but Fail to Affect Total Parasite Proliferation. *Biology (Basel)*. 2019 Oct 11;8(4):78. doi: 10.3390/biology8040078.

**Grob D**, Conejeros I, Velásquez ZD, Preußner C, Gärtner U, Alarcón P, Burgos RA, Hermosilla C, Taubert A. *Trypanosoma brucei brucei* Induces Polymorphonuclear Neutrophil Activation and Neutrophil Extracellular Traps Release. *Front Immunol*. 2020 Oct 22;11:559561. doi: 10.3389/fimmu.2020.559561.

**Grob D**, Conejeros I, López-Osorio S, Velásquez ZD, Segeritz L, Gärtner U, Schaper R, Hermosilla C, Taubert A. Canine *Angiostrongylus vasorum*-Induced Early Innate Immune Reactions Based on NETs Formation and Canine Vascular Endothelial Cell Activation In Vitro. *Biology (Basel)*. 2021 May 12;10(5):427. doi: 10.3390/biology10050427..

Demattio L, Conejeros I, **Grob D**, Gärtner U, Taubert A, Hermosilla C, Wehrend A. *Neospora caninum*-induced NETosis in canine colostrum polymorphonuclear neutrophils. *Journal of Reproductive Immunology*. 2022 Sept 154:103749. doi: 10.1016/j.jri.2022.103749

**Grob D.**, Larrazabal C., Velmer T., Janssen C., Gärtner U., Taubert A., Hermosilla, C., Conejeros I. *Trypanosoma brucei brucei*-induced aggregated nets (aggnets) are dependent on purinergic receptors P2X1 and P2Y6 (manuscript in preparation)

**Grob D.**, Larrazabal C., Conejeros I., Lopez-Osorio S., Taubert A., Hermosilla, C. *Sarcoptes scabiei* soluble antigen increases intracellular calcium concentration, ROS production and evokes weak NET release in bovine Polymorphonuclear neutrophils (manuscript in preparation)

## Conference contributions

**Grob D**, Conejeros I, Velásquez ZD, Preußner C, Bindereif A, Gardner H, Hermosilla C, Taubert A. *Trypanosoma brucei* stages induce bovine NETosis. Talk at the meeting of the German Society of Veterinary (DVG), specialist group of Parasitologist 17-19 June 2019, Leipzig, Germany, Proceedings pp. 13

**Grob D**, Conejeros I, Lopez-Osorio S, Velásquez ZD, Segeritz L, Gärtner U, Schäper R, Taubert A, Hermosilla C. Molecular mechanisms of *Angiostrongylus vasorum*-triggered NETosis in canine PMN. Talk Presentation. Meeting of the German Society of Parasitology (DGP), 15-17 March 2021 Bohn, Germany (online).

**Grob D**, Conejeros I, Lopez-Osorio S, Velásquez ZD, Segeritz L, Gärtner U, Schäper R, Taubert A, Hermosilla C. Molecular mechanisms of *Angiostrongylus vasorum*-triggered NETosis in canine PMN. Poster Presentation. Neutrophils International Symposium. 31 May – 1 June 2021 (online).

**Grob D**, Conejeros I, Lopez-Osorio S, Velásquez ZD, Segeritz L, Gärtner U, Schäper R, Taubert A, Hermosilla C. Molecular mechanisms of *Angiostrongylus vasorum*-triggered NETosis in canine PMN. Talk Presentation. Meeting of the German Society of Veterinary (DVG), specialist group of parasitology 28-30 June 2021 (online).

**Grob D**, Conejeros I, Larrazabal, C, López-Osorio S, Velásquez ZD, Taubert A, Hermosilla C. Oxidative responses, calcium flux and NET formation in *Sarcoptes scabiei* mites- and antigen-exposed bovine neutrophils. Meeting of the German Society of Veterinary (DVG), specialist group of parasitology 28-30 June 2021 (online).

**Grob D**, Conejeros I, Lopez-Osorio S, Velásquez ZD, Segeritz L, Gärtner U, Schäper R, Taubert A, Hermosilla C. Molecular mechanisms of *Angiostrongylus vasorum*-triggered NETosis in canine PMN. Poster Presentation. 28th International Conference of the World Association for the Advancement of the Veterinary Parasitology (WAAVP), 19-22 July 2021. Dublin, Ireland (online).

**Grob D**, Larrazabal C, Conejeros I, López-Osorio S, Taubert A, Hermosilla C. Oxidative responses, calcium efflux and NET formation in *Sarcoptes scabiei* mites and antigen-exposed bovine neutrophils. Poster Presentation. 28th International Conference of the World Association for the Advancement of the Veterinary Parasitology (WAAVP), 19-22 July 2021. Dublin, Ireland (online).

Larrazabal C, **Grob D**, Velásquez ZD, Hermosilla C, Taubert A., Conejeros I. Ca<sup>++</sup> signaling in *Besnoitia besnoiti* tachyzoite invasion and development in primary bovine host endothelial cells. Meeting of the world association for the advancement of veterinary parasitology (WAAVP), 19-22 July 2021. Dublin, Ireland (online).

**Grob D**, Larrazabal C, Conejeros I, López-Osorio S, Taubert A, Hermosilla C. *Sarcoptes scabiei* antigens trigger oxidative responses, calcium efflux and ROS production but weak NETosis in bovine polymorphonuclear. Poster Presentation. Meeting of the German Society of Veterinary (DVG), specialist group of parasitology 23-25 May 2022. Berlin, Germany.

**Grob D**, Gärtner U., Taubert A, Hermosilla, C., Conejeros I. *Trypanosoma brucei brucei*-induced aggregated NETs (*aggNETs*) are dependent on purinergic receptors P2X1 and P2Y6. Oral Presentation. Meeting of the German Society of Veterinary (DVG), specialist group of parasitology 23-25 May 2022. Berlin, Germany

## TABLE OF CONTENTS

1. INTRODUCTION.....	1
<b>1.1. Host parasite interactions</b> .....	1
<b>1.1.1. Phylum Euglenozoa</b> .....	2
<b>1.1.2. Phylum Alveolata, subphylum Apicomplexa</b> .....	10
<b>1.1.3. Phylum Nematelminthes</b> .....	13
<b>1.2. Polymorphonuclear neutrophils (PMN) and PMN-derived innate immune responses</b> .....	15
<b>1.2.1. PMN recruitment cascade</b> .....	16
<b>1.2.2. Microbicide activity of PMN</b> .....	17
<b>1.2.3. Neutrophil extracellular traps (NETs)</b> .....	19
<b>1.2.4. Role of ATP purinergic signaling in NET formation</b> .....	22
<b>1.3. Parasite-induced NET formation</b> .....	23
2. ORIGINAL PUBLICATIONS.....	26
<b>2.1. <i>Trypanosoma brucei brucei</i> induces polymorphonuclear neutrophil activation and neutrophil extracellular traps release</b> .....	26
<b>2.2. Canine <i>Angiostrongylus vasorum</i>-induced early innate immune reactions based on NETs formation and canine vascular endothelial cell activation in vitro</b> .....	42
<b>2.3. Histone H2A and bovine neutrophil extracellular traps induce damage of <i>Besnoitia besnoiti</i>-infected host endothelial cells but fail to affect total parasite proliferation</b> .....	61
<b>2.4. <i>Neospora caninum</i>-induced NETosis in canine colostral polymorphonuclear neutrophils</b> .....	81
<b>2.5. <i>Trypanosoma brucei brucei</i>-induced aggregated NETs (<i>aggNETS</i>) are dependent on purinergic receptors P2X1 and P2Y6</b> .....	89
<b>2.6. <i>Sarcoptes scabiei</i> soluble antigen increases intracellular calcium concentration, ROS production and evokes weak NET release in bovine polymorphonuclear neutrophils</b> .....	121
3. DISCUSSION .....	152
4. ZUSAMMENFASSUNG.....	164
5. SUMMARY .....	167
6. REFERENCES.....	169
7. ACKNOWLEDGMENTS.....	189
8. DECLARATION .....	190
9. FUNDING .....	191

## **ABBREVIATIONS**

Food and Agriculture Organization	<b>FAO</b>
Adenosin triphosphate	<b>ATP</b>
Adenosine monophosphate	<b>AMP</b>
Aggregated NETs	<b><i>aggNETs</i></b>
Bovine umbilical vein endothelial cells	<b>BUVEC</b>
Calcium carbonate	<b>CaCO<sub>3</sub></b>
Calcium oxalate	<b>CaOx</b>
Calcium phosphate	<b>CaP</b>
Calcium pyrophosphate dihydrate	<b>CPP</b>
Canine aortic endothelial cells	<b>CAEC</b>
Card Agglutination Test for Trypanosomes	<b>CAAT</b>
CXC-chemokine receptor 4	<b>CXCR4</b>
Diffused NETs	<b><i>diffNETs</i></b>
Diphenyleiodonium	<b>DPI</b>
DNA area and NETosis analysis	<b>DANA</b>
Equilibrate nucleoside transporters	<b>ENTs</b>
Extracellular acidification Rate	<b>ECAR</b>
Extracellular trap	<b>ET</b>
Glycosylphosphatidylinositol	<b>GPI</b>
Granulocyte colony-stimulating factor	<b>G-CSF</b>
Human african trypanosomiasis	<b>HAT</b>
Immunofluorescence	<b>IF</b>
Immunoglobulin M	<b>IgM</b>
Interferon $\gamma$	<b>INF-<math>\gamma</math></b>
Interleukin-23	<b>IL-23</b>
Monosodium urate crystals	<b>MSU</b>
Myeloperoxidase	<b>MPO</b>
Natural killer	<b>NK</b>
Neutrophil elastase	<b>NE</b>
Neutrophil extracellular traps	<b>NETs</b>
Nicotinamide adenine dinucleotide phosphate	<b>NADPH</b>
Nuclear area expansion	<b>NAE</b>
Oxygen consumption rate	<b>OCR</b>

Pathogen-associated molecular patterns	<b>PAMPs</b>
Patter-recognition receptors	<b>PRRs</b>
Peptidylarginine deiminase 4	<b>PAD4</b>
Phenylhydrazone	<b>FCCP</b>
Phorbol myristate acetate	<b>PMA</b>
Polymerase chain reaction	<b>PCR</b>
Polymorphonuclear neutrophil	<b>PMN</b>
P-selectin glycoprotein ligand 1	<b>PSGL1</b>
Reactive oxygen species	<b>ROS</b>
<i>Sarcoptes scabiei</i> antigen	<b>ScAg</b>
Scanning electron microscopy	<b>SEM</b>
Spread NETs	<b><i>spr</i>NETs</b>
Tumor necrosis factor alpha	<b>TNF<math>\alpha</math></b>
Variable surface glycoprotein	<b>VSG</b>
World Health Organization	<b>WHO</b>



# 1. INTRODUCTION

## 1.1. Host parasite interactions

Parasites are organisms that live in a close association with another organism, often related to relevant infectious diseases in veterinary and human medicine, worldwide. In this sense, by studying the close and complex interaction between parasites and their hosts, it is possible to discover new and fascinating insights into parasitic relationships (da Silva and Langoni 2009; Hermosilla et al. 2012; Thomson et al. 2017). Several mechanisms are involved in final endogenous location, life cycle, pathogenesis, immunology and host homeostasis driven by parasitic infections, including not only mechanical or physiological effects, but also metabolic disorders, cellular detriment and immunological changes among others (da Silva and Langoni 2009; Thomson et al. 2017).

Veterinary parasitology embraces several parasitic groups, being subdivided in two subkingdoms: the Protozoa (unicellular parasites) and Metazoa (multicellular parasites). In general, the life cycle of parasites will develop within a suitable host, where they have established their microhabitat to ensure their developments and perpetuating their life cycles (Poulin 2014). Likewise, depending on the species, migration through host tissues and/or organs might occur. Consistently, remarkable examples of this feature can be seen in protozoan *Toxoplasma gondii* and metazoan *Ascaris suum*. *T. gondii* is a globally spread cyst-forming coccidian parasite, having as intermediate hosts all warm-blooded terrestrial as well as marine animals (Tenter et al. 2000; Villagra-Blanco et al. 2019) and as definitive hosts members of the family Felidae (Dubey 2008). After oral ingestion of *T. gondii*-sporulated oocysts (containing sporozoites) or tissue cyst (containing bradyzoites), the parasite will rapidly multiply in the intestine of the final- or facultative intermediate host. After this, they migrate to form tissue cysts, having a high affinity for muscular and neural tissues (Tenter et al. 2000). Consistently, *A. suum* is one of the most frequent nematodes of pig industry and having a relevant economic impact in the field. After oral ingestion of eggs containing the infective larvae 3 (L<sub>3</sub>), hatched L<sub>3</sub> will migrate from the small intestine into the liver of final host, via portal system, thereafter reaching lungs to finally colonize small intestine lumen. Regarding endogenous migration routes, several stages of taxonomically different parasites will develop in the cardiovascular/lymphatic system, generating a critical situation, considering the close interaction between the different cells of the host innate immune system, including endothelium/epithelial cells, complement factors and different leukocytes (Muñoz Caro et al. 2014; Hermosilla et al. 2014; Muñoz-Caro et al. 2018; Zhou et al. 2019; Peixoto et al. 2021).

# 1. Introduction

## 1.1.1. Phylum Euglenozoa

Systematically the euglenozoan parasite *Trypanosoma brucei brucei* belongs to the class Kinetoplastea (subphylum Kinetoplasta). It is a member of the order Trypanosomatida belonging to the family Trypanosomatidae (*trypanon*:drill; *soma*:body). In mammalian hosts, trypanosomatids can develop freely in blood and body fluids, while some species of this family, such as *Trypanosoma cruzi*, requires to infect host cells in order to complete its life cycle (Molinari and Moreno 2018). Morphologically, *T. b. brucei* are curved elongated parasites that depending on their life cycle stage, have a range from 12 to 35  $\mu\text{m}$  in length and 1.5 to 3.5  $\mu\text{m}$  in width (Hoare 1972). As an extracellular parasite, *T. b. brucei* possess one flagellum originating at the basal body that emerges from the so called “flagellar pocket”, extending for the entire length of the trypanosome starting at the anterior part of it (see Figure 1). Remarkably, all members of this order have kinetoplasts, a unique form of mitochondrial DNA that has a disc-shaped form, where the flagellar pocket is established as an invagination of plasma membrane (MacLean et al. 2013). Mechanistically, the flagella movement, also named flagella wave, cause a forward parasite movement and simultaneous rotations around its axis. This movement permits trypanosomes to swim by producing a “travelling wave” that cross along the flagellum, pushing the surrounding liquid in one direction and generating a propulsion force into opposite direction (Krüger and Engstler 2018).

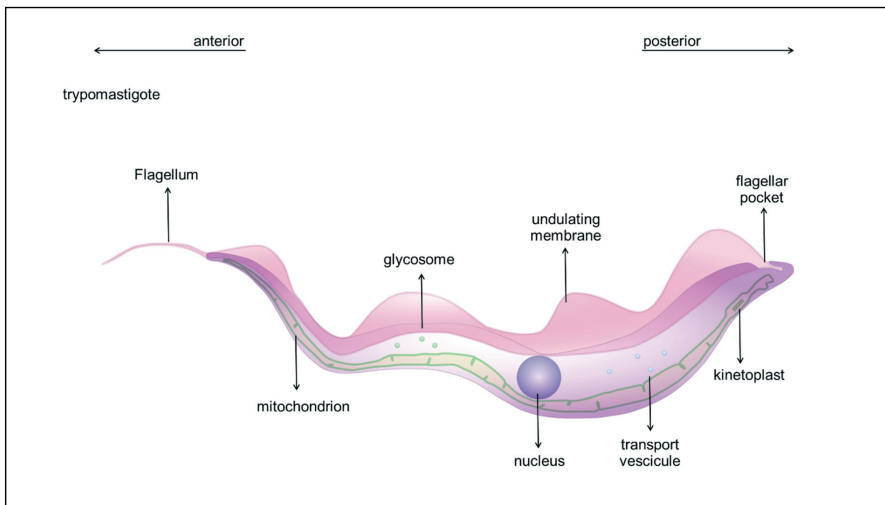


**Figure 1.** Schematic representation of a *T. b. brucei* trypomastigote morphology. Adapted from MacLean et al 2013

# 1. Introduction

---

Parasitic *Trypanosoma* species are classified in two categories according to their life cycles: Salivaria and Stercoraria. In the first group, *Trypanosoma* spp. develop in the anterior digestive tract of invertebrate vectors (insects) and transmitted via insect saliva whereas in the second group they develop in the posterior part of the insect gut and transmitted via insect faeces (Desquesnes et al. 2013). Among the members of the Salivaria, *T. brucei* includes sub-species such as *T. b. gambiense*, *T. b. rhodesiense* and *T. b. brucei*. The overall importance of *T. b. gambiense* and *T. b. rhodesiense* is due to its participation as causal agents of the human African trypanosomiasis (HAT), also known as sleeping sickness. Epidemiologically, these species are extended in sub-Saharan Africa countries (between 14°N and 20°S) due to the habitat of their vectors, the tsetse fly (*Glossina* spp.) (Brun et al. 2010; Malvy and Chappuis 2011; Radwanska et al. 2018). Additionally, HAT is classified into East African- and West African disease depending on the species, i. e. *T. b. rhodesiense* and *T. b. gambiense*, respectively (Simarro et al. 2011). Both HAT infections are differentiated by their incubation period, where *T. b. rhodesiense* shows a more rapid and progressive replication when compared to *T. b. gambiense* (Kennedy 2006; Simarro et al. 2011). Nevertheless, in both cases the disease can be fatal if untreated (Kennedy 2006). Noteworthy, humans living in endemic areas are capable to overcome infection and neutralize the functions of trypanosome lytic factor 1 (TLF1) and trypanosome lytic factor 2 (TLF2), both known to be relevant in pathogenesis of HAT. Both, TLF1 and TLF2 are high-density lipoproteins (HDL) and their efficient neutralization provides innate immune protection to humans against *T. b. brucei* infections in endemic areas (Ponte-Sucre 2016). Fortunately, extended sanitary efforts in Africa have controlled HAT between 1949 and 1965 with only few new registered cases per year. Nowadays, an increase in the incidence has been observed needing further monitoring efforts (Kennedy 2006).

## 1.1.1.1. *T. b. brucei* infection of cattle

Contrastingly to HAT, *T. b. brucei* infection of cattle is largely less controlled. This last aspect, takes special relevance since bovines have pivotal role as natural host reservoirs allowing perpetuation of this parasite among diverse African ecosystems. In the case of cattle, the disease caused by *T. b. brucei* is locally named as 'Nagana' ("powerless/useless" in the Zulu language), thereby restricting agricultural development and significantly contributing to poverty in affected areas (Steverding 2008; Radwanska et al. 2018). The disease often affects animals if a proper early diagnosis is not performed (Maudlin 2006). The relevance of Nagana is ancient, since evidence reveals the presence of African animal trypanosomiasis (AAT) in ancient Egypt, where a veterinary papyrus from Kahun Papyri (dating from the 2<sup>nd</sup> millennium BC) exhibits

## 1. Introduction

---

information of a cattle with a disease which resembles Nagana (Steverding 2008). In 1895, the Scottish pathologist and microbiologist David Bruce (1855–1931) officially identified *T. b. brucei* as etiological cause of Nagana (Steverding 2008). Clinically, AAT symptoms are considered as non-specific, including body condition detriment, pale mucous membranes, change of feces consistence and abnormal body temperature. Therefore, AAT is considered as a wasting disease, in which there is a slow progressive loss of health condition accompanied by increasing anaemia and weakness to the point of extreme emaciation, collapse and even death (Uilenberg 1998). Initially, *T. b. brucei*-infected animals will show variable appetite, tending to leave their herds, looking for protection from sun and standing with ears and tail hanging and ignoring insects. Increased lacrimation is also seen in *T. b. brucei*-infected animals (Uilenberg 1998). Overall, the infection becomes evident 7-10 days after tsetse bites, with a raise in body temperature and an increase of heart and respiratory rates (Uilenberg 1998).

The economic importance of *T. b. brucei*-infection in endemic areas is large, having negative implications in the development of Sub-Saharan African countries. In this context, livestock production plays a fundamental role in economic and socio-cultural role of rural or small households, acting as food and nutrition supply, source of power for farm work and capital accumulation (Alsan 2015; Abro et al. 2021). It is estimated that AAT can cause 3 million deaths of cattle with an annual direct economic loss of US\$ 1–1.2 billion in Sub-Saharan African production systems (Uilenberg 1998). Furthermore, considering indirect economical losses, these countries can lose up to 4.75 billion USD per year due to Nagana (Uilenberg 1998; Abro et al. 2021). Mitigation strategies includes sale of agricultural products (64%); search assistance from family and friends (54%); sale/lease of family belongings (22%); credit acquirement (22%) and use of personal savings (17%) (Bukachi et al. 2017), highlighting the economic impact of AAT.

### 1.1.1.2. *T. b. brucei* life cycle and host-parasite interactions

In the vertebrate host, motile extracellular stages of *T. b. brucei*, known as trypomastigotes, live and proliferate freely within blood circulation and multiply asexually by longitudinal fission-driven replication, being thereafter taken by female tsetse (*Glossina*) flies during their blood meals (see Figure 2). The critical role of *Glossina* spp. flies becomes evident in AAT ecology and epidemiology as AAT is strictly limited to the African continent where genus *Glossina* occurs in different biomes.

# 1. Introduction

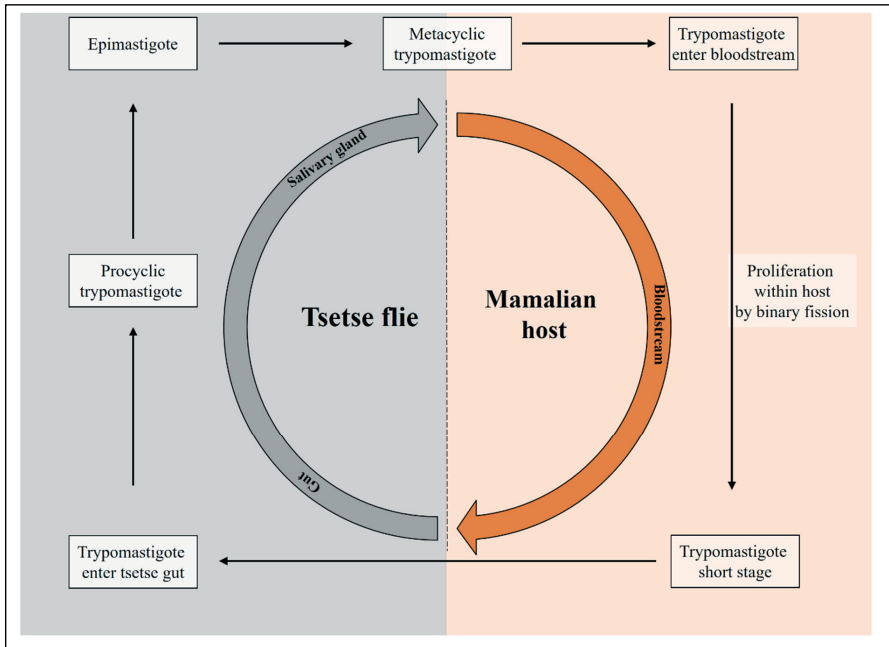


**Figure 2.** Schematic *T. b. brucei* life cycle. Adapted from Deplazes 2016.

Taxonomically, tsetse flies of the genus *Glossina* belong to the family Glossinidae (*Glossa*: tongue) within the order Diptera. The members of this family are dark-brown, with a piercing apparatus (i. e. proboscis) directed forward which surpasses by far the head (caput) of all *Glossina* spp. Additionally, the fold of the two wings exhibit in resting position a ‘tongue-like’ structure, representing a typical feature of tsetse flies and allowing to differentiate them from other dipteran genera. African *Glossina* flies are grouped in three different species, i. e. *Glossina palpalis*, *Glossina fusca* and *Glossina morsitans*, being the last one the most important for Nagana transmission (Krafsur and Maudlin 2018). Biologically, adult female *Glossina* flies are obligate hematophagous (non-parasitic tsetse males feed on nectar) and have a life span of 2 and 5 months. Differing to other dipteran flies, female tsetse flies mate and thereafter generate only one egg which is carried within a uterine-like organ, where the larvae will develop from L<sub>1</sub> into L<sub>3</sub> over 7 to 10 days (Demirbas-Uzel 2018). Thereafter, it will be deposited in sheltered places where they immediately pupate. It must be noticed that larval development requires 7-10 days; nevertheless, the pupal period requires approximately 30 days at a temperature of 25 °C (Tobe 1978; Demirbas-Uzel 2018).

## 1. Introduction

---

The tsetse flies are infected by non-dividing stumpy forms of the parasite (shorter form, 12 to 26  $\mu\text{m}$ ) present in the host bloodstream. The slender or long trypomastigotes (30 to 40  $\mu\text{m}$ ) are the previous stages which proliferate asexually in the bloodstream (please refer to Figure 2) (Tyler et al. 1997). After insect ingestion, slender forms are killed rapidly when compared to stumpy forms which survive longer within tsetse intermediary hosts (Silvester et al. 2017), differentiating into the next stage. In the fly, *T. b. brucei* stumpy forms transform into epimastigote stages within midgut and salivary glands. This process requires approximately 3 to 5 weeks (Brun et al. 2010). Once *T. b. brucei*-infected tsetse fly will have another blood meal, injected epimastigotes through proboscis will develop into metacyclic trypanosomes and an inflammatory reaction within dermal connective tissue will occur, generating a characteristic lesion named “chancre”, followed by draining from the lymphatic and bloodstream system (Hope-Rapp et al. 2009). The overall description of life cycle stages refers mainly to morphological features identified by the shape, kinetoplast position in relation to nucleus and the extent of the flagellar apparatus. As such, trypomastigotes have a nuclear kinetoplast and body-attached flagellum, while epimastigotes have a prenuclear kinetoplast (Cavalcanti and de Souza 2018). It is necessary to highlight, that unlike other members of the genus *Trypanosoma* (i.e. *T. cruzi*), *T. b. brucei* does not have amastigote stages (Tyler et al. 2003).

Epidemiologically, it has been established that the completion of the life cycle of *T. b. brucei*, requires the presence of domestic- and wild animals (Rotureau and Van Den Abbeele 2013). Additionally, the existence of natural reservoir hosts in Africa allows the perpetuation of *T. b. brucei* life cycle with ease, and will add a challenge for disease control or eradication programs (Rotureau and Van Den Abbeele 2013).

One of the most dangerous complications of *T. b. brucei*-induced trypanosomiasis is that parasites can infect brain parenchyma and cerebrospinal fluid (Malvy and Chappuis 2011). This is due to the capacity of this blood-dwelling parasite to migrate through the blood-brain-barrier (BBB). Moreover, *T. b. brucei* is able to survive within the bloodstream, evading the adaptive immune response through efficient and constant antigenic variation (Malvy and Chappuis 2011). This antigenic variation is driven by the presence of so-called variable surface glycoproteins (VSG), which consist of a layer of complex proteins on the surface of these parasites, which are anchored to their membranes by glycosylphosphatidylinositol (GPI) molecules, allowing survival and maintenance over time of parasite infection (Matthews 2005; Moreno et al. 2019). GPI-anchored glycoproteins are extremely abundant on the surface of trypomastigotes, having approximately  $10^7$  copies covering the whole cell plasma membrane

## 1. Introduction

---

(Mugnier et al. 2016). Moreover, VSG molecules coating trypanosomes can function in a selective way by removing specific antibodies from the surface of the cell, allowing to dampen the host antibody response (Engstler et al. 2007). In this sense, VSG proteins can be described as a barrier based on surface proteins on which host antibodies will attach, being thereafter selectively removed by an endocytic process that occurs in the parasite flagellar pocket allocated in the posterior cell pole (Engstler et al. 2007; Mugnier et al. 2016). This process is highly linked to activation of humoral adaptive immune response, where immunoglobulin M (IgM) is the first antibody isotype to be detected after *T. b. brucei* infection, and being cleared more quickly than other isotypes such as IgG from the parasite surface (Mugnier et al. 2016). Interestingly, it has been shown that clearance of IgG from trypomastigotes cell surface is directional and very fast, i. e. within 30 to 60 s. All of these immune complexes will be sorted out to the posterior part of *T. b. brucei* trypomastigotes, where they will accumulate. Thereafter, endocytic uptake of accumulated antibody-antigen complexes will occur, as stated above via parasitic flagellar pocket (Engstler et al. 2007). This last evasion strategy dramatically limits the development of vaccines against AAT by conventional humoral-based systems, being nowadays unfeasible due to the participation of VSG and endocytosis capacities of *T. brucei* trypomastigotes (Mugnier et al. 2016).

### 1.1.1.3. Diagnosis of AAT

One characteristic of AAT is its highly fluctuating parasitaemia within affected hosts. This parasitaemia is normally high in the early phase of infection and lower in the chronic phase. This situation generates a challenging scenario for proper diagnosis as many times during chronic infection less extracellular stages will be detected in the blood (Desquesnes et al. 2022). In general terms, there are three main established diagnostic strategies: microcopy-, DNA- and antibody-based detection (Desquesnes et al. 2022). The parasite detection/diagnosis is normally based on microscopic examination of fresh blood, Giemsa-staining of blood smears, hematocrit concentration and buffy coat methods (Woo 1970; Murray et al. 1977). The advantage of microscope-based techniques relies on the use of standard equipment and low cost for AAT diagnosis in rather poorer countries of Africa. In the case of the hematocrit concentration, it has been established that it is better suited when large number of animals will be assessed for occurrence of AAT. Moreover, hematocrit concentration- and buffy coat methods are able to provide the packed cell volume, which allows to estimate the level of anemia of *T. b. brucei*-infected animals, being one of the most critical indicators of clinical manifested Nagana (Desquesnes et al. 2022). Additionally, several primer pairs have been designed for the

## 1. Introduction

---

amplification of *T. b. brucei*-specific DNA, based on highly repetitive satellite DNA probes (Health 2021). The advantage of these molecular diagnostic techniques rely on their specificity, allowing not only differentiation to subgenus-, subspecies- or even to genotype levels depending on the primer set here used, but also to detect infections in the insect vector as well as wildlife animals as reported elsewhere (Masiga et al. 1996).

Serological-based diagnostic methods are valuable epidemiological tools to analyze large numbers of animals for presence, emergence, re-emergence or even spread of AAT into previously non-endemic geographic areas, considering the persistence of specific antibodies raised against *T. b. brucei* circulating in the blood even after parasite elimination. Despite of other multiple diagnostic techniques standardized for Nagana detection [e. g. indirect fluorescent antibody test (IFAT), antibody detection, ELISA, Westerblots], the most standardized technique used in Africa is the so-called ‘Card Agglutination Test for Trypanosomes’ (CATT) (Desquesnes et al. 2022). This test is based on the detection of specific IgM antibodies, and is suitable for detection of early. *T. b. brucei*-infections (Asonganyi et al. 1990; Desquesnes et al. 2022). Importantly, CATT can be performed in not specialized laboratories as frequently reported for rural African areas (Desquesnes et al. 2022). Nevertheless, the specificity of this technique in animals has not been totally determined, showing strong cross-reactions between *T. b. brucei* and other salivarian trypanosomes such as *T. b. congolense* (Asonganyi et al. 1990; Desquesnes et al. 2022).

### 1.1.1.4. Treatment and control of AAT

FAO (United Nations)- recommendations still represent the best international guidelines for suitable chemotherapy, chemoprophylaxis, control and eradication of Nagana. Chemotherapy include various ‘trypanocides’, a group of drugs which work by killing or inhibiting the development of these parasites within the host (Keating et al. 2015; Seangseerattanukulchai and Piratae 2021). Since *T. b. brucei* can avoid the host immune system by VSG-driven mechanisms, the use of certain trypanocides permits to hamper parasitic multiplication, allowing the host immune system to overcome and control the infection (Keating et al. 2015; Seangseerattanukulchai and Piratae 2021). Historically, different attempts of animal treatments were performed in the twentieth century, including tartar emetic (antimony potassium tartate) treatments which resulted in successful therapy of affected animals. Nevertheless, this treatment generated irritation in the area of injection and required multiples doses to achieve therapeutic effects, thereby limiting its use. Nowadays, the mostly used drugs in the last 35 years are diminazene aceturate-, homidium salt- and isometadium chloride-based trypanocides (Keating

## 1. Introduction

---

et al. 2015; Seangseerattanukulchai and Piratae 2021). Diminazene aceturate is a yellow powder/solution that is administered intramuscularly and tissues at the site of injection will be stained by the drug for a period of 14 days, dramatically limiting the commercial value of animal meat (Keating et al. 2015; Seangseerattanukulchai and Piratae 2021). Additionally, homidium salt derivatives includes homidium bromide (HB) and homidium chloride (HC) and exclusively to be applied via intramuscular routes. Skin irritations have frequently been reported for HB- and HC intramuscular application. At therapeutic dosages, no toxicity problems have been observed in treated animals, but drug resistance development to both drugs is an emerging problem in numerous African countries. Likewise, since both HB and HC salts have carcinogenic properties for humans, the use of gloves by operators is imperative, limiting their use in poorly equipped African farms. Finally, all above mentioned chemotherapies have to be administered by intramuscular injection resulting in severe skin irritations which might be considered as serious disadvantage for certain ethnic animal farmers (e. g. Massai) where cattle possess an enormous value. Moreover, these drugs have a known little margin of safety regarding their therapeutic doses. Nonetheless, some of these compounds can be used either as curative or as prophylactic drugs, depending on the dosage administered (curative dose: 0.25–0.5 mg/kg; prophylactic dose: 0.5–1 mg/kg) (Latif et al. 2019).

Since pharmacological control of the disease has several limitations in endemic areas, vector control is the most available and reliable strategy for disease control. Several control methods has been established for tsetse flies within their natural habitats. Bush clearing of the vegetation used by these flies has been the oldest way to control their populations, and is still performed by local farmers, but is limited due to the vegetation reappearance with following fly reestablishment. Additionally, elimination of wild host animals can be feasible, based on the fact that tsetse flies need to feed blood regularly as there is no diapause during the life cycle; thereby reducing bites of wild mammal hosts will limit their survival strategies. Nevertheless, this method is often discarded considering ecological implications of this approach (Latif et al. 2019). Historically, control of tsetse fly populations was achieved by spraying with insecticides on surfaces and air (i. e. aerial spraying) of endemic regions. This strategy relays on the fact that ground spraying will affect places where tsetse flies rest and breed. Moreover, aerial spraying can be considered the more safely strategy as side effects against other insect species are less severe (Perkins 2004). Nevertheless, the use of aerosol spray will depend on the terrain where it will be performed and, the possibility of resistance development against insecticides cannot be discarded (Perkins 2004). Alternatively, WHO recommends the use of impregnated traps with insecticides either for sampling or for efficient vector control, being imbued with

## 1. Introduction

---

pyrethroids (in general) in order to increase efficiency (Organization 2013; Latif et al. 2019). Black- and blue textile fabrics are the ones used to construct these tsetse traps, considering the fact that blue is the more attractive colour for these vectors whereas black encourage tsetse flies to land. For this reason, the black part is normally found covering the inside of recommended tsetse traps. Furthermore, WHO recommends that the blue fabric consists of a polyester-cotton mix, because this will help to fight degradation of material in tropical conditions (Organization 2013).

Another technique is the use of olfactory baits for these flies. They are developed by applying urine in designed dispensers close to the animals. Normally aged urine from cows is here used, as it is widely available and free (Hassanali et al. 1986). Lastly, animals sprayed with insecticides can be used as “live baits” as well. For “live baits” the insecticide has to be applied either as spray or as pour-on solution; the last ones will be efficient if the necessary number of animals is treated. Also, application of insecticides close to the belly and/or legs of cattle at 2-week intervals can kill tsetse flies just as effectively as spraying the whole animal body every month. Sadly, these alternative applications are too expensive for most farmers in many poor African countries (Torr et al. 2007).

Overall, one of largest problems related with the effectiveness of products to combat Nagana efficiently, are still related to the missing access of these products by local farmers and their high economic costs. The local market is rather uncertain, non-controlled and not very profitable for these products throughout African countries (Bauer et al. 1995).

### 1.1.2. Phylum Alveolata, subphylum Apicomplexa

Apicomplexa is a subphylum including exclusively obligate unicellular parasites of numerous vertebrate- and invertebrate hosts (Votýpka et al., 2017), including major parasite species of medical and veterinary relevance such as *Plasmodium* spp. causing malaria and *Toxoplasma gondii* causing toxoplasmosis. Moreover, they are complex organisms with a variety of morphological shapes, depending on the species, the genus and the life cycle, and being surrounded by a three-layered membranous structure, called pellicle, forming the characteristic banana-shape of apicomplexans (Šlapeta 2013). Three classes of apicomplexan parasites are known: hematozoa, gregarine and coccidian, being the last one organized in two families: Eimeriidae and Sarcocystidae (Votýpka et al., 2017; Lindsay and Dubey, 2020).

The mechanism of pathogenesis of Eimeriidae and Sarcocystidae is a consequence of its obligate intracellular life cycle, which culminates with the lysis of infected host cell as these

## 1. Introduction

---

parasites replicate (Black and Boothroyd, 2000). Both families have similar features regarding their life cycles, being divided into sexual- and asexual cycles. Asexual cycles present one or more merogonic proliferation, which will develop in the intermediary and/or in the definitive host. Sexual cycle is known as gametogonic proliferation (i. e. gamogony), which will occur only in the definitive host by the development of microgamonts and macrogamonts and, as a consequence, the formation of sporozoites contained in a structure named oocyst (Votýpka et al., 2017; Lindsay and Dubey, 2020). The family Sarcocystidae includes various relevant coccidian genera, e. g. *Toxoplasma*, *Besnoitia*, *Sarcocystis*, *Hammondia* and *Neospora*, which all will form tissue cysts containing bradyzoites within different intermediate hosts according to their life cycles. In all members of family Sarcocystidae, the gamogony, i. e. the sexual replication, will exclusively occur in definitive hosts, mainly in carnivorous or omnivorous species.

Knowledge on the general survival mechanisms of apicomplexan parasites has improved in the last decades, and has allowed to explore in detail host-parasite interactions, host immune reactions (Hermosilla et al., 2012; Taubert et al., 2010), host cell modulation (Taubert et al., 2010; Velásquez et al., 2021), parasite metabolism among others (Silva et al., 2021; Larrazabal et al., 2021), all of which is of great importance for the development of control strategies and better understanding of the apicomplexan diseases.

### 1.1.2.1. *Besnoitia besnoiti*

*B. besnoiti* is a cyst-forming coccidian parasite and the causal agent of bovine besnoitiosis. The first report related with this disease was in 1884 by Cadéac who described bovine besnoitiosis as a skin disease in cattle. In 1912, the French parasitologists Besnoit and Robin found that the disease was caused by an apicomplexan parasite (Cortes et al. 2014). Bovine besnoitiosis has been spreading during the last year on a larger scale, and being reported endemically in Portugal, Spain, France, Hungary, Germany and Italy. Mortality rate is less than 1% where only few *B. besnoiti*-infected animals will develop clinical symptoms (Alvarez-García et al. 2013).

The complete life cycle of *B. besnoiti* has not been clarified, but most likely to be heteroxenic with carnivores (e. g. felids) acting as definitive hosts and cattle as intermediate hosts (Basso et al. 2011), where they alternate tachyzoites and bradyzoites stages in intermediate hosts, which gather into macroscopic cysts located inside cells of subcutaneous connective tissue (Alvarez-García et al. 2013; Cortes et al. 2014). The disease has two phases: the acute phase, occurring within 11-13 days after infection, and the chronic phase, developing while affected animal's recovers (Alvarez-García et al. 2013; Cortes et al. 2014). Acute phase is characterized by fever,

## 1. Introduction

---

respiratory disorders, serous nasal- and ocular discharges, anorexia and generalized edema of the skin, as a consequence of fast replicating tachyzoites in macrophages, monocytes, polymorphonuclear neutrophils (PMN) and endothelial cells within the blood/lymph vessel of the host (Basso et al. 2011; Muñoz-Caro et al., 2015). Chronic phase of bovine besnoitiosis will manifest with strong skin alterations as a consequence of cutaneous and subcutaneous skin-cysts of up to 0.5 mm in diameter, hyperkeratosis, hyperpigmentation, alopecia and infertility in bulls due to orchitis (Basso et al. 2011; Alvarez-García et al. 2013).

### 1.1.2.2. *Neospora caninum*

*N. caninum* is a cyst-forming coccidian protozoa and being a major cause of abortion in cattle, small ruminants (Benavides et al. 2022) and causal agent of neurological disorders in young dogs. The first description of the parasite was performed in 1984 in dogs of Norway but the genus and species identification was completed in 1988 (Dubey et al. 1988). *N. caninum* infections have been reported worldwide, including Australia, New Zealand, Europe, Korea, Japan and Americas. Quantitative studies have demonstrated that between 12 to 42% of aborted fetuses in cattle industry of USA, New Zealand, Netherlands and Germany are a consequence of bovine neosporosis (Dubey 2003).

Canids have been described to act as intermediate- as well as definitive host of *N. caninum* (Lindsay et al. 2001; Dubey 2003). Life cycle has three different infectious intracellular stages, including tachyzoites, bradyzoites and sporozoites. Overall, intracellular tachyzoites represent a minor infection source in comparison to bradyzoites, which are enclosed in thin-walled tissue cysts (0.3-1.0 µm). Vertical- or diaplacental transmission in dairy cattle is the main infective route for bovine neosporosis but also environmental sporulated oocysts shed by *N. caninum*-infected dogs can initiate infections. As stated above, *N. caninum* can be transmitted transplacental/vertically and postnatally. Postnatal transmission will occur after the ingestion of infected tissues with tachyzoites and/or ingestion of tissue/organs containing cysts (Dubey 2003). Patent canids (i. e. domestic dogs, wolves, coyotes) have been described as important risk factors of bovine neosporosis by excreting millions of un-sporulated *N. caninum*-oocysts into the environment. Exogenous oocysts will then sporulate within 24-48 h if environmental conditions are optimal (i. e. adequate humidity, temperature and oxygen concentrations), and thereby contaminating premises of farms for many months with these highly resistant stages (Dubey 2003; Almería 2013).

Clinical symptoms in cattle relay mainly in abortion, from 3 months of gestation to term. *N. caninum*-infected fetuses will die inside the uterus or being reabsorbed, mummified and/or

## 1. Introduction

---

autolyzed. Additionally, either asymptomatic neonatal calves or with clinical signs can be born (Dubey 2003). Affected calves will manifest mainly neurologic signs, underweight, with limbs flexed or hyperextended (Dubey 2003).

### 1.1.3. Phylum Nematelminthes

The phylum Nematelminthes represents a large and diverse group of non-segmented round worms, capable to inhabit water and different type of soils, and having a high number of species (> 20.000 species) within this metazoan phylum (Dorris et al. 1999; Seesao et al. 2017). They can be classified in several superfamilies, including Strongyloidea, Ancylostomatoidea, Trichonstrongyloidea and Metastrongyloidea among others. This last superfamily includes the family Angiostrongylidae with numerous parasites of high veterinary- and human medicine relevance. The nematodes of Angiostrongylidae family are parasites inhabiting blood vessels and lungs of various host species (i. e. carnivores, marsupials, rodents). Males have a well-developed bursa, while females have a vulva on their caudal position. *Angiostrongylus* species have an indirect life cycle requiring the presence of mollusks (terrestrial and aquatic species) acting as obligate intermediate hosts, in order to fulfill their biology (Ferdushy and Hasan 2010; Schnyder et al. 2017).

#### 1.1.3.1. *Angiostrongylus vasorum*: the French heartworm

*A. vasorum* is a cardiopulmonary parasite that belongs to the class Nematoda (superfamily Metastrongyloidea) and having mainly canids, including domestic and wild ones (e. g. foxes, wolves) as final hosts (Ferdushy and Hasan 2010; Schug et al. 2018; Silva et al. 2021). The first certified description of this parasite was probably made in 1853 by Serres, in the city of Toulouse in the south-western of France, where a hunting dog with non-specific signs such as apathy and loss of appetite was treated. After a few days the animal was found dead and necropsy revealed an increased volume of the right ventricle containing a huge number of “worms” of approximately 15 mm of length. These heartworms were found not only in the right ventricle but also in the right auriculum and described as *A. vasorum* (Schnyder et al. 2017).

Morphologically, *A. vasorum* is a slender nematode, with a length of 18-25 mm for females while the males are shorter and reaching only 14-18 mm, with a bursa copulatrix. In addition, female nematodes of *A. vasorum* have two morphological features: *i*) the white uteri/ovaries are coiled around the intestine, and *ii*) additionally by having the vulva opening at the posterior part of their bodies (Ferdushy and Hasan 2010).

# 1. Introduction

---

*A. vasorum* is worldwide distributed (Ferdusky and Hasan 2010; Schnyder et al. 2017) and has been found during the last years in previously considered non-endemic geographic areas. Thus, canine angiostrongylosis is now being considered as an emerging disease in Europe, North- and South America (Helm et al. 2015; Penagos-Tabares et al. 2019). In Europe the distribution of the parasite is variable, having hyperendemic regions of *A. vasorum*-positive animals with surrounding areas which can show much lower prevalences (Schug et al. 2018). Recent geographical studies show that *A. vasorum*-infected dogs are expanding from Southwest Germany to Northeastern parts (Maksimov et al. 2017).

## 1.1.3.2. Life cycle and symptomatology of canine angiostrongylosis

The life cycle of *A. vasorum* is heteroxenous, requiring presence of terrestrial gastropods as obligate intermediate hosts. Adults live in the pulmonary artery and right heart of the host, the eggs, unsegmented 70 to 80 by 40 to 50  $\mu\text{m}$ , are transported to the capillary from the lungs, where L<sub>1</sub>, first stage larvae with a size of 310 to 400  $\mu\text{m}$ , will develop (Morgan et al. 2005). Larvae will travel to the alveoli, where they will be ingested and thereafter released to the environment with the feces. After this, L<sub>1</sub> must be ingested by terrestrial mollusks (e. g. snails, semi-slugs and slugs) to continue developing the cycle. Inside of them, L<sub>1</sub> will develop into L<sub>3</sub> in approximately 3 weeks. Several gastropod species have been recognized as suitable intermediate hosts, accordingly to the part of Europe where the life cycle is developing: in central Europa *Arion rufus*, *Arion lusitanicus*, *Arion ater* and also *Limax maximus* represent the main intermediate host species. It has been also reported that frogs can act as intermediate and/or paratenic hosts (Helm et al. 2015). Ingested larvae 3 (L<sub>3</sub>) through gastropod uptake will break through the intestinal wall and travel by using the lymphatic system to lymph nodes and thereafter to right heart and lung arteries of final hosts. The period of prepatency for *A. vasorum* is between 6 - 8 weeks and the patency period can be up to 5 years (Morgan et al. 2005).

Symptoms of canine angiostrongylosis include dry cough, dyspnea, exercise intolerance, weight loss, vomitus, abdominal pain, lumbar pain, neurological signs, heart failure, bleeding diatheses and sudden death. Canine angiostrongylosis can be classified in an early- and late phase (Morgan et al. 2005). In recent *A. vasorum*-infected dogs it was reported that resting animals might show no evident clinical signs; nevertheless, considering the already established presence of the parasite within right heart and *arteria pulmonaris*, tachycardia, tachypnea and heavy productive coughing can be observed. Additionally, sputum containing blood have been reported. On the other hand, in long established *A. vasorum*-infections the symptoms just described above can also be seen even in resting dogs. In chronic canine angiostrongylosis

## 1. Introduction

---

cases, all above mentioned signs can be accompanied with reduced appetite, anemia and ascites (Ferdushy and Hasan 2010; Schnyder et al. 2017).

### 1.1.3.3. Diagnosis and other insights of *A. vasorum*-infections

The diagnosis of the infection is performed by searching for the presence of L<sub>1</sub> in feces and sputum by using either the Baermann funnel technique or the bronchial lavage (BAL). The recovery of larvae from the feces or BAL is exclusively possible in the intermittent patency period of the infection (Bolt et al. 1994). Serological and molecular techniques (e. g. Western blot, ELISA, PCR) for diagnosis have been developed and considered to be highly sensitive methods for the diagnosis (Lunn et al. 2003; Morgan et al. 2005; Schnyder et al., 2017). The main goal of all these techniques is to generate detailed epidemiological data on occurrence of canine angiostrongylosis in domestic dog populations and also in wildlife (e. g. foxes, wolves) from different countries where only traditional *post mortem* studies are routinely performed, aiming to better understand parasite transmission and spread of disease (Morgan et al. 2005). The treatment recommended for *A. vasorum*-infected dogs include benzimidazole, such as mebendazole and febendazole. Benzimidazole-based drugs have been described to bind to microtubulin and causing disruption of microtubule polymerization as primary anthelmintic mechanism (Schmidt 1998). Also, levamisole and macrocyclic lactones have been used against this lungworm species (Ferdushy and Hasan 2010; Schnyder et al. 2017).

Clinically, Schnyder et al. reported in 2010 that an indicator of chronic inflammation in *A. vasorum*-infected dogs, are leukocytosis and neutrophilia; likewise, mediators of the immune system -strongly related to inflammatory processes- will be increased as consequence of damage of vasculature, situation that have been proved in cases of manifested canine angiostrongylosis (Schnyder et al. 2017). Interestingly, another heartworm that affect canids, *Dirofilaria immitis*, has also been shown to increase the activation of endothelium *in vivo* and *in vitro* (Mupanomunda et al. 1997). Activation of endothelial cells might lead to vessel hypertrophy that will suffer parasitized arteries as a consequence of *A. vasorum*-induced activation (Glaus et al. 2010). Due to its marked angiotropism, studies on endothelium activation and endothelium-derived pro-inflammation might help to clarify the pathogenesis of bleeding disorders observed in certain *A. vasorum*-infected dogs (Schnyder et al., 2017).

### 1.2. Polymorphonuclear neutrophils (PMN) and PMN-derived innate immune responses

PMN are able to react against several pathogen organisms -including virus, bacteria, fungi and/or parasites- due to the fact that they are capable to invade the normal homeostatic

# 1. Introduction

---

environment of the host (Brinkmann et al. 2004; Papayannopoulos 2018; Mozzini and Girelli 2020). All invasive foreign pathogens will be exposed to different components of the innate immune system, including endothelial/epithelial barriers, circulating leukocytes [i. e. PMN, monocytes, macrophages], dendritic cells (DCs) and natural killer (NK) cells (Brinkmann and Zychlinsky 2012; Hermosilla et al. 2014). An important attribute of circulating leukocytes relies on the ability to stick on the surface of activated endothelium as a consequence of stimulation with several inflammatory mediators (i. e. histamines, bradykines, chemokines, cytokines) that are released from sentinel leukocytes when they are able to sense the presence of pathogens, and being able to migrate to the site of infection (Kolaczkowska and Kubes 2013). In this context, PMN are the first leukocytes to arrive to the site of infection, playing a fundamental role in the control against foreign pathogens (Brinkmann et al. 2004; Muñoz Caro et al. 2014; Papayannopoulos 2018; Mozzini and Girelli 2020). PMN are characterized by having a polymorphic-segmented nucleus and various types of cytoplasmic granules (Paape et al. 2003; Kobayashi et al. 2017). They are classified as short-lived cells, having a half-life of 8.9 h in the bovine and 8 h in the human system. PMN are produced in large numbers in the bone marrow from hematopoietic precursor cells, where granulocyte colony-stimulating factor (G-CSF) commit PMN generation and turning them into myeloblasts. Following a maturation process which includes promyelocytes, myelocytes, metamyelocytes, band cells and finally PMN (Rosales 2018). Senescent PMN are cleared from circulation in the liver, spleen and bone marrow, by sensing the CXC-chemokine receptor 4 (CXCR4) expressed in these aged PMN. A negative regulation of the release of new developed PMN from the bone marrow is also possible. For instance, clearance of apoptotic PMN is performed mainly by Kupffer cells or DCs, mainly regulated by interleukin-23 (IL-23)/IL-17/G-CSF cytokine axis (Kolaczkowska and Kubes 2013). In case of bovines, it is important to highlight that unlike many animal species where PMN comprise the majority of leukocytes circulating in blood, bovine PMN corresponds to only 25% of total counts (Paape et al. 2003) conforming less than half of total leukocytes (Bassel and Caswell 2018).

## 1.2.1. PMN recruitment cascade

The multi-lobulated nucleus allows PMN to line the nuclear lobes in a straight line, allowing rapid migration between activated endothelial cells, and thereby being the first ones to arrive to the site of infection or inflammation (Paape et al. 2003). As above stated, in most tissues and organs PMN migrate driven by chemoattractant signals (Metzemaekers et al. 2020) and this process has five recognized steps: tethering, rolling, adhesion, crawling and transmigration

## 1. Introduction

---

(Kolaczkowska and Kubes 2013; Wang and Chen 2018). Recruitment of PMN is initiated with initial changes on endothelium surface which occur upon stimulation by inflammatory mediators or activation of pattern-recognition receptors (PRR) interacting with infective agents. Thereafter, PMN-tethering and -rolling will occur, mediated by various selectins (i. e. E-selectin, P-selectin); these two selectins have a partially overlapping function to maximize PMN recruitment (Kolaczkowska and Kubes 2013). On endothelial cells, interactions of ligands present on PMN surface (i. e. P-selectin glycoprotein ligand 1 [PSGL1]) will occur, triggering a strong adhesion to receptors of the integrin family such as CD11b and CD18 (Kolaczkowska and Kubes 2013; Choudhury et al. 2019). The complete activation is a two-steps process, requiring the priming to specific pro-inflammatory cytokines (i. e.  $\text{TNF}\alpha$ ) or exposure of PRR to pathogen-associated molecular patterns (PAMPs) (Summers et al. 2010). Then, PMN normally transmigrate using endothelial cell-to-cell junctions, considering that they are able to actively crawl between cell components and relaying on interactions between receptors and ligands (Phillipson et al. 2006). Finally, in order to leave the vasculature, PMN cross the endothelium and thereafter the basal membrane. Migration through endothelial barrier can be paracellular (between endothelial cells) or transcellular (through endothelial cells), being the first one the most commonly performed by activated PMN, since transcellular migration is slower (20-30 min) (Phillipson et al. 2008; Woodfin et al. 2011). Worthwhile to mention is the fact that PMN recruitment might occur without participation of selectins and/or integrins, since PMN lacking these molecules are also capable to adhere to blood vessels of lungs as reported elsewhere (Kolaczkowska and Kubes 2013).

### 1.2.2. Microbicide activity of PMN

Mechanistically, antimicrobial functions include phagocytosis, degranulation, production of reactive oxygen species (ROS) and and release of neutrophil extracellular traps (NETs) (see Figure 3) (Brinkmann et al. 2004; Fuchs et al. 2007; Rosales 2018; Pérez-Figueroa et al. 2021). Phagocytosis is a process that involves the ingestion of microorganisms into a phagocytic vacuole, where after maturation becomes a phagolysosome where the microorganism is destroyed by the action of low pH and degrading enzymes (Rosales 2018). In addition, mature PMN granules and secretory vesicles are sequentially developed in PMN differentiation: primary granules (azurophilic) are found at the promyelocyte stages and known to be myeloperoxidase (MPO)-positive and lysozyme-positive; secondary granules (specific) can be observed in myelocytic stages containing high levels of lactoferrin and finally, tertiary granules (gelatinase) containing the majority of antimicrobial proteins (Paape et al. 2003; Sheshachalam

## 1. Introduction

et al. 2014; Rosales 2018). The three types of granules can be found in bovine PMN where tertiary granules tend to be larger than azurophilic- and secondary granules.

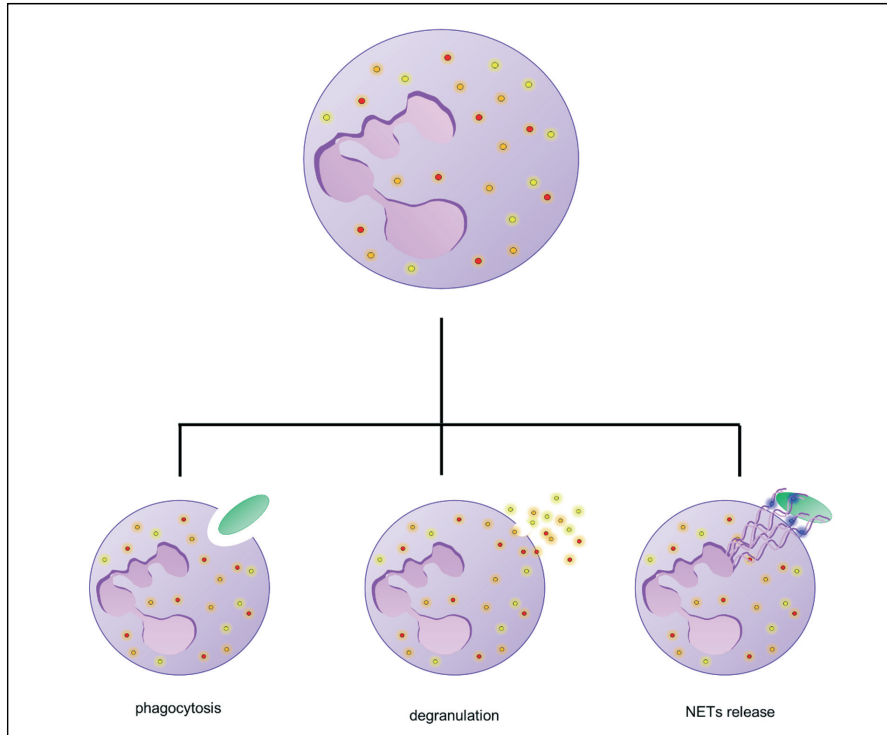


**Figure 3.** Schematic representation of the main effector mechanisms in PMN. Adapted from Kolaczowska *et al* 2013

The formation of ROS, produced by oxidative burst activities, is a characteristic property of all mammalian PMN and critical for fulfilling appropriate host defense since impaired ROS production is associated with an increase susceptibility to infections (Hampton et al. 1998). This mechanism is mediated by nicotinamide adenine dinucleotide phosphate (NADPH) oxidase (NOX), a multi subunit enzyme responsible of shuttling electrons, using  $O_2$  as final acceptor generating superoxide anion ( $O_2^-$ ) as final product and thereafter used as substrate for hydrogen peroxide ( $H_2O_2$ ) by enzymatic dismutation through superoxide dismutase (Rinaldi et al. 2007). Overall, PMN-mediated ROS production can be either NOX-dependent or NOX-independent; nevertheless, since both events can occur simultaneously, is unlikely to ignore the interaction that both elements might have during their antimicrobial responses (Nauseef 2004; Rinaldi et al. 2007; Moghadam et al. 2021). Accordingly, MPO contained in azurophilic

## 1. Introduction

---

granules has a fundamental role catalyzing the conversion of hydrogen peroxide into more toxic hypohalous acids (e. g. HClO) thereby increasing PMN bactericidal activity (Rinaldi et al. 2007; Moghadam et al. 2021). The overall generation of ROS can occur intra- or extracellularly, considering NOX location on the cellular membrane. As such, NOX internalization into phagosome will develop in generation of intracellular ROS (Hampton et al. 1998). Formation of extracellular ROS will occur either by production from NOX located on PMN cell membrane or escape of ROS molecules from early phagosomes that were not completely sealed (Hampton et al. 1998; Rinaldi et al. 2007).

### 1.2.3. Neutrophil extracellular traps (NETs)

It has been demonstrated that upon stimulation of PMN, the nucleus will start to lose its normal shape. Following this, the nuclear envelope and the granule membranes will disintegrate, allowing the mixture of decondensed chromatin with protein granules that will be then released to bind and kill microorganism. This complex and delicate mechanism is known as the formation of neutrophil extracellular traps (NETs). Since its first description in 2004 by Brinkman et al. (Brinkmann et al. 2004), it has become a relevant topic of PMN physiology, changing our understanding on how these cells efficiently kill and trap pathogens far beyond their life span (Hermosilla et al., 2014). Detailed NETs-related studies have consistently supported that NETs are mainly composed of nuclear DNA decorated with different histones, antimicrobial peptides and proteins derived from different granules present in PMN cytoplasm, including NE, MPO, pentraxin, lactoferrin and gelatinase (Brinkmann et al. 2004; Hahn et al. 2013). Thus, released NETs provide a high local concentration of antimicrobial molecules that can entrap and kill microbes, providing an effective mechanism to avoid foreign pathogen spread, minimizing simultaneously the damage to surrounding tissues (Fuchs et al. 2007; Hahn et al. 2013).

Within PMN physiology, phorbol 12-myristate 13-acetate (PMA) stimulation unleash a fast and consistent activation of mammalian PMN. In the case of PMA-triggered NET formation, the release of decondensed chromatin decorated with histones, nuclear swelling and membrane perforation of PMN will inevitably occur (Brinkmann et al. 2004; Yipp and Kubes 2013; Masuda et al. 2016). NET formation, also known as NETosis, was initially thought as a mandatory cellular death process different from apoptosis or necrosis (Fuchs et al., 2007; Steinberg and Grinstein 2007). However, recent evidence has shown that PMN do not necessarily undergo cell death after NET formation (Clark et al. 2007). In this sense, NET formation can additionally occur with the conservation of normal PMN functions, including

## 1. Introduction

---

phagocytosis, crawling and chemotaxis, known nowadays as vital NETosis. Currently, NET formation can be classified in literature as suicidal- or vital NETosis, respectively. Suicidal NETosis requires activation of Raf-MERK-ERK pathways and NOX-dependent production of ROS (Yipp and Kubes 2013; Masuda et al. 2016). This pathway includes also peptidylarginine deiminase 4 (PAD4)-dependent citrullination of histones (i. e. H1, H2A/H2B, H3, H4), necessary for DNA decondensation, which will result in mixture of extracellular DNA with citrullinated histones as well as granular components. In 2007, Fuchs et al. proved that the process of NET formation is triggered PMA and *Staphylococcus aureus* after a period of 3 h, where PMN developed very significant morphological changes as result of large quantities of oxidants produced by NOX activity (Fuchs et al. 2007). The NOX-dependent process is initiated by PMN losing their normal nuclei segmentation and their characteristic lobular forms. Likewise, granular membranes disappear and the granular components are thereafter mixed. The cell death process finishes with the release of unfolded chromatin to the extracellular space within 3 h to conduct their antimicrobial functions extracellularly (Fuchs et al. 2007). However, INF- $\gamma$ -primed eosinophils can also extrude DNA against specific stimuli, in a fast and non-lytic process. In this case, DNA-conforming eosinophil extracellular traps (EET) can be released from mitochondria (Yousefi et al. 2008; Pilszczek et al. 2010). Interestingly, the same group reported that when PMN were primed with GM-CSF and thereafter stimulated with LPS, DNA extrusion occurred from the same source (Yousefi et al. 2008). In mammalian-derived vital NETosis, PMN can as well release DNA of mitochondrial origin without losing nuclei components and continuing performing other functions. In line, vital NETosis was recently reported to occur against apicomplexan *Besnoitia besnoiti*. Activation of bovine PMN occurred within 5 to 30 min after co-culture, unveiling the formation of pseudopods and fast migration of PMN towards *B. besnoiti* bradyzoites (Zhou et al. 2020b). Observation of an elongated structure tossed out quickly from activated PMN after 30 min of co-culture with tachyzoites was also documented. The early time point of its occurrence and the non-lytic PMN phenotype casting this “tongue-like” structure confirmed *B. besnoiti*-mediated vital NETosis in bovine PMN (Zhou et al. 2020b). This last pathway allows the coexistence of NETs release and conventional PMN host defense (Yipp and Kubes 2013). Moreover, vital NETosis requires vesicular mobilization of DNA from inside the nuclei into the extracellular space. These vesicles will travel and fuse with the nuclear membrane, passing through the cytoplasm, allowing NETs to be delivered outside the cell without rupture of plasma membrane and, consequently, not destroying the cell. This process has been described as ROS-independent and

## 1. Introduction

---

reported as a fast defense process ( $\leq 30$  min) when compared to suicidal NETosis (Yipp and Kubes 2013; Masuda et al. 2016).

Remarkably, PMN have been proved to be abundant in colostrum, the most important protective nutrient for neonates considering pivotal role of passive transmission of maternal immunity (i. e. antibodies, leukocytes) to the newborn in marine and terrestrial mammals, (Gonzalez and Dus Santos 2017). It is known that colostrum PMN will distribute through neonates body after intestinal absorption, allowing to suspect a primordial role in the development of newborn innate immune response and defense against neonatal infective agents (Williams, 1993), including apicomplexan parasites such as *Cryptosporidium parvum*, *T. gondii* and *N. caninum* (Demattio et al. 2022).

Concerning NETs types, there are at least three NETs phenotypes based on their sizes and forms. Specifically, spread NETs (*sprNETs*) are consisted as smooth and elongated web-like structures, being composed exclusively of thin fibers of 15-17  $\mu\text{m}$  diameter. Diffused NETs (*diffNETs*) are described as a complex of extracellular decondensed chromatin with a diameter of 15-20  $\mu\text{m}$ . Lastly, aggregated NETs (*aggNETs*) are usually described as “a ball of yarn”, with a diameter of 20  $\mu\text{m}$  or more. Due to participating of numerous PMN undergoing simultaneously NETs, *aggNETs* have been the focus of recent investigations. For instance, *aggNETs* can have anti-inflammatory properties through degradation of pro-inflammatory cytokines in human gout (Schauer et al., 2014). Conversely, in uncontrolled *aggNETs* release these extracellular structures might have pathophysiological implications through either anti- or pro-inflammatory properties (Schauer et al. 2014; Sil et al. 2017; Hidalgo et al. 2019). Accumulation of *aggNET* can actively prevent dissemination of large and highly motile *Haemonchus contortus*- and *Dirofilaria immitis* larvae (Muñoz-Caro et al., 2015c; Muñoz-Caro et al., 2018), thereby permitting to orchestrate and establish the resolution of inflammatory mediators and/or large parasites (Muñoz-Caro et al., 2018; Knopf et al. 2019; Hahn et al. 2019; Mahajan et al. 2019). Potent *aggNETs* inducers are monosodium urate (MSU) crystals produced during the course metabolic gout in the human- and mouse systems (Schauer et al., 2014). PMN are able to ingest MSU crystals and respond initially by releasing inflammatory mediators to the environment and also by forming *aggNETs* (Schauer et al. 2014).

Additionally, it has been reported that release of inflammatory mediators by activated PMN can be high at intermediate cell densities ( $20\text{-}40 \times 10^6$  cells/cm<sup>3</sup>). Above these densities, mediator release by normal PMN is overcome by *aggNETs*-proteolytic degradation properties. Therefore, proteolysis of pro-inflammatory mediators primarily will depend on PMN densities

## 1. Introduction

---

and not necessarily on the size of aggregates (Hahn et al. 2019). Interestingly, Schauer et al. (2014) reported that within 10 min of incubation with MSU crystals (10 mg/mL) PMN are able to induce formation of *aggNETs* in humans (Schauer et al. 2014). Similarly, formation of *aggNETs* acting in a dose-dependent manner after MSU crystal exposure, suggested that this phenotype could also occur *in vivo* during pro-inflammatory gout disease (Schauer et al., 2014; Hahn et al., 2019). Since surrounding PMN are continuously recruited to the site of *aggNETs* after formation of the crystalline core, the final size of these aggregates can increase significantly (Hahn et al. 2019). Nevertheless, the mechanism underlying rapid control and termination of MSU-triggered inflammation by *aggNETs* still remains unclear (Schauer et al. 2014).

### 1.2.4. Role of ATP purinergic signaling in NET formation

PMN have a major role during early stages of the inflammatory response, associated to a quick reaction against environment disturbances. Nucleotides, especially ATP, and nucleosides (ADO) are fundamental metabolites in energy metabolism. In healthy tissues, ATP is synthesized by anaerobic glycolysis or oxidative phosphorylation and intracellularly stored, being almost undetectable extracellularly (Kolaczkowska and Kubes 2013; Wang and Chen 2018). On the other hand, ADO is generated from hydrolysis of AMP by 5-nucleotidase or by hydrolysis of S-adenosyl-homocysteine, being released from multiple cell types and considered for their ubiquitous presence of equilibrate nucleoside transporters (ENTs) (Wang and Chen 2018). Interestingly, when its presence is detected extracellularly, for example released by cells undergoing lysis, it can be sensed as an important pro-inflammatory modulator, acting as a damage associated molecular pattern (DAMP) or “dangerous signal”/“find me signal” (Dosch et al. 2018; Rubenich et al. 2021). Mechanistically, ATP and ADO are detected by P2- and P1 purinergic receptors, respectively, modulating several cell functions (Antonioli et al. 2013). P1 receptors belong to the G-protein-coupled metabotropic receptors, and are localized in PMN, where they play an important role in PMN migration (Antonioli et al. 2013). Conversely, P2 receptors are divided in two types: ionotropic (P2XRs) and metabotropic (P2YRs). P2XRs are ATP-gated trimeric ion channels becoming permeable to  $\text{Na}^+$ ,  $\text{K}^+$  and  $\text{Ca}^{++}$  after ATP binding while P2YRs belong to the G-protein-coupled receptors classification. These receptors have seven characteristic hydrophobic transmembrane regions (Idzko et al. 2014). The coordination between the two types of purinergic receptors play an important role in PMN activation during bacterial infection and against apicomplexan *C. parvum* (Kolaczkowska and Kubes 2013; Antonioli et al. 2013; Alarcón et al. 2020; Hasheminasab et al. 2022). P2Y receptors have been

## 1. Introduction

---

described to have a mayor influence on PMN activation, where release of IL-8 is enhanced by P2 receptors; even so, P2Y6 induces IL-8 secretion in the case of human monocytes, thereby modulating in a paracrine manner the *in vitro* PMN migration (Kukulski et al. 2007). Remarkably, extracellular release of ATP represents also an autocrine messenger for PMN, amplifying the chemotaxis gradient through P2Y2R activation, acting as a positive feedback for PMN gradient sensing (Chen et al. 2006).

Interestingly, purinergic signaling plays essential role in mediating PMN chemotaxis as well (Chen et al., 2006). Extracellular ATP and positive stimulation via the P2Y2R receptor of PMN is able to activate a mechanism that is required for PMN gradient sensing, thus a process directly involved in PMN chemotaxis (Chen et al. 2006). Released ATP will be hydrolyzed to ADO by nucleotidases expressed on PMN membrane, activating signaling mechanisms related to the migration speed of activated PMN (Chen et al. 2006; Wang and Chen 2018). In this line, activation of P2X1R receptor by extracellular ATP fails to induce PMN directional chemotaxis, but it increases random PMN migration (Wang et al. 2017). Additionally, it has been reported that P2X1 signaling may participate in PMN recruitment cascade by promoting PMN transmigration but neither rolling nor adhesion, directly affecting the process of PMN recruitment cascade (Kolaczowska and Kubes 2013). Related to NETs release, it has been shown that UDP itself is not able to initiate NET formation in human-derived PMN. Nonetheless, UDP has a direct effect on P2Y6 receptor in studies performed with MSU crystals as potent NETs inducers (Sil et al. 2017; Wang and Chen 2018). Lastly, P2Y2R has been classified as an activator of ROS production in PMN and directly involved with various PMN anti-microbial functions (Fuchs et al. 2007; Brinkmann and Zychlinsky 2007; Branzk and Papayannopoulos 2013).

### 1.3. Parasite-induced NET formation

In general terms, NETs are structures released from PMN involved in several physio-pathological processes and as a pivotal innate defense mechanism against several pathogens, including also protozoan- and metazoan parasites (Fuchs et al. 2007; Brinkmann and Zychlinsky 2007; Hermosilla et al. 2014; Papayannopoulos 2018; Villagra-Blanco et al. 2019).

In the case of parasites, NETs have been a relevant topic of research since the first publications of human-, mouse- and bovine PMN casting NETs against *Plasmodium falciparum*, *Leishmania amazonensis* and *Eimeria bovis* published in 2008, 2009 and 2010, respectively (Baker et al. 2008; Guimarães-Costa et al. 2009; Behrendt et al. 2010). The conserved nature of NETs against various parasite species has been observed from apicomplexan protozoans until large

# 1. Introduction

---

sized nematodes and trematodes (Behrendt et al. 2010; Bonne-Année et al. 2014; Muñoz-Caro et al. 2014, 2015c, 2016; Maksimov et al. 2016; Mendez et al. 2018; Peixoto et al. 2021).

Parasite-infected endothelial cells support the recruitment of PMN, this last process related to changes in endothelial morphology and adhesion molecule expression (Hermosilla et al. 2006; Taubert et al. 2006). It triggers chemokine production resulting in a pro-inflammatory environment which will finally mediate PMN mobilization to parasite-affected endothelium area (Hermosilla et al. 2012; Dehghani and Panitch 2020). The role of NET-derived adverse effects against parasite-infected endothelial cells *in vivo* and *in vitro* is still a matter of study, particularly for apicomplexan parasites infecting endothelium (Conejeros et al. 2019).

As previously mentioned, the role of intake of colostrum containing PMN in mammalian neonates is essential for increasing defense against invasive agents. Thus, it has been demonstrated that ingestion of colostrum plays a fundamental role during the first 24 h for the healthy development of newborns (Inoue and Tsukahara 2021). The predominant cell type in colostrum are PMN (41-84%) (Lee and Outteridge 1981). Conversely, milk secreted 48 h post deliver and/or formula milk without bioactive components (i. e. PMN) cannot replace colostrum (Inoue and Tsukahara 2021). After the intake, leukocytes will distribute through the body of the neonate, where they will develop an immune-regulatory function, considering the known tropism they show to affected tissues (Williams 1993). Yet, little is known on colostrum-derived NETosis, which could potentially influence newborn calf development (Demattio et al. 2022).

Taking into consideration the biological differences among parasite species, the evaluation on how PMN and endothelial/epithelial cells are modulated by taxonomically different parasites becomes a key element to better understand the pathophysiological implications driven by host infection or even the outcome of parasitic diseases affecting vessel endothelium (Maksimov et al. 2016), intestinal-, pulmonary- or even reproductive epithelium (Brazil et al., 2013; Szturmowicz and Demkow, 2021; Zambrano et al., 2022). Extraordinarily, marine mammals (i. e. pinnipeds and cetaceans) cast suicidal leukocyte extracellular traps against the presence of the apicomplexan parasites *T. gondii* and *N. caninum* –as seen for terrestrial mammals–, thus being able to entrap and immobilize these parasites, demonstrating that this cell death process is an ancient and well-conserved host innate defense mechanism (Villagra-Blanco et al. 2019).

The main objectives of this doctoral thesis were to conduct comparative evaluation studies on NETs formation triggered by evolutionary divergent groups of parasites such the euglenozoan extracellular living haemoflagellate *T. b. brucei*, the angiotropic nematode *A. vasorum*, the

## 1. Introduction

---

intracellular apicomplexan *N. caninum* and the mite species *Sarcoptes scabiei*. Also, first investigations on canine colostrum-derived PMN reactions, including NETosis and phagocytosis, were assessed. Comparative studies presented here will permit to generate comprehensive understanding regarding various signaling pathways, NET-derived endothelium damage, PRR, PAMP, phenotypes of NETs and also provide novel data on the extension and limitations of NETs formation as innate response against intracellular, extracellular dwelling parasites as well as large-sized and highly motile parasites (i. e. nematodes, trematodes and mites).

## 2. ORIGINAL PUBLICATIONS

### 2.1. *TRYPANOSOMA BRUCEI BRUCEI* INDUCES POLYMORPHONUCLEAR NEUTROPHIL ACTIVATION AND NEUTROPHIL EXTRACELLULAR TRAPS RELEASE

This chapter is based on the following publish paper:

**Grob D**, Conejeros I, Velásquez ZD, Preußner C, Gärtner U, Alarcón P, Burgos RA, Hermosilla C, Taubert A. *Trypanosoma brucei brucei* Induces Polymorphonuclear Neutrophil Activation and Neutrophil Extracellular Traps Release. *Front Immunol.* 2020 Oct 22;11:559561. doi: 10.3389/fimmu.2020.559561.

Eigener Anteil in der Publikation:

Projektplanung	50 %, zusammen mit Ko-Autoren und Betreuern
Durchführung des Versuches	60 %, weitestgehend selbständig
Auswertung der Experimente	60 %, weitestgehend selbständig
Erstellung der Publikation	60 %, weitestgehend selbständig

## 2.1 *Trypanosoma brucei brucei* induces polymorphonuclear neutrophil activation and neutrophil extracellular traps release



# *Trypanosoma brucei brucei* Induces Polymorphonuclear Neutrophil Activation and Neutrophil Extracellular Traps Release

Daniela Grob<sup>1\*</sup>, Iván Conejeros<sup>1</sup>, Zahady D. Velásquez<sup>1</sup>, Christian Preußner<sup>2</sup>, Ulrich Gärtner<sup>3</sup>, Pablo Alarcón<sup>4</sup>, Rafael A. Burgos<sup>4</sup>, Carlos Hermosilla<sup>1</sup> and Anja Taubert<sup>1</sup>

<sup>1</sup> Institute of Parasitology, Biomedical Research Center Seltersberg (BFS), Justus Liebig University Giessen, Giessen, Germany, <sup>2</sup> Institute of Biochemistry, Department of Biology and Chemistry, Justus Liebig University Giessen, Giessen, Germany, <sup>3</sup> Institute of Anatomy and Cell Biology, Justus Liebig University Giessen, Giessen, Germany, <sup>4</sup> Laboratory of Inflammation Pharmacology, Institute of Pharmacology and Morphophysiology, Universidad Austral de Chile, Valdivia, Chile

### OPEN ACCESS

#### Edited by:

Jan Fric,  
International Clinical Research Center  
(FNUSA-ICRC), Czechia

#### Reviewed by:

Anderson Guimarães-Costa,  
Federal University of Rio de  
Janeiro, Brazil  
Markus H. Hoffmann,  
University of Erlangen  
Nuremberg, Germany

#### \*Correspondence:

Daniela Grob  
daniela.grob@vetmed.uni-giessen.de

#### Specialty section:

This article was submitted to  
Molecular Innate Immunity,  
a section of the journal  
Frontiers in Immunology

Received: 06 May 2020

Accepted: 18 August 2020

Published: 22 October 2020

#### Citation:

Grob D, Conejeros I, Velásquez ZD,  
Preußner C, Gärtner U, Alarcón P,  
Burgos RA, Hermosilla C and  
Taubert A (2020) *Trypanosoma brucei*  
*brucei* Induces Polymorphonuclear  
Neutrophil Activation and Neutrophil  
Extracellular Traps Release.  
Front. Immunol. 11:559561.  
doi: 10.3389/fimmu.2020.559561

*Trypanosoma brucei brucei* trypomastigotes are classical blood parasites of cattle, these stages might become potential targets for circulating polymorphonuclear neutrophils (PMN). We here investigated NETs extrusion and related oxygen consumption in bovine PMN exposed to motile *T. b. brucei* trypomastigotes *in vitro*. Parasite exposure induced PMN activation as detected by enhanced oxygen consumption rates (OCR), extracellular acidification rates (ECAR), and production of total and extracellular reactive oxygen species (ROS). Scanning electron microscopy (SEM) showed that co-cultivation of bovine PMN with motile trypomastigotes resulted in NETs formation within 120 min of exposure. *T. b. brucei*-induced NETs were confirmed by confocal microscopy demonstrating co-localization of extruded DNA with neutrophil elastase (NE) and nuclear histones. Immunofluorescence analyses demonstrated that trypomastigotes induced different phenotypes of NETs in bovine PMN, such as aggregated NETs (*aggNETs*), spread NETs (*sprNETs*), and diffuse NETs (*diffNETs*) with *aggNETs* being the most abundant ones. Furthermore, live cell 3D-holotomographic microscopy unveiled detailed morphological changes during the NETotic process. Quantification of *T. b. brucei*-induced NETs formation was estimated by DNA and nuclear area analysis (DANA) and confirmed enhanced NETs formation in response to trypomastigote stages. Formation of NETs does not result in a decrease of *T. b. brucei* viability, but a decrease of 26% in the number of motile parasites. Referring the involved signaling pathways, trypomastigote-induced NETs formation seems to be purinergic-dependent, since inhibition via NF449 treatment resulted in a significant reduction of *T. b. brucei*-triggered DNA extrusion. Overall, future studies will have to analyze whether the formation of *aggNETs* indeed plays a role in the outcome of clinical disease and bovine African trypanosomiasis-related immunopathological disorders, such as increased intravascular coagulopathy and vascular permeability, often reported to occur in this disease.

**Keywords:** *Trypanosoma brucei brucei*, NETs formation, PMN, *aggNETs*, purinergic receptors

# 2.1 *Trypanosoma brucei brucei* induces polymorphonuclear neutrophil activation and neutrophil extracellular traps release

## INTRODUCTION

Animal African trypanosomiasis (AAT), also known as Nagana, has been recognized as a devastating and still neglected cattle disease in sub-Saharan Africa for centuries (1). The causal agent of AAT is the haemoflagellate parasite *Trypanosoma brucei brucei*, being transmitted by blood-meal bites of female tsetse flies (*Glossina* spp.). It is still considered as a major cause of mortality and morbidity in domestic cattle, sheep, goats, and horses. Pathogenesis of AAT is complex and starts with primary, localized inflammatory lesions at the site of *T. b. brucei* inoculation after successful tsetse bites, followed by intensive local asexual parasite multiplication and dissemination of the trypomastigote stage via lymphatic and blood vessels to regional lymph nodes, internal organs, central nervous system, cerebellum, and spinal cord (2–4). Consequently, clinical manifestations of AAT include generalized lymphadenopathy, splenomegaly, increased vascular permeability, edema, haemostasis, intravascular coagulopathies, anemia, tissue hypoxia, formation of immune complexes, glomerulonephritis, severe immunosuppression, and sudden death. *T. b. brucei*-infected cattle with or without clinical symptoms are considered as the main parasite reservoirs for AAT in Africa (5).

In the sub-Saharan African region, AAT in domestic livestock causes reduction of meat and milk production, restraining the labor function of *T. b. brucei*-infected animals, thereby causing high economic losses. Accordingly, economic benefits of tsetse fly elimination programs have been estimated for up to US\$ 4.5 billion per year by avoiding the death of 3 million cattle per year, as well as sheep, horses, and goats. In terms of zoonotic potential, the closely related species *T. brucei gambiense* and *T. brucei rhodesiense* are the causative agents of human African trypanosomiasis (HAT) or sleeping sickness, which is lethal if untreated and classified as well as a neglected tropical disease by the World Health Organization (WHO) (6).

*In vivo*, direct contact of *T. b. brucei* stages with leukocytes of the host innate immune system occurs during the parasite-endogenous replication phase, for example, (i) after initial tsetse bite-mediated inoculation of procyclic trypomastigotes into the skin, (ii) when metacyclic trypomastigotes enter the lymphatic/blood vessels, and (iii) when metacyclic trypomastigotes replicate in diverse organs. Polymorphonuclear neutrophils (PMN) are the most abundant leukocyte population in lymph and bloodstream and rapidly recruited from circulation to sites of infection (7–9). In this context, local pro-inflammatory responses in skin lesions in AAT, resulting in focal edema, were associated with PMN recruitment and granuloma formation surrounding *T. b. brucei* replication sites (10). PMN reacts against protozoan and metazoan parasites by different effector mechanisms which include the release of immunomodulatory molecules [e.g., cytokines, chemokines (CXCL1, CXCL8, CXCL10) (11, 12)], phagocytosis, production of reactive oxygen species (ROS), and release of neutrophil extracellular traps (NETs) (11, 13, 14). So far, different parasite species were identified to induce either nicotinamide adenine dinucleotide phosphate (NADPH) oxidase (NOX)-dependent or

NOX-independent NETs formation (15, 16). During parasite-triggered NETs release, nuclear chromatin decondensation is facilitated by protein arginine deiminase 4 (PAD4)-mediated citrullination of histones (16–18). NETs-related enzymes, such as neutrophil elastase (NE) and myeloperoxidase (MPO), translocate to the nucleus and fuse with chromatin (19). Finally, PMN membrane disintegration is mediated either by enhanced ROS production (20) or by actions of lytic proteins, such as gasdermin-D, mediating membrane pore formation and subsequent NETs extrusion into the extracellular matrix (21). NETs release is a regulated molecular process which depends on energy metabolism (22, 23), activation of NOX and generation of ROS and Ca<sup>++</sup>-influx as second messengers among others (9). Overall, the NETotic process can occur in a NOX-dependent and a NOX-independent mode, being classified as suicidal NETosis, vital NETosis or vesicular NETosis, respectively (24). Suicidal NETosis includes the stimulation of PMN, translocation of NE and MPO into nucleus resulting in degradation of nuclear histones and PAD4-mediated chromatin decondensation after the disintegration of the nuclear membrane and final PMN death (7, 19, 20, 24). In contrast, vital NETosis is described as a process in which PMN not necessarily will die. Here, PMN release NETs from mitochondrial origin without losing cell vitality, being nowadays addressed as non-lytic NETs (16, 24–26).

Zoonotic relevant euglenozoan parasites, such as *Leishmania* spp. and *Trypanosoma cruzi*, were recently described to trigger NETs release in different hosts, such as humans, mice, opossums and dogs, evidencing NETs formation as an ancient and evolutionary well-conserved innate effector mechanism among mammalian species (4, 11, 13, 14, 16, 27–30). So far, data on the role of NETs against highly motile *T. b. brucei* trypomastigotes are entirely lacking.

Data on metabolic requirements of PMN during parasite-triggered NETs formation are limited (31). Nevertheless, it is known that extracellular adenosine 5'-triphosphate (ATP) availability and activation of P2 purinergic receptors play fundamental roles in PMN activation (31). Thus, P2-mediated purinergic signaling pathways are involved in the regulation of essential functions of PMN, such as chemotaxis, phagocytosis, oxidative burst, degranulation (31). Consistently, P2-mediated purinergic pathways seem crucial in *Neospora caninum*- and *Besnoitia besnoiti*-mediated NETosis (15, 23). Considering these data, we here aimed to evaluate the role of purinergic signaling in *T. b. brucei* triggered NETs formation.

In the current work, PMN activation was estimated by analysis of oxygen consumption rates (OCR), extracellular acidification rates (ECAR), and ROS production. Also, we observed by using scanning electron microscopy (SEM), confocal- and live cell three-dimensional (3D) holotomographic microscopy that exposure of bovine PMN with trypomastigotes resulted in the formation of different phenotypes of NETs *in vitro*. Quantification of *T. b. brucei*-triggered NETs release was performed by DNA and nuclear area expansion (NAE) ["DNA area and NETosis analysis" (DNA)] analysis; *T. b. brucei*-triggered NETs formation also revealed as purinergic-dependent, since PMN treatment with the inhibitor NF449 decreases the release of extracellular DNA.

# 2.1 *Trypanosoma brucei brucei* induces polymorphonuclear neutrophil activation and neutrophil extracellular traps release

Grob et al.

*T. b. brucei*-Induced NETs

## MATERIALS AND METHODS

### Ethics Statements

This study was conducted following the Justus Liebig University Giessen (JLU) Animal Care Committee Guidelines. Protocols were approved by Ethics Commission for Experimental Animal Studies of Federal State of Hesse (Regierungspräsidium Giessen; A9/2012; JLU-No.521\_AZ) and in accordance to European Animal Welfare Legislation: ART13TFEU and current applicable German Animal Protection Laws.

### Parasites

*Trypanosoma brucei brucei* trypomastigotes of the strain 427 (32) were grown on plastic T-25 cm<sup>2</sup> tissue culture flasks (Greiner) in SDM-79 cell culture medium (General Electric Health) supplemented with 10% fetal calf serum (FCS; Greiner) for parasite proliferation. The medium was changed every 4 days, as described by Cross and Manning (33).

### Isolation of Bovine PMN

Healthy adult dairy cows ( $n = 9$ ) served as blood donors. Blood was obtained by puncture of the jugular vein and 30 ml was collected in 12 ml heparinized sterile plastic tubes (Kabe Labortechnik). Then, 20 ml of heparinized blood was diluted in 20 ml sterile phosphate-buffered saline (PBS) with 0.02% ethylenediaminetetraacetic acid (EDTA) (Sigma-Aldrich), layered on top of 12 ml Bicolll<sup>®</sup> separating solution (density = 1.077 g/l; Biochrom AG) and centrifuged (800 × g, 45 min). After the removal of plasma and peripheral blood mononuclear cells (PBMC), cells were suspended in sterile 25 ml bi-distilled water and gently mixed during 40 s to lyse erythrocytes. Osmolarity was rapidly restored by adding 4 ml of 10x Hanks balanced salt solution (HBSS; Biochrom AG). For complete erythrocyte lysis, this step was repeated twice and bovine PMN were later suspended in sterile RPMI 1640 cell culture medium (Sigma-Aldrich). PMN were counted in a Neubauer haemocytometer. Finally, freshly isolated bovine PMN were allowed to rest at 37°C and 5% carbon dioxide (CO<sub>2</sub>) atmosphere for 30 min before experimental use.

### Quantification of Oxygen Consumption Rates and Extracellular Acidification Rates in *T. b. brucei*-Exposed Polymorphonuclear Neutrophils

Activation of bovine PMN was monitored using Seahorse XF<sup>®</sup> analyzer (Agilent). Briefly,  $1 \times 10^6$  PMN from three donors were pelleted at  $500 \times g$  for 10 min at room temperature (RT). After removal of the supernatant, cells were re-suspended in 0.5 ml of XF<sup>®</sup> assay medium (Agilent) supplemented with 2 mM of L-glutamine, 1 mM pyruvate, and 10 mM glucose.  $1 \times 10^5$  cells, corresponding to 50  $\mu$ l of the cell solution, were gently placed in each well of an eight-well XF<sup>®</sup> analyzer plate (Agilent) pre-coated for 30 min with 0.001% poly-L-lysine (Sigma-Aldrich). Then, 50  $\mu$ l of XF<sup>®</sup> assay medium (Agilent) were added to blank wells (= no cell-controls). Finally, 130  $\mu$ l of XF assay medium (Agilent) was added to all wells (180  $\mu$ l total volume) and cells were incubated at 37°C without

CO<sub>2</sub> supplementation for 45 min before Seahorse XF<sup>®</sup> analyzer measurement. When rotenone/antimycin A was used to inhibit mitochondrial complexes I and III, a 5  $\mu$ M solution was added to the respective port and injected previously to the addition of *T. b. brucei* trypomastigotes (final concentration 0.5  $\mu$ M). On the other hand, *T. b. brucei* trypomastigotes were suspended in XF assay medium (Agilent, 300,000 parasites/20  $\mu$ l) and placed in one of the four injection ports of the instrument. For PMN controls, only 20  $\mu$ l of XF<sup>®</sup> assay medium (Agilent) was dispensed. The metabolic assay included basal measurement of three readings followed by injection of vital trypomastigotes or medium and 30 readings over time. The total assay duration was 240 min. Background subtraction, determination of OCR, ECAR, and the area under the curve (AUC) of obtained registries were performed by using Wave<sup>®</sup> software (Desktop Version, Agilent).

### Estimation of Extracellular and Total Reactive Oxygen Species Production

Estimation of total ROS production was achieved as described for bovine PMN by (34). Briefly,  $2 \times 10^5$  PMN were stimulated with  $3 \times 10^5$  *T. b. brucei* trypomastigotes in the presence of 500  $\mu$ M of luminol for total ROS production and 100  $\mu$ M of isoluminol in the presence of 4 U/ml horseradish peroxidase (HRP) to evaluate extracellular superoxide production. After stimulation, luminescence was monitored every 30 min for 120 min using a luminometer (Promega Glomax). Data are presented as relative chemiluminescence units (RLU).

### Scanning Electron Microscopy (SEM) Analysis

Bovine PMN ( $n = 3$ ) were co-cultured with vital *T. b. brucei* trypomastigotes (ratio 1:3) for 120 min on coverslips (10 mm of diameter; Thermo Fisher Scientific) pre-coated with 0.01% poly-L-lysine (Sigma-Aldrich) at 37°C and 5% CO<sub>2</sub>. After incubation, cells were fixed in 2.5% glutaraldehyde (Merck), post-fixed in 1% osmium tetroxide (Merck), washed in distilled water, dehydrated, critical point dried by CO<sub>2</sub>-treatment and sputtered with gold particles. Finally, all samples were visualized via a Philips XL30<sup>®</sup> scanning electron microscope at the Institute of Anatomy and Cell Biology, JLU Giessen, Germany.

### *T. b. brucei*-Triggered NETs Visualized by Immunofluorescence Analysis

Bovine PMN ( $n = 3$ ) were co-cultured with *T. b. brucei* trypomastigotes (ratio 1:3) for 120 min (37°C and 5% CO<sub>2</sub> atmosphere) on coverslips (15 mm diameter, Thermo Fisher Scientific) pre-treated with 0.01% poly-L-lysine (Sigma-Aldrich). After corresponding incubation time, the cells were fixed in 4% paraformaldehyde (Merck) and stored at 4°C until further use. To visualize NETs structures, Sytox Orange<sup>®</sup> (1:1,000, Life Technologies) was used to stain extracellular DNA, anti-histones (H1, H2A/H2B, H3, and H4, 1:500, Merck #MAB3422) and anti-neutrophil elastase (NE) (1:500, Abcam #ab68672) antibodies were used to detect NETs-specific components/proteins. Therefore, fixed samples were washed three times with sterile PBS and blocked (60 min, RT) in 2%

## 2.1 *Trypanosoma brucei brucei* induces polymorphonuclear neutrophil activation and neutrophil extracellular traps release

Grob et al.

*T. b. brucei*-Induced NETs

bovine serum albumin (BSA; Sigma-Aldrich) containing 0.3% Triton X-100 (Thermo Fischer Scientific) and incubated in primary antibody solutions for 120 min at RT. After incubation, three washing steps were performed with sterile PBS and incubated in secondary antibody solutions (Alexa 488 goat anti-mouse IgG #A110011, Alexa 405 goat anti-rabbit IgG #A31556, 1:500, Invitrogen) for 120 min at RT in complete darkness. Finally, the samples were washed three times with sterile PBS and mounted upside-down with Fluoromount G<sup>®</sup> (Thermo Fischer Scientific). Visualization of NETs formation was achieved using an inverted IX81<sup>®</sup> epifluorescence microscope equipped with an XM 10<sup>®</sup> digital camera (both Olympus) or by applying confocal microscopy (Zeiss LSM 710<sup>®</sup>).

### Analysis of Neutrophil Extracellular Traps Phenotypes

For quantification of different NETs phenotypes [i.e., spread NETs (*spr*NETs), diffuse NETs (*diff*NETs), and aggregated NETs (*agg*NETs)] we followed the description by (35, 36). Briefly, bovine PMN ( $n = 3$ ) were seeded ( $2 \times 10^5$ /sample, in duplicates) on 0.01% poly-L-lysine (Sigma-Aldrich) pre-coated coverslips (Thermo Fischer Scientific) and exposed to *T. b. brucei* trypomastigotes ( $6 \times 10^5$ , 1:3 PMN: parasite ratio) for 120 min (37°C, 5% CO<sub>2</sub>). Afterwards, samples were fixed in 2% paraformaldehyde (Merck) and stored at 4°C until further analysis. The phenotypes *spr*NETs, *diff*NETs, and *agg*NETs were visualized by staining extracellular DNA with Sytox Orange<sup>®</sup> (5 μM, Life Technologies), anti-NE (1:500, Abcam #ab68672), and anti-histones (H1, H2A/H2B, H3, and H4; 1:500, Merck #MAB3422) antibodies as previously described (37, 38). For visual quantification, five random power vision pictures were taken from each experimental condition using an inverted IX81<sup>®</sup> fluorescence microscope equipped with an XM 10<sup>®</sup> digital camera (both Olympus) and analyzed microscopically based on typical morphological characteristics according to Muñoz-Caro et al. (36).

### *T. b. brucei* Motility Assays

Motility evaluation of alive *T. b. brucei* trypomastigotes cocultured with bovine PMN ( $n = 3$ ; ratio 1:3) for 2 h at 37°C and 5% CO<sub>2</sub> controlled-atmosphere on a 12-well transparent bottom microplate (Falcon). After the incubation time, motility was scored by direct observation using an inverted IX81<sup>®</sup> phase-contrast microscope (Olympus<sup>®</sup>). After counting, the results are shown as a percentage of motile trypomastigotes.

### *T. b. brucei* Viability Measurement by Trypan Blue Staining

Viability evaluation of alive *T. b. brucei* trypomastigotes cocultured with bovine PMN ( $n = 3$ ; ratio 1:3) for 2 h at 37°C and 5% CO<sub>2</sub> controlled-atmosphere was performed on a 12-well transparent bottom microplate (Falcon). After incubation, Trypan blue staining (Sigma Aldrich) was added to the medium in a 1:10 dilution. After 2 min, viability was evaluated by visual observation using an inverted IX81<sup>®</sup> microscope (Olympus). The results are expressed as a percentage of alive trypomastigotes.

### Nuclear Area Expansion-Based Quantification of Neutrophil Extracellular Traps-Formation Using DNA Area and NETosis Analysis Software

For NAE-based quantification of *T. b. brucei*-induced NETs formation, DANA I/II software was used following developers recommendations (39). In brief, bovine PMN ( $n = 3$ ) were left in plain medium (RPMI 1640, Sigma-Aldrich) for 30 min and then exposed to *T. b. brucei* trypomastigotes for 120 min at a 1:3 ratio. PMN were then fixed in 2% paraformaldehyde (Merck) and stained with 5 μM Sytox Orange<sup>®</sup> (Life Technologies) for 30 min at RT. Five images were randomly taken for each condition using an inverted microscope (Olympus IX 81<sup>®</sup>) and NAE was analyzed using DANA I- and II-software. Cells presenting a decondensed nucleus and exceeding the threshold of 90 μm<sup>2</sup> of the nuclear area were considered as PMN undergoing NETs formation.

### Live Cell Imaging of *T. b. brucei*-Induced Neutrophil Extracellular Traps Release Using 3D-Holotomographic Microscopy

In total,  $1 \times 10^6$  isolated bovine PMN were pelleted (300 × g, 10 min, RT). The supernatant was carefully discarded and cells were suspended in 2 ml imaging medium containing 0.1% BSA (Sigma-Aldrich), 2 μM 1,5-bis[[2-(di-methylamino)ethylamino]-4,8-dihydroxyanthracene-9,10-dione (DRAQ5) (Thermo Scientific), and 0.5 μM Sytox Green<sup>®</sup> (Life Technologies). One ml of this cell solution was seeded in an Ibidi<sup>®</sup> plastic cell plate (35 mm<sup>2</sup> diameter with low profile) and placed in a top stage incubation chamber (Ibidi) at 5% CO<sub>2</sub> and 37°C. Resting time of 30 min was used to let PMN settle down in the plastic cell plate. Then,  $1.5 \times 10^6$  motile *T. b. brucei* trypomastigotes were added to the center of the plastic cell plate. Image acquisition was set for refractive index (RI; 3D tomography), for 4,6-diamidino-2-phenylindole (DAPI) channel (blue) for DRAQ5 and fluorescein channel (green) for Sytox Green<sup>®</sup> (Life Technologies) detection, applying time-lapse settings (image acquisition every minute over 180 min) using a Nanolive Fluo-3D Cell Explorer<sup>®</sup> (Nanolive). At the end of the experiment, each channel was exported separately using Steve<sup>®</sup> software v.2.6 (Nanolive) and managed with Image J<sup>®</sup> software (Fiji version 1.7, NIH). In addition, digital staining was performed based on the values of refractive index (RI) of the obtained images.

### Pharmacological Inhibition of Purinergic Receptors and Mitochondrial Activity

Bovine PMN ( $n = 3$ ) were suspended in sterile HBSS buffer (Sigma-Aldrich) at a final concentration of  $1 \times 10^6$  cells/ml. Sytox Green<sup>®</sup> (5 μM; Life Technologies) was added and cells were seeded ( $1 \times 10^5$  cells in 50 μl/well) in a 96-well plate transparent bottom microplate (Greiner). The plate was warmed for 30 min at 37°C and thereafter inhibitors were added at a final concentration of 100 μM for NF449 (inhibitor of the purinergic receptors, Tocris, #7038), 1 mM for N-(Methoxysuccinyl)-Ala-Ala-Pro-Val-chloromethyl ketone (CMK; neutrophil elastase inhibitor;

## 2.1 *Trypanosoma brucei brucei* induces polymorphonuclear neutrophil activation and neutrophil extracellular traps release

Grob et al.

*T. b. brucei*-Induced NETs

Sigma-Aldrich, #M0398), rotenone/antimycin A (inhibitor of complexes I and III, 5  $\mu$ M, Agilent), and phenylhydrazine (FCCP, disruptor of mitochondrial membrane potential, 0.5  $\mu$ M, Agilent). Meanwhile, the parasites were pelleted and suspended in sterile HBSS at a concentration of  $3 \times 10^5$  specimen/50  $\mu$ l. The kinetic of NETs formation was followed by spectrofluorometric analysis at an excitation wavelength of 504 nm and an emission wavelength of 523 nm by using an automated multiplate monochrome reader (Variokan Flash<sup>®</sup>; Thermo Scientific) and registered every 2 min for a total of 120 min. Furthermore, for NF449 inhibition studies, bovine PMN, and trypomastigotes were seeded on 0.01% poly-L-lysine pre-coated coverslips (Greiner) as previously described. After 120 min of exposure, cells were fixed in 2% paraformaldehyde (Roth) and stained with Sytox Orange<sup>®</sup> (Life Technologies) for 30 min at RT. Five power vision field images were randomly taken for each condition using an inverted epifluorescence IX81<sup>®</sup> microscope (Olympus) equipped with a XM 10<sup>®</sup> digital camera (Olympus) for further analysis.

### Assessment of the Influence of Motility in *T. b. brucei*-Induced DNA Release

Bovine PMN ( $n = 3$ ) were suspended in sterile HBSS buffer (Sigma-Aldrich) at a final concentration of  $1 \times 10^6$  cells/ml. Sytox Green<sup>®</sup> (5  $\mu$ M; Life Technologies) was added and cells were seeded ( $1 \times 10^5$  cells in 50  $\mu$ l/well) in a 96-well plate transparent bottom microplate (Greiner). The plate was warmed for 30 min at 37°C. Meanwhile, the parasites were heat-inactivated by treatment of 1 h at 50°C, using a Thermomixer 5436 (Eppendorf). After this, alive and heat-inactivated trypomastigotes were pelleted and suspended in sterile HBSS at a concentration of  $3 \times 10^5$  parasites/50  $\mu$ l. The kinetic of NETs formation was followed as described previously.

### Statistical Analysis

For all experiments in the current study, except for NAE estimation and inhibitor experiments, statistical significance was defined by a  $p$ -value of  $< 0.05$  by applying non-parametric analyses: Mann-Whitney test when two experimental conditions were compared and Kruskal-Wallis test followed by Dunn's *post-hoc* test for multiple comparisons. Shapiro-Wilk normality test was performed on the data of inhibitors. Differences were estimated by ANOVA. All graphs (mean  $\pm$  SD), AUC calculations and statistical analyses were performed using Graph Pad<sup>®</sup> Prism software (v.7.03).

## RESULTS

### *T. b. brucei* Trypomastigotes Induce Activation of Bovine Polymorphonuclear Neutrophils

To evaluate the activation of PMN exposed to *T. b. brucei* trypomastigotes, we performed a series of experiments using Seahorse instrumentation (Agilent). As illustrated in Figure 1, after obtaining basal OCR and proton efflux rates (PER) of plain PMN, live parasites induced a fast and sustained increase in OCR (Figure 1A) and PER (Figure 1C). As shown in Figures 1B,D,

analysis of the area under the curve (AUC) revealed a significant increase ( $p < 0.05$ ) in OCR upon parasite exposure. Also, significantly enhanced PER findings ( $p < 0.01$ ) were detected in parasite-exposed PMN when compared to un-stimulated PMN controls. Observed OCR increase was not prevented by rotenone treatment (Figures 1E,F); indicating a contribution of both, NOX and mitochondrial activity, in the increase of OCR in the activation of PMN induced by *T. b. brucei* trypomastigotes. To evaluate if the OCR was linked to ROS production, total ROS, and extracellular ROS production were evaluated in PMN exposed to *T. b. brucei*. Current data shows that *T. b. brucei* induces total and extracellular ROS (Figures 1G,J); however, this increase does not achieve statistical significance when neither AUC (Figures 1H,K) nor the final luminescence value at 120 min (Figures 1I,L) of the obtained registries are analyzed most probably due to inter-individual variation.

### *T. b. brucei* Trypomastigotes Induce Neutrophil Extracellular Traps Formation in Bovine Polymorphonuclear Neutrophils

SEM analysis unveiled that exposure of bovine PMN to *T. b. brucei* trypomastigotes (asterisks Figures 2A–D) for 120 min induced the formation of both, thick and fine chromatin strands of fibers released from dead PMN (arrows Figures 2A–D). This observation was confirmed as NETs structures since using confocal microscopy, the co-localization of extracellular DNA with histones and NE allowed to confirm the presence of these typical NETs proteins associated with the chromatin released from PMN (Figures 2E–H).

### *T. b. brucei* Trypomastigotes Trigger Different Phenotypes of Neutrophil Extracellular Traps

Different NETs phenotypes were detected in trypomastigote-exposed PMN. These NETs phenotypes have previously been described for other parasite species capable to induce NETs [(35, 36, 40); Figure 3 and Supplementary Figures 2, 3]. Correspondingly, *diff*NETs were identified as a complex of extracellular decondensed chromatin with a size of 15–20  $\mu$ m diameter, *spr*NETs consisted of smooth and elongated web-like structures being composed exclusively of thin fibers with a diameter of 15–17  $\mu$ m and *agg*NETs were characterized by a “ball of yarn” shape and sizes of more than 20  $\mu$ m. Interestingly, interactions of *T. b. brucei* trypomastigotes with PMN mainly triggered *agg*NETs after 2 h of co-cultivation. Besides, also *diff*NETs and *spr*NETs were detected but at a minor proportion (Figure 3M).

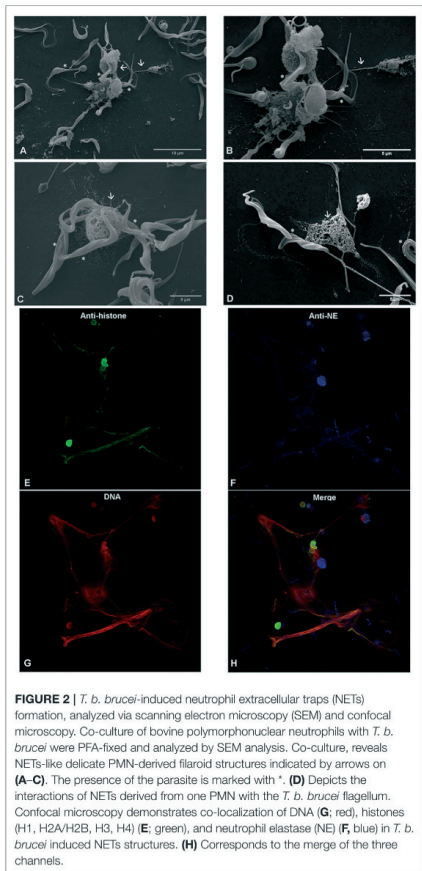
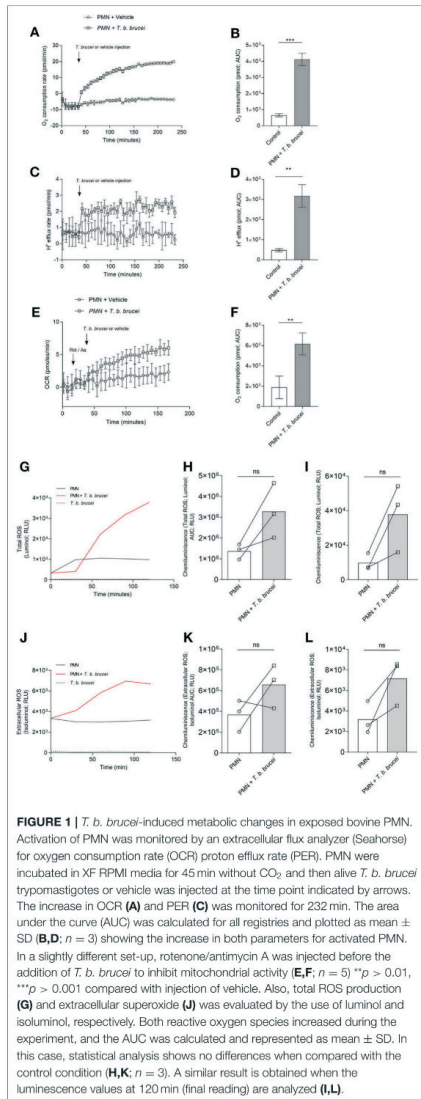
### Bovine Neutrophil Extracellular Traps Slightly Decrease the Motility of *T. b. brucei* Trypomastigotes Without Affecting the Viability of the Parasite

To evaluate and quantify the effect of bovine PMN against the parasite, we evaluated the motility of *T. b. brucei* after 2 h of co-cultivation with PMN. Figure 3N depicts the motility of the parasite after co-cultivation with bovine PMN demonstrating that 50.17% of the parasites are motile against 66.24% of the

## 2.1 *Trypanosoma brucei brucei* induces polymorphonuclear neutrophil activation and neutrophil extracellular traps release

Grob et al.

*T. b. brucei*-Induced NETs



trypomastigotes in the PMN-free condition. Also, in the same set-up, the viability of the trypomastigotes was evaluated. As is depicted in Figure 3O, activated bovine PMN are not able to kill *T. b. brucei* trypomastigotes, indicating that NETs can entrap in a non-lethal way a small number of parasites.

### 3D-Holotomographic Live-Cell Imaging of *T. b. brucei*-Mediated Neutrophil Extracellular Traps

To be as close as possible to the *in vivo* situation, we performed 3D-holotomographic live-cell imaging (3D Cell Explorer<sup>®</sup>,

## 2.1 *Trypanosoma brucei brucei* induces polymorphonuclear neutrophil activation and neutrophil extracellular traps release

Grob et al.

*T. b. brucei*-Induced NETs

Nanolive) to visualize the interactions between bovine PMN and *T. b. brucei* trypomastigotes. The morphology of a non-activated bovine PMN is illustrated in **Figure 4A**, complemented with 3D rendering and digital staining based on refractive index (RI) (**Figures 4A,B**), thereby allowing for the differentiation of some classical structures of these cells, such as a segmented nucleus (purple), granular cytosol, and plasmatic membrane (green). Additionally, **Figure 4B** illustrates an interaction of PMN and parasites.

To complement the results obtained by immunofluorescence microscopy in fixed cells, a live cell microscopy experiment was here performed, allowing a closer look to interactions and morphological changes. **Figure 4C** shows single images of the time-lapse experiment. The complete video of the live-cell imaging experiment can be found on the **Supplementary Video 1**. As depicted in **Figure 4C**, an increase on Sytox Green<sup>®</sup> signal (= extracellular DNA release; green) was observed after 120 min of co-culture. This signal was correlated with a change in nuclear shape as illustrated by DRAQ5 staining (blue). This finding confirms that *T. b. brucei* trypomastigotes indeed trigger DNA release. 3D-digital staining allowed for illustration of distinct morphological changes as protrusion and bubbling of bovine PMN membrane (**Figure 4C**; lower panel). Also, bovine PMN during confrontation with highly motile *T. b. brucei* shows nuclear expansion during the time and further lysis. Thus, especially cytoplasmic expansion and changes in nuclear shape were observed after 154 min whilst within the first 24 min of exposure, hardly any morphological change could be noted. The complete video registry of the 3D rendering of a unique cell is shown in **Supplementary Video 2**. Finally, after 180 min, we were able to detect the considerable expansion of PMN nuclei, thereby obviously reflecting the initiation of the NETotic process.

### Quantification of Neutrophil Extracellular Traps Formation via Nuclear Area Expansion-Based DNA Area and NETosis Analysis

Nuclear area expansion (NAE) and chromatin decondensation is an early event of the NETs formation as described by (19). For this reason, we analyzed *T. b. brucei*-triggered NAE in PMN and estimated the percentage of cells undergoing NETs release using the software tool "DNA area and NETosis analysis" (DANA) as reported before (39) to guarantee an observer-independent estimation. To evaluate if exposure to *T. b. brucei* trypomastigotes indeed affected the DNA area of PMN nuclei after exposure, a total of 201 cells were analyzed for each experimental condition and the data were illustrated as frequency histograms (**Figure 5C**). However, we were unable to detect significant changes in mean values of the nuclear area within interactions between motile *T. b. brucei* and bovine PMN (**Figure 5C**) most probably resulting from high inter-donor variations, which are often reported for non-syngenic beings. On the other hand, when the percentage of cells forming NETs was calculated by DANA, this approach documented induction of NETs formation by the parasites. Thus,  $28.3\% \pm 3.57$  of PMN released NETs

upon trypomastigote exposure, compared to  $6.25\% \pm 2.62$  in non-exposed control cells (**Figure 5D**).

### *T. b. brucei*-Induced Neutrophil Extracellular Traps Formation Seems to Be Dependent on Purinergic Signaling

We also investigated the role of the purinergic signaling pathway to study whether *T. b. brucei*-triggered NETs release is an energy and ATP-dependent process. Therefore, bovine PMN were pre-treated with different inhibitors: 100  $\mu\text{M}$  of NF449 as an inhibitor of purinergic receptors and CMK 1 mM as neutrophil elastase inhibitor. As an interesting finding, the pre-treatment of PMN with NF449 almost completely abolished parasite-triggered NETs formation when compared to non-treated controls (**Figures 6A–D**). However, blocking NE activity with CMK did not affect parasite-triggered NETs formation. These data indicate that *T. b. brucei*-induced NETs formation seems to be dependent on purinergic-mediated ATP binding but is seemingly independent of NE activity. Also, other inhibitors of key signaling pathways in NETs formation were tested. Interestingly, NADPHOX inhibitor (DPI); glycolysis inhibitor (2-deoxy-D-glucose) and PAD-4 inhibitor (Cl-amide) have no effect over NETs formation –measured as DNA extrusion- on bovine PMN confronted to *T. b. brucei* trypomastigotes (**Supplementary Figure 4**). It is important to mention that, as a limitation of our study the lack of positive controls in our inhibition experiments makes impossible to know if the inhibitors worked properly in our experimental settings.

### Evaluation of Mitochondrial Activity Inhibitors on *T. b. brucei*-Mediated NETosis

To evaluate if the mitochondrial activity is involved on the NETotic process, experiments were performed using the inhibitors rotenone mixed with rotenone/antimycin A (inhibitor of complex I and III, Agilent) and phenylhydrazine (FCCP, disruptor of mitochondrial membrane potential, Agilent). The treatment with rotenone/antimycin A resulted in partial, but no significant inhibition of the parasite triggered-NETs formation (**Figure 6E**).

### Heat Inactivation Does Not Hamper *T. b. brucei*-Triggered Neutrophil Extracellular Traps Release

To determine the influence on NETs formation of alive *T. b. brucei* trypomastigotes against immotile parasites we used heat-inactivated trypomastigotes. After 2 h of co-cultivation, we confirmed that alive trypomastigotes induced an increase in NETs release and the release of NETs by heat-inactivated parasites showed a non-significant decrease in comparison with live non-treated parasites (**Figure 6F**).

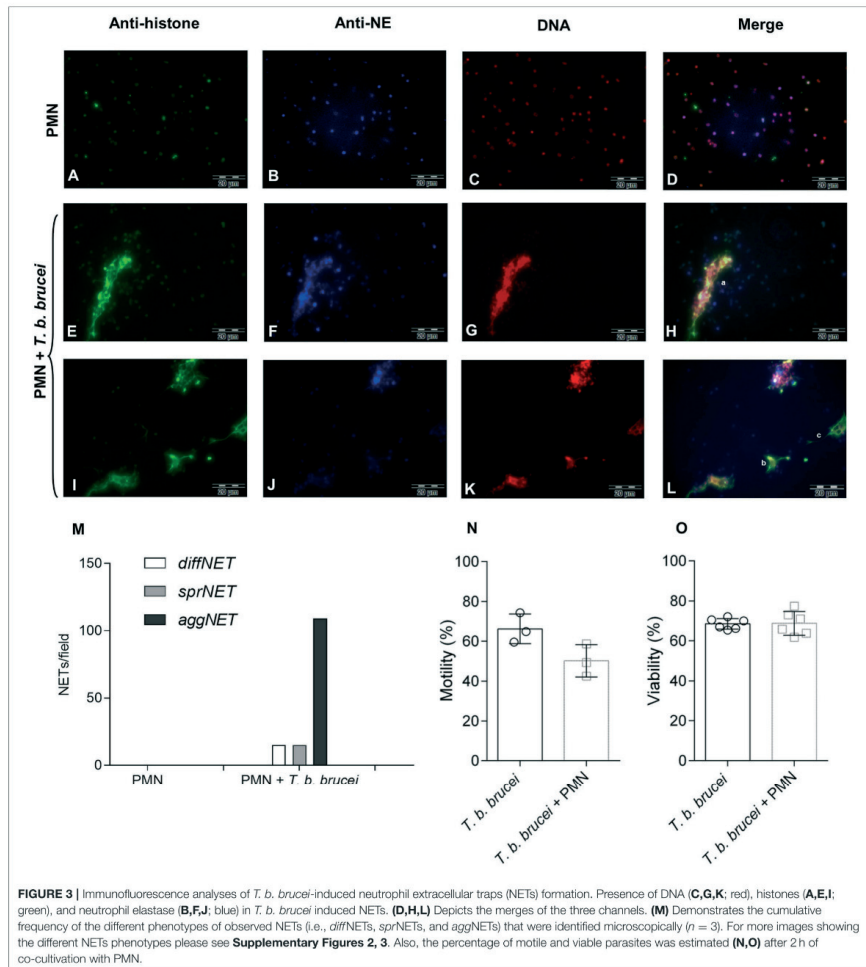
## DISCUSSION

This study shows for the first time that bovine PMN cast NETs in response to motile *T. b. brucei* trypomastigotes *in vitro*. After the first description of NETs formation as pivotal innate immune

## 2.1 *Trypanosoma brucei brucei* induces polymorphonuclear neutrophil activation and neutrophil extracellular traps release

Grob et al.

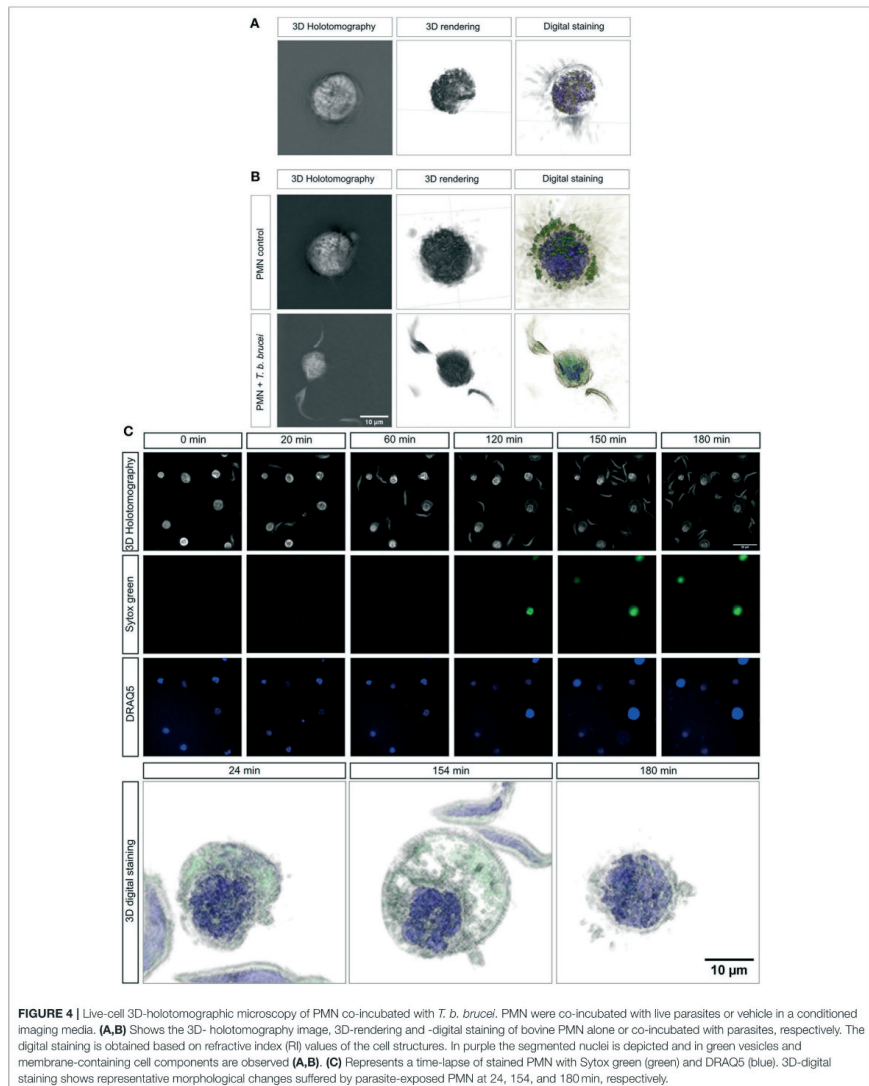
*T. b. brucei*-Induced NETs



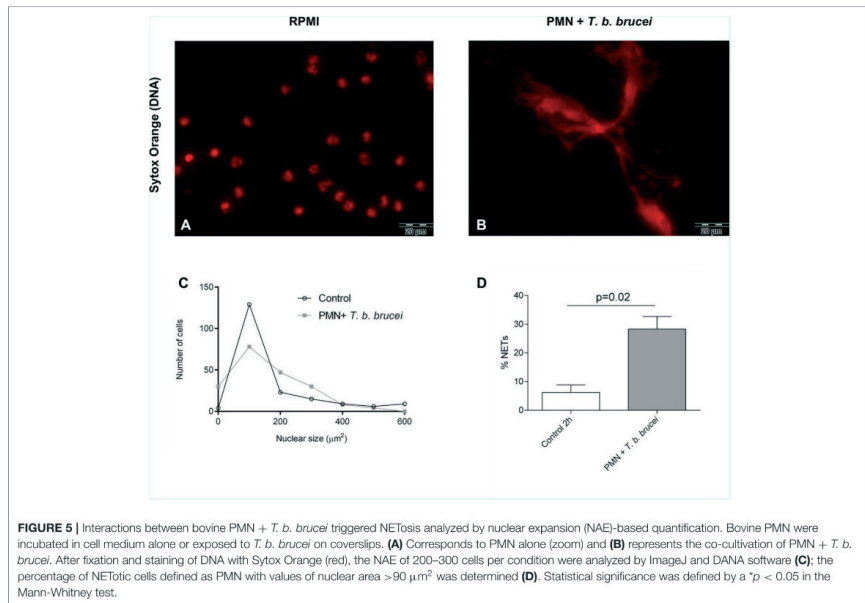
effector mechanism against invasive bacteria in 2004 (7), several reports have confirmed the relevance of this ancient defense mechanism not only against bacteria but also against several protozoan and metazoan parasites (16, 30, 37). However, little is known on NETs triggered by the genus *Trypanosoma*. So

far, only two studies report on *T. cruzi*-induced NETosis in human- (28), opossum- and canine-derived PMN (13). In the case of human PMN, it has been described that *T. cruzi*-mediated NETosis is triggered via TLRs, specifically by TLR 2 and TLR 4 (28).

## 2.1 *Trypanosoma brucei brucei* induces polymorphonuclear neutrophil activation and neutrophil extracellular traps release



## 2.1 *Trypanosoma brucei brucei* induces polymorphonuclear neutrophil activation and neutrophil extracellular traps release



In contrast to *T. cruzi*, *T. b. brucei* includes obligate extracellular stages (41) meaning that endogenous parasites are permanently exposed to leukocytes either present in blood/lymphatic stream or being attracted to *T. b. brucei*-infected tissues/organs *in vivo* (42, 43). Nonetheless, trypanosomes are well-known to effectively escape host cell immune responses. Consistently, *T. b. brucei* trypomastigotes are reported to constantly remodel their cell surface via viable surface antigens (VSA), explaining their ability to evade adverse immune reactions (42).

PMN display different effector mechanisms to combat parasites, such as phagocytosis, ROS production and NETosis (11, 16). Of note, ROS production seems essential for NETs extrusion (20, 21, 44). This process is linked to both, an increase in OCR and enhancement of proton efflux rates (PER) (45) which are necessary for proper NETs formation (22). Consistently, OCR and PER were found rapidly enhanced in bovine PMN after incubation with motile *T. b. brucei* trypomastigotes. These notorious increases were sustained for more than 240 min of stimulation, thereby suggesting considerable ROS production and induction of PMN-derived metabolic activities. We observed a fast increasing tendency in PMN confronted with *T. b. brucei* trypomastigotes in both, total ROS and extracellular superoxide. This tendency does not show statistical significance, mainly due

to the low number of animals studied and inter-donor variation (38, 46). The OCR consumption was also increased in the presence of rotenone/antimycin A mixture, as an indirect way to measure the contribution of NADPHOX and mitochondrial complexes in the observed increase. Our results show that the mitochondrial activity, critical for other PMN functions as chemotaxis, phagocytosis, and respiratory burst (47) has a partial involvement also in extracellular DNA release from bovine PMN.

To measure morphological changes during the early phase of the NETotic process, we performed DANA, as described before (39). DANA-based analysis of NAE in exposed PMN is accepted as an indicator of early NETs formation process as demonstrated previously (19, 48, 49). In this study, we used DANA to better characterize interactions of PMN and *T. b. brucei* trypomastigotes. This approach allowed NETs-forming PMN quantification. However, in contrast to other reports, we did not find significant differences among the nuclear area after undergoing cytoplasmic changes at 2 h of parasite confrontation. This discrepancy may be because PMN in our study have been stimulated with vital parasites and not by classical NETs inducer molecules, such as phorbol myristate acetate (PMA), zymosan, ionophores, cytokines/chemokines, or lipopolysaccharide (LPS) (15, 50, 51). By using the default threshold of DANA for the nuclear area of 90  $\mu\text{m}^2$ , we were able to detect a significant

## 2.1 *Trypanosoma brucei brucei* induces polymorphonuclear neutrophil activation and neutrophil extracellular traps release

Grob et al.

*T. b. brucei*-Induced NETs

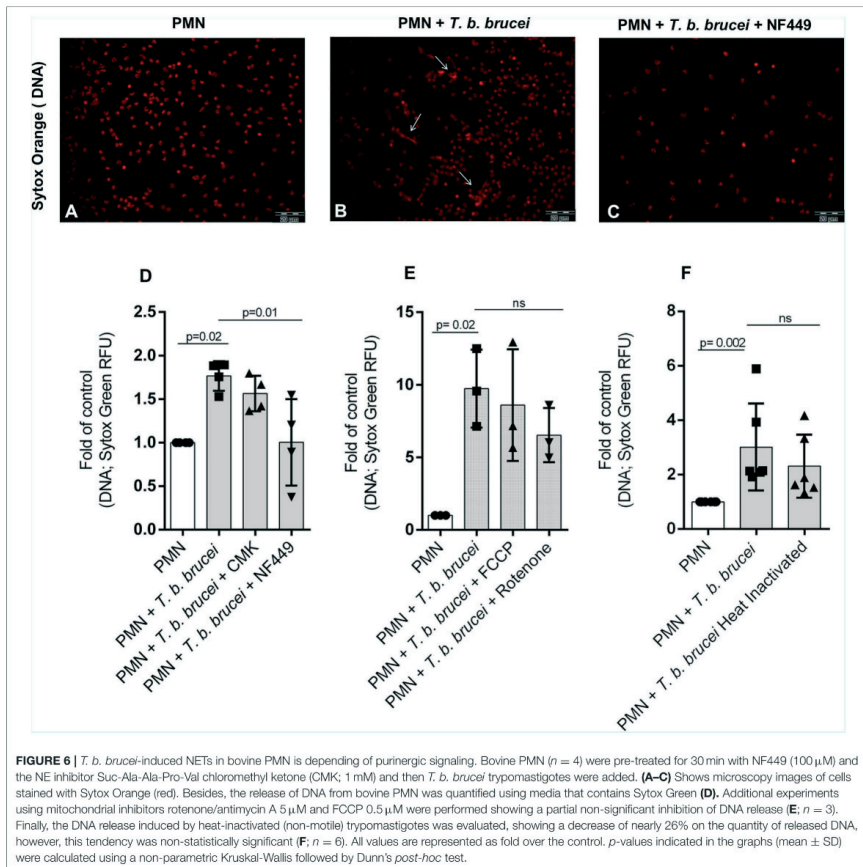


**FIGURE 6 |** *T. b. brucei*-induced NETs in bovine PMN is depending of purinergic signaling. Bovine PMN ( $n = 4$ ) were pre-treated for 30 min with NF449 (100  $\mu$ M) and the NE inhibitor Suc-Ala-Ala-Pro-Val chloromethyl ketone (CMK; 1 mM) and then *T. b. brucei* trypomastigotes were added. (A–C) Shows microscopy images of cells stained with Sytox Orange (red). Besides, the release of DNA from bovine PMN was quantified using media that contains Sytox Green (D). Additional experiments using mitochondrial inhibitors rotenone/antimycin A 5  $\mu$ M and FCCP 0.5  $\mu$ M were performed showing a partial non-significant inhibition of DNA release (E;  $n = 3$ ). Finally, the DNA release induced by heat-inactivated (non-motile) trypomastigotes was evaluated, showing a decrease of nearly 26% on the quantity of released DNA, however, this tendency was non-statistically significant (F;  $n = 6$ ). All values are represented as fold over the control.  $p$ -values indicated in the graphs (mean  $\pm$  SD) were calculated using a non-parametric Kruskal-Wallis followed by Dunn's *post-hoc* test.

increase in the percentage of NETs-forming cells triggered by *T. b. brucei* trypomastigotes (Figure 5) corresponding well to results obtained by direct visualization. Also, it must be noted that DANA was used successfully in the human and murine system, with the present report being the first attempt to quantify NETs formation by DANA in bovine PMN.

To confirm our observations in living cells, we additionally performed live-cell imaging using a 3D Cell Explorer<sup>®</sup> microscope (Nanolive) and an Ibidi<sup>®</sup> top-stage chamber (Ibidi) to keep the temperature and CO<sub>2</sub> atmosphere conditions stable. Overall this technical approach allowed for the generation

of 3D rendering and digital staining-based images of PMN in different activation stages and activities, i.e., resting PMN, activated ones, PMN in close contact to trypomastigotes-, and/or cells casting NETs. Classical morphological features of bovine PMN were obtained, such as the abundant presence of cytoplasmic granules, polymorphic nuclei, attachment activity, and laminopod formation (52–54). Overall, co-culture of bovine PMN and trypomastigotes induced an increase of nuclear size after 120 min post-incubation strongly suggesting NETotic process. Moreover, we were able to detect nuclear degeneration after 180 min post-parasite exposure by 3D-digital staining,

## 2.1 *Trypanosoma brucei brucei* induces polymorphonuclear neutrophil activation and neutrophil extracellular traps release

Grob et al.

*T. b. brucei*-Induced NETs

which may indicate a late NETotic process, as previously reported (19).

Interestingly, *T. b. brucei*-induced NETs formation resulted in different phenotypes of NETs, which is in accordance to other reports on parasite-induced NETosis (12, 35, 36). Thus, *T. b. brucei*-stimulated PMN predominantly cast *aggNETs* and *sprNETs*; *diffNETs* were also extruded but to a minor extent, corresponding well to previous findings on large-sized *D. immitis* larvae-induced NETs (36). Immunopathological implications of this observations are related to the fact that *aggNETs* are proposed to have anti-inflammatory effects via sequestration and detoxification of histones (55) and the proteolysis of cytokines and chemokines (56) whereas *sprNETs* and *diffNETs* are pro-inflammatory in the early phase of the immune response (57). In this context, loss of the continuity of the blood-brain barrier is necessary for the increased leukocyte counts in cerebrospinal fluid (CSF) and the presence of *T. b. brucei* in the CSF of affected animals (58). Considering this, NETs induce endothelial damage by the presence of histones (43, 59, 60) and provides a scaffold for the alternative complement pathway (61). Moreover, it was reported that *aggNETs* involve a higher number of PMN, suggesting a rather marked PMN attraction and activation after the first contact with these rather large and motile haemoflagellates. Interestingly, PMN can distinguish the sizes of pathogens and selectively release NETs in response to them (62). Taking PMN sensing capacities into account, we here hypothesize that not only size but also movements might influence in *T. b. brucei*-triggered NETs, based in observations of tiny and immotile bacteria or viruses. Interestingly, previous reports showed that movement in flagellated bacteria (63) and also on parasites (36) is important for NETs release. Even so, viability and motility experiments were performed, showing that in our experimental conditions triggered NETs did not promote the killing of this parasitological stage, helping us to hypothesize that NETs have a role on immobilization than the viability of the parasite (12, 36).

Purinergic receptors are involved in several activities of PMN, such as chemotaxis, phagocytosis, oxidative burst, apoptosis, and degranulation (31, 64). In line, it was recently reported that extracellular ATP regulates PMN chemotaxis via P2Y<sub>2</sub> receptors and that P2Y receptors are involved in PMN adhesion to the endothelium (31). Even so, studies have demonstrated that *T. cruzi* can induce calcium intake using the Pannexin-1 channel, which allows cells to release ATP to the environment. This could help to trigger the PMN activation, considering the chemotactic effect (65). In this study, we found that purinergic receptors indeed play a role in *T. b. brucei*-induced NETs formation, since the inhibition of this receptors by using NF449 decreased NETs formation to a considerable extent, which is in accordance to previous parasite-based reports (23, 66). However, since we used a concentration 10–100 times higher than some of these previous reports, we cannot discard an influence of G protein-coupled receptors (GPCRs). Further experiments will be performed to establish which purinergic receptors are involved in the activation of bovine PMN. On the other hand, treatments with rotenone/antimycin A and FCCP, both inhibitors of mitochondrial function, partially reduced the NETs formation,

suggesting a partial role of mitochondrial activity in *T. b. brucei* induced NETs release. Interestingly, a critical role for the mitochondrial function of bovine PMN in response to platelet-activating factor (PAF) was recently demonstrated (64). In addition, no inhibition was observed when the other inhibitors as CMK (elastase inhibitor), DPI (NADPHOX inhibitor), Cl-amide (PAD4 inhibitor) were used. Since we did not demonstrate the activity of our inhibitors by the use of positive controls, we cannot do conclusive statements on this regard. Moreover, the possibility of that PAD4 and elastase have redundant functions on NETs formation induced by *T. b. brucei* cannot be discarded.

NETs are mainly composed of decondensed chromatin alongside with citrullinated nuclear histones and enzymatic granular components, such as NE, MPO, lactoferrin, calprotectin, LL37, pentraxin, proteinase 3 (P3) and cathepsin G (CG) among others (19, 67). Current co-localization experiments on PMN-derived DNA being decorated with histones and NE on *T. b. brucei*-triggered extracellular structures proved that NETs are induced by trypomastigotes. PMN activation and extrusion of nuclear DNA was also documented by live cell 3D-holotomographic microscopy indicating that NETs indeed are formed as a response to large and motile pathogens when compared to virus, bacteria or fungi. Furthermore, our data showed that almost a third of PMN (28.3% ± 3.57) being confronted with *T. b. brucei* stages released NETs.

Overall, we here present novel data on PMN-derived NETs formation against highly motile and rather large extracellular *T. b. brucei* trypomastigotes (compared to bacteria, fungi or virus) as part of the host innate immune responses *in vitro*. Considering blood/lymph localization of *T. b. brucei* *in vivo*, parasite entanglement via NETs release could be of particular importance since immobilized trypomastigotes might become potential targets for other leukocytes being attracted to sites of parasite entrapment or intravascular NETs release. The pivotal role of purinergic-dependent signaling is also postulated but needs further investigation since other members of this receptor family might as well-participate in *T. b. brucei*-mediated NETs release. However, the complete role of NETs-derived effects on these euglenozoan parasites as well as possible NETs-derived damage on exposed endothelium (60) of lymph/blood vessels *in vivo* is not yet clear and will be addressed in the near future. The same holds for the possible role of *T. b. brucei*-triggered NETs release in the immunopathology of AAT such as intravascular coagulopathies or vascular permeabilization.

### DATA AVAILABILITY STATEMENT

The raw data supporting the conclusions of this article will be made available by the authors, without undue reservation.

### ETHICS STATEMENT

The animal study was reviewed and approved by Regierungspräsidium Giessen; 147 A9/2012; JLU-No.521\_AZ (Ethic Commission for 146 Experimental Animal Studies of Federal State of Hesse).

# 2.1 *Trypanosoma brucei brucei* induces polymorphonuclear neutrophil activation and neutrophil extracellular traps release

Grob et al.

*T. b. brucei*-Induced NETs

## AUTHOR CONTRIBUTIONS

AT, CH, and IC conceptualization and supervision. DG investigation (PMN isolation, *T. b. brucei* cell culture, immunofluorescence, DANA analyses, and inhibition experiments), formal analyses, data visualization, and wrote the original draft. IC carried out the investigation (SEM, Nanolive, Seahorse) and data visualization. ZV obtained confocal microscopy images, performed Nanolive video analysis, and data visualization. CP provided the *T. b. brucei* cell culture for this study. RB and PA conceptualization of inhibition experiments. IC, PA, RB, AT, and CH reviewed the manuscript. CH and AT funding acquisition. All authors contributed to the article and approved the submitted version.

## FUNDING

DG was funded by the Chilean Scholarship Program Doctorado Becas Chile Number /2019-72200437 from the National Agency for Research and Development. The publication fees were

partially funded by the Open Access Publication Fund from JLU Giessen.

## ACKNOWLEDGMENTS

We are deeply thankful to Prof. Dr. Albrecht Bindereif for providing us with the *T. b. brucei*, forming part of the LOEWE-Center DRUID (Novel Drug Targets against Poverty-Related and Neglected Tropical Infectious Diseases). The authors would like to acknowledge Anika Seipp, Institute of Anatomy and Cell Biology, JLU Giessen, Germany, for her technical support in SEM analyses. We further thank all staff members of JLU Giessen teaching and research station Oberer Hardthof.

## SUPPLEMENTARY MATERIAL

The Supplementary Material for this article can be found online at: <https://www.frontiersin.org/articles/10.3389/fimmu.2020.559561/full#supplementary-material>

## REFERENCES

- Kennedy PG. Human African trypanosomiasis-neurological aspects. *J Neurol.* (2006) 253:411–6. doi: 10.1007/s00415-006-0093-3
- Connor RJ. The impact of nagana. *Onderstepoort J Vet Res.* (1994) 61:379–83.
- Kennedy PGE. Clinical features, diagnosis, and treatment of human African trypanosomiasis (sleeping sickness). *Lancet Neurol.* (2013) 12:186–94. doi: 10.1016/s1474-4422(12)70296-x
- Ponte-Sucré A. An overview of *Trypanosoma brucei* infections: an intense host-parasite interaction. *Front Microbiol.* (2016) 7:2126. doi: 10.3389/fmicb.2016.02126
- Stijlemans B, Leng L, Brys L, Sparkes A, Vansintjan L, Caljon G, et al. MIF contributes to *Trypanosoma brucei* associated immunopathogenicity development. *PLoS Pathog.* (2014) 10:e1004414. doi: 10.1371/journal.ppat.1004414
- World Health Organization and WHO Expert Committee on the Control and Surveillance of Human African Trypanosomiasis. *Control and Surveillance of Human African Trypanosomiasis: Report of a WHO Expert Committee.* Geneva: World Health Organization (2013). Available online at: <https://apps.who.int/iris/handle/10665/95732> (accessed August, 2020).
- Brinkmann V, Reichard U, Gossmann C, Fauler B, Uhlemann Y, Weiss DS, et al. Neutrophil extracellular traps kill bacteria. *Science.* (2004) 303:1532–5. doi: 10.1126/science.1092385
- Urban CF, Reichard U, Brinkmann V, Zychlinsky A. Neutrophil extracellular traps capture and kill *Candida albicans* yeast and hyphal forms. *Cell Microbiol.* (2006) 8:668–76. doi: 10.1111/j.1462-5822.2005.00659.x
- Papayannopoulos V. Neutrophil extracellular traps in immunity and disease. *Nat Rev Immunol.* (2018) 18:134–47. doi: 10.1038/nri.2017.105
- Caljon G, Mabile D, Stijlemans B, De Trez C, Mazzone M, Tacchini-Cottier E, et al. Neutrophils enhance early *Trypanosoma brucei* infection onset. *Sci Rep.* (2018) 8:11203. doi: 10.1038/s41598-018-29527-y
- Hermosilla C, Caro TM, Silva LM, Ruiz A, Taubert A. The intriguing host innate immune response: novel anti-parasitic defence by neutrophil extracellular traps. *Parasitology.* (2014) 141:1489–98. doi: 10.1017/S0031182014000316
- Muñoz-Caro T, Rubio RM, Silva LM, Magdowski G, Gartner U, McNeilly TN, et al. Leucocyte-derived extracellular trap formation significantly contributes to *Haemonchus contortus* larval entrapment. *Parasit Vect.* (2015) 8:607. doi: 10.1186/s13071-015-1219-1
- de Buhr N, Bonilla MC, Jimenez-Soto M, von Kockritz-Blickwede M, Dolz G. Extracellular trap formation in response to *Trypanosoma cruzi* infection

- in granulocytes isolated from dogs and common opossums, natural reservoir hosts. *Front Microbiol.* (2018) 9:966. doi: 10.3389/fmicb.2018.00966
- Pereira MA, Alexandre-Pires G, Camara M, Santos M, Martins C, Rodrigues A, et al. Canine neutrophils cooperate with macrophages in the early stages of *Leishmania infantum* in vitro infection. *Parasite Immunol.* (2019) 41:e12617. doi: 10.1111/pim.12617
- Villagra-Blanco R, Silva LMR, Gartner U, Wagner H, Failing K, Wehrend A, et al. Molecular analyses on *Neospora caninum*-triggered NETosis in the caprine system. *Dev Comp Immunol.* (2017) 72:119–27. doi: 10.1016/j.dci.2017.02.020
- Villagra-Blanco R, Silva LMR, Conejeros I, Taubert A, Hermosilla C. Pinniped- and cetacean-derived ETosis contributes to combating emerging apicomplexan parasites (*Toxoplasma gondii*, *Neospora caninum*) circulating in marine environments. *Biology.* (2019) 8:12. doi: 10.3390/biology8010012
- Li P, Li M, Lindberg MR, Kennett MJ, Xiong N, Wang Y. PAD4 is essential for antibacterial innate immunity mediated by neutrophil extracellular traps. *J Exp Med.* (2010) 207:1853–62. doi: 10.1084/jem.20100239
- Leshner M, Wang S, Lewis C, Zheng H, Chen XA, Santy L, et al. PAD4 mediated histone hypercitrullination induces heterochromatin decondensation and chromatin unfolding to form neutrophil extracellular trap-like structures. *Front Immunol.* (2012) 3:307. doi: 10.3389/fimmu.2012.00307
- Papayannopoulos V, Metzler KD, Hakkim A, Zychlinsky A. Neutrophil elastase and myeloperoxidase regulate the formation of neutrophil extracellular traps. *J Cell Biol.* (2010) 191:677–91. doi: 10.1083/jcb.201006052
- Fuchs TA, Abed U, Gossmann C, Hurwitz R, Schulze I, Wahn V, et al. Novel cell death program leads to neutrophil extracellular traps. *J Cell Biol.* (2007) 176:231–41. doi: 10.1083/jcb.200606027
- Ravindran M, Khan MA, Palaniyan N. Neutrophil extracellular trap formation: physiology, pathology, and pharmacology. *Biomolecules.* (2019) 9:365. doi: 10.3390/biom9080365
- Azevedo EP, Rocha NC, Guimaraes-Costa AB, de Souza-Vieira TS, Ganilho J, Saraiva EM, et al. A metabolic shift toward pentose phosphate pathway is necessary for amyloid fibril- and phorbol 12-myristate 13-acetate-induced neutrophil extracellular trap (NET) formation. *J Biol Chem.* (2015) 290:22174–83. doi: 10.1074/jbc.M115.640094
- Zhou E, Conejeros I, Gartner U, Mazurek S, Hermosilla C, Taubert A. Metabolic requirements of *Besnoitia besnoiti* tachyzoite-triggered NETosis. *Parasitol Res.* (2020) 119:4545–57. doi: 10.1007/s00436-019-06543-z
- Yipp BG, Kubes P. NETosis: how vital is it? *Blood.* (2013) 122:2784–94. doi: 10.1182/blood-2013-04-457671

## 2.1 *Trypanosoma brucei brucei* induces polymorphonuclear neutrophil activation and neutrophil extracellular traps release

Grob et al.

T. b. brucei-induced NETs

25. Yousefi S, Gold JA, Andina N, Lee JJ, Kelly AM, Kozlowski E, et al. Catapult-like release of mitochondrial DNA by eosinophils contributes to antibacterial defense. *Nat Med*. (2008) 14:949–53. doi: 10.1038/nm.1855
26. Pilszczek FH, Salina D, Poon KK, Fahey C, Yipp BG, Sibley CD, et al. A novel mechanism of rapid nuclear neutrophil extracellular trap formation in response to *Staphylococcus aureus*. *J Immunol*. (2010) 185:7413–25. doi: 10.4049/jimmunol.1000675
27. Thalhofer CJ, Chen Y, Sudan B, Love-Homan L, Wilson ME. Leukocytes infiltrate the skin and draining lymph nodes in response to the protozoan *Leishmania infantum chagasi*. *Infect Immun*. (2011) 79:108–17. doi: 10.1128/IAI.00338-10
28. Sousa-Rocha D, Thomaz-Tobias M, Diniz LF, Souza PS, Pinge-Filho P, Toledo KA. *Trypanosoma cruzi* and its soluble antigens induce NET release by stimulating toll-like receptors. *PLoS ONE*. (2015) 10:e0139569. doi: 10.1371/journal.pone.0139569
29. de Menezes JB, Saraiva EM, da Rocha-Azevedo B. The site of the bite: *Leishmania* interaction with macrophages, neutrophils and the extracellular matrix in the dermis. *Parasit Vectors*. (2016) 9:264. doi: 10.1186/s13071-016-1540-3
30. Silva LM, Munoz-Caro T, Burgos RA, Hidalgo MA, Taubert A, Hermosilla C. Far beyond phagocytosis: phagocyte-derived extracellular traps act efficiently against protozoan parasites *in vitro* and *in vivo*. *Mediators Inflamm*. (2016) 2016:5898074. doi: 10.1155/2016/5898074
31. Wang X, Chen D. Purinergic regulation of neutrophil function. *Front Immunol*. (2018) 9:399. doi: 10.3389/fimmu.2018.00399
32. Palfi Z, Jae N, Preusser C, Kaminska KH, Bujnicki JM, Lee JH, et al. SMN-assisted assembly of snRNP-specific Sm cores in trypanosomes. *Genes Dev*. (2009) 23:1650–64. doi: 10.1101/gad.526109
33. Cross GA, Manning JC. Cultivation of *Trypanosoma brucei* spp. in semi-defined and defined media. *Parasitology*. (1973) 67:315–31. doi: 10.1017/0003182000046540
34. Rinaldi M, Moroni P, Paape MJ, Bannerman DD. Evaluation of Assays for the measurement of bovine neutrophil reactive oxygen species. *Vet Immunol Immunopathol*. (2007) 115:107–25. doi: 10.1016/j.vetimm.2006.09.009
35. Lange MK, Penagos-Tabares F, Munoz-Caro T, Gartner U, Mejer H, Schaper R, et al. Gastroph-derived haemocyte extracellular traps entrap metachryloid larval stages of *Angiostrongylus vasorum*, *Aelurostrongylus abstrusus* and *Troglostrongylus brevior*. *Parasit Vectors*. (2017) 10:50. doi: 10.1186/s13071-016-1961-z
36. Muñoz-Caro T, Conejeros I, Zhou E, Pikhovych A, Gartner U, Hermosilla C, et al. *Dirofilaria immitis* microfilariae and third-stage larvae induce canine NETosis resulting in different types of neutrophil extracellular traps. *Front Immunol*. (2018) 9:968. doi: 10.3389/fimmu.2018.00968
37. Muñoz-Caro T, Machado Ribeiro da Silva L, Rentería-Solis Z, Taubert A, Hermosilla C. Neutrophil extracellular traps in the intestinal mucosa of *Eimeria*-infected animals. *Asian Pacific J Trop Biomed*. (2016) 6:301–7. doi: 10.1016/j.apjtb.2016.01.001
38. Zhou E, Conejeros I, Velasquez ZD, Muñoz-Caro T, Gartner U, Hermosilla C, et al. Simultaneous and positively correlated NET1 formation and autophagy in *Besnoitia besnoiti* tachyzoite-exposed bovine polymorphonuclear neutrophils. *Front Immunol*. (2010) 10:1131. doi: 10.3389/fimmu.2010.01131
39. Rebernick R, Fahmy I, Glover C, Bawadekar M, Shim D, Holmes CL, et al. DNA Area and NETosis Analysis (DNA): a high-throughput method to quantify neutrophil extracellular traps in fluorescent microscope images. *Biol Proced Online*. (2018) 20:7. doi: 10.1186/s12575-018-0072-y
40. Schauer C, Janko C, Muñoz LE, Zhao Y, Kienhofer D, Frey B, et al. Aggregated neutrophil extracellular traps limit inflammation by degrading cytokines and chemokines. *Nat Med*. (2014) 20:511–7. doi: 10.1038/nm.3547
41. Brun R, Blum J, Chappuis F, Burri C. Human African trypanosomiasis. *Lancet*. (2010) 375:148–59. doi: 10.1016/S0140-6736(09)60829-1
42. Stijlemans B, Caljon G, Van Den Abbeele J, Van Ginderachter JA, Magez S, De Trez C. Immune evasion strategies of *Trypanosoma brucei* within the mammalian host: progression to pathogenicity. *Front Immunol*. (2016) 7:233. doi: 10.3389/fimmu.2016.00233
43. Silvester E, Ivens A, Matthews KR. A gene expression comparison of *Trypanosoma brucei* and *Trypanosoma congolense* in the bloodstream of the mammalian host reveals species-specific adaptations to density-dependent development. *PLoS Negl Trop Dis*. (2018) 12:e0006863. doi: 10.1371/journal.pntd.0006863
44. Poirier AC, Schmitt P, Rosa RD, Vanhove AS, Kieffer-Jaquinet S, Rubio TP, et al. Antimicrobial histones and DNA traps in invertebrate immunity: evidences in *Crassostrea gigas*. *J Biol Chem*. (2014) 289:24821–31. doi: 10.1074/jbc.M114.576546
45. Chacko BK, Kramer PA, Ravi S, Johnson MS, Hardy RW, Ballinger SW, et al. Methods for defining distinct bioenergetic profiles in platelets, lymphocytes, monocytes, and neutrophils, and the oxidative burst from human blood. *Lab Invest*. (2013) 93:690–700. doi: 10.1038/labinvest.2013.53
46. Hoffmann JH, Schaeckel K, Gaiser MR, Fink AH, Hadaschik EN. Interindividual variation of NETosis in healthy donors: quantification and application of a refined method for extracellular trap quantification. *Exp Dermatol*. (2016) 25:895–900. doi: 10.1111/exd.13125
47. Fossati G, Moulding DA, Spiller DG, Moots RJ, White MRH, Edwards SW. The mitochondrial network of human neutrophils: role in chemotaxis, phagocytosis, respiratory burst activation, and commitment to apoptosis. *J Immunol*. (2003) 170:1964–72. doi: 10.4049/jimmunol.170.4.1964
48. Giusti D, Bini E, Terryn C, Didier K, Le Jan S, Gatoullat G, et al. NET formation in bullous pemphigoid patients with relapse is modulated by IL-17 and IL-23 interplay. *Front Immunol*. (2019) 10:701. doi: 10.3389/fimmu.2019.00701
49. van Breda SV, Vokolova L, Neugebauer C, Rossi SW, Hahn S, Hasler P. Computational methodologies for the *in vitro* and *in situ* quantification of neutrophil extracellular traps. *Front Immunol*. (2019) 10:1562. doi: 10.3389/fimmu.2019.01562
50. Kirchner T, Moller S, Klinger M, Solbach W, Laskay T, Behnen M. The impact of various reactive oxygen species on the formation of neutrophil extracellular traps. *Mediators Inflamm*. (2012) 2012:849136. doi: 10.1155/2012/849136
51. Muñoz-Caro T, Hermosilla C, Silva LM, Cortes H, Taubert A. Neutrophil extracellular traps as innate immune reaction against the emerging apicomplexan parasite *Besnoitia besnoiti*. *PLoS ONE*. (2014) 9:e91415. doi: 10.1371/journal.pone.0091415
52. Paape MJ, Bannerman DD, Zhao X, Lee JW. The bovine neutrophil: structure and function in blood and milk. *Vet Res*. (2003) 34:597–627. doi: 10.1051/vetres:2003024
53. Behrendt JH, Hermosilla C, Hardt M, Failing K, Zahner H, Taubert A. PMN-mediated immune reactions against *Eimeria bovis*. *Vet Parasitol*. (2008) 151:97–109. doi: 10.1016/j.vetpar.2007.11.013
54. Bassel LL, Caswell JL. Bovine neutrophils in health and disease. *Cell Tissue Res*. (2018) 371:617–37. doi: 10.1007/s00441-018-2789-y
55. Knopf J, Leppkes M, Schett G, Herrmann M, Muñoz LE. Aggregated NETs sequester and detoxify extracellular histones. *Front Immunol*. (2019) 10:2176. doi: 10.3389/fimmu.2019.02176
56. Hahn J, Schauer C, Czeglery C, Kling I, Petru I, Schmid B, et al. Aggregated neutrophil extracellular traps resolve inflammation by proteolysis of cytokines and chemokines and protection from anti-proteases. *FASEB J*. (2019) 33:1401–14. doi: 10.1096/fj.201800152x
57. Mahajan A, Grünboom A, Petru I, Podolska MJ, Kling I, Maueröder C, et al. Frontline science: Aggregated neutrophil extracellular traps prevent inflammation on the neutrophil-rich ocular surface. *J Leukocyte Biol*. (2019) 105:1087–98. doi: 10.1002/HLB.110718-249RF
58. Masake RA, Nantulya VM, Akol GW, Musoke AJ. Cerebral trypanosomiasis in cattle with mixed *Trypanosoma congolense* and *T. brucei* brucei infections. *Acta Trop*. (1984) 41:237–46.
59. Safarizadeh M, Jueneemann C, Queisser MA, Lochnit G, Barreto G, Galuska SP, et al. Neutrophil extracellular traps directly induce epithelial and endothelial cell death: a predominant role of histones. *PLOS ONE*. (2012) 7:e32366. doi: 10.1371/journal.pone.0032366
60. Conejeros I, Velasquez ZD, Grob D, Zhou E, Salecker H, Hermosilla C, et al. Histone H2A and bovine neutrophil extracellular traps induce damage of *Besnoitia besnoiti*-infected host endothelial cells but fail to affect total parasite proliferation. *Biology*. (2019) 8:78. doi: 10.3390/biology8040078
61. Schreiber A, Rousselle A, Becker JU, von Mässenhausen A, Linkermann A, Kettritz R. Necroptosis controls NET generation and mediates complement activation, endothelial damage, and autoimmune vasculitis. *Proc Natl Acad Sci USA*. (2017) 114:E9618–25. doi: 10.1073/pnas.1708247114

## 2.1 *Trypanosoma brucei brucei* induces polymorphonuclear neutrophil activation and neutrophil extracellular traps release

Grob et al.

*T. b. brucei*-Induced NETs

62. Branzk N, Lubojemska A, Hardison SE, Wang Q, Gutierrez MG, Brown GD, et al. Neutrophils sense microbe size and selectively release neutrophil extracellular traps in response to large pathogens. *Nat Immunol.* (2014) 15:1017–25. doi: 10.1038/ni.2987
63. Floyd M, Winn M, Cullen C. Swimming motility mediates the formation of neutrophil extracellular traps induced by flagellated *Pseudomonas aeruginosa*. *PLoS Pathog.* (2016) 12:e1005987. doi: 10.1371/journal.ppat.1005987
64. Quiroga J, Alarcón P, Manosalva C, Taubert A, Hermosilla C, Hidalgo MA, et al. Glycolysis and mitochondrial function regulate the radical oxygen species production induced by platelet-activating factor in bovine polymorphonuclear leukocytes. *Vet Immunol Immunopathol.* (2020) 226:110074. doi: 10.1016/j.vetimm.2020.110074
65. Barriá I, Güiza I, Cifuentes F, Zamorano P, Sáez JC, González J, et al. *Trypanosoma cruzi* infection induces pannexin-1 channel opening in cardiac myocytes. *Am J Trop Med Hygiene.* (2018) 98:105–12. doi: 10.4269/ajtmh.17-0293
66. Villagra-Blanco R, Silva LMR, Muñoz-Caro T, Yang Z, Li J, Gartner U, et al. Bovine polymorphonuclear neutrophils cast neutrophil extracellular traps against the abortive parasite *Neospora caninum*. *Front Immunol.* (2017) 8:606. doi: 10.3389/fimmu.2017.00606
67. Urban CF, Ermer D, Schmid M, Abu-Abed U, Goosmann C, Nacken W, et al. Neutrophil extracellular traps contain calprotectin, a cytosolic protein complex involved in host defense against *Candida albicans*. *PLoS Pathog.* (2009) 5:e1000639. doi: 10.1371/journal.ppat.1000639

**Conflict of Interest:** The authors declare that the research was conducted in the absence of any commercial or financial relationships that could be construed as a potential conflict of interest.

Copyright © 2020 Grob, Conejeros, Velásquez, Preußner, Gartner, Alarcón, Burgos, Hermosilla and Taubert. This is an open-access article distributed under the terms of the Creative Commons Attribution License (CC BY). The use, distribution or reproduction in other forums is permitted, provided the original author(s) and the copyright owner(s) are credited and that the original publication in this journal is cited, in accordance with accepted academic practice. No use, distribution or reproduction is permitted which does not comply with these terms.

## 2.2. CANINE *ANGIOSTRONGYLUS VASORUM*-INDUCED EARLY INNATE IMMUNE REACTIONS BASED ON NETS FORMATION AND CANINE VASCULAR ENDOTHELIAL CELL ACTIVATION IN VITRO

This chapter is based on the following publish paper:

Grob, D., Conejeros, I., López-Osorio, S., Velásquez, Z. D., Segeritz, L., Gärtner, U., Schaper, R., Hermosilla, C., & Taubert, A. (2021). Canine *Angiostrongylus vasorum*-Induced Early Innate Immune Reactions Based on NETs Formation and Canine Vascular Endothelial Cell Activation In Vitro. *Biology*, 10(5), 427.

Eigener Anteil in der Publikation:

Projektplanung	50 %, zusammen mit Ko-Autoren und Betreuern
Durchführung des Versuches	50 %, weitestgehend selbständig
Auswertung der Experimente	50 %, weitestgehend selbständig
Erstellung der Publikation	60 %, weitestgehend selbständig

## 2.2 Canine *Angiostrongylus vasorum*-induced early innate immune reactions based on NETs formation and canine vascular endothelial cell activation *in vitro*.



Article

### Canine *Angiostrongylus vasorum*-Induced Early Innate Immune Reactions Based on NETs Formation and Canine Vascular Endothelial Cell Activation In Vitro

Daniela Grob <sup>1,\*</sup>, Iván Conejeros <sup>1,†</sup>, Sara López-Osorio <sup>1,2</sup>, Zahady D. Velásquez <sup>1</sup>, Lisa Segeritz <sup>1</sup>, Ulrich Gärtner <sup>3</sup>, Roland Schaper <sup>4</sup>, Carlos Hermosilla <sup>1</sup> and Anja Taubert <sup>1</sup>

<sup>1</sup> Institute for Parasitology, Justus Liebig University Giessen, 35392 Giessen, Germany;

Ivan.Conejeros@vetmed.uni-giessen.de (I.C.); sara.lopezo@udea.edu.co (S.L.-O.);

zahady.velasquez@vetmed.uni-giessen.de (Z.D.V.); Lisa.C.Segeritz@vetmed.uni-giessen.de (L.S.);

Carlos.R.Hermosilla@vetmed.uni-giessen.de (C.H.); Anja.Taubert@vetmed.uni-giessen.de (A.T)

<sup>2</sup> Grupo de Investigación CIBAV, Universidad de Antioquia UdeA, Medellín 050034, Colombia

<sup>3</sup> Institute of Anatomy and Cell Biology, Justus Liebig University Giessen, 35392 Giessen, Germany;

ulrich.gaertner@anatomie.med.uni-giessen.de

<sup>4</sup> Elanco Animal Health, 40789 Monheim, Germany; roland.schaper@elancoah.com

\* Correspondence: Daniela.Grob@vetmed.uni-giessen.de

† Equally contributed.



**Citation:** Grob, D.; Conejeros, I.; López-Osorio, S.; Velásquez, Z.D.; Segeritz, L.; Gärtner, U.; Schaper, R.; Hermosilla, C.; Taubert, A. Canine *Angiostrongylus vasorum*-Induced Early Innate Immune Reactions Based on NETs Formation and Canine Vascular Endothelial Cell Activation In Vitro. *Biology* **2021**, *10*, 427. <https://doi.org/10.3390/biology10050427>

Academic Editor:  
Francesca Mancianti

Received: 29 March 2021

Accepted: 8 May 2021

Published: 12 May 2021

**Publisher's Note:** MDPI stays neutral with regard to jurisdictional claims in published maps and institutional affiliations.



**Copyright:** © 2021 by the authors. Licensee MDPI, Basel, Switzerland. This article is an open access article distributed under the terms and conditions of the Creative Commons Attribution (CC BY) license (<https://creativecommons.org/licenses/by/4.0/>).

**Simple Summary:** *Angiostrongylus vasorum* is a cardiopulmonary nematode that affects canids, residing in the pulmonary artery and right atrium/ventricle. Due to its location, the parasite will have a close interaction with the different components of the innate immune system, including endothelial cells and polymorphonuclear neutrophils (PMN). Here we evaluated the expression of adhesion molecules of canine aortic endothelial cells (CAEC), and NETs formation by co-culture of freshly isolated canine PMN with *A. vasorum* L3. Overall, we found distinct inter-donor variations in adhesion molecule expression among CAEC isolates. Additionally, PMN and *A. vasorum* co-culture induced NETs release without affecting larval viability.

**Abstract:** Due to its localization in the canine blood stream, *Angiostrongylus vasorum* is exposed to circulating polymorphonuclear neutrophils (PMN) and the endothelial cells of vessels. NETs release of canine PMN exposed to *A. vasorum* infective stages (third stage larvae, L3) and early pro-inflammatory immune reactions of primary canine aortic endothelial cells (CAEC) stimulated with *A. vasorum* L3-derived soluble antigens (*AvAg*) were analyzed. Expression profiles of the pro-inflammatory adhesion molecules ICAM-1, VCAM-1, P-selectin and E-selectin were analyzed in *AvAg*-stimulated CAEC. Immunofluorescence analyses demonstrated that motile *A. vasorum* L3 triggered different NETs phenotypes, with spread NETs (*sprNETs*) as the most abundant. Scanning electron microscopy confirmed that the co-culture of canine PMN with *A. vasorum* L3 resulted in significant larval entanglement. Distinct inter-donor variations of P-selectin, E-selectin, ICAM-1 and VCAM-1 gene transcription and protein expression were observed in CAEC isolates which might contribute to the high individual variability of pathological findings in severe canine angiostrongylosis. Even though canine NETs did not result in larval killing, the entanglement of L3 might facilitate further leukocyte attraction to their surface. Since NETs have already been documented as involved in both thrombosis and endothelium damage events, we speculate that *A. vasorum*-triggered NETs might play a critical role in disease outcome *in vivo*.

**Keywords:** *Angiostrongylus vasorum*; canine PMN; NETs formation; primary canine aortic endothelial cells; adhesion molecules

## 2.2 Canine *Angiostrongylus vasorum*-induced early innate immune reactions based on NETs formation and canine vascular endothelial cell activation *in vitro*.

### 1. Introduction

*Angiostrongylus vasorum* is a metastrongyloid nematode causing cardiopulmonary disorders in domestic dogs [1–3]. *In vivo*, *A. vasorum* resides in pulmonary arteries and the right side of the heart of domestic dogs and other carnivores [4–6]. The life cycle is heteroxenous and various terrestrial gastropod genera act as obligate intermediate hosts. They become infected by the consumption of first-stage larvae (L1) released into the environment by feces of *A. vasorum*-infected canids [7–9]. In gastropods, *A. vasorum* L1 develop into infective third-stage larvae (L3) which are ingested by definitive hosts to achieve the life cycle [10]. Over the last decades, canine angiostrongylosis has geographically spread into previously non-endemic areas and life-threatening cases have increasingly been reported [11–14]. Nowadays, canine angiostrongylosis is considered an emerging disease not only in Europe but also in North and South America [9,13,15–17]. *A. vasorum*-infected dogs show a wide range of clinical signs from mild coughing to neurological disorders, along with the presence of respiratory symptoms, coagulopathies (e.g., vascular thrombosis, diathesis, hemorrhages), gastrointestinal disorders, leukophilia and hypercalcemia representing common findings [18–20].

Based on its life cycle and migratory routes in the final host, direct contacts of different *A. vasorum* stages (i.e., L3, pre-adults and adults) with both canine polymorphonuclear neutrophils (PMN) and vascular endothelial cells will indeed occur *in vivo*. PMN are the most abundant leukocytes and represent the first line of defense in mammalian hosts [21–23]. PMN are recruited immediately after pathogen invasion and exhibit different effector mechanisms: degranulation of immunomodulatory molecules, generation of reactive oxygen species (ROS), phagocytosis and NETosis (release of neutrophil extracellular traps, NETs). NETs are delicate extracellular structures formed by decondensed chromatin, mainly via PAD4-mediated citrullination, and adorned with antimicrobial components, such as myeloperoxidase (MPO), neutrophil elastase (NE), lactoferrin, calprotectin, LL37, pentraxin, proteinase 3 or cathepsin G [21,24,25]. Meanwhile, different NET phenotypes were reported, including diffuse (*diff*NETs), spread (*spr*NETs), aggregated (*agg*NETs), cell free and anchored NETs [26–28]. *diff*NETs consist of globular and compact forms with sizes of 15–20 nm diameter whilst *spr*NETs are smooth and elongated web-like structures with extremely thin fibers of 15–17 nm diameter [29,30]. *agg*NETs are large conglomerates with sizes >50 µm in diameter and released by a high number of PMN undergoing NETosis [29–32].

So far, canine PMN have been shown to cast NETs in response to LPS, PMA [33], sodium arsenite [34], platelet activating factor (PAF) [35], *Neospora caninum* [36] and the heartworm *Dirofilaria immitis* [30]. Even though NETs in general were proven effective against nematode stages of *Haemonchus contortus*, *Strongyloides stercoralis*, *Ostertagia ostertagi* and *Brugia malayi* [30,37–40], nothing is currently known on canine NETosis against *A. vasorum*. So far, only one study has reported on *A. vasorum*-triggered phagocyte-derived extracellular traps (ETs) formation in the gastropod immune system [8].

Endothelial cells are highly immunoreactive and rapidly produce a broad range of molecules (e.g., adhesion molecules, cytokines, chemokines) upon activation, thereby triggering pro-inflammatory responses [41,42]. Interestingly, tight interactions between activated endothelium and NETs, but also adverse effects of NETs on endothelial integrity, were reported [14,43]. As indication of chronic inflammation, leukocytosis and neutrophilia have already been described in *A. vasorum*-infected animals [20]. Likewise, immune-mediated inflammation and damage of lung vasculature were also reported for *A. vasorum* infections in dogs [20,44]. However, detailed analysis of endothelial activation during *A. vasorum* infection in dogs is scarce. Interestingly, the closely related nematode *Angiostrongylus cantonensis* induces an increase in the blood–brain barrier via metalloproteinase 9 upregulation [45], thereby suggesting endothelial cell activation. In this context, related to the case of another heartworm that affect canids, *D. immitis*, it is well-known that its presence in the blood stream of the host causes endothelial cell activation and inflammation, a situation demonstrated *in vivo* and *in vitro* [46], situation attributed to progressive pulmonary en-

## 2.2 Canine *Angiostrongylus vasorum*-induced early innate immune reactions based on NETs formation and canine vascular endothelial cell activation *in vitro*.

derteritis and muscular hypertrophy of arteriole walls [44,47]. Activated endothelial cells not only trigger leukocyte recruitment and adhesion but also secrete von Willebrand factor (vWF), a large multifunctional glycoprotein with strong adhesive properties mediating adhesion of platelets at the site of the vascular damage [48–51]. As an indirect evidence of infection-induced endothelial cell activation, increased vWF concentrations were found in 32% of *A. vasorum*-infected dogs suffering bleeding disorders [12].

To our best knowledge, we here show for the first time that motile axenic *A. vasorum* L3 and soluble *A. vasorum* L3 antigens (AvAg) induce both significant NET formation and canine endothelial cell activation, and suggest that these reactions may contribute to individual disease outcome.

### 2. Materials and Methods

#### 2.1. Gastropod Maintenance and Isolation of Axenic *Angiostrongylus vasorum* Third-Stage Larvae (L3)

Terrestrial leopard slugs (*Limax maximus*) were bred and maintained in fully-automated climate incubators (model ECP01E; Sniijders Scientific B.V. Tilburg, the Netherlands) according to [8]. Briefly, breeding and maintenance was performed under controlled conditions: 50% humidity, 10 h of dark/10 h of illumination corresponding to circadian cycles, plus 2 h for dusk and dawn each, temperature ranging from 10 to 16 °C (night/day). *L. maximus* were kept on wet paper towels in plastic boxes equipped with Petri dishes for food supply and a plastic dim housing area (Techniplast, Hohenpeissenberg, Germany) for slug retreat.

*A. vasorum* first-stage larvae (L1) were isolated via the Baermann funnel technique from feces of experimentally infected dogs (kindly provided by the Institute of Parasitology, University of Veterinary Medicine of Hannover, Hannover, Germany) as described elsewhere [8]. Approximately 10 mL of sediment containing migrated L1 were collected and pelleted (800 × g, 5 min, 20 °C). The supernatant was discarded and larval numbers were determined microscopically (Olympus CX41). Three leopard slugs (*L. maximus*) were orally infected with 2000 vital larvae each and according to [8,17].

#### 2.2. Isolation of Canine PMN

Blood samples were collected from healthy adult Beagle dogs ( $n = 7$ ; Marshall BioResources, kept at Elanco Animal Health, Monheim, Germany) and used for canine PMN isolation. Heparinized blood was diluted in an equal volume of sterile PBS with 0.02% EDTA (Sigma-Aldrich, Darmstadt, Germany) and placed on Biocoll Separating Solution® (Biochrom AG, Berlin, Germany). The samples were centrifuged at 800 × g for 45 min at RT. The cell pellet was gently re-suspended, diluted in 27 mL of distilled water and shaken for 20 s to lyse erythrocytes according to [30]. Then, osmolarity was adjusted by adding 3 mL of 10 × Hanks Salt Solution (HBSS, Biochrom AG, Berlin, Germany). Canine PMN were washed twice (400 × g, 10 min, RT), re-suspended in sterile RPMI 1640 medium (Sigma-Aldrich, Darmstadt, Germany), counted in a Neubauer hemocytometer chamber and incubated at 37 °C with 5% CO<sub>2</sub> for 30 min before experimental use.

#### 2.3. Scanning Electron Microscopy (SEM) Analysis

Canine PMN were co-cultured with axenic vital *A. vasorum* L3 (6 larvae/sample) on poly-L-lysine (Sigma-Aldrich, Darmstadt, Germany) pre-coated coverslips (60 min, RT). After incubation, the samples were fixed in HEPES solution (Sigma-Aldrich; 0.3 M, pH 7.35) containing 1.5% paraformaldehyde and glutaraldehyde (both Merck, Darmstadt, Germany) (60 min, RT), post-fixed in 1% osmium tetroxide (Merck, Darmstadt, Germany), washed in sterile distilled water, dehydrated, critical point dried by CO<sub>2</sub> treatment and sprayed with gold. Thereafter, samples were analyzed with a Philips XL30® scanning electron microscope at the Institute of Anatomy and Cell Biology, Justus Liebig University Giessen, Giessen, Germany.

## 2.2 Canine *Angiostrongylus vasorum*-induced early innate immune reactions based on NETs formation and canine vascular endothelial cell activation *in vitro*.

### 2.4. NET Visualization by Immunofluorescence

Canine PMN ( $4.2 \times 10^5/400 \mu\text{L}$ ) were seeded on 15 mm diameter poly-L-lysine treated coverslip glasses (Nunc, Schwerte, Germany) and placed in a 12 well plate (Greiner, Frickenhausen, Germany) in sterile RPMI 1640 medium (without phenol red, supplemented with 1% penicillin/streptomycin, Sigma-Aldrich, Darmstadt, Germany). Co-culture of axenic *A. vasorum* L3 with canine PMN was performed for 90 min ( $2 \times 10^5$  PMN were stimulated with 10 larvae/well,  $37^\circ\text{C}$ , 5%  $\text{CO}_2$ ). Thereafter, samples were fixed in 4% paraformaldehyde (Merck, Darmstadt, Germany) and kept at  $4^\circ\text{C}$  until further analysis. Canine NET structures were visualized by staining extracellular DNA with DAPI (4',6-diamidino-2-phenylindole, Thermo Fisher Scientific, Langenselbold, Germany). For the detection of histones and NE decorating NETs structures, the following primary antibodies were used: anti-global histone (H1, H2A/H2B, H3, H4) (clone H11-4, 1:500; Merck Millipore cat #MAB3422) and anti-NE (cat # Ab68672, 1:500, Abcam, Berlin, Germany). Briefly, samples were washed with sterile PBS, blocked in 3% bovine serum albumin (BSA) (Sigma-Aldrich; 60 min, RT) + 0.3% Triton X-100 (Thermo Fischer Scientific, Langenselbold, Germany) for 60 min at RT and then incubated with respective primary antibodies for 3 h at RT. Then, samples were washed three times with sterile PBS and incubated in secondary antibody solutions (Alexa 594 goat anti-mouse IgG H&L #A11005, Alexa 488 goat anti-rabbit IgG #A11008, 1:500, RT). Finally, samples were washed three times with sterile PBS and mounted upside-down with Fluoromount G<sup>®</sup> with DAPI (Thermo Fischer Scientific). Visualization of NETs was achieved using an inverted IX81 fluorescence microscope equipped with an XM10 digital camera (both Olympus, Hamburg, Germany). Five random pictures were taken from each experimental condition to analyze the presence of NETs and NET phenotypes.

### 2.5. Assessment of Different NET Phenotypes

NET phenotypes were quantified by immunofluorescence microscopy as previously described elsewhere [27]. Therefore, five randomly taken pictures were analyzed by manual counting, based on morphological and morphometric characteristics for each phenotype of canine NETs, as previously described [8,30].

### 2.6. Nuclear Decondensation-Based Quantification Using DANA Software

To further confirm parasite-induced NET induction and to evaluate effects within the dynamic NETotic process, we additionally analyzed *A. vasorum* L3-triggered nuclear area expansion (NAE) in canine PMN. Nuclear expansion-based quantification of NETs relied on the method described by [25] and the software DANA I and DANA II was applied according to the developer's recommendations. In brief, freshly isolated canine PMN ( $n = 7$  donors,  $2 \times 10^5$  PMN/well) were left in plain medium (RPMI 1640, Sigma-Aldrich, Darmstadt, Germany) for 30 min and then exposed to 10 L3/well for 90 min. After incubation, samples were fixed using 2% paraformaldehyde (Merck, Darmstadt, Germany) and stained with DAPI (Thermo Fischer Scientific, Langenselbold, Germany) for 30 min RT. Five microscopic images were randomly taken for each condition using an inverted microscope (Olympus IX 81), having a total of 203 PMN in the control and 178 in the stimulated group. Nuclear areas of PMN were analyzed using DANA software.

### 2.7. Isolation of Primary Canine Aortic Endothelial Cells (CAEC)

Four aortic arteries from four adult healthy male Beagle dogs were donated from Elanco Animal Health, Monheim, Germany. Arteries were kept at  $4^\circ\text{C}$  in sterile 0.9% HBSS-HEPES buffer (pH 7.4; Gibco) supplemented with 1% penicillin (500 U/mL; Sigma-Aldrich) and streptomycin (500  $\mu\text{g}/\text{mL}$ ; Sigma-Aldrich, Darmstadt, Germany). For isolation of aortic endothelial cells, 0.025% collagenase type II (Worthington Biochemical Corporation, Lakewood, NJ, USA) was infused into the vessel lumen, the aorta was ligated with clamps and incubated for 20 min at  $37^\circ\text{C}$  in 5%  $\text{CO}_2$  atmosphere. After gently massaging aortas, infused collagenase II-cell suspension was collected and immediately supplemented with

## 2.2 Canine *Angiostrongylus vasorum*-induced early innate immune reactions based on NETs formation and canine vascular endothelial cell activation *in vitro*.

1 mL sterile fetal calf serum (FCS; Gibco, Langensfeld, Germany) to inactivate collagenase II. After two washing steps ( $400 \times g$ , 10 min, 4 °C), the cells were suspended in endothelium cell growth medium (ECGM; PromoCell, Heidelberg, Germany), plated in 25 cm<sup>2</sup> plastic culture flasks (Nunc, Roskilde, Denmark) and kept at 37 °C in 5% CO<sub>2</sub> atmosphere until reaching confluent cell layers. Culture medium was changed every 2–3 days.

### 2.8. Preparation of *Angiostrongylus vasorum* L3 Soluble Antigen (AvAg)

Twenty *A. vasorum* L3 were used for soluble antigen preparation (AvAg). Therefore, larval stages were frozen in liquid nitrogen and thereafter grounded in 300 µL sterile phosphate-buffered saline (PBS; 1×) in a previously UV-sterilized and cooled mortar (−80 °C for 1 h). The resulting suspension was sonicated in an ice bath with a Sonorex Super RK31<sup>®</sup> bath-type sonicator (Bandelin, five cycles of 15 s) and centrifuged ( $10,000 \times g$ , 20 min, 4 °C). Final protein concentration of PBS-soluble supernatants was estimated via Coomassie Plus (Bradford, UK) Assay Kit<sup>®</sup> (Thermo Scientific). AvAg was stored at −20 °C until further use.

### 2.9. Total RNA Isolation and qRT-PCR

CAEC were seeded in 6-well plastic plates (Greiner, Frickenhausen, Germany) until confluence (37 °C and 5% CO<sub>2</sub>). Thereafter, CAEC monolayers were exposed to 1 ng/mL of soluble AvAg and incubated at 37 °C with 5% CO<sub>2</sub>. At 3, 6, 12 and 24 h post stimulation, total RNA was harvested by applying RTL lysis buffer (Qiagen, Hilden, Germany) directly on the well. RNA isolation was performed with RNeasy kit (Qiagen, Hilden, Germany) according to manufacturer instructions and followed by a DNase (Thermo Scientific, Langensfeld, Germany) digestion (37 °C, 30 min) to remove genomic contamination. DNase was then inactivated by heating (65 °C, 10 min). Efficiency of DNA digestion was confirmed by including no-RT-controls in each qRT-PCR experiment. In total, 1 µg of DNase-treated total RNA was reversely transcribed with SuperScript IV enzyme (Thermo Scientific, Langensfeld, Germany), according to manufacturer instructions. cDNA synthesis was performed for 10 min at 23 °C, then 10 min at 50 °C. The enzyme was then inactivated by heating (80 °C) for 10 min.

Probes were labelled at the 5'-end with the reporter dye FAM (6-carboxyfluorescein) and at the 3'-end with the quencher dye TAMRA (6-carboxytetramethyl-rhodamine) (refer to Table 1). PCR amplification was performed in an automated fluorometer Rotor-GeneQ cyclor (Qiagen, Hilden, Germany) using a 96-well optical plates (Greiner, Frickenhausen, Germany). Samples were analyzed in duplicate. For PCR, 2 µL cDNA (corresponding to 25 ng total RNA) were used in a 10 µL PCR reaction mixture containing 5 µL PerfeCTa FastMix II (QuantaBio, Beverly, MA, USA), 400 nM of each primer and 200 nM probe. Amplification conditions were the same for all targets assayed: one cycle at 95 °C for 5 min, one cycle at 94 °C for 15 min and one cycle at 60 °C for 60 min. Semiquantitative analyses used comparative C<sub>t</sub> method ( $\Delta\Delta C_t$  method, [52]) and reported as *n*-fold differences in comparison to one of the samples arbitrarily chosen as calibrator). Canine ribosomal protein L32 (RPL32), ribosomal protein S19 (RPS19) and hypoxanthine phosphoribosyl-transferase (HPRT) genes were used as housekeeper genes. TNF $\alpha$  (10 ng/mL for 24 h, Serotec) was used a positive control.

## 2.2 Canine *Angiostrongylus vasorum*-induced early innate immune reactions based on NETs formation and canine vascular endothelial cell activation *in vitro*.

**Table 1.** Sequences of canine probes and primers used for qRT-PCR experiments

Target	Primers		Tm
	Forward/Reverse		
<i>Canis lupus</i> E-selectin	5'-TGGCTTCAGAGTCTCAGGT-3'	5'-TCAAAGCACTGCACCTAAC-3'	60 °C
<i>Canis lupus</i> P-selectin	5'-CAAAAAGCCTCTCACCGAAG-3'	5'-ATGCATTCCTCTTGCTGCT-3'	60 °C
<i>Canis lupus</i> ICAM-1	5'-CAGGGTTGCCAGGTACAGTT-3'	5'-AGTATGGGCTCAGTGGGTTG-3'	60 °C
<i>Canis lupus</i> VCAM-1	5'-TCCATCGTGAGGAAGTAG-3'	5'-CAGCCTGGTTAATCCCTTCA-3'	60 °C
<i>Canis lupus</i> RPL32	5'-CCTCAGACCTCTGGTGAAGC-3'	5'-TCAAGCTCCTTGACGTTGTG-3'	60 °C
<i>Canis lupus</i> RPS19	5'-TGTCAGGCTACCTCGGAGT-3'	5'-GCCTTCAGCCTCTTCTTCT-3'	60 °C
<i>Canis lupus</i> HPRT	5'-AAGCTTGTGGTGAAAAGGA-3'	5'-CAATGGACTCCAGATGCTT-3'	60 °C
Probes			
<i>Canis lupus</i> E-selectin	5'-TTTGTACAGCTGTGACAAGGG-3'		60 °C
<i>Canis lupus</i> P-selectin	5'-GCTATACAGCCTCCTGCCAG-3'		60 °C
<i>Canis lupus</i> ICAM-1	5'-CATTGGCTAAGCTGCTTTCC-3'		60 °C
<i>Canis lupus</i> VCAM-1	5'-GAGCAGCGGCTAAGTAATG-3'		60 °C
<i>Canis lupus</i> RPL32	5'-GGCACCAGTCAGACCGATAT-3'		60 °C
<i>Canis lupus</i> RPS19	5'-CAGTACCCAGCAGATTGTG-3'		60 °C
<i>Canis lupus</i> HPRT	5'-CCCCTCGAAGTGTGGCTAT-3'		60 °C

### 2.10. Protein Isolation and Western Blot Analyses

CAEC were seeded in 6-well plastic plates (Greiner, Frickenhausen, Germany) until confluence at 37 °C and 5% CO<sub>2</sub> atmosphere. Then, CAEC layers were stimulated with 1 ng/mL *AoAg* for 3, 6, 12 and 24 h (37 °C, 5% CO<sub>2</sub>). Thereafter, samples were subjected to protein isolation: proteins from CAEC were extracted by cell sonication (20 s, 5 cycles) in RIPA buffer (50 mM Tris-HCl, pH 7.4; 1% NP-40; 0.5% Na-deoxycholate; 0.1% SDS; 150 mM NaCl; 2 mM EDTA; 50 mM NaF; all Roth) supplemented with a protease inhibitor cocktail (1:200, Sigma-Aldrich). Cell homogenates were centrifuged (10,000 × *g*, 10 min, 4 °C) to sediment intact cells and nuclei. The RIPA buffer-soluble protein content of supernatants was quantified via Coomassie Plus (Bradford) Assay Kit<sup>®</sup> (Thermo Scientific, Langensfeld, Germany) following the manufacturer's instructions.

For immunoblotting, samples were supplemented with 6 M urea protein loading buffer. After boiling (95 °C) for 5 min, proteins (20 µg/slot) were separated in 12% or 15% polyacrylamide gels via electrophoresis (100 V, 1.5 h; *tetra* system, BioRad, Dreieich, Germany). Proteins were then transferred to polyvinylidene difluoride (PVDF) membranes (Millipore) (300 mA, 2 h at 4 °C). Blots were blocked in 3% BSA in TBS (50 mM Tris-Cl, pH 7.6; 150 mM NaCl containing 0.1% Tween (blocking solution); Sigma-Aldrich (Darmstadt, Germany) for 1 h at RT and then incubated overnight at 4 °C in primary antibodies against vinculin (1:1000, #sc-73,614, Santa Cruz), E-selectin (1:500, #TA318934, OriGene, Herford, Germany), P-selectin (1:500, #TA318936, OriGene, Herford, Germany) and VCAM-1 (1:500, #TA502391, OriGene, Herford, Germany) diluted in blocking solution. Vinculin detection was used as loading control for sample normalization. Following three washings in TBS-Tween 0.1% buffer (Sigma-Aldrich, Darmstadt, Germany), blots were incubated for 30 min at RT with secondary antibodies (goat anti-mouse IgG peroxidase-conjugated (1:40,000,

## 2.2 Canine *Angiostrongylus vasorum*-induced early innate immune reactions based on NETs formation and canine vascular endothelial cell activation *in vitro*.

#31,430, Pierce, Langensfeld, Germany); goat anti-rabbit IgG peroxidase-conjugated (1:40,000, #31,460, Pierce, Langensfeld, Germany) diluted in blocking solution. After three further washings in TBS-Tween 0.1% buffer, signal detection was accomplished by an enhanced chemo-luminescence detection system (ECL<sup>®</sup> plus kit, GE Healthcare) and recorded using a ChemoCam<sup>®</sup> Imager (Intas Science Imaging, Göttingen, Germany). Protein sizes were controlled by a protein ladder (PageRuler Plus<sup>®</sup> Prestained Protein Ladder ~10–250 kDa, Thermo Fisher Scientific, Langensfeld, Germany). Protein band intensities were quantified by Image J<sup>®</sup> (NIH), Fiji Gel Analyzer plugin.

### 2.11. Statistical Analysis

For all analyses except for NAE analysis in which ANOVA was applied, statistical significance was defined by a  $p$  value  $\leq 0.05$  determined by non-parametric analyses: Mann-Whitney test when two experimental conditions were compared and Kruskal-Wallis test followed by Dunn's post-hoc test for multiple comparisons. All graphs (mean  $\pm$  SD) and statistical analyses were performed using Graph Pad<sup>®</sup> software (v.7.03).

## 3. Results

### 3.1. *Angiostrongylus vasorum* L3 Trigger NET Formation in Canine PMN and Led to Differential NET Phenotype Formation

SEM analysis demonstrated that co-culture of canine PMN with live *A. vasorum* L3 induced the formation of NET-like thick and fine DNA fibers originating from dead PMN attached to L3 stages (Figure 1, arrows). As such, robust PMN-derived structures contacted and firmly entrapped *A. vasorum* L3. However, not all canine PMN participated in NETs release after exposure to highly motile larval stages. As such, a large number of PMN did not show morphological changes and a small number of non-NETotic PMN were also found to be firmly attached to the parasite's cuticle (Figure 1A–C).

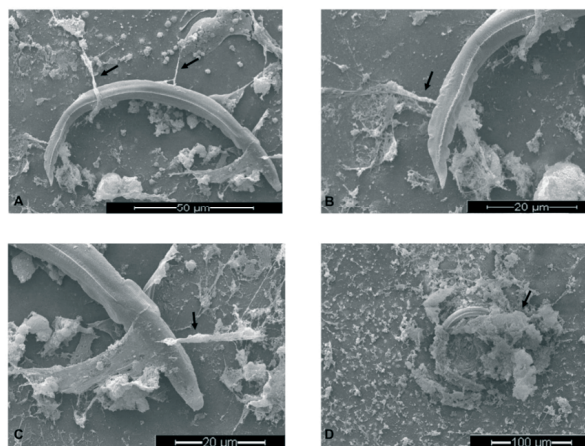


**Figure 1.** *Angiostrongylus vasorum* L3-induced neutrophil extracellular traps (NETs) analyzed via scanning electron microscopy (SEM) analysis. Fine spread NETs (*spr*NETs) entrapping the L3 (A–C) and robust aggregated NETs (*agg*NETs) (D) were the most predominant phenotypes of NETs. Arrows point to NET-like delicate PMN-derived structures in co-culture assays.

## 2.2 Canine *Angiostrongylus vasorum*-induced early innate immune reactions based on NETs formation and canine vascular endothelial cell activation *in vitro*.

To prove that these *A. vasorum* L3-triggered structures were, indeed, NETs, immunofluorescence analyses were performed to detect classical NETs components. DAPI staining confirmed the DNA nature of extracellular NET-like structures extruding from ruptured canine PMN after exposure to *A. vasorum* L3 larvae (Figure 2D,H). Additionally, co-localization analyses revealed the simultaneous presence of NE (Figure 2B–F) and global histones (Figure 2A–E) in DNA-positive (Figure 2C–G) canine NETs (Figure 2D–H).

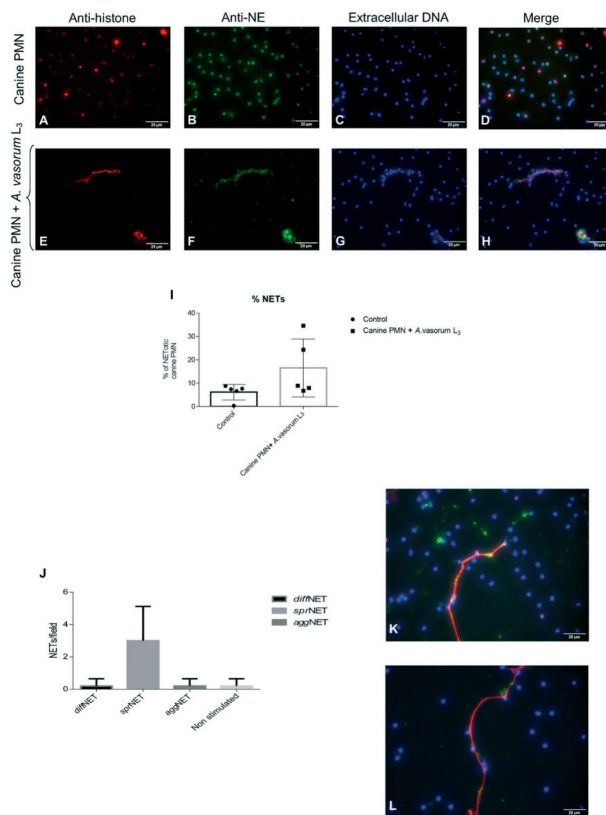


**Figure 2.** Immunofluorescence analyses of *Angiostrongylus vasorum* L3-induced neutrophil extracellular trap (NET) formation. Co-localization analyses on extracellular DNA, histones, and neutrophil elastase were performed. Presence of extracellular DNA (C,G; blue), anti-histone (A,E; red) and anti-NE (B,F; green) was confirmed. (D,H) depicts the merging of the three channels. (I) reveals the percentage of *A. vasorum* L3-triggered NETosis. (J–L) demonstrate the presence of spread NETs (*spr*NETs).

## 2.2 Canine *Angiostrongylus vasorum*-induced early innate immune reactions based on NETs formation and canine vascular endothelial cell activation *in vitro*.

When considering different NET phenotypes, vital *A. vasorum* L3 mainly triggered the formation of *spr*NETs (Figure 2J), consisting of smooth and elongated web-like structures of decondensed chromatin and antimicrobial proteins with a diameter of 15–17  $\mu\text{m}$  (Figure 2K–L). To a lesser extent, the formation of *diff*NET- and *agg*NET-phenotypes was induced. Whilst the former were composed of extracellular chromatin complexes covering a larger area and decorated with antimicrobial proteins of globular and compact form, *agg*NETs were much larger in size ( $\geq 50 \mu\text{m}$ ) and originated from groups of NETotic PMN. Overall, mainly *agg*NETs appeared rigid enough to immobilize these large and highly motile larval stages.

Observer-based estimation of cell numbers of performing NETs revealed that 13.2% of PMN released NETs when confronted with vital *A. vasorum* L3 (Figure 2I). In comparison, only 5.3% of the total PMN population reacted in this manner in control conditions (unstimulated PMN). Figure 3A depicts the normal structure of a canine PMN and its nucleus. When canine PMN were exposed to *A. vasorum* L3 stages, we observed a mean expansion of the NAE of  $102.1 \pm 35.64 \mu\text{m}^2$  in control cells, whilst in parasite-encountering cells this area increased to  $146.9 \pm 39.11 \mu\text{m}^2$  (controls vs. *A. vasorum*:  $p = 0.02$ ; Figure 3B–D).

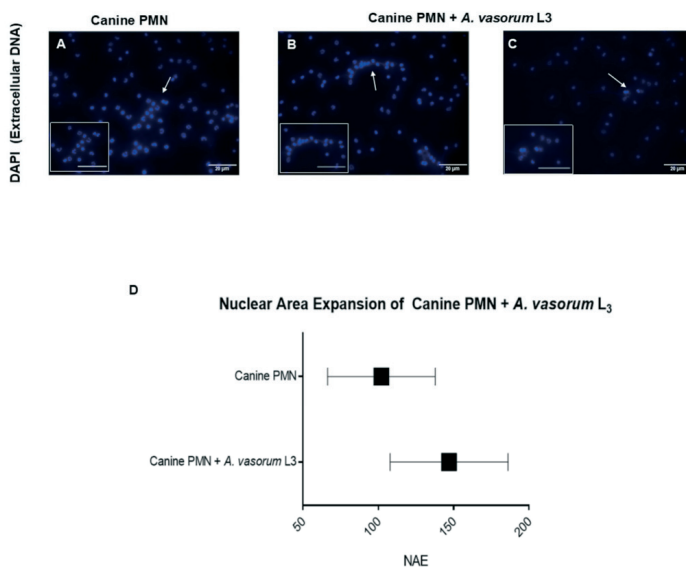


**Figure 3.** Nuclear expansion (NAE)-based quantification of *A. vasorum* L3-triggered NETs. Canine PMN were incubated in cell medium alone or exposed to *A. vasorum* L3. (A) depicts canine PMN alone; (B,C) illustrates co-cultivation of canine PMN + *A. vasorum*. Box placed on the left bottom depicts an isolated magnification of canine PMN alone and canine PMN co-cultured with axenic *A. vasorum* L3. NAE was analyzed by ImageJ® and DANA software. (D) shows the nuclear area increase of NETotic cells after co-cultures.

## 2.2 Canine *Angiostrongylus vasorum*-induced early innate immune reactions based on NETs formation and canine vascular endothelial cell activation *in vitro*.

### 3.2. *AvAg* Induces Canine Endothelial Cell Activation and Donor-Dependent Adhesion Molecule Expression

CAEC were stimulated with *AvAg* (PBS-soluble L3 protein extract) and samples were analysed via a kinetic approach (3, 6, 12 and 24 h after stimulation). To monitor endothelial cell activation, the expression of the adhesion molecules P-selectin, E-selectin, VCAM-1 and ICAM-1 was assessed. To achieve this, qRT-PCR and Western blotting were performed to quantify mRNA abundance and to estimate protein expression, respectively. In this context, ICAM-1 was not estimated, considering that the commercially available primary antibodies did not work reliably for the canine samples. In all cases, results showed highly variable responses depending on individual canine endothelial cell donors/CAEC isolates (Figures 4 and 5). Referring to mRNA expression, we observed one “non-respondent” CAEC (isolate 2) during the experiments, which hampered significance (based on animal trial restrictions, we could not enhance the number of CAEC isolates), but which might also reflect the true *in vivo* situation in individual dogs suffering canine angiostrongylosis. Nevertheless, the other two isolates (isolates 1 and 3) reacted upon *AvAg* stimulation, thereby indicating endothelial cell activation, but followed different reaction patterns (Figure 4). Interestingly, *AvAg*-stimulated CAEC isolate 1 showed a rather high level of E-selectin, P-selectin and VCAM-1 gene transcripts (Figure 4) when compared to the other isolates. At 12 h post incubation, a peak of E-selectin mRNA expression was observed (Figure 4A) in 2/3 isolates. For P-selectin, a more or less constantly high mRNA abundance was detected but only in isolate 1, whereas ICAM-1 seemed to increase at 6 h post stimulation in 2/3 isolates (Figure 4C). A further increase in 1/3 isolates was observed for ICAM-1 24 h post incubation (Figure 4C). VCAM-1 mRNA expression showed the most variable results with no coincidence between the three isolates (Figure 4D). For positive controls, CAEC isolates were stimulated with TNF- $\alpha$  for 24 h. Given that these data revealed a high variability between CAEC donors for all adhesion molecules tested, this might also indicate an extraordinary individual reactivity of canine endothelial cell isolates, even in response to such a potent stimulant (Figure 4).

Considering protein expression, adhesion molecule-related results in principle mirrored the reactivities observed in mRNA-based experiments, and revealed highly variable inter-animal responses (Figure 5). Overall, the distinct adhesion molecule regulation in each CAEC isolate reflected an *AvAg*-driven endothelial cell activation. E-selectin expression increased at 6 h post incubation in 2/3 isolates. In 1/3 isolates this peak already occurred at 3 h post incubation (or earlier). In 1/3 isolates a  $\geq 3$ -fold increase of E-selectin expression when compared to control was observed at 24 h of incubation (Figure 5B). P-selectin protein expression also showed a peak of around two-fold at 6 h post *AvAg* stimulation in 2/3 isolates, decreasing at 12 h for 2/3 isolates and with a further increase at 24 h (Figure 5C). The latter increase was more pronounced in 1/3 isolates with a four-fold up-regulation of P-selectin protein expression compared to control conditions (Figure 5C). Finally, in line with mRNA expression data, VCAM-1 abundance showed the most variable results in stimulated CAEC (Figure 5D). Thus, a first peak of expression was observed at 3 h post incubation in 1/3 isolates and a second, less pronounced peak at 12 h. In 1/3 isolates the peak occurred at 6 h, but at a much lower level than in isolate 2. Overall, we observed an increased expression of E-selectin, P-selectin and VCAM-1 at protein level in the three different CAEC isolates stimulated with soluble *AvAg*, which indeed reflected an antigen-driven activation of these endothelial cells. However, regarding the quantity or kinetics of protein expression, the pattern remains inconclusive due to high inter-isolate variations.

## 2.2 Canine *Angiostrongylus vasorum*-induced early innate immune reactions based on NETs formation and canine vascular endothelial cell activation *in vitro*.

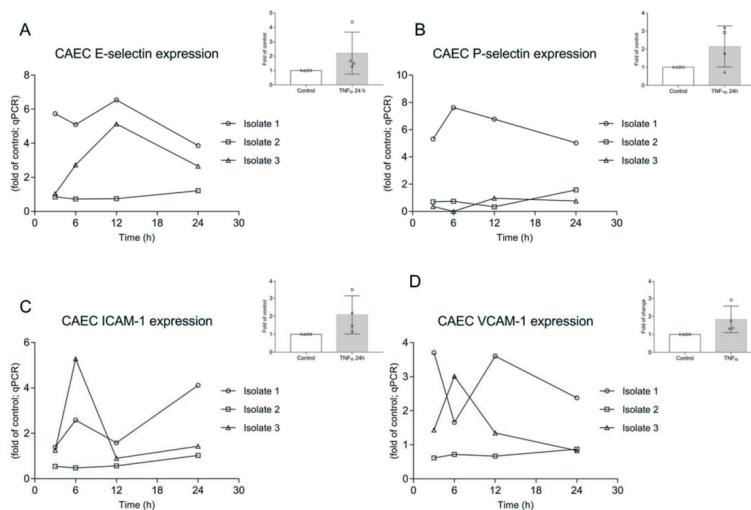


**Figure 4.** Adhesion molecule gene transcription in *A. vasorum* antigen (*AvAg*)-stimulated canine endothelial cells. CAEC were stimulated with soluble *A. vasorum* L3 antigen (*AvAg*; 1 ng/mL) and after 3, 6, 12 and 24 h of incubation total RNA was isolated, reverse transcribed and assayed for E-selectin (A), P-selectin (B), ICAM-1 (C) and VCAM-1 (D) gene transcription via qPCR. Data are expressed as *n*-fold of controls (non-stimulated CAEC). TNF- $\alpha$  stimulation was used as positive control.

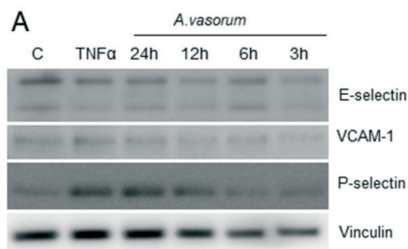


**Figure 5.** Cont.

## 2.2 Canine *Angiostrongylus vasorum*-induced early innate immune reactions based on NETs formation and canine vascular endothelial cell activation *in vitro*.

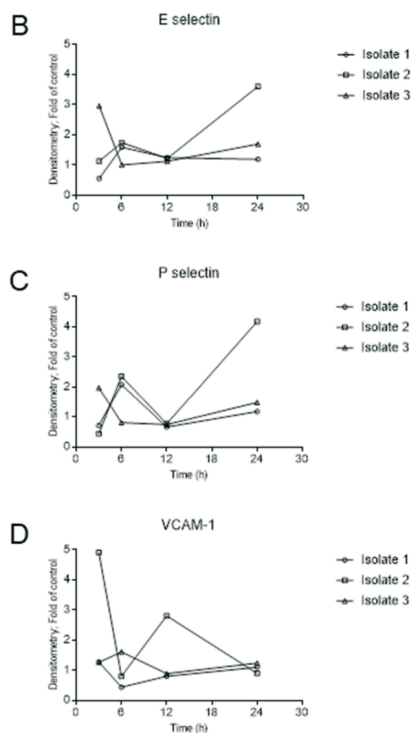


**Figure 5.** Adhesion molecule protein expression in *A. vasorum* antigen (*AvAg*)-stimulated canine endothelial cells. CAEC cells were stimulated with *A. vasorum* L3 antigen (*AvAg*; 1 ng/mL) and after 3, 6, 12 and 24 h of incubation, total protein was extracted. Non-stimulated CAEC served as negative controls. The expression of E-selectin (B), P-selectin (C) and VCAM-1 (D) was studied by Western blotting (A); representative illustration of one CAEC isolate and densitometric analysis of protein bands. TNF- $\alpha$  was used as positive control of CAEC stimulation. The detection of vinculin was used as loading control for sample normalization. Complete Western Blot acquisitions from E-selectin, P-selectin, VCAM-1 and vinculin is depicted in the Supplementary Figure S1.

### 4. Discussion

After ingestion by the definitive host, *A. vasorum* L3 larval stages must first migrate through the intestinal wall to reach mesenteric lymph nodules where they moult into L4 within the first four days post infection (p.i.), and then invade lymph/blood vessels, and later on the pulmonary arteries, ventricle, atrium and auricle of the right section of heart [1,5,53,54]. Following the definitive host infection, *A. vasorum* are constantly exposed to the definitive host innate immune environment, mainly composed of cell barriers [e.g., digestive mucosa (epithelial cells), endothelium], cells of the innate immune

## 2.2 Canine *Angiostrongylus vasorum*-induced early innate immune reactions based on NETs formation and canine vascular endothelial cell activation *in vitro*.

system (e.g., PMN), complementary factors, antimicrobial peptides, cytokines/chemokines, among others. However, studies on early innate canine immune reactions against *A. vasorum* stages are scarce. Given that PMN infiltration is common in *A. vasorum*-infected dogs [54–56] and that NETs formation was recently reported as an effective PMN-derived defense mechanism against nematode stages [30,32,37,39,40], we here analysed *A. vasorum* L3-induced NETosis as part of early innate immune responses in the canine system. Considering that *A. vasorum* circulating antigens are in direct contact with highly immunoreactive host endothelial cells of vessels *in vivo*, vasculitis, perivasculitis and thrombosis are consistently reported for canine angiostrongylosis [54,56]. Therefore, we further studied canine endothelium-derived responses to soluble *AvAg*. Overall, we here provide first evidence of *A. vasorum*-induced formation of different NET phenotypes, NET-mediated larval entanglement and activation of canine endothelial cells (based on pro-inflammatory adhesion molecule up-regulation).

NETs are composed of decondensed chromatin decorated with histones and granular components, such as calprotectin, NE, MPO, cathepsin G, proteinase 3, lactoferrin, LL37, pentraxin and gelatinase, among others [21,57]. Consistently, typical NET-associated components were here confirmed for *A. vasorum* L3-induced NETs by demonstrating colocalization of NE and histones on DNA-rich extracellular fibres being released from canine PMN. In line with other reports on parasites triggering NETosis [8,27,30,58], the induction of different NET phenotypes was here observed. In principle, all types (*spr*NETs, *diff*NETs, *agg*NETs) were detected upon contact of canine PMN with *A. vasorum* L3; however, the most abundant were *spr*NETs, which is consistent with findings on *D. immitis*-triggered NETosis [30]. Referring to functionality of different NET phenotypes, *agg*NETs are reported to have anti-inflammatory properties via sequestration and detoxification of global histones and proteolysis of pro-inflammatory chemokines and cytokines [29,59,60], whilst *spr*NETs and *diff*NETs exhibit pro-inflammatory effects in the early phase of innate response [61]. In the current study, *A. vasorum*-triggered NET formation was quantified via NAE-based estimations using DANA, thereby reflecting early reactions during the NETotic process. This technique was recently demonstrated as useful and reliable in identifying early NETotic cells during parasite encounter [62]. In the current study, an increase in NAE in *A. vasorum* L3-confronted canine PMN confirmed the parasite-triggered induction of NETotic cells and these data corresponded well to observer-based microscopic observations of NETs. Worth noting, DANA has already been successfully performed before in human, murine and bovine systems [25,27,63,64], with the current report representing the first application for canine PMN.

Studies on helminth-triggered NETosis documented the efficiency and strength of delicate extracellular fibers in capturing these large-sized parasites [8,32,37,39,62,65]. Strikingly, mammalian PMN seem able to recognize or sense large-sized parasites [66] and to rapidly cast NETs in response, in order to immobilize these pathogens [67]. On a mechanistic level, NE is slowly released into the cytosol after PMN encounter a pathogen via a route that does not involve membrane fusion, thereby facilitating NE translocation into the nucleus, which finally results in chromatin decondensation and NETs release [66]. Considering the high motility of *A. vasorum* L3, attachment of these larvae onto coverslips is revealed as problematic, even when applying adhesion-promoting compounds, such as poly-L-lysine [8,32,62]. Irrespective of coverslip treatments, vital *A. vasorum* L3 were consistently moving away from PMN to areas of coverslips where PMN were less abundant. Despite these efforts of escape, PMN successfully captured several larvae as visualized by SEM; nevertheless, future studies are required to confirm the importance of this observation *in vivo*. Current observations mainly indicated suicidal NETs formation, which corresponds well to previous NET-related reports on motile protozoan and metazoan parasites [8,27,30,38,62].

Given that PMN are highly present in the blood circulation, complex interactions between this innate immune cell type and activated endothelial cells of blood and lymphatic vessels have been described and also play a fundamental role in the pathogenesis of various parasite infections [42,68–70]. Thus, changes in the permeability of endothelium

## 2.2 Canine *Angiostrongylus vasorum*-induced early innate immune reactions based on NETs formation and canine vascular endothelial cell activation *in vitro*.

upon inflammation or parasite infection are common [42,71]. Analyses of the expression of typical adhesion molecules serve as indicator of endothelial cell activation. Therefore, we here monitored expression profiles of P-selectin, E-selectin, VCAM-1 and ICAM-1 in parasite antigen-stimulated canine primary endothelial cells. Even though adhesion molecule-related reactions proved highly variable between time points and isolates, they reflected *AvAg*-driven endothelial activation, thus forming part of early host innate immune response against *A. vasorum*. This variation in endothelium-derived pro-inflammatory reactions were also confirmed between the different CAEC donors used. Therefore, individual variations concerning host innate reactions might be linked to different clinical manifestations during canine angiostrongylosis as previously reported [18]. In line with the current data, several studies on canine angiostrongylosis reported on pathological findings which are in the long term necessarily linked to endothelial cell activation. Thus, formation and endothelial adhesion of antigen-antibody-complexes, thrombus formation and vessel inflammation lead to altered endothelial physiology and integrity [54–56]. An indirect evidence of endothelial alteration in canine angiostrongylosis comes from vWF-related findings. vWF is considered as a typical marker of activated endothelial cells. It captures circulating platelets to the site of vascular injury and mediates subsequent platelet activation and aggregation [72,73]. Interestingly, vWF serum levels were consistently found elevated in naturally *A. vasorum*-infected dogs [12,74], thereby most likely reflecting endothelial cell activation. Multimers of vWF, released from activated endothelium, were recorded as spontaneously recruiting excessive circulating platelets and PMN, thereby promoting intravascular thrombosis [72], which is commonly observed in severe cases of canine angiostrongylosis [54,56]. Of note, the metalloprotease ADAMTS13, which is also present in PMN granules [75], specifically cleaves vWF-A2 domains to regulate the size and activity of vWF multimers [76,77], thereby hampering thrombus formation [73,78]. Linking these events, several studies showed that NETs are also involved in venous and arterial thrombus formation [73]. Moreover, NETs directly interact via electrostatic forces and by DNA or H2A with endothelium [42,76] and eventually directly affect endothelial physiology. Taking into account that both vWF and NETs own pro-thrombotic and pro-inflammatory properties, it seems plausible to speculate that interactions between *A. vasorum*-induced NETs and vWF might promote the development of coagulopathies and bleeding disorders in clinical canine angiostrongylosis [12]. Moreover, future studies are necessary to link both processes in order to better understand the whole complex cascade of *A. vasorum*-induced coagulopathies and bleeding disorders *in vivo*.

### 5. Conclusions

Overall, we here demonstrated for the first time that exposure of primary canine endothelial cells to soluble *AvAg* resulted in pro-inflammatory activation as part of early host innate immune response against axenic *A. vasorum* L3. Finally, *A. vasorum* L3 was able to strongly induce NETosis in canine PMN and *spr*NETs being the most abundant phenotype observed.

**Supplementary Materials:** The following are available online at <https://www.mdpi.com/article/10.3390/biology10050427/s1>, Figure S1: Complete Western Blot acquisitions from E-Selectin, P-Selectin, VCAM-1 and Vinculin.

**Author Contributions:** C.H., A.T., R.S. and I.C.: conceptualization and experimental design. D.G., S.L.-O., and L.S., isolated, purified, and provided the parasites and canine PMN for this study. U.G. conducted scanning electron microscopy analysis. R.S., participated in design of project and experiments by isolating, purifying and providing parasites and blood for the current investigation and reviewed manuscript. L.S. and D.G., analyzed the data and carried out most of NETs experiments. Z.D.V., performed adhesion molecule expression experiments. I.C., analyzed the data of expression experiments. L.S., D.G., I.C. and C.H., prepared the manuscript. All authors have read and agreed to the published version of the manuscript.

## 2.2 Canine *Angiostrongylus vasorum*-induced early innate immune reactions based on NETs formation and canine vascular endothelial cell activation *in vitro*.

**Funding:** D.G. is funded by the Chilean Scholarship Program Doctorado Becas Chile Number/2019-72200437 from the National Agency for Research and Development. The publication fees were partially funded by the Open Access Publication Fund from JLU Giessen.

**Institutional Review Board Statement:** This study was carried out in accordance with the recommendations of the local animal care and use committee and by governmental authorities (LANUV #200/A176 and #200/A154) extended Elanco Animal Health (Monheim, Germany).

**Informed Consent Statement:** Not applicable.

**Data Availability Statement:** The raw data supporting the conclusions of this article will be made available by the authors, without undue reservation.

**Acknowledgments:** The authors would like to acknowledge Anika Seipp, Institute of Anatomy and Cell Biology, Justus Liebig Universität Giessen, Giessen, Germany, for her technical support in scanning electron microscopy analyses. We further thank all staff members of Elanco Animal Health GmbH, Germany, which were involved in the maintenance of *A. vasorum* life cycle and sample collection.

**Conflicts of Interest:** The author R.S. was employed at Elanco Animal Health, Monheim, Germany, at the moment of research. The authors declare that this study was mainly financed by the Institute of Parasitology, Justus Liebig University Giessen, Germany, and partially supported by Elanco Animal Health, Monheim, Germany. All other authors declare no competing interests.

### References

1. Traversa, D.; Di Cesare, A.; Conboy, G. Canine and feline cardiopulmonary parasitic nematodes in Europe: Emerging and underestimated. *Parasites Vectors* **2010**, *3*, 62. [\[CrossRef\]](#)
2. Schnyder, M.; Bilbrough, G.; Hafner, C.; Schaper, R. *Angiostrongylus vasorum*, “The French Heartworm”: A Serological Survey in Dogs from France Introduced by a Brief Historical Review. *Parasitol. Res.* **2017**, *116*, 31–40. [\[CrossRef\]](#) [\[PubMed\]](#)
3. Alho, A.M.; Meireles, J.; Schnyder, M.; Cardoso, L.; Belo, S.; Deplazes, P.; de Carvalho, L.M. *Dirofilaria immitis* and *Angiostrongylus vasorum*: The current situation of two major canine heartworms in Portugal. *Vet. Parasitol.* **2018**, *252*, 120–126. [\[CrossRef\]](#) [\[PubMed\]](#)
4. Hermosilla, C.; Kleinertz, S.; Silva, L.M.; Hirtzmann, J.; Huber, D.; Kusak, J.; Taubert, A. Protozoan and helminth parasite fauna of free-living Croatian wild wolves (*Canis lupus*) analyzed by scat collection. *Vet. Parasitol.* **2017**, *233*, 14–19. [\[CrossRef\]](#) [\[PubMed\]](#)
5. Schug, K.; Kramer, F.; Schaper, R.; Hirtzmann, J.; Failing, K.; Hermosilla, C.; Taubert, A. Prevalence survey on lungworm (*Angiostrongylus vasorum*, *Crenosoma vulpis*, *Eucoleus aerophilus*) infections of wild red foxes (*Vulpes vulpes*) in central Germany. *Parasites Vectors* **2018**, *11*, 85. [\[CrossRef\]](#) [\[PubMed\]](#)
6. Gavrilović, P.; Dobrosavljević, I.; Vasković, N.; Todorović, I.; Živulj, A.; Kureljušić, B.; Pavlović, I. Cardiopulmonary parasitic nematodes of the red fox (*Vulpes vulpes*) in Serbia. *Acta Vet. Hung.* **2019**, *67*, 60–69. [\[CrossRef\]](#)
7. Patel, Z.; Gill, A.C.; Fox, M.T.; Hermosilla, C.; Backeljau, T.; Bruegelmans, K.; Keevash, E.; McEwan, C.; Aghazadeh, M.; Elson-Riggins, J.G. Molecular identification of novel intermediate host species of *Angiostrongylus vasorum* in Greater London. *Parasitol. Res.* **2014**, *113*, 4363–4369. [\[CrossRef\]](#)
8. Lange, M.K.; Penagos-Tabares, F.; Muñoz-Carro, I.; Gärtner, U.; Mejer, H.; Schaper, K.; Hermosilla, C.; Taubert, A. Gastro-pod-derived haemocyte extracellular traps entrap metastrongyloid larval stages of *Angiostrongylus vasorum*, *Aelurostrongylus abstrusus* and *Troglostrongylus brevior*. *Parasites Vectors* **2017**, *10*, 50. [\[CrossRef\]](#) [\[PubMed\]](#)
9. Penagos-Tabares, F.; Lange, M.K.; Vélez, J.; Hirtzmann, J.; Gutiérrez-Arboleda, J.; Taubert, A.; Hermosilla, C.; Chaparro Gutiérrez, J.J. The invasive giant African snail *Lissachatina fulica* as natural intermediate host of *Aelurostrongylus abstrusus*, *Angiostrongylus vasorum*, *Troglostrongylus brevior*, and *Crenosoma vulpis* in Colombia. *PLoS Negl. Trop. Dis.* **2019**, *13*, e0007277. [\[CrossRef\]](#)
10. Morgan, E.R.; Shaw, S.E.; Brennan, S.F.; De Waal, T.D.; Jones, B.R.; Mulcahy, G. *Angiostrongylus vasorum*: A real heartbreaker. *Trends Parasitol.* **2005**, *21*, 49–51. [\[CrossRef\]](#) [\[PubMed\]](#)
11. Taubert, A.; Pantchev, N.; Vrhovec, M.G.; Bauer, C.; Hermosilla, C. Lungworm infections (*Angiostrongylus vasorum*, *Crenosoma vulpis*, *Aelurostrongylus abstrusus*) in dogs and cats in Germany and Denmark in 2003–2007. *Vet. Parasitol.* **2009**, *159*, 175–180. [\[CrossRef\]](#) [\[PubMed\]](#)
12. Adamantos, S.; Waters, S.; Boag, A. Coagulation status in dogs with naturally occurring *Angiostrongylus vasorum* infection. *J. Small Anim. Pr.* **2015**, *56*, 485–490. [\[CrossRef\]](#) [\[PubMed\]](#)
13. Helm, J.; Roberts, L.; Jefferies, R.; Shaw, S.E.; Morgan, E.R. Epidemiological survey of *Angiostrongylus vasorum* in dogs and slugs around a new endemic focus in Scotland. *Vet. Rec.* **2015**, *177*, 46. [\[CrossRef\]](#) [\[PubMed\]](#)
14. Maksimov, P.; Hermosilla, C.; Taubert, A.; Staubach, C.; Sauter-Louis, C.; Conraths, F.J.; Vrhovec, M.G.; Pantchev, N. GIS-supported epidemiological analysis on canine *Angiostrongylus vasorum* and *Crenosoma vulpis* infections in Germany. *Parasites Vectors* **2017**, *10*, 108. [\[CrossRef\]](#) [\[PubMed\]](#)

## 2.2 Canine *Angiostrongylus vasorum*-induced early innate immune reactions based on NETs formation and canine vascular endothelial cell activation *in vitro*.

15. Conboy, G.A. Canine angiostrongylosis: The French heartworm: An emerging threat in North America. *Vet. Parasitol.* **2011**, *176*, 382–389. [[CrossRef](#)]
16. Lange, M.K.; Penagos-Tabares, F.; Hirtzmann, J.; Failing, K.; Schaper, R.; Van Bourgonie, Y.R.; Backeljau, T.; Hermosilla, C.; Taubert, A. Prevalence of *Angiostrongylus vasorum*, *Aelurostrongylus abstrusus* and *Crenosoma vulpis* larvae in native slug populations in Germany. *Vet. Parasitol.* **2018**, *254*, 120–130. [[CrossRef](#)] [[PubMed](#)]
17. Penagos-Tabares, F.; Lange, M.K.; Seipp, A.; Gärtner, U.; Mejer, H.; Taubert, A.; Hermosilla, C. Novel approach to study gastropod-mediated innate immune reactions against metastrongyloid parasites. *Parasitol. Res.* **2018**, *117*, 1211–1224. [[CrossRef](#)] [[PubMed](#)]
18. Chapman, P.S.; Boag, A.K.; Guitian, J.; Boswood, A. *Angiostrongylus vasorum* infection in 23 dogs (1999–2002). *J. Small Anim. Pr.* **2004**, *45*, 435–440. [[CrossRef](#)] [[PubMed](#)]
19. Koch, J.; Willesen, J.L. Canine pulmonary angiostrongylosis: An update. *Vet. J.* **2009**, *179*, 348–359. [[CrossRef](#)] [[PubMed](#)]
20. Schnyder, M.; Fahrion, A.; Riond, B.; Ossent, P.; Webster, P.; Kranjc, A.; Glaus, T.; Deplazes, P. Clinical, laboratory and pathological findings in dogs experimentally infected with *Angiostrongylus vasorum*. *Parasitol. Res.* **2010**, *107*, 1471–1480. [[CrossRef](#)] [[PubMed](#)]
21. Brinkmann, V.; Reichard, U.; Goosmann, C.; Fauler, B.; Uhlemann, Y.; Weiss, D.S.; Weinrauch, Y.; Zychlinsky, A. Neutrophil extracellular traps kill bacteria. *Science* **2004**, *303*, 1532–1535. [[CrossRef](#)]
22. Fuchs, T.A.; Abed, U.; Goosmann, C.; Hurwitz, R.; Schulze, I.; Wahn, V.; Weinrauch, Y.; Brinkmann, V.; Zychlinsky, A. Novel cell death program leads to neutrophil extracellular traps. *J. Cell Biol.* **2007**, *176*, 231–241. [[CrossRef](#)]
23. Papayannopoulos, V. Neutrophil extracellular traps in immunity and disease. *Nat. Rev. Immunol.* **2018**, *18*, 134–147. [[CrossRef](#)]
24. Urban, C.F.; Reichard, U.; Brinkmann, V.; Zychlinsky, A. Neutrophil extracellular traps capture and kill *Candida albicans* yeast and hyphal forms. *Cell. Microbiol.* **2006**, *8*, 668–676. [[CrossRef](#)]
25. Papayannopoulos, V.; Metzler, K.D.; Hakkim, A.; Zychlinsky, A. Neutrophil elastase and myeloperoxidase regulate the formation of neutrophil extracellular traps. *J. Cell Biol.* **2010**, *191*, 677–691. [[CrossRef](#)] [[PubMed](#)]
26. Tanaka, K.; Koike, Y.; Shimura, T.; Okigami, M.; Ide, S.; Toyama, Y.; Okugawa, Y.; Inoue, Y.; Araki, T.; Uchida, K.; et al. In Vivo Characterization of Neutrophil Extracellular Traps in Various Organs of a Murine Sepsis Model. *PLoS ONE* **2014**, *9*, e111888. [[CrossRef](#)]
27. Grob, D.; Conejeros, I.; Velásquez, Z.D.; Preußer, C.; Gärtner, U.; Alarcón, P.; Burgos, R.A.; Hermosilla, C.; Taubert, A. Trypanosoma brucei brucei Induces Polymorphonuclear Neutrophil Activation and Neutrophil Extracellular Traps Release. *Front. Immunol.* **2020**, *11*, 559561. [[CrossRef](#)] [[PubMed](#)]
28. Imlau, M.; Conejeros, I.; Muñoz-Caro, T.; Zhou, E.; Gärtner, U.; Ternes, K.; Taubert, A.; Hermosilla, C. Dolphin-derived NETosis results in rapid *Toxoplasma gondii* tachyzoite ensnarement and different phenotypes of NETs. *Dev. Comp. Immunol.* **2020**, *103*, 103527. [[CrossRef](#)] [[PubMed](#)]
29. Schauer, C.; Janko, C.; Muñoz, L.E.; Zhao, Y.; Kienhöfer, D.; Frey, B.; Lell, M.; Manger, B.; Rech, J.; Naschberger, E.; et al. Aggregated neutrophil extracellular traps limit inflammation by degrading cytokines and chemokines. *Nat. Med.* **2014**, *20*, 511–517. [[CrossRef](#)] [[PubMed](#)]
30. Muñoz-Caro, T.; Conejeros, I.; Zhou, E.; Pikhovych, A.; Gärtner, U.; Hermosilla, C.; Kulke, D.; Taubert, A. *Dirofilaria immitis* Microfilariae and Third-Stage Larvae Induce Canine NETosis Resulting in Different Types of Neutrophil Extracellular Traps. *Front. Immunol.* **2018**, *9*, 968. [[CrossRef](#)]
31. Hakkim, A.; Fuchs, T.A.; Martinez, N.E.; Hess, S.; Prinz, H.; Zychlinsky, A.; Waldmann, H. Activation of the Raf-MEK-ERK pathway is required for neutrophil extracellular trap formation. *Nat. Chem. Biol.* **2010**, *7*, 75–77. [[CrossRef](#)]
32. Muñoz-Caro, T.; Mena Huertas, S.J.; Conejeros, I.; Alarcón, F.; Hidalgo, M.A.; Burgos, R.A.; Hermosilla, C.; Taubert, A. *Eimeria* bovis-triggered neutrophil extracellular trap formation is CD11b-, ERK 1/2-, p38 MAP kinase- and SOCE-dependent. *Vet. Res.* **2015**, *46*, 23. [[CrossRef](#)] [[PubMed](#)]
33. Li, R.H.L.; Ng, G.; Tablin, F. Lipopolysaccharide-induced neutrophil extracellular trap formation in canine neutrophils is dependent on histone H3 citrullination by peptidylarginine deiminase. *Vet. Immunol. Immunopathol.* **2017**, *193*–194, 29–37. [[CrossRef](#)] [[PubMed](#)]
34. Wei, Z.; Zhang, X.; Wang, J.; Wang, Y.; Yang, Z.; Fu, Y. The formation of canine neutrophil extracellular traps induced by sodium arsenic in polymorphonuclear neutrophils. *Chemosphere* **2018**, *196*, 297–302. [[CrossRef](#)]
35. Jeffery, U.; Kimura, K.; Gray, R.; Lueth, P.; Bellaire, B.; LeVine, D. Dogs cast NETs too: Canine neutrophil extracellular traps in health and immune-mediated hemolytic anemia. *Vet. Immunol. Immunopathol.* **2015**, *168*, 262–268. [[CrossRef](#)]
36. Wei, Z.; Hermosilla, C.; Taubert, A.; He, X.; Wang, X.; Gong, P.; Li, J.; Yang, Z.; Zhang, X. Canine Neutrophil Extracellular Traps Release Induced by the Apicomplexan Parasite *Neospora caninum* in vitro. *Front. Immunol.* **2016**, *7*, 436. [[CrossRef](#)]
37. Bonne-Année, S.; Kerepesi, L.A.; Hess, J.A.; Wesolowski, J.; Paumet, F.; Lok, J.B.; Nolan, T.J.; Abraham, D. Extracellular traps are associated with human and mouse neutrophil and macrophage mediated killing of larval *Strongyloides stercoralis*. *Microbes Infect.* **2014**, *16*, 502–511. [[CrossRef](#)] [[PubMed](#)]
38. Muñoz-Caro, T.; Rubio, R.M.; Silva, L.M.; Magdowski, G.; Gartner, U.; McNeilly, T.N.; Taubert, A.; Hermosilla, C. Leucocyte-derived extracellular trap formation significantly contributes to *Haemonchus contortus* larval entrapment. *Parasites Vectors* **2015**, *8*, 607. [[CrossRef](#)]

## 2.2 Canine *Angiostrongylus vasorum*-induced early innate immune reactions based on NETs formation and canine vascular endothelial cell activation *in vitro*.

39. McCoy, C.J.; Reaves, B.J.; Giguère, S.; Coates, R.; Rada, B.; Wolstenholme, A.J. Human Leukocytes Kill *Brugia malayi* Microfilariae Independently of DNA-Based Extracellular Trap Release. *PLoS Negl. Trop. Dis.* **2017**, *11*, e0005279. [[CrossRef](#)] [[PubMed](#)]
40. Mendez, J.; Sun, D.; Tuo, W.; Xiao, Z. Bovine neutrophils form extracellular traps in response to the gastrointestinal parasite *Ostertagia ostertagi*. *Sci. Rep.* **2018**, *8*, 17598. [[CrossRef](#)]
41. Maksimov, P.; Hermosilla, C.; Kleinertz, S.; Hirtzmann, J.; Taubert, A. *Besnoitia besnoiti* infections activate primary bovine endothelial cells and promote PMN adhesion and NET formation under physiological flow condition. *Parasitol. Res.* **2016**, *115*, 1991–2001. [[CrossRef](#)]
42. Conejeros, I.; Velásquez, Z.D.; Grob, D.; Zhou, E.; Salecker, H.; Hermosilla, C.; Taubert, A. Histone H2A and Bovine Neutrophil Extracellular Traps Induce Damage of *Besnoitia besnoiti*-Infected Host Endothelial Cells but Fail to Affect Total Parasite Proliferation. *Biology* **2019**, *8*, 78. [[CrossRef](#)]
43. Zhou, E.; Conejeros, I.; Gärtner, U.; Mazurek, S.; Hermosilla, C.; Taubert, A. Metabolic requirements of *Besnoitia besnoiti* tachyzoite-triggered NETosis. *Parasitol. Res.* **2020**, *119*, 545–557. [[CrossRef](#)]
44. Glaus, T.; Schnyder, M.; Dennler, M.; Tschuor, F.; Wenger, M.; Sieber-Ruckstuhl, N. Natural infection with *Angiostrongylus vasorum*: Characterisation of 3 dogs with pulmonary hypertension. *Schweiz. Arch. Tierheilkd.* **2010**, *152*, 331–338. [[CrossRef](#)]
45. Chiu, P.S.; Lai, S.C. Matrix metalloproteinase-9 leads to blood–brain barrier leakage in mice with eosinophilic meningoencephalitis caused by *Angiostrongylus cantonensis*. *Acta Trop.* **2014**, *140*, 141–150. [[CrossRef](#)]
46. Mupanomunda, M.; Williams, J.F.; MacKenzie, C.D.; Kaiser, L. *Dirofilaria immitis*: Heartworm infection alters pulmonary artery endothelial cell behavior. *J. Appl. Physiol.* **1997**, *82*, 389–398. [[CrossRef](#)]
47. Kramer, L.; Grandi, G.; Passeri, B.; Gianelli, P.; Genchi, M.; Dzimianski, M.T.; Supakorndej, P.; Mansour, A.M.; Supakorndej, N.; McCall, S.D.; et al. Evaluation of lung pathology in *Dirofilaria immitis*-experimentally infected dogs treated with doxycycline or a combination of doxycycline and ivermectin before administration of melarsomine dihydrochloride. *Vet. Parasitol.* **2011**, *176*, 357–360. [[CrossRef](#)]
48. Lip, G.Y.; Blann, A. von Willebrand factor: A marker of endothelial dysfunction in vascular disorders? *Cardiovasc. Res.* **1997**, *34*, 255–265. [[CrossRef](#)]
49. Brott, D.A.; Katein, A.; Thomas, H.; Lawton, M.; Montgomery, R.R.; Richardson, R.J.; Loudon, C.S. Evaluation of von Willebrand Factor and von Willebrand Factor Propeptide in Models of Vascular Endothelial Cell Activation, Perturbation, and/or Injury. *Toxicol. Pathol.* **2014**, *42*, 672–683. [[CrossRef](#)]
50. Levine, D.N.; Cianciolo, R.E.; Linder, K.E.; Bizikova, P.; Birkenheuer, A.J.; Brooks, M.B.; Salous, A.K.; Nordone, S.K.; Bellinger, D.A.; Marr, H.; et al. Endothelial alterations in a canine model of immune thrombocytopenia. *Platelets* **2019**, *30*, 88–97. [[CrossRef](#)]
51. Denis, C.V. Molecular and Cellular Biology of von Willebrand Factor. *Int. J. Hematol.* **2002**, *75*, 3–8. [[CrossRef](#)]
52. Livak, K.J.; Schmittgen, T.D. Analysis of relative gene expression data using real-time quantitative PCR and the 2<sup>-</sup>(Delta Delta C(T)) Method. *Methods* **2001**, *25*, 402–408. [[CrossRef](#)]
53. Di Cesare, A.; Traversa, D. Canine angiostrongylosis: Recent advances in diagnosis, prevention, and treatment. *Vet. Med.* **2014**, *5*, 181–192. [[CrossRef](#)]
54. Rinaldi, L.; Cortese, L.; Meomartino, L.; Pagano, T.B.; Pepe, P.; Cringoli, G.; Papparella, S. *Angiostrongylus vasorum*: Epidemiological, clinical and histopathological insights. *BMC Vet. Res.* **2014**, *10*, 236. [[CrossRef](#)]
55. Barçante, J.M.; Barçante, T.A.; Dias, S.R.; Vieira, L.Q.; Lima, W.S.; Negrão-Corrêa, D. A method to obtain axenic *Angiostrongylus vasorum* first-stage larvae from dog feces. *Parasitol. Res.* **2003**, *89*, 89–93. [[CrossRef](#)]
56. Bourque, A.C.; Conboy, G.; Miller, L.M.; Whitney, H. Pathological Findings in Dogs Naturally Infected with *Angiostrongylus vasorum* in Newfoundland and Labrador, Canada. *J. Vet. Diagn. Investig.* **2008**, *20*, 11–20. [[CrossRef](#)]
57. Neumann, A.; Brogden, G.; Von Köckritz-Blickwede, M. Extracellular Traps: An Ancient Weapon of Multiple Kingdoms. *Biology* **2020**, *9*, 34. [[CrossRef](#)]
58. Zhou, E.; Conejeros, I.; Velásquez, Z.D.; Muñoz-Caro, T.; Gärtner, U.; Hermosilla, C.; Taubert, A. Simultaneous and Positively Correlated NET Formation and Autophagy in *Besnoitia besnoiti* Tachyzoite-Exposed Bovine Polymorphonuclear Neutrophils. *Front. Immunol.* **2019**, *10*, 1131. [[CrossRef](#)]
59. Hahn, J.; Schauer, C.; Czegley, C.; Kling, L.; Petru, L.; Schmid, B.; Weidner, D.; Reinwald, C.; Biermann, M.H.C.; Blunder, S.; et al. Aggregated neutrophil extracellular traps resolve inflammation by proteolysis of cytokines and chemokines and protection from antiproteases. *FASEB J.* **2019**, *33*, 1401–1414. [[CrossRef](#)]
60. Knopf, J.; Leppkes, M.; Schett, G.; Herrmann, M.; Muñoz, L.E. Aggregated NETs Sequester and Detoxify Extracellular Histones. *Front. Immunol.* **2019**, *10*, 2176. [[CrossRef](#)]
61. Mahajan, A.; Grüneboom, A.; Petru, L.; Podolska, M.J.; Kling, L.; Maueröder, C.; Dahms, F.; Christiansen, S.; Günter, L.; Krenn, V.; et al. Frontline Science: Aggregated neutrophil extracellular traps prevent inflammation on the neutrophil-rich ocular surface. *J. Leukoc. Biol.* **2019**, *105*, 1087–1098. [[CrossRef](#)]
62. Peixoto, R.; Silva, L.M.R.; López-Osorio, S.; Zhou, E.; Gärtner, U.; Conejeros, I.; Taubert, A.; Hermosilla, C. *Fasciola hepatica* induces weak NETosis and low production of intra- and extracellular ROS in exposed bovine polymorphonuclear neutrophils. *Dev. Comp. Immunol.* **2021**, *114*, 103787. [[CrossRef](#)]
63. Van Breda, S.V.; Vokalova, L.; Neugebauer, C.; Rossi, S.W.; Hahn, S.; Hasler, P. Computational Methodologies for the *in vitro* and *in situ* Quantification of Neutrophil Extracellular Traps. *Front. Immunol.* **2019**, *10*, 1562. [[CrossRef](#)] [[PubMed](#)]

## 2.2 Canine *Angiostrongylus vasorum*-induced early innate immune reactions based on NETs formation and canine vascular endothelial cell activation *in vitro*.

64. Rebernick, R.; Fahmy, L.; Glover, C.; Bawadekar, M.; Shim, D.; Holmes, C.L.; Rademacher, N.; Potluri, H.; Bartels, C.M.; Shelif, M.A. DNA Area and NETosis Analysis (DNA): A High-Throughput Method to Quantify Neutrophil Extracellular Traps in Fluorescent Microscope Images. *Biol. Proced. Online* **2018**, *20*, 7. [[CrossRef](#)] [[PubMed](#)]
65. Guo, A.J.; Wang, L.; Meng, X.L.; Zhang, S.H.; Sheng, Z.A.; Wei, Z.K.; Luo, X.N.; Huang, W.Y.; Zhu, X.Q.; Zhang, X.C.; et al. Newly eysted juveniles of *Fasciola gigantica* trigger the release of water buffalo neutrophil extracellular traps *in vitro*. *Exp. Parasitol.* **2020**, *211*, 107828. [[CrossRef](#)] [[PubMed](#)]
66. Branzk, N.; Lubojemska, A.; Hardison, S.E.; Wang, Q.; Gutierrez, M.G.; Brown, G.D.; Papayannopoulos, V. Neutrophils sense microbe size and selectively release neutrophil extracellular traps in response to large pathogens. *Nat. Immunol.* **2014**, *15*, 1017–1025. [[CrossRef](#)]
67. Silva, L.M.; Muñoz-Caro, T.; Burgos, R.A.; Hidalgo, M.A.; Taubert, A.; Hermosilla, C. Far beyond Phagocytosis: Phagocyte-Derived Extracellular Traps Act Efficiently against Protozoan Parasites *in vitro* and *In Vivo*. *Mediat. Inflamm.* **2016**, *2016*, 5898074. [[CrossRef](#)]
68. Deckert-Schlüter, M.; Schlüter, D.; Hof, H.; Wiestler, O.D.; Lassmann, H. Differential Expression of ICAM-1, VCAM-1 and Their Ligands LFA-1, Mac-1, CD43, VLA-4, and MHC Class II Antigens in Murine Toxoplasma Encephalitis: A Light Microscopic and Ultrastructural Immunohistochemical Study. *J. Neuropathol. Exp. Neurol.* **1994**, *53*, 457–468. [[CrossRef](#)]
69. Hermosilla, C.; Ruiz, A.; Taubert, A. *Eimeria bovis*: An update on parasite–host cell interactions. *Int. J. Med. Microbiol.* **2012**, *302*, 210–215. [[CrossRef](#)]
70. Raza, A.; Ghanchi, N.K.; Sarwar Zubairi, A.; Raheem, A.; Nizami, S.; Beg, M.A. Tumor Necrosis Factor - $\alpha$ , Interleukin-10, Interleukin and Vascular Adhesion Molecules Are Possible Biomarkers of Disease Severity in Complicated *Plasmodium vivax* Isolates from Pakistan. *PLoS ONE* **2013**, *8*, e81363. [[CrossRef](#)]
71. DiStasi, M.R.; Ley, K. Opening the flood-gates: How neutrophil-endothelial interactions regulate permeability. *Trends Immunol.* **2009**, *30*, 547–556. [[CrossRef](#)] [[PubMed](#)]
72. Löf, A.; Müller, J.P.; Brehm, M.A. A biophysical view on von Willebrand factor activation. *J. Cell. Physiol.* **2018**, *233*, 799–810. [[CrossRef](#)] [[PubMed](#)]
73. Yang, J.; Wu, Z.; Long, Q.; Huang, J.; Hong, T.; Liu, W.; Lin, J. Insights into Immunothrombosis: The Interplay among Neutrophil Extracellular Trap, von Willebrand Factor, and ADAMTS13. *Front. Immunol.* **2020**, *11*, 610696. [[CrossRef](#)]
74. Whitley, N.T.; Corzo-Mendez, N.; Carmichael, N.G.; McGarry, J.W. Cerebral and conjunctival haemorrhages associated with von Willebrand factor deficiency and canine angiostrongylosis. *J. Small Anim. Pr.* **2005**, *46*, 75–78. [[CrossRef](#)]
75. Pillai, V.G.; Bao, J.; Zander, C.B.; McDaniel, J.K.; Chetty, P.S.; Seeholzer, S.H.; Bdeir, K.; Cines, D.B. Human neutrophil peptides inhibit cleavage of von Willebrand factor by ADAMTS13: A potential link of inflammation to TTP. *Blood* **2016**, *128*, 110–119. [[CrossRef](#)]
76. Grässle, S.; Huck, V.; Pappelbaum, K.I.; Gorzelanny, C.; Aponte-Santamaría, C.; Baldauf, C.; Gräter, F.; Schneppenheim, R.; Obser, T.; Schneider, S.W. von Willebrand Factor Directly Interacts With DNA From Neutrophil Extracellular Traps. *Arter. Thromb. Vasc. Biol.* **2014**, *34*, 1382–1389. [[CrossRef](#)]
77. Thälín, C.; Hisada, Y.; Lundström, S.; Mackman, N.; Wallén, H. Neutrophil Extracellular Traps: Villains and Targets in Arterial, Venous, and Cancer-Associated Thrombosis. *Arter. Thromb. Vasc. Biol.* **2019**, *39*, 1724–1738. [[CrossRef](#)] [[PubMed](#)]
78. Zhang, X.; Halvorsen, K.; Zhang, C.Z.; Wong, W.P.; Springer, T.A. Mechanoenzymatic Cleavage of the Ultralarge Vascular Protein von Willebrand Factor. *Science* **2009**, *324*, 1330–1334. [[CrossRef](#)]

### **2.3. HISTONE H2A AND BOVINE NEUTROPHIL EXTRACELLULAR TRAPS INDUCE DAMAGE OF *BESNOITIA BESNOITI*-INFECTED HOST ENDOTHELIAL CELLS BUT FAIL TO AFFECT TOTAL PARASITE PROLIFERATION**

This chapter is based on the following publish paper:

Conejeros, I.; Velásquez, Z.D.; Grob, D.; Zhou, E.; Salecker, H.; Hermosilla, C.; Taubert, A. Histone H2A and Bovine Neutrophil Extracellular Traps Induce Damage of *Besnoitia besnoiti*-Infected Host Endothelial Cells but Fail to Affect Total Parasite Proliferation. *Biology* 2019, 8, 78.

Eigener Anteil in der Publikation:

Projektplanung	40 %, zusammen mit Ko-Autoren und Betreuern
Durchführung des Versuches	40 %, weitestgehend selbständig
Auswertung der Experimente	40 %, weitestgehend selbständig
Erstellung der Publikation	40 %, weitestgehend selbständig

## 2.3 Histone H2A and bovine neutrophil extracellular traps induce damage of *Besnoitia besnoiti*-infected host endothelial cells but fail to affect total parasite proliferation



Article

### Histone H2A and Bovine Neutrophil Extracellular Traps Induce Damage of *Besnoitia besnoiti*-Infected Host Endothelial Cells but Fail to Affect Total Parasite Proliferation

Iván Conejeros \*<sup>†</sup>, Zahady D. Velásquez <sup>†</sup>, Daniela Grob, Ershun Zhou, Hannah Salecker, Carlos Hermosilla and Anja Taubert

Institute of Parasitology, Biomedical Research Center Seltersberg, Justus Liebig University-Giessen, 35392 Giessen, Germany; zahady.velasquez@vetmed.uni-giessen.de (Z.D.V.); daniela.grob@vetmed.uni-giessen.de (D.G.); ershun.zhou@vetmed.uni-giessen.de (E.Z.); hannah.salecker@vetmed.uni-giessen.de (H.S.); carlos.r.hermosilla@vetmed.uni-giessen.de (C.H.); anja.taubert@vetmed.uni-giessen.de (A.T.)

\* Correspondence: ivan.conejeros@vetmed.uni-giessen.de; Tel.: +49-641-99-38478

<sup>†</sup> These authors contributed equally.

Received: 19 July 2019; Accepted: 9 October 2019; Published: 11 October 2019



**Abstract:** *Besnoitia besnoiti* tachyzoites infect and develop in bovine endothelial cells in vivo and trigger the release of neutrophil extracellular traps (NETs) from bovine polymorphonuclear neutrophils (PMN). The purpose of this study was to analyze if pure *B. besnoiti* tachyzoite-triggered NETs would damage endothelial host cells and subsequently influence intracellular development and proliferation of *B. besnoiti* tachyzoites in primary bovine endothelial cells. For comparison purposes, isolated A23187-induced NETs were also used. Thus, we here evaluated endothelial host cell damage triggered by histone 2A (H2A) and *B. besnoiti* tachyzoite-induced NET preparations and furthermore estimated the effects of PMN floating over *B. besnoiti*-infected endothelium under physiological flow conditions on endothelial host cell viability. Overall, all treatments (H2A, *B. besnoiti*-triggered NETs and floating PMN) induced endothelial cell death of *B. besnoiti*-infected host cells. However, though host cell damage led to significantly altered intracellular parasite development with respect to parasitophorous vacuole diameter and numbers, the total proliferation of the parasite over time was not significantly affected by these treatments thereby denying any direct effect of NETs on intracellular *B. besnoiti* replication.

**Keywords:** NETs; BUVEC; PMN; endothelium; innate; DNA; histones; *Besnoitia*

#### 1. Introduction

The obligate intracellular parasite *Besnoitia besnoiti* (*B. besnoiti*) replicates in vivo in endothelium and represents the causal agent of besnoitiosis in cattle. Bovine besnoitiosis has a high impact on animal welfare and cattle production. Since 2010, bovine besnoitiosis has been classified as an emerging disease by the European Food Safety Authority (EFSA). Within the life cycle of *B. besnoiti*, cattle act as intermediate hosts whilst the definitive host, shedding oocysts, is still unknown [1–3].

Polymorphonuclear neutrophils (PMN) and endothelium are key players of host innate immune responses both interacting with *B. besnoiti* stages during acute infection [4]. In addition to classical effector mechanisms, such as reactive oxygen species (ROS) production, phagocytosis and degranulation, PMN are able to extrude chromatin structures decorated with granular proteins that are able to ensnare and eventually kill pathogens. These structures were first reported by Brinkmann et al. [5] and named

## 2.3 Histone H2A and bovine neutrophil extracellular traps induce damage of *Besnoitia besnoiti*-infected host endothelial cells but fail to affect total parasite proliferation

---

neutrophil extracellular traps (NETs). They are involved in several physiopathological processes and are described as a defense mechanism that is directed against pathogens (bacteria, fungi, parasites) but also induced by soluble mediators (for review on NET inducers and respective mechanisms please refer to [6,7]). In case of apicomplexan parasites, NETs were reported to be released by PMN of different donor origin in response to stages of *B. besnoiti* [4], *Neospora caninum* [8,9], *Toxoplasma gondii* [10,11], *Eimeria bovis* [12,13], *Plasmodium falciparum* [14], and *Cryptosporidium parvum* [15], thereby highlighting the conserved nature of NETs formation throughout parasite and host species. Specifically regarding *B. besnoiti*-triggered NET formation the process is correlated with a simultaneous increase in autophagy, a process that involves AMPK phosphorylation indicating some insights about the controlling mechanisms in *B. besnoiti*-triggered NETs formation [16].

Direct interactions of PMN or NETs with endothelium at physiological conditions have already been reported [17–19] and indicated a critical role of PMN in the pathophysiology of endothelium impairment. Nonetheless, few data are still available with respect to NET-derived effects on parasite-infected endothelium *in vitro* and *in vivo*. In general, endothelial cells react upon parasite infections by a broad spectrum of immune-related reactions, such as upregulation of adhesion molecules (e.g., ICAM-1, VCAM-1, P-selectin, E-selectin), chemokines and PMN adhesion onto activated endothelium [12,20–24]. With this regard, our previous data showed that *B. besnoiti* infections induced the following early innate immune reactions in primary bovine umbilical endothelial cells (BUVEC): i) Increased gene transcription of adhesion and inflammatory molecules (ICAM-1, CXCL1, CXCL8, CCL5, and COX-2), ii) augmented PMN adhesion to BUVEC layers and iii) release of NETs under physiological flow conditions [20].

PMN-derived NETs affect endothelium by increasing endothelial cell (EC) layer permeability and directly damaging single endothelial cells [25,26]. Additionally, NETs induce the expression of leukocyte adhesion molecules in activated ECs and, consequently, enhance local inflammatory responses [27]. EC damage is mainly explained by transiently increased abundance of proteases/proteins in the microenvironment of vessels. Major NET components that were already proven as inducers of EC damage include histone 2A (H2A) [26]. Core histones are the most abundant proteins on NETs (70% of all NET-associated proteins) and H2A represents the 26.9% of the total NETs protein content [28]. Moreover, differences in cytotoxicity are dependent of the histone type, being H2A, H2B, and H4 individually more cytotoxic than a mixture of histones [29]. In addition, a critical role of histone H4 in lytic cell death of smooth muscle cells and endothelial cells in a mice model of atherosclerosis was reported recently [30]. Altogether, this evidence highlights the importance of NET-derived histones in tissue damage originated by NET-releasing neutrophils.

The aim of the current study was to determine whether bovine PMN and especially *B. besnoiti* tachyzoite-triggered NETs in addition to a major single NET component, such as H2A [27], induce cytotoxicity and damage in ECs and further alter intracellular *B. besnoiti* tachyzoite development in endothelial host cells. The current methods included fluorescence- and confocal microscopy applying static or physiological flow conditions on *B. besnoiti*-infected and non-infected primary bovine umbilical vein endothelial cells (BUVEC). Respective analyses were performed on BUVEC treated with H2A and NET preparations triggered by *B. besnoiti* tachyzoites. For comparison purposes, NETs were also induced by the calcium ionophore and PMN activator A23187 [31–35]. This compound has been successfully used to stimulate PMN and isolate NETs from humans [36].

Current data revealed that *B. besnoiti*-triggered NETs and H2A induced cytotoxicity and damage in *B. besnoiti*-infected bovine endothelial cells. With respect to parasite intracellular development, *B. besnoiti* parasitophorous vacuole (PV) diameter and number per host cell were found diminished in treated BUVEC. However, total tachyzoite proliferation over time was not significantly affected by NET-derived treatments, thereby denying a direct effect of NETs on intracellular *B. besnoiti* replication.

## 2.3 Histone H2A and bovine neutrophil extracellular traps induce damage of *Besnoitia besnoiti*-infected host endothelial cells but fail to affect total parasite proliferation

---

neutrophil extracellular traps (NETs). They are involved in several physiopathological processes and are described as a defense mechanism that is directed against pathogens (bacteria, fungi, parasites) but also induced by soluble mediators (for review on NET inducers and respective mechanisms please refer to [6,7]). In case of apicomplexan parasites, NETs were reported to be released by PMN of different donor origin in response to stages of *B. besnoiti* [4], *Neospora caninum* [8,9], *Toxoplasma gondii* [10,11], *Eimeria bovis* [12,13], *Plasmodium falciparum* [14], and *Cryptosporidium parvum* [15], thereby highlighting the conserved nature of NETs formation throughout parasite and host species. Specifically regarding *B. besnoiti*-triggered NET formation the process is correlated with a simultaneous increase in autophagy, a process that involves AMPK phosphorylation indicating some insights about the controlling mechanisms in *B. besnoiti*-triggered NETs formation [16].

Direct interactions of PMN or NETs with endothelium at physiological conditions have already been reported [17–19] and indicated a critical role of PMN in the pathophysiology of endothelium impairment. Nonetheless, few data are still available with respect to NET-derived effects on parasite-infected endothelium in vitro and in vivo. In general, endothelial cells react upon parasite infections by a broad spectrum of immune-related reactions, such as upregulation of adhesion molecules (e.g., ICAM-1, VCAM-1, P-selectin, E-selectin), chemokines and PMN adhesion onto activated endothelium [12,20–24]. With this regard, our previous data showed that *B. besnoiti* infections induced the following early innate immune reactions in primary bovine umbilical endothelial cells (BUVEC): i) Increased gene transcription of adhesion and inflammatory molecules (ICAM-1, CXCL1, CXCL8, CCL5, and COX-2), ii) augmented PMN adhesion to BUVEC layers and iii) release of NETs under physiological flow conditions [20].

PMN-derived NETs affect endothelium by increasing endothelial cell (EC) layer permeability and directly damaging single endothelial cells [25,26]. Additionally, NETs induce the expression of leukocyte adhesion molecules in activated ECs and, consequently, enhance local inflammatory responses [27]. EC damage is mainly explained by transiently increased abundance of proteases/proteins in the microenvironment of vessels. Major NET components that were already proven as inducers of EC damage include histone 2A (H2A) [26]. Core histones are the most abundant proteins on NETs (70% of all NET-associated proteins) and H2A represents the 26.9% of the total NETs protein content [28]. Moreover, differences in cytotoxicity are dependent of the histone type, being H2A, H2B, and H4 individually more cytotoxic than a mixture of histones [29]. In addition, a critical role of histone H4 in lytic cell death of smooth muscle cells and endothelial cells in a mice model of atherosclerosis was reported recently [30]. Altogether, this evidence highlights the importance of NET-derived histones in tissue damage originated by NET-releasing neutrophils.

The aim of the current study was to determine whether bovine PMN and especially *B. besnoiti* tachyzoite-triggered NETs in addition to a major single NET component, such as H2A [27], induce cytotoxicity and damage in ECs and further alter intracellular *B. besnoiti* tachyzoite development in endothelial host cells. The current methods included fluorescence- and confocal microscopy applying static or physiological flow conditions on *B. besnoiti*-infected and non-infected primary bovine umbilical vein endothelial cells (BUVEC). Respective analyses were performed on BUVEC treated with H2A and NET preparations triggered by *B. besnoiti* tachyzoites. For comparison purposes, NETs were also induced by the calcium ionophore and PMN activator A23187 [31–35]. This compound has been successfully used to stimulate PMN and isolate NETs from humans [36].

Current data revealed that *B. besnoiti*-triggered NETs and H2A induced cytotoxicity and damage in *B. besnoiti*-infected bovine endothelial cells. With respect to parasite intracellular development, *B. besnoiti* parasitophorous vacuole (PV) diameter and number per host cell were found diminished in treated BUVEC. However, total tachyzoite proliferation over time was not significantly affected by NET-derived treatments, thereby denying a direct effect of NETs on intracellular *B. besnoiti* replication.

## 2.3 Histone H2A and bovine neutrophil extracellular traps induce damage of *Besnoitia besnoiti*-infected host endothelial cells but fail to affect total parasite proliferation

vital tachyzoites of *B. besnoiti*. Harvesting of *B. besnoiti* tachyzoites was performed as described previously [4].

### 2.5. Detection of Extracellular DNA and Protein Markers of NETs by Confocal and Fluorescence Microscopy

Bovine PMN were co-cultured with *B. besnoiti* tachyzoites (ratio 1:4) for 3 h (37 °C and 5% CO<sub>2</sub> atmosphere) on 0.01% poly-L-lysine pretreated coverslips (15 mm diameter, Thermo Fisher Scientific, Braunschweig, Germany), fixed by adding 4% paraformaldehyde (Merck) in PBS and stored at 4 °C until further staining.

For NETs visualization, 4',6-Diamidine-2'-phenylindole (DAPI) was used to stain DNA and anti-histone (clone H11-4, 1:200; Merck Millipore (Darmstadt, Germany), #MAB3422) and anti-NE (AB68672, 1:200, Abcam, Cambridge, UK) antibodies were used to stain specific proteins on ETs structures. Therefore, fixed samples were washed three times with PBS, incubated with permeabilization solution (3% BSA, 0.3% Triton X-100 in PBS) for 60 min at room temperature (RT) and incubated with corresponding primary antibodies diluted in permeabilization solution for overnight at 4 °C. Thereafter, samples were washed thrice with PBS and incubated in secondary antibody solutions (Alexa Fluor 488 goat anti-rabbit IgG #A-11008 or Alexa Fluor 594 goat anti-mouse IgG, #A-11005; both Life Technologies (Eugene, Oregon, USA) 30 min, 1:500 in permeabilization solution, RT). Finally, samples were washed thrice in PBS and mounted in DAPI-containing mounting media (Fluoromount G with DAPI; Thermo Fisher Scientific). Visualization was achieved applying confocal microscopy (Zeiss LSM 710, Oberkochen, Germany). Image processing was carried out with Fiji ImageJ software (NIH, USA (<https://imagej.net/Fiji>)) using Z-project and merged channel plugins restricted to overall adjustments of brightness and contrast.

### 2.6. Preparation of *B. besnoiti* Tachyzoite- or A23187-Induced NETs

Isolation of NETs was performed as previously described by Barrientos et al. [36] with some modifications. Briefly,  $1.5 \times 10^6$  bovine PMN/well were seeded in 12-well culture plates and stimulated either with A23187 (5  $\mu$ M) or  $6 \times 10^6$  *B. besnoiti* tachyzoites (= 1:4 PMN:tachyzoites ratio) for 3 h (37 °C, 5% CO<sub>2</sub>). After incubation, the medium was carefully aspirated and wells were washed twice with 1 mL of PBS. Then, 400  $\mu$ L of *AluI* (4 U/mL, New England Biolabs, Ipswich, Massachusetts, USA) were added and plates were incubated for 20 min at 37 °C and 5% CO<sub>2</sub>. Thereafter, samples were recovered and centrifuged for 5 min at 300  $\times$  g to remove cells and debris. NET preparations were immediately stored at -80 °C until further quantification and use.

DNA content of NET preparations was estimated by Quant-iT PicoGreen (Thermo Fisher Scientific). Briefly, 2  $\mu$ L of each NET sample was mixed with 98  $\mu$ L of TE buffer (1 M Tris pH 7.4; 0.5 M EDTA pH = 8.0) and incubated for 5 min at room temperature (RT), protected from light. Afterwards, DNA content was quantified in a Varioskan fluorescence automated multiplate reader (Thermo Scientific, USA) applying exposition/emission wavelengths of 480/520 nm, respectively. All DNA measurements were performed in duplicates. A standard  $\lambda$ -DNA curve was used to interpolate the DNA concentration of the samples.

### 2.7. Estimation of NET-, DNA- and Histone 2A (H2A)-Induced Endothelial Cell Death

Three different BVVEC isolates were cultured to 100% confluency on 96- or 24-well plates (Greiner Bio-One, Frickenhausen, Germany) depending on the experiment setting. For H2A-related experiments, cells were treated with 10 or 100  $\mu$ g H2A/mL for 4 h or 12 h. For DNA and NET preparations experiments cells were treated for 12 h. To control the influence of components of NETs, *B. besnoiti* secreted and excreted substances and to test if a single protein such as BSA can influence the observed results we also tested BSA (incubation for 4 h and 12 h) at the same concentrations used for histone H2A (10 and 200  $\mu$ g/mL), viable and heat-inactivated *B. besnoiti* tachyzoites and supernatants recovered from *B. besnoiti* cell culture after 3 h of infection, named excretory secretory (E/S) components at two different dilutions. At each time point, the medium was removed and cells were analyzed for

## 2.3 Histone H2A and bovine neutrophil extracellular traps induce damage of *Besnoitia besnoiti*-infected host endothelial cells but fail to affect total parasite proliferation

---

cytotoxic effects via live/dead staining (5  $\mu$ M Sytox Orange<sup>®</sup> (Thermo Fisher Scientific) diluted in modified ECGM medium, 10 min, RT, in the dark). Fluorescence intensity was estimated at 574/570 nm excitation and emission wavelengths, respectively.

### 2.8. Physiological Flow Condition Experiments

Three different BUVEC isolates were cultured in  $\mu$ -slide-0.4 Luer chambers (IBIDI<sup>®</sup>, Martinsried, Germany) until confluency. BUVEC layers were infected with *B. besnoiti* tachyzoites 12 h before performing flow condition experiments or left uninfected for controls. Culture plates were mounted on the stage of a motorized inverted microscope (Olympus Microscope IX81, Hamburg, Germany) using a top-stage incubator (IBIDI<sup>®</sup>, Martinsried, Germany) with a controlled atmosphere of 5% CO<sub>2</sub> and 37 °C. The chambers containing non-infected or *B. besnoiti*-infected BUVEC were connected to a pump flow system using Luer adapters and a constant physiological wall shear stress of 1.0 dyn/cm<sup>2</sup> was applied (syringe pump sp100i; World Precision Instruments, Friedberg, Germany) for 5 min of perfusion of either pure medium or a solution 5 x 10<sup>6</sup> PMN/mL. After perfusion, plates were carefully removed from IBIDI<sup>®</sup> chambers, cells were fixed in 4% paraformaldehyde at RT for 10 min and finally washed thrice with sterile PBS for further staining.

### 2.9. Determination of Endothelial Cell Damage Using Isolectin GS-IB4

PFA-fixed BUVEC layers were treated with blocking/permeabilization solution (PBS with 3% BSA, 0.1% saponin; 1 h, RT). Thereafter, the samples were incubated in isolectin GS-IB4 which binds predominantly to the cell membrane of blood vessel endothelia [37]. Isolectin GS-IB4 conjugated with Alexa Fluor 594 (Molecular Probes, Eugene, Oregon, USA) was used at a concentration of 20  $\mu$ g/mL, diluted in blocking/permeabilization solution and the samples were stained for 20 min at RT, in a humidified chamber according to Tanaka et al. [38]. Then, samples were washed thrice in PBS and mounted using DAPI-containing mounting medium Fluoromount G<sup>®</sup> (Thermo Fisher Scientific). Of each sample, five random microscopic images were taken applying identical conditions of exposition, light intensity and compensation (Olympus Microscope IX81). Image processing was carried out by Fiji ImageJ<sup>®</sup> using merged-channel-plugins restricted to overall adjustment of brightness and contrast. In brief, images were converted to eight bit and greyscale color. A sharpen filter was applied followed by the color threshold selection, selecting min error algorithm, and defined as background the isolectin-negative regions. The lack of isolectin-derived signals in BUVEC layers was defined as EC damage. For calculation, data from isolectin-negative area were divided by those of the total area to obtain the percentage of EC damage in each analyzed image. Overall, data from a total of 15 images (resulting from three different BUVEC isolates, and three different PMN isolations) were included in the calculation. A workflow of the procedure to obtain endothelial damage values is presented in the supplementary material (Supplementary Figure S5).

### 2.10. Determination of *B. besnoiti* Rosette Number and Parasitophorous Vacuoles (PV) Diameter

Three different BUVEC isolates were included in all experiments. For each experimental condition, five microscopic images of *B. besnoiti*-infected BUVEC and non-treated controls were randomly taken via phase contrast microscopy (Olympus Microscope IX81<sup>®</sup>). The number of *B. besnoiti* rosettes present in the PV of infected host cells were counted and PV sizes reflecting differential stages of tachyzoite replication were measured manually by three independent observers using the Image J<sup>®</sup> software (NIH).

### 2.11. Quantification of *B. besnoiti* Tachyzoites by qPCR

The number of free-released *B. besnoiti* tachyzoites (extracellular tachyzoites in cell culture supernatants) was determined by qPCR using primers described previously by Cortes et al. [39].

## 2.3 Histone H2A and bovine neutrophil extracellular traps induce damage of *Besnoitia besnoiti*-infected host endothelial cells but fail to affect total parasite proliferation

### 2.12. Graphical Representation of Results and Statistical Analyses

Statistical significance was defined by a  $p$ -value  $< 0.05$ . If not otherwise stated,  $p$ -value was determined using the Kruskal-Wallis test followed by Dunn's multiple comparisons test. Data are presented as bar graphs (showing mean  $\pm$  SD) or box-whiskers graphs (showing middle line at median and lines at maximum and minimum values). Capital letter N is used to denote the number of biological replicates (BUVEC isolates) and minuscule letter n is used when the analysis referred to *B. besnoiti* rosettes numbers. All statistical analyses and graphs were performed via the Graph Pad® v. 7.03 software (San Diego, CA, USA).

## 3. Results

### 3.1. *B. besnoiti* Tachyzoites Induce Bovine NETs

Markers of NETs of granular origin, such as neutrophil elastase, were detected colocalizing with histone and DNA when bovine PMN were confronted with *B. besnoiti* tachyzoites at 1:4 ratio for 3 h and observed under confocal microscopy after immunostaining (Figure 1A) or after DNA staining with Sytox Orange (Supplementary Figure S4). Tachyzoites being trapped in NETs were also observed (white triangles) alongside a pointed distribution of neutrophil elastase in NETs (Figure 1B). Images are representative for the experiments conducted with PMN from three different animals. Colocalization of extracellular DNA with these proteins confirmed typical characteristics of NETs. Using the NETs quantification method proposed by González et al. [40] it was estimated that 15% of bovine PMN that were confronted with *B. besnoiti* tachyzoites release NETs (Supplementary Figure S2).

### 3.2. H2A, *B. besnoiti* Tachyzoite- and A23187-Derived NET Preparations Are All Cytotoxic for BUVEC

Cell death was determined by a live/dead-staining with Sytox Orange® (Thermo Fisher Scientific, Waltham, MA USA), which only enters into cells with compromised membranes (= dead cells). Overall, treatments of BUVEC with H2A at 200  $\mu$ g/mL resulted in significantly enhanced cell death when applied for 4 h (H2A 200  $\mu$ g/mL versus nontreated control:  $p = 0.04$ ; Figure 2A) or 12 h (H2A 200  $\mu$ g/mL versus non-treated control:  $p = 0.01$ ; Figure 2B). In addition, we tested if pure NET preparations obtained from bovine PMN being stimulated either with *B. besnoiti* tachyzoites (Bb-NETs) or the calcium ionophore A23187 (A23187-NETs) also induced BUVEC death in a static system. In this context, A23187 induced NETs in the bovine system in 39.5% of the cells at the working concentration of 5  $\mu$ M (Supplementary Figure S1). Preparation of pure NETs resulted in concentrations of  $161.5 \pm 35$  ng DNA/mL for A23187-NETs and  $169 \pm 17$  ng DNA/mL for Bb-NETs. Overall, an average of 40 ng DNA per  $10^6$  PMN was obtained. For the estimation of cytotoxic effects on BUVEC, NETs were used at two different concentrations defined as 1X and 2X corresponding to a final concentration of 3.3 and 6.6 ng DNA/mL, respectively. Respective data showed that Bb-NET (1X versus non-treated control:  $p = 0.03$ ) induced significant cytotoxic effect after 12 h of exposure. On the other hand, both A23187-NET conditions (1X, 2X) showed increased cytotoxicity, but without reaching statistical significance. (Figure 2C). When the influence of protein alone (BSA), *B. besnoiti* tachyzoites (live and heat-killed), and excretory/secretory molecules (E/S) (Figure 2D,E) was analyzed, we found that only viable *B. besnoiti* tachyzoites induced cytotoxicity in BUVEC after 12 h of incubation (Figure 2E).

### 3.3. PMN Induce Endothelial Cell Damage in *B. besnoiti*-Infected BUVEC Under Flow Conditions

We recently showed that PMN being perfused over *B. besnoiti*-infected BUVEC show increased endothelial adhesion and additionally form NETs [2]. Here, we applied a constant physiological shear stress of 1 dyn/cm<sup>2</sup> onto BUVEC and additionally conducted the experiments under controlled temperature (37 °C) and atmosphere (5% CO<sub>2</sub>) conditions. Medium was perfused over BUVEC layers infected with *B. besnoiti* tachyzoites for 12 h for a time period of 5 min under presence or absence of floating bovine PMN. Non-infected BUVEC were used as controls. Following perfusion, BUVEC layers were assayed for the EC damage marker isolectin-IB4 coupled to Alexa Fluor 594 and stained

## 2.3 Histone H2A and bovine neutrophil extracellular traps induce damage of *Besnoitia besnoiti*-infected host endothelial cells but fail to affect total parasite proliferation

Biology 2019, 8, 78

7 of 19

with DAPI as nuclear marker (exemplary images are illustrated in Figure 3A). Unmerged and phase contrast images confirming PMN adhesion on BUVEC layers are presented in supplementary material (Supplementary Figure S3). Overall, perfusion of PMN over non-infected BUVEC induced EC damage ( $17.48\% \pm 10.58\%$ ), whilst perfusion of medium alone hardly affected BUVEC layers ( $2.83\% \pm 0.47\%$ ) (Figure 3B). Interestingly, when PMN were perfused over *B. besnoiti*-infected cell layers, EC damage increased to  $35.47\% \pm 9.20\%$  at 12 h of infection (Figure 3B). Given that perfusion of medium alone did not induce considerable EC damage in *B. besnoiti*-infected BUVEC ( $3.43\% \pm 0.57\%$  Figure 3B), the former effect could not be due to an enhanced sensitivity of infected BUVEC towards shear stress conditions. Consequently, medium only-related data on non-infected and *B. besnoiti*-infected cells did not differ significantly.

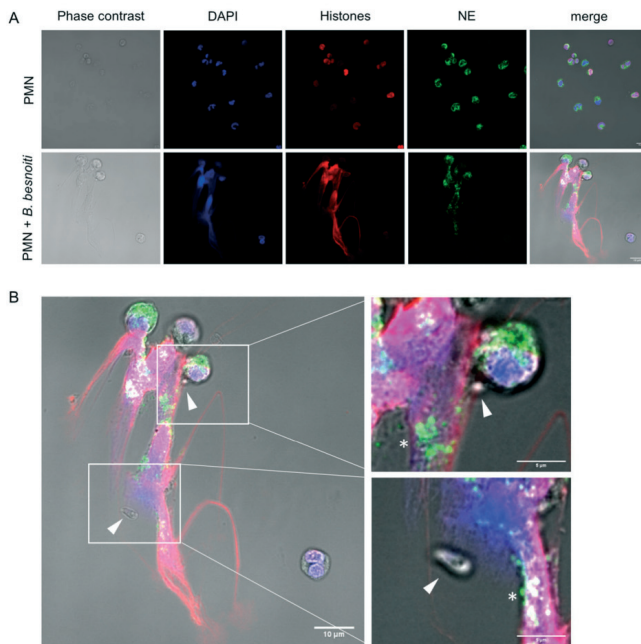


**Figure 1.** *B. besnoiti* tachyzoites induce neutrophil extracellular traps (NETs).  $2 \times 10^5$  bovine polymorphonuclear neutrophils (PMN) were confronted with plain medium (control) or  $8 \times 10^5$  *B. besnoiti* tachyzoites (1:4 ratio) for 3 h at  $37^\circ\text{C}$  and  $5\% \text{CO}_2$ . Samples were fixed and immune-stained for neutrophil elastase (green) and histones (red). The coverslips were mounted in mounting media containing 4',6-Diamidino-2-phenylindole DAPI to stain DNA (blue). Representative image of NETs in response to *B. besnoiti* tachyzoites is shown in (A). In (B) a zoom shows the detail of NETs trapping *B. besnoiti* tachyzoites (white triangle). In addition, the dotted distribution of neutrophil elastase in NETs is observed (white asterisk).

## 2.3 Histone H2A and bovine neutrophil extracellular traps induce damage of *Besnoitia besnoiti*-infected host endothelial cells but fail to affect total parasite proliferation

Biology 2019, 8, 78

8 of 19

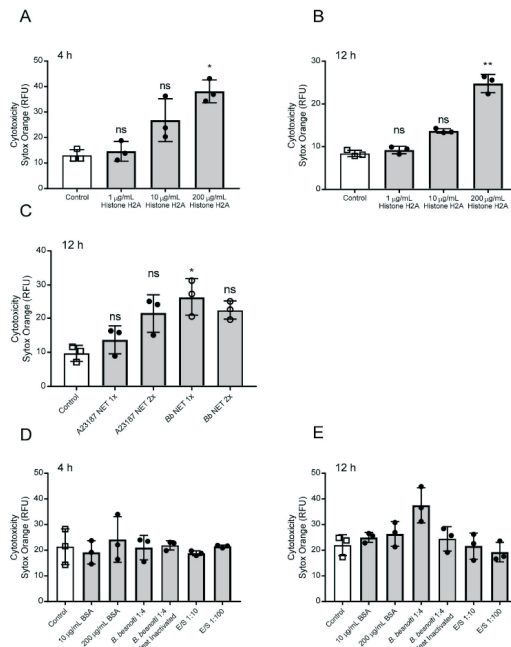


**Figure 2.** Histone 2A (H2A) and NETs preparations induce cell death in bovine umbilical vein endothelial cells (BUVEC). Three different BUVEC isolates were treated with H2A at concentrations of 1–200 µg/mL for 4 (A) h and 12 (B) h and with NETs preparations from bovine PMN confronted with *B. besnoiti* tachyzoites (*Bb* NET) or stimulated with A23187 (A23187 NET) for 12 h (C). For control purposes BUVEC were incubated with bovine serum albumin (BSA), heat killed, and viable *B. besnoiti* tachyzoites and excretory/secretory (E/S) molecules for 4 h (D) and 12 (E) h. Cell death was evaluated using Sytox Orange® staining. Bars represent mean ± SD. Statistical significance (ns = non-significant, \*  $p < 0.05$ ; \*\*  $p < 0.01$ ;  $p < 0.001$ ) was determined by Kruskal-Wallis test followed by a Dunn’s post-test comparing experimental versus control conditions (N = 3), all experiments were performed in duplicates.

### 3.4. H2A Treatments Decrease PV Diameter in *B. besnoiti*-Infected Host Cells but Does Not Affect the Number of Rosettes and Total Tachyzoite Production Over Time

Since we observed that H2A, NETs and PMN induced cytotoxicity and damage on infected BUVEC under static and physiological flow conditions, we next analyzed whether treatments with H2A as a major component of NETs may also influence intracellular development of *B. besnoiti* (for experimental set-up see Figure 4A). Therefore, we determined *B. besnoiti* PV diameters which reflect the typical division stages of *B. besnoiti* tachyzoites (Figure 4A). In addition, we quantified the number of rosettes present in each host cell. Overall, H2A treatments induced a decrease of the PV diameter independent of the time point of H2A supplementation (Figure 4C). As such, this effect

## 2.3 Histone H2A and bovine neutrophil extracellular traps induce damage of *Besnoitia besnoiti*-infected host endothelial cells but fail to affect total parasite proliferation

Biology 2019, 8, 78

9 of 19

was observed at time points, 4 h and 12 hours post infection (h.p.i.) and at both H2A concentrations (10 and 100  $\mu\text{g/mL}$ ) (H2A-treated versus untreated: 100  $\mu\text{g}$ , 4 h:  $p = <0.0001$ ; 10  $\mu\text{g}$ , 4 h:  $p = <0.0001$ ; 100  $\mu\text{g}$ , 12 h:  $p = <0.0001$ ). Referring to mean rosette numbers/host cell, no significant difference was observed between non-treated and H2A-treated samples when varying PV loads per host cell were statistically analyzed within one condition. Given that up to 15 rosettes were detected in non-treated cells, PV number-derived categories were formed and compared to each other. Following this strategy, no changes in mean PV numbers in H2A-treated BUVEC were observed (Figure 5A) whilst the general infection rate remained unchanged (Figure 5B). Accordingly, when estimating tachyzoite production over time (30 h), no significant differences were observed between H2A-treated cells and untreated controls (Figure 5C).

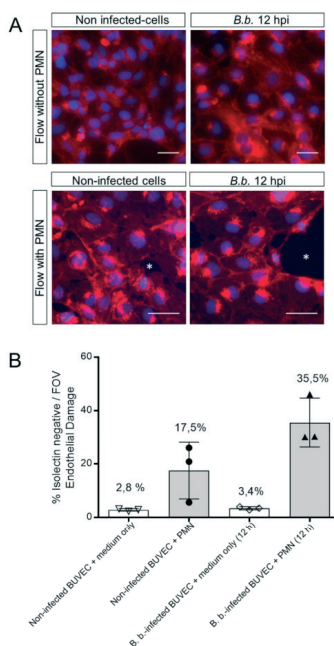


**Figure 3.** PMN induce damage on *B. besnoiti*-infected BUVEC under physiological flow conditions. PMN or medium alone were perfused at a constant shear stress of 1  $\text{dyn/cm}^2$  over *B. besnoiti*-infected and non-infected BUVEC at 12 h.p.i. After 5 min of perfusion, cell layers were fixed and stained with DAPI for nuclei and with Alexa Fluor 594-conjugated isoelectin-IB4 that predominantly binds endothelium and observed under fluorescence microscopy. Endothelial damage is calculated dividing the isoelectin-negative surface (white asterisks, A, representative images) by the total surface of the field of view. Column graph represents results of the percentage of endothelial damage after analyzing five random pictures from three different BUVEC isolates per each experimental condition (B). FOV = Field of view. Number over the bars indicates the mean % and error bars  $\pm$  SD.

## 2.3 Histone H2A and bovine neutrophil extracellular traps induce damage of *Besnoitia besnoiti*-infected host endothelial cells but fail to affect total parasite proliferation

Biology 2019, 8, 78

10 of 19

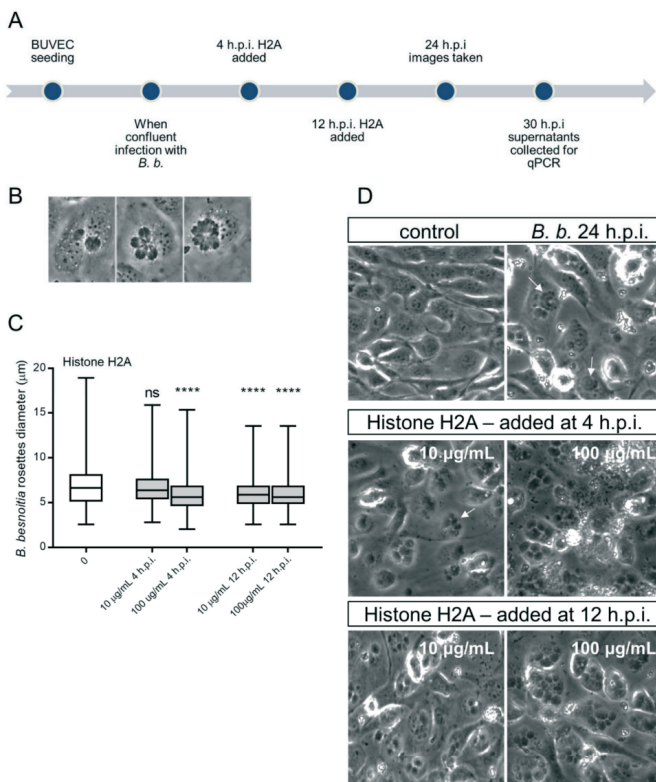


**Figure 4.** Histone 2A (H2A) treatment of *B. besnoiti*-infected BUVEC reduces *B. besnoiti* parasitophorous vacuole (PV) diameter. BUVEC (three different isolates, N = 3) were treated with H2A at 10 or 100 µg/mL at 4 and 12 h.p.i. (for experimental procedure refer to Figure 4A). At 24 h.p.i. experimental conditions were documented by five randomly taken images using a phase contrast microscope (B,D). (B) Shows the typical development of *B. besnoiti* rosettes within 24 h of infection (non-synchronous tachyzoite division leads to the formation of 2-mers to 16-mers). Here, the diameter of each *B. besnoiti* PV was measured ( $n = 825$ ) and plotted as box and whiskers plot (C), line at median, bars indicating maximum and minimum values. Statistical significance, N = 3 (ns = non significant, \*\*\*\*  $p < 0.0001$ ) was determined by Kruskal-Wallis test followed by a Dunn's post-test comparing experimental versus control condition at 4 and 12 h.p.i. In (D) a representative image of each experimental condition is shown, white arrows indicate *B. besnoiti* rosettes inside host BUVEC cell.

## 2.3 Histone H2A and bovine neutrophil extracellular traps induce damage of *Besnoitia besnoiti*-infected host endothelial cells but fail to affect total parasite proliferation

Biology 2019, 8, 78

11 of 19

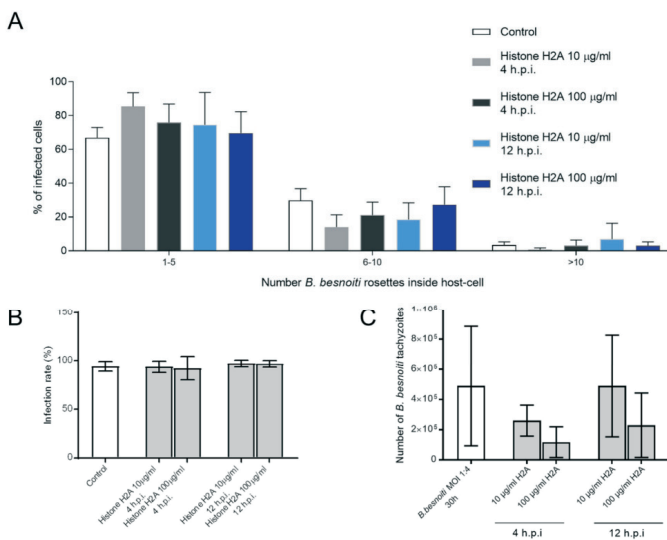


**Figure 5.** Histone 2A (H2A) did not affect the number of intracellular *B. besnoiti* rosettes. *B. besnoiti*-infected BUVEC (three different isolates, N = 3) were treated with H2A (10 or 100 µg/mL) at 4 and 12 h.p.i. At 24 h.p.i. cell layers were analyzed by randomly taking five microscopic images using phase contrast microscopy. The total number of *B. besnoiti* rosettes per host cell was determined and the percentage of host cells carrying different numbers of PV was estimated and sub-grouped in different categories (with 1–5, 6–10 and >10 rosettes/cell, respectively; (A)). Furthermore, the infection rate (B) and the total number of tachyzoites being released into cell supernatant within 30 h.p.i. was estimated via qPCR (C). Bar graph shows mean ± SD. (n = 238).

### 3.5. Treatments of *B. besnoiti*-Infected BUVEC with Bb-NETs and A23187-NETs Affect PV Development and Total Tachyzoite Production

Overall, treatments of *B. besnoiti*-infected BUVEC layers with Bb-NETs or A23187-NETs at 4 and 12 h.p.i. differentially affected *B. besnoiti* PV diameter. Whilst A23187-NETs induced a significant diminishment of PV size at both time points of treatment (A23187-NETs-1X (4 h) versus untreated control:  $p < 0.0001$ ; A23187-NETs-1X (12 h) versus untreated control:  $p = 0.052$ ; A23187-NETs-2X (12 h) versus untreated control:  $p < 0.0001$ ), treatments with Bb-NETs had no effects when performed at 4 h.p.i. (Figure 6A). However, in the case of later Bb-NET treatments (12 h.p.i.), a significant decrease of PV diameters was estimated for 1X concentration (Bb-NETs-1X (12 h):  $p = 0.012$ ) (Figure 6A, lower panel). When rosette numbers/host cell were analyzed and normalized as percentage of the infected host cells which contained one to 15 rosettes, we observed a decrease in the number of host cells which contained only one *B. besnoiti* rosette per cell in the case of Bb-NET and A23187-NET treatments (Figure 7A). When estimating total tachyzoite production and release over 30 h, a striking difference was observed when comparing Bb-NET- and A23187-NET-related treatments: Whilst total tachyzoite proliferation was not altered by Bb-NETs (Figure 7B), treatments with A23187-NETs led to a significant and dramatic (almost 10-fold) increase of tachyzoite numbers present in cell culture

## 2.3 Histone H2A and bovine neutrophil extracellular traps induce damage of *Besnoitia besnoiti*-infected host endothelial cells but fail to affect total parasite proliferation

Biology 2019, 8, 78

12 of 19

supernatants (Figure 7B). This effect was independent of both, A23187-NET concentration and the time point of supplementation.

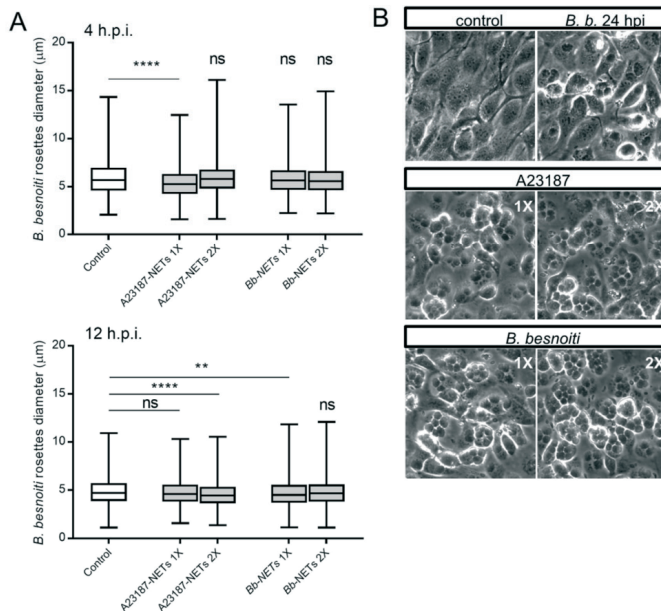


**Figure 6.** *Bb*-NETs and A231887-NETs induced a decrease in rosette diameter in *B. besnoiti*-infected BUVEC. *Bb*-NETs or A231887-NETs were added at two different concentrations (1X and 2X) to infected BUVEC cells (three different isolates,  $N = 3$ ) at 4 (A, upper panel) and 12 (A, lower panel) h.p.i. At 24 h.p.i. experimental conditions were documented within five random pictures using a phase contrast microscope and the diameter of *B. besnoiti* rosettes was determined ( $n = 1115$ ). Box and whiskers plot, line at median, bars indicating maximum and minimum values. Statistical significance was determined by Kruskal-Wallis test followed by a Dunn's post-test comparing experimental versus control condition at 4 and 12 h.p.i. (A). Representative images infected BUVEC cells to which *Bb* and A23187 NETs were added at 12 h.p.i. are shown (B). ns = non significant, \*\*  $p < 0.01$ , \*\*\*\*  $p < 0.0001$ .

## 2.3 Histone H2A and bovine neutrophil extracellular traps induce damage of *Besnoitia besnoiti*-infected host endothelial cells but fail to affect total parasite proliferation

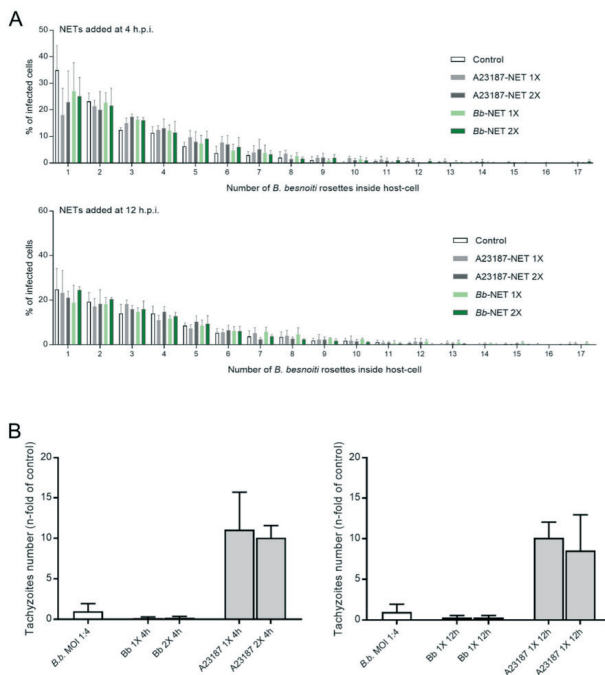


**Figure 7.** Effects of *Bb*-NET and A23187-NET treatments on intracellular *B. besnoiti* rosettes formation and tachyzoite release. *B. besnoiti*-infected BUVEC (three different isolates, N = 3), were treated with *Bb*-NETs or A23187-NETs at 1X and 2X concentrations at 4 and 12 h.p.i. All treatments were performed in duplicates. At 24 h.p.i. cells were analyzed by randomly taking five images for each experimental condition using phase contrast microscopy. The total number of *B. besnoiti* rosettes per host cell at 4 ( $n = 1115$ ) and 12 h.p.i. ( $n = 970$ ) was determined and the percentage of host cells carrying different numbers of rosettes was calculated (A). In addition, the total number of tachyzoites being released into cell supernatant within 30 h.p.i. was estimated via qPCR (B). Bars represent mean  $\pm$  SD.

### 4. Discussion

*B. besnoiti* tachyzoites predominantly infect host endothelial cells from different organs and vessels in vivo [20]. In the acute stage, the toxic effect has been related to increased vascular permeability. It is described that these lesions are mainly located in small- and medium-sized vessels, but also in arteries [2]. In this report we used primary endothelial cells isolated from three different animals in order to be as close as possible to the in vivo situation.

We have recently demonstrated that *B. besnoiti* tachyzoites are NET-inducers [4] and that perfusion of bovine PMN over *B. besnoiti*-infected bovine endothelial cells leads to enhanced PMN adhesion and NET deposition on endothelium [20]. NETs are able to entrap *B. besnoiti* tachyzoites thereby hampering the parasite from active host cell invasion. Previously, it was reported that NETs affected

## 2.3 Histone H2A and bovine neutrophil extracellular traps induce damage of *Besnoitia besnoiti*-infected host endothelial cells but fail to affect total parasite proliferation

tachyzoite-derived host cell invasion since infection rates in primary BUVEC cells decreased by more than 25% when PMN-pre-exposed *B. besnoiti* tachyzoites were used for infection. This effect was reversed by the addition of DNase, highlighting that NET can potentially affect the continuous infection and proliferation cycles [4]. Additionally, in the acute phase of besnoitiosis leukopenia is observed, an effect that is explained by increased tissue emigration and margination [41]. It is tempting to assume that, as proposed for other intracellular protozoan parasites as *Leishmania* [42], tachyzoite-mediated NETs formation and the corresponding entrapment, induces a series of events involving—at least—mononuclear phagocytes and an inflammatory responses that can restrict the site of the acute infection. Histopathological examination of chronically infected animals has shown inflammatory infiltrates composed by lymphocytes, macrophages, and plasma cells. In some cases, infiltration and disruption of tissue cysts by inflammatory cells was also observed [43]. Adaptive immune reactions of cattle to *B. besnoiti* have been also reviewed [2] and are not covered in this report. Altogether, this evidence gives insights on the multifactorial, complex, and interrelated immune response of cattle to *B. besnoiti* in the acute and chronic stages of the infection.

In this report we confirmed the previous observation and calculated that 15% of PMN release NETs in response to *B. besnoiti* tachyzoites and that the calcium ionophore A23187 induces NETs in the 39.5% and 67.7% of the cells at 5  $\mu$ M and 25  $\mu$ M concentration, respectively. On this respect, it must be considered that several NETs quantification systems are described and that the current results must be interpreted in the context of similar methodologies (image analysis) in order to establish correct comparisons [40,44,45]. In addition, we present for the first time evidence that pure NET preparations as well as PMN perfusion under physiological shear stress conditions lead to damage and cell death of parasite-infected endothelial host cells. In addition, we demonstrate that, though PV sizes appear to be affected by NET treatments, NET-related endothelial cell damage fails to significantly influence total parasite proliferation. The current finding emphasizes the hypothesis that excess NET formation may contribute to pathogenesis driven by cell-toxic side-effects and that these immune defence-related structures fail to exert lethal effects on tachyzoite stages.

In the current study, we worked with pure NET preparations that were released from bovine PMN either in response to *B. besnoiti* tachyzoites or after stimulation with the calcium ionophore A23187. In this regard, isolation of NETs was achieved by partial digestion of the DNA backbone by the enzyme nuclease *AluI* as demonstrated by Barrientos et al. [28]. We here obtained comparable quantities of DNA for both inducers (161.5  $\pm$  35 ng/mL for A23187-NETs and 169.17  $\pm$  17 ng/mL for *Bb*-NETs). These DNA values are one order of magnitude below the ones described for human PMN stimulated with A23187 [36] when normalized as  $\mu$ g of DNA per  $1 \times 10^6$  PMN. This difference might rely on species-specific differences in the activity of human and bovine PMN [46] and on peculiarities of PMN activation induced by calcium influxes in cattle [32]. No other data exist so far on the recovery or isolation of parasite-induced NETs to conduct a reliable comparison. However, it is expected that NETs derived from *B. besnoiti* tachyzoites and A23187-stimulated PMN contains neutrophil elastase, histones, and MPO considering the detection of these proteins in immunofluorescence of NETs induced by *B. besnoiti* tachyzoites in vitro under static and flow conditions [4,20].

H2A is a key component of NETs and NET-derived H2A was recently reported as a potent inducer of epithelial- and endothelial cell death in both, primary and permanent cell lines [26]. In line, the current data confirmed this effect for primary bovine endothelial cells and additionally showed that cytotoxicity for BUVEC was also observed when cell layers were treated with A23187-NETs and *Bb*-NETs. Considering that histones present in NETs show a lower molecular mass compared to chromatin-derived histones (which may be due to post-translational modifications [28]) and are not as concentrated as when pure H2A is applied, different molecules present in NETs may also have driven these effects. In addition, given that *B. besnoiti*-infected BUVEC generally showed a high infection rate (at least 95% of BUVEC were infected) it additionally appears unlikely that exclusively non-infected cells died within the infected cell layer.

## 2.3 Histone H2A and bovine neutrophil extracellular traps induce damage of *Besnoitia besnoiti*-infected host endothelial cells but fail to affect total parasite proliferation

The current study furthermore evaluated endothelial damage under controlled atmosphere and physiological flow conditions by means of the specific marker isolectin IB-4, a lectin derived from *Griffonia simplicifolia* that preferentially binds to endothelium in blood vessels [29], and which was used before in NETs-endothelium damage related studies [38]. The current estimation of the endothelial damage showed that *B. besnoiti*-infected endothelial cells were indeed significantly affected by perfused bovine PMN. Endothelium-PMN interactions, mainly referring to leukocyte adhesion cascades, have extensively been studied comprising a series of steps and signaling pathways [17]. In the case of *B. besnoiti*-infected endothelium, it is known that infection leads to changes in BUVEC host cell metabolism [47]. Moreover, gene expression of the cytokines CXCL1, CXCL8, CCL2, and CCL5 and the adhesion molecules VCAM-1, P-selectin, ICAM-1, and E-selectin was increased in *B. besnoiti*-infected BUVEC at 12 h.p.i. and, in this context, induction of PMN adhesion and NET release occurred under flow [20]. In this study we add evidence that bovine PMN can also induce damage on activated endothelium at the same time point through PMN adhesion and NET release. These lethal effects most probably are due to a transient higher concentration of proteases as hypothesized by others [48].

As an interesting finding, we here showed that the presence of H2A but also of A23187-NETs and Bb-NETs led to a decrease of intracellular PV diameter thereby reflecting earlier developmental stages with less numbers of tachyzoites (two- and four-mers of tachyzoites have a smaller diameter than 8- or 16-mers). Noteworthy, this phenomenon occurred irrespective of the time point of *B. besnoiti* infection. The two time points here used, i.e., 4 and 12 h.p.i., reflect *B. besnoiti* replication at the beginning (4 hp.i.: before first division) and in the middle (12 h.p.i.: after two divisions) of first merogony, but before lysis of infected BUVEC occurs (from 20 h ongoing). It must be noted that different *B. besnoiti* strains exhibit different lytic cycle characteristics in vitro when a permanent cell line (MARC-145) is used as a host cell [49]. Our results cannot be compared in terms of the lytic cycle since we use the Bb1Evora04 *B. besnoiti* strain, that was not included in this study and as a host cell we used isolated primary cells (BUVEC). Thus, the timepoint to measure endothelial damage were rationally selected based on the gene expression profile of BUVEC cells infected with *B. besnoiti* tachyzoites and the formation of NETs over infected endothelium [20]. At a first glance, the effects on PV diameter could indicate a direct detrimental effect of H2A or NET preparations on tachyzoite development. However, when host cells were analyzed for rosettes numbers, less cells carrying only one rosette were detected in the case of A23187- and Bb-NET treatments. This effect can be linked to selective endothelial cell death, which leads to the release of (obviously) vital tachyzoites which then “rescue” themselves by invading neighboring cells. Since they first have to establish within these new host cells, proliferation onset is delayed, and smaller PVs are found. We consistently observed similar effects in other adverse cell culture conditions, e.g., when cells died out of nutritional deficits. As a general finding, this effect only occurs when single BUVEC die within a total cell layer, not when a cell layer entirely detaches. In agreements with this hypothesis, total *B. besnoiti* tachyzoite production was not significantly affected in NET-treated BUVEC. The latter data clearly indicated that direct lethal effects of NET preparations on intracellular tachyzoites did not occur.

In contrast to H2A or Bb-NETs, treatments of *B. besnoiti*-infected BUVEC with A23187-NETs led to a striking and significant increase of *B. besnoiti* tachyzoite production and release into cell culture supernatants within 30 h of infection. The basis of these effects remains unclear although it is known that NET-derived protein composition varies according to the stimuli and may therefore exert different reactions. However, it must be taken into account that existing data mainly refer to PMA-stimulated PMN [28,50], and that also a dependence on the PMN donor species as well as on the quantity of key components present in NETs has been reported [36]. Nevertheless, since Behrendt et al. [51] reported on A23187-induced tachyzoite host cell egress in case of the closely related coccidian parasites *Toxoplasma gondii* and *Neospora caninum*, the increase of free tachyzoites may also have been induced by residues of A23187 compound present in NET preparations (even though these preparations were thoroughly washed before use). However, Behrendt et al. [51] reported that A23187-induced tachyzoite egress largely depends on PV maturity and on A23187 concentration. Thus, exclusively

## 2.3 Histone H2A and bovine neutrophil extracellular traps induce damage of *Besnoitia besnoiti*-infected host endothelial cells but fail to affect total parasite proliferation

Biology 2019, 8, 78

16 of 19

10  $\mu\text{M}$  A23187 treatments led to egress of tachyzoites from immature PV. Interestingly, reactions were species-dependent since already 1  $\mu\text{M}$  of this compound caused egress of 86% of *T. gondii* tachyzoites but had no effect on *N. caninum* tachyzoites. Given that we here used 5  $\mu\text{M}$  A23197 for NET induction but removed the compound by consecutive washings rather argues against A23187-induced egress as cause for enhanced tachyzoite numbers in cell culture supernatants.

Regarding the mechanisms that can explain our results on, we can hypothesize based on the evidence that shows direct effects of NETs over endothelium: Activation of endothelial pro-MMP-2 and impairment in vasorelaxation by NET through externalization of neutrophil-MMP-9 [52], direct damage to the endothelium by the most prominent histone on NET:H2A; or even degradation products of histones [26,29]. In this context, histones directly activate TLR2 and TLR4 [53] and the corresponding inflammatory signaling cascades [54]. Nevertheless, if these mechanisms are indeed involved in the modulation of intracellular *B. besnoiti* development is unknown so far and may be a matter of further research. Finally, since our data did not include parasite viability or posterior infection rate as parameters is not possible to give a conclusion on this regard.

### 5. Conclusions

Overall, we here present new data on the damaging capacity of *B. besnoiti* tachyzoite- and A23197-triggered NETs and H2A and showed that PV diameter and number of rosettes/host cell may have been affected by NET-driven host cell death. However, NETs induced by *B. besnoiti* tachyzoites do not influence the total parasite proliferation on infected primary endothelial cells.

**Supplementary Materials:** The following are available online at <http://www.mdpi.com/2079-7737/8/4/78/s1>. Figure S1: Immunofluorescence on PMN releasing NETs in response to A23187 5 and 25  $\mu\text{M}$  and determination of % of PMN releasing NET in these conditions. Figure S2: Estimation of the % of PMN releasing NETs in response to *B. besnoiti* tachyzoites and PMA 100 nM. Figure S3. Additional Images of DAPI/Isolectin IB4 staining of experimental conditions. Figure S4. Additional figures showing *B. besnoiti* tachyzoites inducing bovine NETs. Figure S5. Workflow illustrating the procedure of image analysis to obtain endothelial damage percentages shown in Figure 3.

**Author Contributions:** Conceptualization, A.T., C.H., I.C., and Z.D.V.; Investigation, Z.D.V., D.G., E.Z., and H.S.; Validation, I.C. and Z.D.V.; Formal Analysis, I.C., Z.D.V., and A.T.; Resources, A.T. and C.H.; Writing—Original Draft Preparation, I.C.; Writing—Review and Editing, Z.D.V., A.T., and C.H.; Supervision, A.T. and C.H.; Project Administration, C.H. and A.T.; Funding Acquisition, A.T.

**Funding:** This research was funded by the German Research Foundation (DFG) grant number [216337519 (TA291/4-2)]. Mr. Ershun Zhou PhD program is funded by a Chinese council scholarship (2015)3022.

**Acknowledgments:** We want to acknowledge Christine Henrich for her excellent technical support and the quantification of *B. besnoiti* tachyzoites production by qPCR.

**Conflicts of Interest:** The authors declare no conflict of interest.

### References

1. Basso, W.; Schares, G.; Gollnick, N.S.; Rütten, M.; Deplazes, P. Exploring the life cycle of *Besnoitia besnoiti*—Experimental infection of putative definitive and intermediate host species. *Vet. Parasitol.* **2011**, *178*, 223–234. [CrossRef] [PubMed]
2. Alvarez-García, G.; García-Lunar, P.; Gutiérrez-Expósito, D.; Shkap, V.; Ortega-Mora, L.M. Dynamics of *Besnoitia besnoiti* infection in cattle. *Parasitology* **2014**, *141*, 1419–1435. [CrossRef] [PubMed]
3. Jacquet, P.; Liénard, E.; Franc, M. Bovine besnoitiosis: Epidemiological and clinical aspects. *Vet. Parasitol.* **2010**, *174*, 30–36. [CrossRef] [PubMed]
4. Muñoz-Caro, T.; Hermosilla, C.; Silva, L.M.R.; Cortes, H.; Taubert, A. Neutrophil Extracellular Traps as Innate Immune Reaction against the Emerging Apicomplexan Parasite *Besnoitia besnoiti*. *PLoS ONE* **2014**, *9*, e91415. [CrossRef] [PubMed]
5. Brinkmann, V. Neutrophil Extracellular Traps Kill Bacteria. *Science* **2004**, *303*, 1532–1535. [CrossRef]
6. Papayannopoulos, V. Neutrophil extracellular traps in immunity and disease. *Nat. Rev. Immunol.* **2018**, *18*, 134–147. [CrossRef]

## 2.3 Histone H2A and bovine neutrophil extracellular traps induce damage of *Besnoitia besnoiti*-infected host endothelial cells but fail to affect total parasite proliferation

7. Brinkmann, V. Neutrophil Extracellular Traps in the Second Decade. *J. Innate Immun.* **2018**, *10*, 414–421. [[CrossRef](#)]
8. Villagra-Blanco, R.; Silva, L.M.R.; Muñoz-Caro, T.; Yang, Z.; Li, J.; Gärtner, U.; Taubert, A.; Zhang, X.; Hermosilla, C. Bovine Polymorphonuclear Neutrophils Cast Neutrophil Extracellular Traps against the Abortive Parasite *Neospora caninum*. *Front. Immunol.* **2017**, *8*, 606. [[CrossRef](#)]
9. Villagra-Blanco, R.; Silva, L.M.R.; Gärtner, U.; Wagner, H.; Failing, K.; Wehrend, A.; Taubert, A.; Hermosilla, C. Molecular analyses on *Neospora caninum*-triggered NETosis in the caprine system. *Dev. Comp. Immunol.* **2017**, *72*, 119–127. [[CrossRef](#)]
10. Yildiz, K.; Gokpinar, S.; Gazyagci, A.N.; Babur, C.; Sursal, N.; Azkur, A.K. Role of NETs in the difference in host susceptibility to *Toxoplasma gondii* between sheep and cattle. *Vet. Immunol. Immunopathol.* **2017**, *189*, 1–10. [[CrossRef](#)]
11. Abi Abdallah, D.S.; Lin, C.; Ball, C.J.; King, M.R.; Duhamel, G.E.; Denkers, E.Y. *Toxoplasma gondii* Triggers Release of Human and Mouse Neutrophil Extracellular Traps. *Infect. Immun.* **2012**, *80*, 768–777. [[CrossRef](#)] [[PubMed](#)]
12. Behrendt, J.H.; Ruiz, A.; Zahner, H.; Taubert, A.; Hermosilla, C. Neutrophil extracellular trap formation as innate immune reactions against the apicomplexan parasite *Eimeria bovis*. *Vet. Immunol. Immunopathol.* **2010**, *133*, 1–8. [[CrossRef](#)] [[PubMed](#)]
13. Muñoz-Caro, T.; Mena Huertas, S.J.; Conejeros, I.; Alarcón, P.; Hidalgo, M.A.; Burgos, R.A.; Hermosilla, C.; Taubert, A. *Eimeria bovis*-triggered neutrophil extracellular trap formation is CD11b-, ERK 1/2-, p38 MAP kinase- and SOCE-dependent. *Vet. Res.* **2015**, *46*, 23. [[CrossRef](#)] [[PubMed](#)]
14. Kho, S.; Minigo, G.; Andries, B.; Leonardo, L.; Prayoga, P.; Poespoprodjo, J.R.; Kenangalem, E.; Price, R.N.; Woodberry, T.; Anstey, N.M.; et al. Circulating Neutrophil Extracellular Traps and Neutrophil Activation Are Increased in Proportion to Disease Severity in Human Malaria. *J. Infect. Dis.* **2019**, *219*, 1994–2004. [[CrossRef](#)]
15. Muñoz-Caro, T.; Lendner, M.; Dausgchies, A.; Hermosilla, C.; Taubert, A. NADPH oxidase, MPO, NE, ERK1/2, p38 MAPK and Ca<sup>2+</sup> influx are essential for *Cryptosporidium parvum*-induced NET formation. *Dev. Comp. Immunol.* **2015**, *52*, 245–254. [[CrossRef](#)]
16. Zhou, E.; Conejeros, I.; Velásquez, Z.D.; Muñoz-Caro, T.; Gärtner, U.; Hermosilla, C.; Taubert, A. Simultaneous and Positively Correlated NET Formation and Autophagy in *Besnoitia besnoiti* Tachyzoite-Exposed Bovine Polymorphonuclear Neutrophils. *Front. Immunol.* **2019**, *10*, 1131. [[CrossRef](#)]
17. Kolaczowska, E.; Kubes, P. Neutrophil recruitment and function in health and inflammation. *Nat. Rev. Immunol.* **2013**, *13*, 159–175. [[CrossRef](#)]
18. Kolaczowska, E.; Jenne, C.N.; Surewaard, B.G.J.; Thanabalasuriar, A.; Lee, W.-Y.; Sanz, M.-J.; Mowen, K.; Opendakker, G.; Kubes, P. Molecular mechanisms of NET formation and degradation revealed by intravital imaging in the liver vasculature. *Nat. Commun.* **2015**, *6*, 6673. [[CrossRef](#)]
19. McDonald, B.; Urrutia, R.; Yipp, B.G.; Jenne, C.N.; Kubes, P. Intravascular Neutrophil Extracellular Traps Capture Bacteria from the Bloodstream during Sepsis. *Cell Host Microbe* **2012**, *12*, 324–333. [[CrossRef](#)]
20. Maksimov, P.; Hermosilla, C.; Kleinertz, S.; Hirtzmann, J.; Taubert, A. *Besnoitia besnoiti* infections activate primary bovine endothelial cells and promote PMN adhesion and NET formation under physiological flow condition. *Parasitol. Res.* **2016**, *115*, 1991–2001. [[CrossRef](#)]
21. Hermosilla, C.; Zahner, H.; Taubert, A. *Eimeria bovis* modulates adhesion molecule gene transcription in and PMN adhesion to infected bovine endothelial cells. *Int. J. Parasitol.* **2006**, *36*, 423–431. [[CrossRef](#)] [[PubMed](#)]
22. Taubert, A.; Krüll, M.; Zahner, H.; Hermosilla, C. *Toxoplasma gondii* and *Neospora caninum* infections of bovine endothelial cells induce endothelial adhesion molecule gene transcription and subsequent PMN adhesion. *Vet. Immunol. Immunopathol.* **2006**, *112*, 272–283. [[CrossRef](#)] [[PubMed](#)]
23. Taubert, A.; Zahner, H.; Hermosilla, C. Dynamics of transcription of immunomodulatory genes in endothelial cells infected with different coccidian parasites. *Vet. Parasitol.* **2006**, *142*, 214–222. [[CrossRef](#)] [[PubMed](#)]
24. Taubert, A.; Wimmers, K.; Ponsuksili, S.; Jimenez, C.A.; Zahner, H.; Hermosilla, C. Microarray-based transcriptional profiling of *Eimeria bovis*-infected bovine endothelial host cells. *Vet. Res.* **2010**, *41*, 70. [[CrossRef](#)] [[PubMed](#)]
25. Schreiber, A.; Rousselle, A.; Becker, J.U.; von Mässenhausen, A.; Linkermann, A.; Kettritz, R. Necroptosis controls NET generation and mediates complement activation, endothelial damage, and autoimmune vasculitis. *Proc. Natl. Acad. Sci. USA* **2017**, *114*, 9618–9625. [[CrossRef](#)] [[PubMed](#)]

## 2.3 Histone H2A and bovine neutrophil extracellular traps induce damage of *Besnoitia besnoiti*-infected host endothelial cells but fail to affect total parasite proliferation

26. Saffarzadeh, M.; Juenemann, C.; Queisser, M.A.; Lochnit, G.; Barreto, G.; Galuska, S.P.; Lohmeyer, J.; Preissner, K.T. Neutrophil Extracellular Traps Directly Induce Epithelial and Endothelial Cell Death: A Predominant Role of Histones. *PLoS ONE* **2012**, *7*, e32366. [[CrossRef](#)]
27. Folco, E.J.; Mawson, H.L.; Vromman, A.; Bernardes-Souza, B.; Franck, G.; Persson, O.; Nakamura, M.; Newton, G.; Luscinskas, F.W.; Libby, P. Neutrophil Extracellular Traps Induce Endothelial Cell Activation and Tissue Factor Production Through Interleukin-1 $\alpha$  and Cathepsin G. *Arterioscler. Thromb. Vasc. Biol.* **2018**, *38*, 1901–1912. [[CrossRef](#)]
28. Urban, C.F.; Ermert, D.; Schmid, M.; Abu-Abed, U.; Goosmann, C.; Nacken, W.; Brinkmann, V.; Jungblut, P.R.; Zychlinsky, A. Neutrophil Extracellular Traps Contain Calprotectin, a Cytosolic Protein Complex Involved in Host Defense against *Candida albicans*. *PLoS Pathog.* **2009**, *5*, e1000639. [[CrossRef](#)]
29. Zlatina, K.; Lütteke, T.; Galuska, S.P. Individual Impact of Distinct Polysialic Acid Chain Lengths on the Cytotoxicity of Histone H1, H2A, H2B, H3 and H4. *Polymers* **2017**, *9*, 720. [[CrossRef](#)]
30. Silvestre-Roig, C.; Braster, Q.; Wichapong, K.; Lee, E.Y.; Teulon, J.M.; Berrebeh, N.; Winter, J.; Adrover, J.M.; Santos, G.S.; Froese, A.; et al. Externalized histone H4 orchestrates chronic inflammation by inducing lytic cell death. *Nature* **2019**, *569*, 236. [[CrossRef](#)]
31. Kankaanranta, H.; Moilanen, E. Flufenamic and tofenamic acids inhibit calcium influx in human polymorphonuclear leukocytes. *Mol. Pharmacol.* **1995**, *47*, 1006–1013. [[PubMed](#)]
32. Burgos, R.A.; Conejeros, I.; Hidalgo, M.A.; Werling, D.; Hermosilla, C. Calcium influx, a new potential therapeutic target in the control of neutrophil-dependent inflammatory diseases in bovines. *Vet. Immunol. Immunopathol.* **2011**, *143*, 1–10. [[CrossRef](#)] [[PubMed](#)]
33. Mahomed, A.G.; Anderson, R. Activation of human neutrophils with chemotactic peptide, opsonized zymosan and the calcium ionophore A23187, but not with a phorbol ester, is accompanied by efflux and store-operated influx of calcium. *Inflammation* **2000**, *24*, 559–569. [[CrossRef](#)] [[PubMed](#)]
34. Doua, D.N.; Khan, M.A.; Grasemann, H.; Palaniyar, N. SK3 channel and mitochondrial ROS mediate NADPH oxidase-independent NETosis induced by calcium influx. *Proc. Nat. Acad. Sci. USA* **2015**, *112*, 2817–2822. [[CrossRef](#)] [[PubMed](#)]
35. Kenny, E.F.; Herzig, A.; Krüger, R.; Muth, A.; Mondal, S.; Thompson, P.R.; Brinkmann, V.; Von Bernuth, H.; Zychlinsky, A. Diverse stimuli engage different neutrophil extracellular trap pathways. *Elife* **2017**, *6*, e24437. [[CrossRef](#)] [[PubMed](#)]
36. Barrientos, L.; Marin-Esteban, V.; de Chaisemartin, L.; Le-Moal, V.L.; Sandré, C.; Bianchini, E.; Nicolas, V.; Pallardy, M.; Chollet-Martin, S. An Improved Strategy to Recover Large Fragments of Functional Human Neutrophil Extracellular Traps. *Front. Immunol.* **2013**, *4*, 166. [[CrossRef](#)] [[PubMed](#)]
37. Laitinen, L. Griffonia simplicifolia lectins bind specifically to endothelial cells and some epithelial cells in mouse tissues. *Histochem. J.* **1987**, *19*, 225–234. [[CrossRef](#)]
38. Tanaka, K.; Koike, Y.; Shimura, T.; Okigami, M.; Ide, S.; Toiyama, Y.; Okugawa, Y.; Inoue, Y.; Araki, T.; Uchida, K.; et al. In vivo characterization of neutrophil extracellular traps in various organs of a murine sepsis model. *PLoS ONE* **2014**, *9*, e111888. [[CrossRef](#)]
39. Cortes, H.C.; Reis, Y.; Gottstein, B.; Hemphill, A.; Leitão, A.; Müller, N. Application of conventional and real-time fluorescent ITS1 rDNA PCR for detection of *Besnoitia besnoiti* infections in bovine skin biopsies. *Vet. Parasitol.* **2007**, *146*, 352–356. [[CrossRef](#)]
40. Gonzalez, A.S.; Bardeol, B.W.; Harbort, C.J.; Zychlinsky, A. Induction and quantification of neutrophil extracellular traps. *Methods Mol. Biol.* **2014**, *1124*, 307–318.
41. Langenmayer, M.C.; Scharf, J.C.; Sauter-Louis, C.; Schares, G.; Gollnick, N.S. Natural *Besnoitia besnoiti* infections in cattle: Hematological alterations and changes in serum chemistry and enzyme activities. *BMC Vet. Res.* **2015**, *11*, 32. [[CrossRef](#)] [[PubMed](#)]
42. Morgado, F.N.; Nascimento, M.T.C.; Saraiva, E.M.; de Oliveira-Ribeiro, C.; Madeira, M.d.F.; da Costa-Santos, M.; Vasconcellos, E.C.F.; Pimentel, M.I.F.; Rosandiski Lyra, M.; Schubach, A.d.O.; et al. Are Neutrophil Extracellular Traps Playing a Role in the Parasite Control in Active American Tegumentary Leishmaniasis Lesions? *PLoS ONE* **2015**, *10*, e0133063. [[CrossRef](#)] [[PubMed](#)]
43. Frey, C.F.; Gutiérrez-Exposito, D.; Ortega-Mora, L.M.; Benavides, J.; Marcén, J.M.; Castillo, J.A.; Casasús, I.; Sanz, A.; García-Lunar, P.; Esteban-Gil, A.; et al. Chronic bovine besnoitiosis: Intra-organ parasite distribution, parasite loads and parasite-associated lesions in subclinical cases. *Vet. Parasitol.* **2013**, *197*, 95–103. [[CrossRef](#)] [[PubMed](#)]

## 2.3 Histone H2A and bovine neutrophil extracellular traps induce damage of *Besnoitia besnoiti*-infected host endothelial cells but fail to affect total parasite proliferation

26. Saffarzadeh, M.; Juenemann, C.; Queisser, M.A.; Lochnit, G.; Barreto, G.; Galuska, S.P.; Lohmeyer, J.; Preissner, K.T. Neutrophil Extracellular Traps Directly Induce Epithelial and Endothelial Cell Death: A Predominant Role of Histones. *PLoS ONE* **2012**, *7*, e32366. [[CrossRef](#)]
27. Folco, E.J.; Mawson, T.L.; Vromman, A.; Bernardes-Souza, B.; Franck, G.; Persson, O.; Nakamura, M.; Newton, G.; Lusinskas, F.W.; Libby, P. Neutrophil Extracellular Traps Induce Endothelial Cell Activation and Tissue Factor Production Through Interleukin-1 $\alpha$  and Cathepsin G. *Arterioscler. Thromb. Vasc. Biol.* **2018**, *38*, 1901–1912. [[CrossRef](#)]
28. Urban, C.F.; Ermert, D.; Schmid, M.; Abu-Abed, U.; Goosmann, C.; Nacken, W.; Brinkmann, V.; Jungblut, P.R.; Zychlinsky, A. Neutrophil Extracellular Traps Contain Calprotectin, a Cytosolic Protein Complex Involved in Host Defense against *Candida albicans*. *PLoS Pathog.* **2009**, *5*, e1000639. [[CrossRef](#)]
29. Zlatina, K.; Lütteke, T.; Galuska, S.P. Individual Impact of Distinct Polysialic Acid Chain Lengths on the Cytotoxicity of Histone H1, H2A, H2B, H3 and H4. *Polymers* **2017**, *9*, 720. [[CrossRef](#)]
30. Silvestre-Roig, C.; Braster, Q.; Wichapong, K.; Lee, E.Y.; Teulon, J.M.; Berrebeh, N.; Winter, J.; Adrover, J.M.; Santos, G.S.; Froese, A.; et al. Externalized histone H4 orchestrates chronic inflammation by inducing lytic cell death. *Nature* **2019**, *569*, 236. [[CrossRef](#)]
31. Kankaanranta, H.; Moilanen, E. Flufenamic and tofenamic acids inhibit calcium influx in human polymorphonuclear leukocytes. *Mol. Pharmacol.* **1995**, *47*, 1006–1013. [[PubMed](#)]
32. Burgos, R.A.; Conejeros, I.; Hidalgo, M.A.; Werling, D.; Hermosilla, C. Calcium influx, a new potential therapeutic target in the control of neutrophil-dependent inflammatory diseases in bovines. *Vet. Immunol. Immunopathol.* **2011**, *143*, 1–10. [[CrossRef](#)] [[PubMed](#)]
33. Mahomed, A.G.; Anderson, R. Activation of human neutrophils with chemotactic peptide, opsonized zymosan and the calcium ionophore A23187, but not with a phorbol ester, is accompanied by efflux and store-operated influx of calcium. *Inflammation* **2000**, *24*, 559–569. [[CrossRef](#)] [[PubMed](#)]
34. Doua, D.N.; Khan, M.A.; Grasemann, H.; Palaniyar, N. SK3 channel and mitochondrial ROS mediate NADPH oxidase-independent NETosis induced by calcium influx. *Proc. Nat. Acad. Sci. USA* **2015**, *112*, 2817–2822. [[CrossRef](#)] [[PubMed](#)]
35. Kenny, E.F.; Herzig, A.; Krüger, R.; Muth, A.; Mondal, S.; Thompson, P.R.; Brinkmann, V.; Von Bernuth, H.; Zychlinsky, A. Diverse stimuli engage different neutrophil extracellular trap pathways. *Elife* **2017**, *6*, e24437. [[CrossRef](#)] [[PubMed](#)]
36. Barrientos, L.; Marin-Esteban, V.; de Chaisemartin, L.; Le-Moal, V.L.; Sandré, C.; Bianchini, E.; Nicolas, V.; Pallardy, M.; Chollet-Martin, S. An Improved Strategy to Recover Large Fragments of Functional Human Neutrophil Extracellular Traps. *Front. Immunol.* **2013**, *4*, 166. [[CrossRef](#)] [[PubMed](#)]
37. Laitinen, L. Griffonia simplicifolia lectins bind specifically to endothelial cells and some epithelial cells in mouse tissues. *Histochem. J.* **1987**, *19*, 225–234. [[CrossRef](#)]
38. Tanaka, K.; Koike, Y.; Shimura, T.; Okigami, M.; Ide, S.; Toiyama, Y.; Okugawa, Y.; Inoue, Y.; Araki, T.; Uchida, K.; et al. In vivo characterization of neutrophil extracellular traps in various organs of a murine sepsis model. *PLoS ONE* **2014**, *9*, e111888. [[CrossRef](#)]
39. Cortes, H.C.; Reis, Y.; Gottstein, B.; Hemphill, A.; Leitão, A.; Müller, N. Application of conventional and real-time fluorescent ITS1 rDNA PCR for detection of *Besnoitia besnoiti* infections in bovine skin biopsies. *Vet. Parasitol.* **2007**, *146*, 352–356. [[CrossRef](#)]
40. Gonzalez, A.S.; Bardoel, B.W.; Harbort, C.J.; Zychlinsky, A. Induction and quantification of neutrophil extracellular traps. *Methods Mol. Biol.* **2014**, *1124*, 307–318.
41. Langenmayer, M.C.; Scharr, J.C.; Sauter-Louis, C.; Schares, G.; Gollnick, N.S. Natural *Besnoitia besnoiti* infections in cattle: Hematological alterations and changes in serum chemistry and enzyme activities. *BMC Vet. Res.* **2015**, *11*, 32. [[CrossRef](#)] [[PubMed](#)]
42. Morgado, F.N.; Nascimento, M.T.C.; Saraiva, E.M.; de Oliveira-Ribeiro, C.; Madeira, M.d.F.; da Costa-Santos, M.; Vasconcelos, E.C.F.; Pimentel, M.I.F.; Rosandiski Lyra, M.; Schubach, A.d.O.; et al. Are Neutrophil Extracellular Traps Playing a Role in the Parasite Control in Active American Tegumentary Leishmaniasis Lesions? *PLoS ONE* **2015**, *10*, e0133063. [[CrossRef](#)] [[PubMed](#)]
43. Frey, C.F.; Gutiérrez-Expósito, D.; Ortega-Mora, L.M.; Benavides, J.; Marcén, J.M.; Castillo, J.A.; Casasús, I.; Sanz, A.; Garcia-Lunar, P.; Esteban-Gil, A.; et al. Chronic bovine besnoitiosis: Intra-organ parasite distribution, parasite loads and parasite-associated lesions in subclinical cases. *Vet. Parasitol.* **2013**, *197*, 95–103. [[CrossRef](#)] [[PubMed](#)]

## **2.4. *NEOSPORA CANINUM*-INDUCED NETOSIS IN CANINE COLOSTRAL POLYMORPHONUCLEAR NEUTROPHILS**

This chapter is based on the following publish paper:

Demattio, L., Conejeros, I., Grob, D., Gärtner, U., Taubert, A., Hermosilla, C., Wehrend, A. *Neospora caninum*-induced NETosis in canine colostrum polymorphonuclear neutrophils. *Journal of Reproductive Immunology* 154, 103749.

Eigener Anteil in der Publikation:

Projektplanung	20 %, zusammen mit Ko-Autoren und Betreuern
Durchführung des Versuches	20 %, weitestgehend selbständig
Auswertung der Experimente	50 %, weitestgehend selbständig
Erstellung der Publikation	10 %, weitestgehend selbständig

## 2.4. *Neospora caninum*-induced NETosis in canine colostrum polymorphonuclear neutrophils

Journal of Reproductive Immunology 154 (2022) 103749



Contents lists available at ScienceDirect

Journal of Reproductive Immunology

journal homepage: [www.elsevier.com/locate/jri](http://www.elsevier.com/locate/jri)



### Neospora caninum-induced NETosis in canine colostrum polymorphonuclear neutrophils

Lukas Demattio<sup>a,\*</sup>, Ivan Conejeros<sup>b,\*</sup>, Daniela Grob<sup>b</sup>, Ulrich Gärtner<sup>c</sup>, Anja Taubert<sup>b</sup>, Carlos Hermosilla<sup>b</sup>, Axel Wehrend<sup>a</sup>

<sup>a</sup> Clinic for Obstetrics, Gynaecology and Andrology, Justus Liebig University Giessen, Giessen, Germany

<sup>b</sup> Institute of Parasitology, Justus Liebig University Giessen, Giessen, Germany

<sup>c</sup> Institute of Anatomy and Cell Biology, Justus Liebig University Giessen, Giessen, Germany

#### ARTICLE INFO

##### Keywords:

*Neospora caninum*  
Colostrum  
Neutrophil extracellular traps  
Canine PMN

#### ABSTRACT

*Neospora caninum* represents an obligate intracellular apicomplexan parasite of the family Sarcocystidae causing severe reproductive disorders in cattle, small ruminants, wild animals and canids worldwide. Neutrophil extracellular traps (NETs) were recently described as effective host defense mechanism of polymorphonuclear neutrophils (PMN) derived from cattle, dogs, goats and dolphins against *N. caninum* tachyzoites. Nonetheless, nothing is known so far on canine colostrum PMN immune reactions against *N. caninum* although breeding bitches represent a susceptible dog cohort and infected bitches may spread tachyzoites through transplacental transmission to their offspring. Thus, isolated colostrum PMN from bitches were assessed for PMN phagocytic activities as well as NETs release against viable *N. caninum* tachyzoites. *In vitro* interactions of canine colostrum-derived PMN with tachyzoites were analyzed at different ratios and time spans. Extracellular chromatin staining was applied in order to unveil classical molecules of NETs, such as neutrophil elastase (NE), global histones (H1, H2A/H2B, H3, H4) and myeloperoxidase (MPO), via antibody-based immunofluorescence microscopy analysis. *N. caninum* tachyzoites induced canine NETs in colostrum PMN and scanning electron microscopy (SEM) analysis revealed NETs formation by colostrum PMN thereby ensnaring tachyzoites after exposure. In summary, NETs released from canine colostrum PMN might represent an early and effective maternal defense mechanism of the definitive host helping neonates to reduce initial intracellular replication of not only parasites but of other invasive pathogens after colostrum consumption.

#### 1. Introduction

Colostrum is one of the most important protective nutrients for the health status of neonates in all marine and terrestrial mammalian species. Consistently, colostrum uptake results in immediate innate resistance to certain invasive pathogens (i. e. viruses, bacteria, parasites and fungi) and the adequate physiological development of neonates of all mammalian species, including newborn children (Godhia and Patel, 2013). One of the major reasons to explain importance of colostrum is the transmission of maternal immunity to the infant (Bandrick et al., 2014). This is mostly driven by the transfer of immunoglobulins (Ganz et al., 2018; Mila et al., 2015). Even in unborn mammalian fetuses or neonate species with hypogammaglobulinemia due to species-specific differences in placental structure, protective effects of colostrum is unprecedentedly important (Chastant-Maillard et al., 2017). In addition to

high levels of maternal antibodies colostrum-mediated immunoprotection is dependent on the abundance of colostrum leukocytes (Gonzalez and Dus Santos, 2017). Within leukocyte populations, polymorphonuclear neutrophils (PMN) are the most abundant in colostrum (Chastant-Maillard et al., 2017; Gonzalez and Dus Santos, 2017). Colostrum-derived leukocytes, including PMN, are also absorbed by neonates via intestine mucosa thereby reaching blood circulation without dying and being capable to display their effector mechanisms, i. e. degranulation, phagocytosis, production of reactive oxygen species (ROS) and release of pro-inflammatory cytokines/chemokines against pathogens (Liebler-Tenorio, Riedel-Caspari, Pohlensa, 2002; Seelig and Beer, 1978; Sheldrake and Husband, 1985). Nonetheless, the exact mechanisms by which colostrum leukocytes reach neonate blood vessels is still not fully understood. There are data in literature showing leukocyte intestinal migration via intercellular transepithelial migration

\* Corresponding authors.

E-mail addresses: [Lukas.Demattio@vetmed.uni-giessen.de](mailto:Lukas.Demattio@vetmed.uni-giessen.de) (L. Demattio), [Ivan.Conejeros@vetmed.uni-giessen.de](mailto:Ivan.Conejeros@vetmed.uni-giessen.de) (I. Conejeros).

<https://doi.org/10.1016/j.jri.2022.103749>

Received 13 August 2022; Accepted 14 September 2022

Available online 15 September 2022

0165-0378/© 2022 The Author(s). Published by Elsevier B.V. This is an open access article under the CC BY-NC-ND license (<http://creativecommons.org/licenses/by-nc-nd/4.0/>).

## 2.4. *Neospora caninum*-induced NETosis in canine colostral polymorphonuclear neutrophils

L. Demattio et al.

Journal of Reproductive Immunology 154 (2022) 103749

(Tuboly et al., 1988).

Moreover, colostrum-derived PMN are known to distribute throughout the neonate's organism after intestinal absorption, where they display a significant immunoregulatory function, while showing significant tropism to immunologically active tissues where they even accumulate (Williams, 1993). Some studies have shown that it makes a significant difference to neonatal development whether they have ingested cell-containing or cell-free colostrum (Langel et al., 2015, 2016). As such, calves fed only cell-free colostrum showed a significant increase in disease incidence in the first days of life and a significant difference in efficiency of immunoreactions to infections (Langel et al., 2015).

However, it has not been investigated whether all colostral leukocytes, after migrating into the colostrum still retain all defense properties they already had in the organism of the dam. The present study deals with colostrum PMN, which are one of the major leukocyte populations in colostrum. These professional phagocytes of the innate cellular immune system are also capable of forming neutrophil extracellular traps (NETs) against invasive pathogens, including protozoan and metazoan parasites (Wei et al., 2016).

*Neospora caninum* is a common apicomplexan protozoa causing abortion in several vertebrate species (Anvari et al., 2020). The main final host of the parasite is the domestic dog (*Canis familiaris*). After sexual gamogony and intracellular release of oocysts into the lumen of canine small intestine unsporulated oocysts will be excreted with feces. Herbivorous animals such as sheep, goats or cattle, which are considered as intermediate hosts (IH), become infected via oral uptake of exogenous sporulated oocysts. In these IH, the parasite forms fast replication tachyzoites which are able to cross the placental barrier and infect the fetus and thereby causing sometimes abortions, especially in the first two trimesters of pregnancy. Diaplacental infection of *N. caninum* has also been reported in the canid definitive host (DH) (Cavalcante et al., 2012).

In both the DH and IH, *N. caninum* tachyzoite stages might become potential targets for various PMN-derived defense mechanisms including extrusion of NETs (Wei et al., 2016). Consistently, NETs release for instance might also occur after colostrum uptake in the intestine of neonates after birth, as well as in their bloodstream during parasitemia within first days of life.

NETs are extruded decondensed nuclear chromatin decorated with granular and cytoplasmic proteins. They are formed by activated PMN. The benefit of NETs is thought to be that invasive pathogens become entangled in chromatin networks formed and becoming in direct contact with NETs-associated anti-microbial peptides and proteins, thus becoming immobilized, killed and easier for other phagocytosis-active cells of the innate immune system to take up. The process of NET formation is also known as NETosis and induced by various stimuli, such as the presence of bacteria, virus, fungi and parasites, and soluble factors (e. i. PMA, zymosan, LPS, calcium ionophores). Moreover, NETosis can also be induced with isolated components of pathogens and parasites (Behrendt et al., 2010; Peixoto et al., 2021). The first step of the NET cascade is the activation of the Raf/MEK/ERK system, which leads to the formation of a multimeric NADPH oxidase (NOX) complex. In addition, the formation of reactive oxygen species (ROS) is initiated. As the reaction proceeds, there is a loss of integrity of intracellular membranes and the release of granular neutrophil elastase (NE), which in turn enters the nucleus of PMN, where it leads to hypertrullination of histones throughout the nucleus, resulting in chromatin decondensation. After the rupture of the nuclear and cellular membrane, decondensed DNA are extruded into extracellular space. The amount of NETs formed is dependent on the strength and amount of the stimulus. Quantitative detection of NETs is possible in several ways. On the one hand, formed NET formations can be detected microscopically, and on the other hand, measurement of released DNA is also possible to achieve (Brinkmann et al., 2012).

Nothing is known so far on the ability of colostral-derived PMN to

form NETs, and the present work describes this phenomenon for the first time on PMN isolated from canine colostrum. Over all, we know that colostral leukocytes, including PMN population, are an important components of maternal immunity transfer to the infant. Until now very little is known on displayed effector mechanisms of absorbed colostral PMN by neonates. The present work aims to investigate properties, such as phagocytosis and NETs formation of colostral PMN exposed to highly pathogenic tachyzoites of *N. caninum*.

## 2. Materials and methods

### 2.1. Parasites

*Neospora caninum* tachyzoites of the strain Nc1 were cultured in vitro in plastic T-25 cm<sup>2</sup> tissue culture flasks (Greiner) in primary bovine umbilical vein endothelial cells (BUVEC) or permanent African green monkey kidney epithelial cells (MAR-145). Viable *N. caninum*-tachyzoites were collected from infected host cell layer supernatants, pelleted [400 × g, 12 min at room temperature (RT)], washed thrice in sterile PBS, counted in a Neubauer hemocytometer (Marienfeld-Superior, Germany) and re-suspended in sterile RPMI 1640 medium (Gibco) until further experimental use.

Also heat-inactivated (killed) and frozen parasites were used for stimulating canine colostral-derived PMN.

### 2.2. Isolation of canine colostral-derived PMN

In total 11 healthy bitches of different parity and races were used with the number divided for the different tests. All dogs have had a physiologic pregnancy length and gave birth to mature puppies. All complexes were free of clinical signs of either inflammation or neoplastic transformations. The colostrum was macroscopic in physiological conditions. All animals were regular patients of the Clinic for Obstetrics, Gynecology and Andrology of Small and Large Animals of the Justus Liebig University Giessen in Germany. All samples were rest volumes of usual diagnostic samples (Aktenzeichen KTV 8–2017).

The samples were taken as soon as possible after birth of the first puppy. The colostrum was milked manually from different complexes on the left and right side. If a cesarean section was necessary, all samples were taken after the procedure before the puppies were allowed to suckle.

Colostral PMN were isolated using density gradient centrifugation. All samples were filtered through a sterile 40 µm nylon filter (Merck, Berlin). Afterwards 100% of the same volume of cold phosphate buffered saline (PBS; 4 °C) were added. The samples were afterwards centrifugated at 600 × g for 15 min at 4 °C. After centrifugation the fatty supernatant was drained and the cell pellet was resuspended in cold PBS and again centrifugated at 600 × g for 15 min at 4 °C. This centrifugation step was repeated one more time. Afterwards remaining pellet was suspended in sterile 1 ml PBS and transferred on to a 250 µl Biocoll® Separating Solution (Merck, Berlin) this was now centrifugated at 800 × g for 45 min at 20 °C. Afterwards supernatant was again discharged and the pellet consisted of PMN and erythrocytes. After this step the suspension contained PMN and Erythrocytes for lysis of Erythrocytes the pelleted cells (600 × g for 15 min at RT) cells were suspended in sterile 25 ml bi-distilled water and gently mixed during 40 s to lyse erythrocytes. Osmolarity was rapidly restored by adding 4 ml of 10x Hanks balanced salt solution (HBSS; Biochrom AG). For further experiments the cells were again solved in PBS.

### 2.3. Counting of colostral PMN

For isolation and counting of colostral PMN fifteen healthy bitches ( $n = 15$ ) were milked in the same way as described above. After isolation of cells, all PMN were stained with 250 µl Turk solution (Merck, Berlin), and then counted in a Neubauer counting chamber. The result was given

## 2.4. *Neospora caninum*-induced NETosis in canine colostrum polymorphonuclear neutrophils

L. Demattio et al.

Journal of Reproductive Immunology 154 (2022) 103749

in cells per ml for all experimental settings. A general mixed model analysis of variance was performed using the program BMDP8V to compare the mammary complexes and the two sides of the mammary gland.

### 2.4. Scanning electron microscopy (SEM) analysis

Canine colostrum PMN ( $n = 3$ ) were co-cultured with vital *N. caninum* tachyzoites (ratio 1:3) for 180 min on coverslips (10 mm of diameter; Thermo Fisher Scientific) pre-coated with 0.01% poly-L-lysine (Sigma-Aldrich) at 37 °C and 5% CO<sub>2</sub> atmosphere. After incubation, cells were prefixed using 2.5% glutaraldehyde (Merck). Post-fixation was performed in 1% osmium tetroxide solution (Merck). Cells were then washed in distilled water, dehydrated and critical point dried by CO<sub>2</sub>-treatment and sputtered with gold particles. Finally, samples were visualized using Philips CL30 scanning electron microscope at the Institute of Anatomy and Cell Biology, Justus Liebig University Giessen, Germany.

As a positive control, the same procedure was performed on cells incubated with the Ca<sup>++</sup> ionophore A23187 (Merck) instead of *N. caninum*-tachyzoites. As negative controls, PMN without stimulants were subjected to the same treatment.

### 2.5. *Neospora caninum*-induced NETs visualized by immunofluorescence microscopy analysis

Canine colostrum PMN ( $n = 5$ ) were co-cultured for 180 min with *N. caninum*-tachyzoites (37 °C, 5% CO<sub>2</sub> atmosphere). This was conducted on glass coverslips (15 mm diameter, Thermo Fisher Scientific) pre-coated with 0.01% poly-L-lysine (Sigma-Aldrich). After incubation, cells were fixed in 1% paraformaldehyde (Merck) and stored at 4 °C until further use. To visualize NET structures DAPI was used to stain DNA and specific antibodies were used to detect NE and global histones (i. e. H1, H2A/H2B, H3, H4) as NET-specific molecules. For this purpose, samples were washed three times with sterile PBS solution (Sigma-Aldrich) and then blocked with 2% bovine serum albumin (BSA; Sigma-Aldrich) containing 0.3% Triton X-100 (Thermo Fischer Scientific) for 60 min at RT and afterwards incubated in primary antibody solutions (Pan-Histone, 1:200, Chemico Int. #MAB3422 and neutrophil elastase (NE), 1:200, Abcam #ab68672) for 120 min at RT. After the incubation period, samples were washed again in triplicates with sterile PBS and incubated with secondary antibodies (Alexa 488 goat anti-mouse IgG #A110011, Alexa 405 goat anti-rabbit IgG #A31556, 1:500, Invitrogen) for 120 min at RT in absolute darkness. As a positive control, the same procedure was performed on cells incubated with Ca<sup>++</sup> ionophore A23187 (Merck) instead of *N. caninum*-tachyzoites. As negative controls, PMN without stimulants were subjected to the same treatment. After a final washing step, samples were mounted upside-down with Fluoromount G® (Thermo Fischer Scientific).

Visualization of NET formations was performed using an inverted IX81® epifluorescence microscope equipped with an XM 10® digital camera (both Olympus).

### 2.6. Analysis of different colostrum NET phenotypes

For the quantification of different colostrum NET phenotypes, i. e. spread NETs (*spNETs*), diffuse NETs (*diffNET*) and aggregated NETs (*aggNETs*), the protocols previously described were here used (Muñoz-Caro et al., 2018). Canine colostrum PMN ( $n = 5$ ) were seeded (1–2 × 10<sup>5</sup>/sample) on 0.01% poly-L-lysine (Sigma-Aldrich) pre-coated coverslips (Thermo Fischer Scientific) and incubated with *N. caninum* tachyzoites as described previously (Villagra-Blanco et al., 2017). NETs were visualized by immunofluorescence microscopy analysis as above-mentioned staining protocols.

For visual quantification, five randomly selected power vision pictures of each experimental approach were taken and evaluated

according to the criteria of (Muñoz-Caro et al., 2018).

### 2.7. Phagocytosis test

In order to evaluate colostrum PMN phagocytosis, a commercial phagocytosis assay kit was used to assess phagocytic capacities of PMN isolated from colostrum (pHrodo™ BioParticles™ Phagocytosis Kits for Flow Cytometry, Invitrogen). Briefly, canine colostrum PMN ( $n = 3$ ) were isolated as described above. Cells were resuspended in 400 µl sterile PBS (1–2 × 10<sup>5</sup>/experiment). To perform the assay, the buffers (A and B) included in the commercial kit, were brought to RT. The cell suspension was divided into four approaches of 100 µl each. To samples 3 and 4, 20 µl of pHrodo™ BioParticles™ dissolved in buffer B, was added and mixed by vortexing. Mixtures 1 and 2 served as negative controls.

Approaches 1 and 3 were placed on ice, and approaches 2 and 4 were incubated at 37 °C for 15 min. After this incubation time, the approaches from the water bath were also placed on ice to stop phagocytosis. 100 µl of lysis buffer A was added, and after brief mixing, incubation was performed at RT for 5 min. After 5 min of incubation, 1 ml of buffer B was added to each of the four preparations and incubated again at RT for 5 min. This was followed by centrifugation for 5 min at 350 × g at RT.

The supernatant was poured off and the pellet resuspended in 0.5 ml wash buffer. Since the analysis could not be performed immediately due to time constraints, the cells were fixed at this point. A commercial cell fixation kit was used for this purpose (BD Cytotfix/Cytoperm™ Fixation/Permeabilization Kit, BD).

The wash buffer was available as a 10x concentrate and therefore diluted 1:10 with distilled water accordingly. This was followed by a centrifugation step for 5 min at 500 × g at RT. The supernatant was discharged and the cells were resuspended in Fix-Perm® solution (Thermo Fischer Scientific). The cells were then incubated at 4 °C for 20 min.

This incubation period was followed by another centrifugation step (5 min, 500 × g at RT). The supernatant was removed and the cells were washed again as described above. The cells treated in this way were resuspended in 250 µl wash buffer. Analysis was performed by flow cytometer (BD Accuri™ C6 Plus®) analysis.

## 3. Results

### 3.1. Counting canine colostrum PMN

In all examined mammary complexes of each bitch, PMN have been found within collected colostrum. The concentration of PMN per ml showed large fluctuations within investigated bitches, but not between the examined mammary complexes in the same dog (Table 1).

Neither differences between the complexes ( $p = 0.34$ ) nor differences between the two sides ( $p = 0.98$ ) of the mammary gland were significant.

### 3.2. *Neospora caninum*-tachyzoites induced suicidal- and vital NETosis in canine colostrum PMN

For ultrastructural detection of *N. caninum*-triggered NETosis, SEM

**Table 1**  
Average amount of PMN in canine colostrum. (L = left; R = right; 1–5: from cranial to caudal).

mammary complex	L3	L4	L5	R3	R4	R5
number	1	14	15	1	15	14
[Cells/ml]	45,000	64,643	64,233	92,500	62,867	62,814
		±	±	±	±	±
		24,465	21,457		21,964	23,535
min	45,000	30,000	34,000	92,500	34,000	30,000
max	45,000	92,000	98,000	92,500	100,000	102,000

3

## 2.4. *Neospora caninum*-induced NETosis in canine colostrum polymorphonuclear neutrophils

L. Demattio et al.

Journal of Reproductive Immunology 154 (2022) 103749

analyses were here conducted. Suicidal NETosis was confirmed by SEM investigations, which revealed that exposure of canine colostrum PMN to vital *N. caninum*-tachyzoites for 180 min triggered development of both thin and thick chromatin fiber strands being extruded from dead PMN (Fig. 1A). Additionally, SEM analysis demonstrated that not all exposed colostrum PMN responded by NET formation as some remained non-activated thereby showing smooth cell surfaces whereas others seeming to be activated demonstrating either rough or irregular surfaces (Fig. 1D, E). Some tachyzoites seemed to be loosely covered by ensnared NETs filaments, but others were almost coated by NETs (Fig. 1A). Furthermore, SEM analyses revealed vital NETosis. Accordingly, in Fig. 1B a vital PMN has been demonstrated extruding an elongated filament toward an aggregation of tachyzoites entrapped in NETs structures.

In this examination, the co-localization of pan histones (i. e. H1,

H2A, H3, H3, H4) and NE on extruded DNA confirmed typical NETs components (Fig. 2).

### 3.3. *Neospora caninum*-tachyzoites triggered different phenotypes of colostrum-derived NETs

Different colostrum-derived NETs phenotypes (i. e. *spr*NETs, *diff*NETs, *agg*NETs) were found in investigated samples after co-culturing with vital *N. caninum* tachyzoites for 180 min. These three different NETs phenotypes have already been described for *Dirofilaria immitis* (Muñoz-Caro et al., 2018). These Nets phenotypes were also described according to the work of (Grob et al., 2020) against *Trypanosoma b. brucei*. The interactions of *N. caninum*-tachyzoites with PMN mainly triggered colostrum-*agg*NETs and *diff*NETs after 3 h of co-cultivation. Some colostrum *spr*NETs were also detected but at a much less

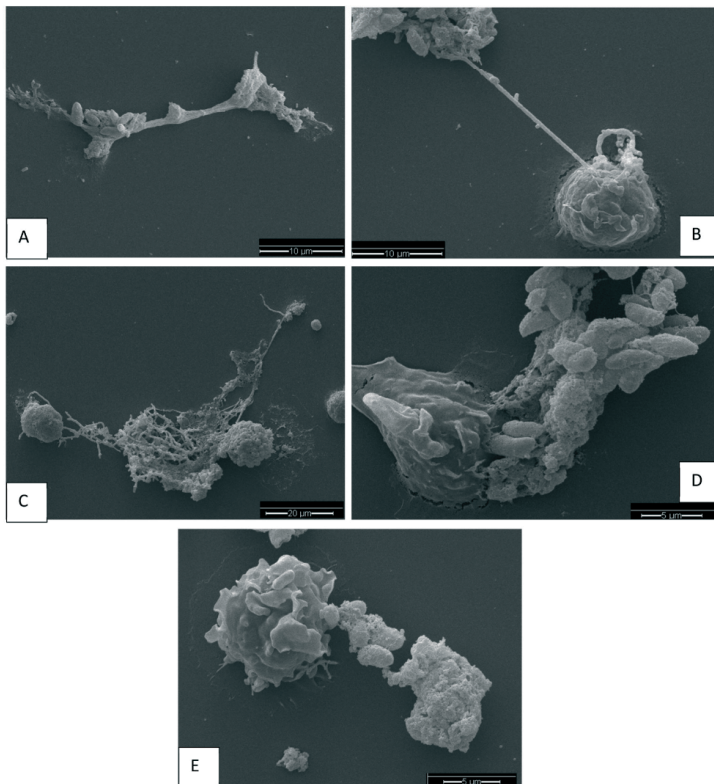


**Fig. 1.** SEM analysis images of canine colostrum PMN. Image A and D clearly show, in decondensed chromatin agglutinated, *Neospora caninum* tachyzoites. Image B likely shows vital NETosis. In detail, an activated colostrum and still alive PMN releases an elongated chromatin filament towards a pre-existing agglutinate of NET-entrapped tachyzoites. In image C, a completely destroyed PMN is visible in the center of the image and showing suicidal NETosis. The thin and thick NET fibers are clearly visible. On the right side of the image there is an activated PMN, on the left side of the image a not yet activated PMN. Image E shows a highly activated PMN, next to parts of a NET and three already agglutinated *Neospora caninum* tachyzoites.

## 2.4. *Neospora caninum*-induced NETosis in canine colostrum polymorphonuclear neutrophils

L. Demattio et al.

Journal of Reproductive Immunology 154 (2022) 103749

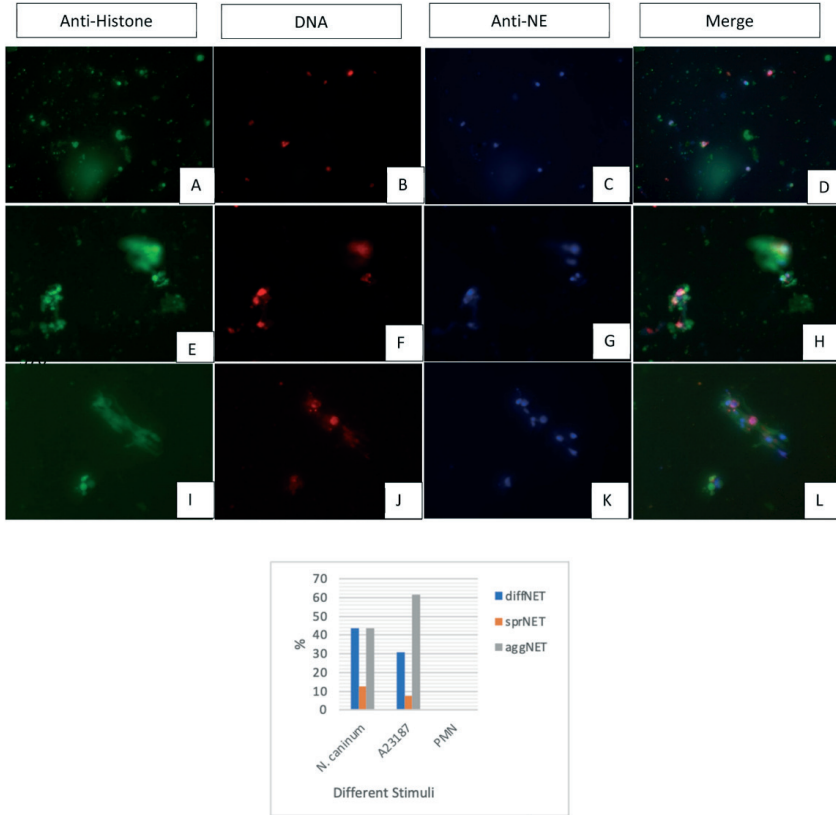


Fig. 2. Shows various immunofluorescences. Images A, E and I show the fluorescence signal of the anti-histone antibodies, images B, F and J show the corresponding signals of the DNA dye (DAPI). Images C, G and K show the fluorescence of the anti-NE (neutrophil elastase) signals and D, H and L show the merge. Row A-D shows the control approach with unstimulated PMN. Rows E-H and I-L show PMN stimulated with *Neospora caninum*.

proportion. These results are shown in Fig. 2.

### 3.4. Phagocytosis test

Evaluation of the phagocytosis assay showed that colostrum-derived PMN from donor animals ( $n = 3$ ) became activated after exposure to bacteria thereby phagocytosing labeled and opsonized *Staphylococcus aureus* strain (Fig. 3). Nonetheless, no significant difference in colostrum PMN phagocytosis rates were detected between phagocytosis activity at 37 °C and samples on ice (negative control,  $p = 0.28$ ). This indicates, that colostrum PMN seem capable in performing phagocytosis and probably also during their presence in neonatal blood circulation and/or in other tissues. Canine colostrum PMN did not die or lose their antimicrobial functions after being secreted into colostrum.

Figure M graphically represents the distribution of the different NET

phenotypes. On the Y-axis are the percentages. On the X-axis, the different stimuli are plotted with the respective NET phenotypes in different colors.

### 3.5. Killed tachyzoites do not hamper *Neospora caninum*-triggered colostrum NETs release

To verify whether inactivated/killed *N. caninum* tachyzoites were also capable to induce colostrum-derived NETosis also heat-inactivated tachyzoites were used. The samples stimulated by dead parasites were examined by SEM microscopy analyses. Applying SEM microscopy analyses to similarly prepared samples showed no morphological differences from colostrum PMN stimulated with live parasite stages.

## 2.4. *Neospora caninum*-induced NETosis in canine colostrum polymorphonuclear neutrophils

L. Demattio et al.

Journal of Reproductive Immunology 154 (2022) 103749

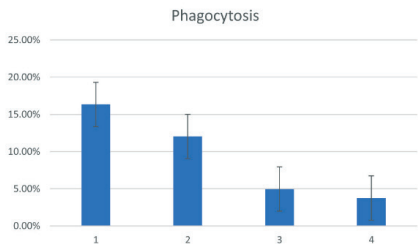


**Fig. 3.** The Fig. 3 shows the average values of phagocytosis activity in percent. The values on one are the average of PMN incubated with opsonized bacteria at 37 °C. On two are the values of the cells with opsonized bacteria on ice. Values under three and four are the colostrum PMN without bacteria at 37 °C (3) and on ice (4).

### 4. Discussion

Vital- and suicidal NETosis are efficient defence processes of activated PMN to ensnare and eliminate invading pathogens (Brinkmann and Zychlinsky, 2012) by extruding web-like extracellular structures which consist of DNA as backbone, citrullinated global histones (H1, H2A/H2B, H3, H4), NE and various anti-microbial peptides/proteins/enzymes such as  $\alpha$ -defensin, lactoferrin, pentraxin, cathelicidin (LL37), cathepsin G, calprotectin and others (Amulic and Hayes, 2011; Hermosilla et al., 2014; Villagra-Blanco et al., 2019). Recently, more attention has been paid on pivotal role of vital- and suicidal NETosis against diverse apicomplexan species such as *Eimeria bovis* (Behrendt et al., 2010; Muñoz-Caro et al., 2015), *Toxoplasma gondii* (Abi Abdallah and Denkers, 2012; Imlau et al., 2020; Reichel et al., 2015), *Cryptosporidium parvum* (Hasheminasab et al., 2022; Silva et al., 2016) *Besnoitia besnoitii* (Conejeros et al., 2019; Zhou et al., 2019) and *N. caninum* (Villagra-Blanco et al., 2017). Even in final host (FH), *N. caninum*-triggered canine NETosis has been described and being NOX<sup>+</sup>, NE<sup>+</sup>, MPO<sup>+</sup>, SOCE<sup>+</sup>, ERK 1/2- and p38 MAPK-dependent (Wei et al., 2016). Herein, for the first time, we demonstrate that vital and killed *N. caninum*-tachyzoites were also capable to induce vital- and suicidal NETosis in exposed canine colostrum PMN, proving that these host innate effector mechanisms are independent of parasite vitality. This phenomenon has also been reported for live and killed sporozoites of *E. bovis* as well as *Haemonchus contortus* larvae (Silva et al., 2016).

This study shows for the first time that canine colostrum PMN are also capable of forming NETs after exposure to vital and dead *N. caninum* tachyzoites. The formation of NETs in response to fast replicating pathogenic tachyzoites might also occur in canine puppies (Cavalcante et al., 2012) thereby demonstrating the biological significance of maternal PMN within the colostrum. This is particularly important for puppies which had been infected vertically within bitch uterus resulting in multi-organ tachyzoite infections. After parturition and lactation of *N. caninum*-infected puppies maternal colostrally transmitted PMN might encounter *N. caninum* not only in the intestine, organs but also in the bloodstream of neonates (Lieberl-Tenorio, Riedel-Caspari, Pohlenza, 2002).

As already stated, NETs represent a significant and well-conserved defense effector mechanism against parasites (Conejeros et al., 2019; Grob et al., 2020; Muñoz-Caro et al., 2018; Villagra-Blanco et al., 2017; Zhou et al., 2019). Nonetheless, in all these studies, PMN isolated from blood were exclusively used. Conversely, in the current study canine colostrum-derived PMN were used. This is to the best of our knowledge the first study ever to look at these colostrum-derived cells and their ability to form NETs. This shows not only that PMN are still alive after their transport into the colostrum, but also that they keep their

immunological competences. This is also shown in the phagocytosis experiment, where it was demonstrated that canine colostrum PMN are still able to phagocytose particles after being exposed to them.

Isolation of PMN from colostrum is significantly more complex and difficult than isolation from peripheral blood or bone marrow (Segawa et al., 2011). One reason for this is generally the significantly higher fat content and, in the case of dogs, additionally the low milkable volume of colostrum. The isolation procedure could be a reason for the high variation in cell numbers obtained in our experimental settings. For our presented investigations, one ml of colostrum was here used when milking was no longer possible. Repeatedly, however, the extraction of PMN from the milk secretion also failed, especially with samples with above-average fat (i. e. 10%) content. Moreover, it was also not completely possible to remove other corpuscular components as well as a residual amount of fat from isolated PMN. However, since there was no colostrum PMN activation (i. e. negative controls), it can be assumed that other components remaining after isolation had neither influence on NET formation or phagocytosis.

With regard to the different *N. caninum*-triggered NETs phenotypes, no clear tendency towards a certain type could be established. In colostrum PMN incubated with vital *N. caninum* tachyzoites, diffNET and aggNET showed an equally occurrence and only sprNET occurred significantly less frequently. Interestingly, positive controls using Ca<sup>++</sup> ionophores showed a tendency towards aggNET (data not shown). These observations differ from other reports in the literature. For instance, Grob et al. (2020) found that bovine PMN from peripheral blood after stimulation with vital *T. brucei brucei* resulted primarily in aggNETs. Other studies with large and highly motile multicellular parasites, i. e. *H. contortus*- and *D. immitis* larvae (Muñoz-Caro et al., 2018) showed a dependence on the size of these stimulating parasites and the phenotypes of NETs formed.

One feature that stood out in the samples that were examined by SEM analysis was the presence of vital NETosis. Basically, there are different possibilities of NET formation, including vital-, suicidal and vesicular NETosis (V Shaji et al., 2020). The difference is the integrity or, in the case of suicidal NETosis, the integrity loss of the plasma membrane (Garza et al., 2018). Usually, the vital NETs are formed very quickly (Zhou et al., 2020). The images of SEM ultrastructural analysis of canine colostrum PMN showed an activated cell emitting a chromatin filament toward a pre-existing NETs extrusion entrapping various tachyzoites. Since actual integrity of PMN could not be confirmed by this methodology, it can only be speculated that this phenomenon corresponds most probably to vital NETosis. However, PMN morphology and integrity of cell surface membrane corresponds well to previously published data on *B. besnoitii*-mediated vital NETosis (Zhou et al., 2020). It would be a proof of a rare phenomenon observed by PMN against apicomplexans and confirming that PMN from colostrum are not only alive but also have the capability of suicidal and vital NETosis against *N. caninum* tachyzoites. This could be a plausible explanation for the outstanding importance of colostrum uptake for neonates after parturition and adding a new aspect of defense supplied not only by immunoglobulins diaplacentally but also by maternal PMN transfer.

The results of phagocytosis test confirm once again that PMN obtained from colostrum are living cells capable of performing their defense functions also in neonates. These results underline previous published data in literature that colostrum leukocytes are key players in passive transfer of maternal immunity to the neonates (Bandrick et al., 2014; Chastant-Maillard et al., 2017; Langel et al., 2015; Meganck et al., 2016; Reber et al., 2008).

Regarding the non-significant difference between the phagocytosis rate at 37 °C and the samples kept on ice, a possible explanation is that phagocytosis occurred very rapidly and already reached a nominal value before the sample could be kept on ice.

The second question initially asked was whether *N. caninum* tachyzoites are capable of stimulating PMN to form NETs. This question can be clearly answered positively as isolated colostrum PMN exposed to

## 2.4. *Neospora caninum*-induced NETosis in canine colostral polymorphonuclear neutrophils

L. Demattio et al.

Journal of Reproductive Immunology 154 (2022) 103749

vital/killed tachyzoites responded by extruding NETs. While none of PMN showed NET formation in the control approach, NETs were formed in the approaches with *N. caninum* as well as in the approaches with ionophores (positive controls). Consequently, it can be assumed that this effector mechanism also takes place when *N. caninum* and colostrum PMN *intra vitam* meet in the neonate and thereby representing an important control strategy against this parasitic species.

Nonetheless, further research is needed to investigate whether this phenomenon can also be investigated *in vivo* and whether tachyzoite-triggered NETs might contribute to hamper intracellular replication and outcome of clinical manifested neosporosis. The results of this study indicate once more, that colostrum transfers passively a significant amount of maternal immunity properties in more ways than just by transferring immunoglobulins.

### Declarations of interest

None.

### References

- Abi Abdallah, D., Denkers, E., 2012. Neutrophils cast extracellular traps in response to protozoan parasites. *Front Immunol.* 3, 382.
- Amulic, B., Hayes, G., 2011. Neutrophil extracellular traps. *Curr. Biol.* 21 (9), R297–R298.
- Anvari, D., Saberi, R., Sharif, M., Sarvi, S., Hosseini, S., Moosazadeh, M., 2020. Seroprevalence of *Neospora caninum* infection in Dog Population Worldwide: A Systematic Review and Meta-analysis. *Acta Parasitol.* 65 (2), 273–290.
- Bandrick, M., Ariza-Nieto, C., Baidoo, S.K., Mollitor, T.W., 2014. Colostral antibody-mediated and cell-mediated immunity contributes to innate and antigen-specific immunity in piglets. *Dev. Comp. Immunol.* 43 (1), 114–120.
- Behrend, J., Ruiz, A., Zahner, H., Taubert, A., Hermosilla, C., 2010. Neutrophil extracellular trap formation as innate immune reactions against the apicomplexan parasite *Eimeria bovis*. *Vet. Immunol. Immunopathol.* 133 (1), 1–8.
- Brinkmann, V., Zychlinsky, A., 2012. Neutrophil extracellular traps: is immunity the second function of chromatin? *J. Cell Biol.* 198 (5), 773–783.
- Cavalcante, G., Soares, R., Nishi, S., Hagen, S., Yannucci, C., Maiorka, P.C., 2012. Experimental infection with *Neospora caninum* in pregnant bitches. *Rev. Bras. Parasitol.* 21 (3), 232–236.
- Chastant-Maillard, S., Aggouli, C., Albarét, A., Fournier, A., Mila, H., 2017. Canine and feline colostrum. *Reprod. Domest. Anim.* 52 (Suppl 2), 148–152.
- Conejeros, I., Velásquez, Z., Groh, D., Zhou, E., Salecker, H., Hermosilla, C., 2019. Histone H2A and Bovine Neutrophil Extracellular Traps Induce Damage of *Besnoitia besnoiti*-Infected Host Endothelial Cells but Fail to Affect Total Parasite Proliferation. *Biol. (Basel)* 8 (4).
- Ganz, S., Bille, M., Gajewski, Z., Wehrend, A., 2018. Inhaltsstoffe des bovinen Kolostrums – eine Übersicht. *Tierarz. Prax. G/N.* 46 (3), 178–189.
- Garza, J., Greiner, S., Bowdridge, S., 2018. Ovine vital neutrophil extracellular traps bind and impair *Haemonchus contortus* L3 in a breed-dependent manner. *Parasite Immunol.* 40 (9), e12572.
- Godhia, M., Patel, N., 2013. Colostrum - its composition, benefits as a nutraceutical: a review. *Curr. Res Nutr. Food Sci.* 1 (1), 37–47.
- Gonzalez, D., Dus, Santos, A., 2017. Bovine colostrum cells - the often forgotten component of colostrum. *JAVMA* 250 (9), 998–1005.
- Groh, D., Conejeros, I., Velásquez, Z., Preußler, C., Gärtner, U., Alarcón, P., 2020. Trypanosoma brucei brucei Induces Polymorphonuclear Neutrophil Activation and Neutrophil Extracellular Traps Release. *Front Immunol.* 11, 559561.
- Hasheminasab, S., Conejeros, I., D Velásquez, Z., Borggrete, T., Gärtner, U., Kamena, F., 2022. ATP Purinergic Receptor P2×1-Dependent Suicidal NETosis Induced by *Cryptosporidium parvum* under Physioxia Conditions. *Biol. (Basel)* 11 (3).
- Hermosilla, C., Caro, T., Silva, L., Ruiz, A., Taubert, A., 2014. The intriguing host innate immune response: novel anti-parasitic defence by neutrophil extracellular traps. *Parasitology* 141 (11), 1489–1498.
- Imlau, M., Conejeros, I., Muñoz-Caro, T., Zhou, E., Gärtner, U., Termes, K., 2020. Dolphin-derived NETosis results in rapid *Toxoplasma gondii* tachyzoite ensternment and different phenotypes of NETs. *Dev. Comp. Immunol.* 103, 103527.
- Langel, S., Wark, W., Garst, S., James, R., McGilliard, M., Peterson-Wolfe, C., 2015. Effect of feeding whole compared with cell-free colostrum on calf immune status: The neonatal period. *J. Dairy Sci.* 98 (6), 3729–3740.
- Langel, S., Wark, W., Garst, S., James, R., McGilliard, M., Peterson-Wolfe, C., 2016. Effect of feeding whole compared with cell-free colostrum on calf immune status: Vaccination response. *J. Dairy Sci.* 99 (5), 3979–3994.
- Liebler-Tenorio, E., Riedel-Caspari, G., Pohlenza, J., 2002. Uptake of colostrum leukocytes in the intestinal tract of newborn calves. *Vet. Immunol. Immunopathol.* 33–40.
- Meganck, V., Opsomer, G., Piepers, S., Cox, E., Goddeeris, B.M., 2016. Maternal colostrum leukocytes appear to enhance cell-mediated recall response, but inhibit humoral recall response in prime-boost vaccinated calves. *J. Reprod. Immunol.* 113, 68–75.
- Mila, H., Feugier, A., Grellet, A., Anne, J., Gonner, M., Martin, M., 2015. Immunoglobulin G concentration in canine colostrum: Evaluation and variability. *J. Reprod. Immunol.* 112, 24–28.
- Muñoz-Caro, T., Lendner, M., Daugschies, A., Hermosilla, C., Taubert, A., 2015. NADPH oxidase, MPO, NE, ERK1/2, p38 MAPK and Ca2+ -influx are essential for *Cryptosporidium parvum*-induced NET formation. *Dev. Comp. Immunol.* 52 (2), 245–254.
- Muñoz-Caro, T., Conejeros, I., Zhou, E., Pikhovych, A., Gärtner, U., 2018. Hermosilla, D. Filariaria Innatis Microfilariae and Third-Stage Larvae Induce Canine NETosis Resulting in Different Types of Neutrophil Extracellular Traps. *Front Immunol.* 9, 968.
- Peixoto, D., Verhein, J., Kiani, R., Kao, J., Nuyujukian, P., Chandrasekaran, C., 2021. Decoding and perturbing decision states in real time. *Nature* 591 (7851), 604–609.
- Reber, A.J., Donovan, D.C., Gabbard, J., Galland, K., Aceves-Avila, M., Holbert, K.A., et al., 2008. Transfer of maternal colostrum leukocytes promotes development of the neonatal immune system Part II. Effects on neonatal lymphocytes. *Vet. Immunol. Immunopathol.* 123 (3–4), 305–313.
- Reichel, M., Muñoz-Caro, T., Sánchez Contreras, G., Rubio García, A., Magdowski, G., Gärtner, U., 2015. Harbour seal (*Phoca vitulina*) PMN and monocytes release extracellular traps to capture the apicomplexan parasite *Toxoplasma gondii*. *Dev. Comp. Immunol.* 50 (2), 106–115.
- Seelg, A., Beer, C., 1978. Transepithelial Migration of leukocytes in the mammary gland of lactating rats. *Biol. Reprod.* 17, 736–744.
- Segawa, T., Ito, T., Suzuki, M., Morimoto, T., Nakanishi, T., Sakai, T., 2011. Hematopoietic cell populations in dolphin bone marrow: Analysis of colony formation and differentiation. *Results Immunol.* 1 (1), 1–5.
- Sheldrake, R., Husband, A., 1985. Intra-uterine uptake of intact maternal lymphocytes by neonatal rats and lambs. *Res Vet. Sci.* 39 (1), 10–15.
- Silva, L., Muñoz-Caro, T., Burgos, R., Hidalgo, M., Taubert, A., Hermosilla, C., 2016. Far beyond Phagocytosis: Phagocyte-Derived Extracellular Traps Act Efficiently against Protozoan Parasites *In Vitro* and *In Vivo*. *Mediat. Inflamm.* 2016, 5898074.
- Tuboly, S., Bernáth, S., Glávits, R., Medveczky, L., 1988. Intestinal absorption of colostrum lymphoid cells in newborn piglets. *Vet. Immunol. Immunopathol.* 20 (1), 75–85.
- Villagra-Blanco, R., Silva, L.M.R., Muñoz-Caro, T., Yang, Z., Li, J., Gärtner, U., 2017. Bovine Polymorphonuclear Neutrophils Cast Neutrophil Extracellular Traps against the Abortive Parasite *Neospora caninum*. *Front Immunol.* 8, 606.
- Villagra-Blanco, R., Silva, L., Conejeros, I., Taubert, A., Hermosilla, C., 2019. Pinniped and Cetacean-Derived NETosis Contributes to Combating Emerging Apicomplexan Parasites (*Toxoplasma gondii*, *Neospora caninum*) Circulating in Marine Environments. *Biol. (Basel)* 8 (1).
- Wei, Z., Hermosilla, C., Taubert, A., He, X., Wang, X., Gong, P., 2016. Canine Neutrophil Extracellular Traps Release Induced by the Apicomplexan Parasite *Neospora caninum* *In Vitro*. *Front Immunol.* 7, 436.
- Williams, P., 1993. Immunomodulating effects of intestinal absorbed maternal colostrum leukocytes by neonatal pigs. *Can. J. Vet. Res.* 57, 1–8.
- Zhou, E., Conejeros, I., Velásquez, Z., Muñoz-Caro, T., Gärtner, U., Hermosilla, C., et al., 2019. Simultaneous and Positively Correlated NET Formation and Autophagy in *Besnoitia besnoiti* Tachyzoite-Exposed Bovine Polymorphonuclear Neutrophils. *Front Immunol.* 10, 1131.
- Zhou, E., Silva, L., Conejeros, I., Velásquez, Z., Hinz, M., Gärtner, U., 2020. *Besnoitia besnoiti* bradyzoite stages induce suicidal- and rapid vital-NETosis. *Parasitology* 147 (4), 401–409.

## **2.5. *TRYPANOSOMA BRUCEI BRUCEI*-INDUCED AGGREGATED NETS (*aggNETS*) ARE DEPENDENT ON PURINERGIC RECEPTORS P2X1 AND P2Y6**

This chapter is based on the following unpublished paper

Grob D., Larrazabal C., Vellmer T., Janzen C. J., Gärtner U., Taubert A, Hermosilla, C., Conejeros I. 2022. *Trypanosoma brucei brucei*-induced aggregated NETs (*aggNETs*) are dependent on purinergic receptors P2X1 and P2Y6 (manuscript in preparation)

Eigener Anteil in der Publikation:

Projektplanung	65 %, zusammen mit Ko-Autoren und Betreuern
Durchführung des Versuches	60 %, weitestgehend selbständig
Auswertung der Experimente	80 %, weitestgehend selbständig
Erstellung der Publikation	70 %, weitestgehend selbständig

## **2.5 *Trypanosoma brucei brucei*-induced aggregated NETs (*aggNETs*) are dependent on purinergic receptors P2X1 and P2Y6**

---

***Trypanosoma brucei brucei*-induced aggregated NETs (*aggNETs*) are dependent on purinergic receptors P2X1 and P2Y6**

<sup>1,\*</sup> Grob D., <sup>1</sup>Larrazabal C., <sup>2</sup>Vellmer T., <sup>2</sup>Janzen C. J., <sup>3</sup>Gärtner U., <sup>1</sup>Taubert A., <sup>1</sup>Hermosilla C., <sup>1</sup>Conejeros I.

<sup>1</sup>Institute of Parasitology, Justus Liebig University of Giessen, Giessen, Germany

<sup>2</sup>Department of Cell & Developmental Biology, Biocenter, University of Würzburg, Würzburg, Germany

<sup>3</sup>Institute of Anatomy and Cell Biology, Justus Liebig University Giessen, Giessen, Germany

### **\*Correspondence:**

**Corresponding author:** Daniela Grob [daniela.grob@vetmed.uni-giessen.de](mailto:daniela.grob@vetmed.uni-giessen.de). Institute of Parasitology, Biomedical Research Center Seltersberg (BFS), Schubertstr. 81, 35392 Giessen, Germany.

**Keywords:** PMN, *Trypanosoma brucei brucei*, *aggNETs*, NF449, MRS2578

## 2.5 *Trypanosoma brucei brucei*-induced aggregated NETs (*aggNETs*) are dependent on purinergic receptors P2X1 and P2Y6

---

### ABSTRACT

*T. b. brucei* is an important parasite that affects both, animal and human health. At acute infection bloodstream trypomastigotes will interact with innate immune cells. Polymorphonuclear neutrophils (PMN) are the most abundant leukocyte in the bloodstream, eliciting several mechanisms in order to control and confront the insulting agent. In the present study, we investigated the induction of *aggNETs* induced by *T. b. brucei*-bloodstream metacyclic trypomastigotes and the role of purinergic signaling in *aggNETs* formation. NETs were studied by scanning electron microscopy (SEM) and immunofluorescence unveiled that co-culture of freshly isolated bovine PMN with *T. b. brucei* bloodstream metacyclic trypomastigotes was able to trigger the formation of *aggNETs* within 4 h. For comparison and as positive controls, we also observed that bovine PMN form *aggNETs* upon stimulation with ionomycin or monosodium urate (MSU) crystals. These results were complemented with live-cell 3D-holotomographic microscopy, allowing to study in better detail the conformation and volume of *aggNETs*. PMN activation also increased the oxygen consumption rate (OCR). Pretreatment of the cells with the inhibitor of P2X1, NF449, and the inhibitor of P2Y6, MRS2578, showed a decrease in both OCR and ECAR. This inhibition was also observed when the *aggNETs* phenotype induced by *T. b. brucei* was studied by immunofluorescence.

## 2.5 *Trypanosoma brucei brucei*-induced aggregated NETs (aggNETs) are dependent on purinergic receptors P2X1 and P2Y6

---

### Introduction

Animal African trypanosomiasis, also known as Nagana in Zulu (“powerless/useless”) is a neglected tropical disease (NTD) that affects sub-Saharan African countries (1,2). The causal agent is the euglenozoan parasite, *Trypanosoma brucei brucei*, able to infect cattle and camels, suidae and antelopes (3). To complete his life cycle, *T. b. brucei* requires an intermediate host and vector. In this case is the tsetse fly (*Glossina* spp.) (3). Once the host becomes infected, the parasite multiply and disseminate trough the blood/lymphatic system along different internal organs of the host (4,5). Clinically, symptoms of infection are considered as rather non-specific, including a general body condition detriment, pale mucous membranes, alterations of the consistency of feces and atypical body temperature (6). The overall clinical development of the disease, usually ends with sudden death. *T. b. brucei*-infected cattle the biggest reservoir of the parasite in endemic areas (7).

Since the parasite develops in the blood, the bloodstream metacyclic trypomastigotes interacts with physical barriers of the of the innate immune system and different cell types, as polymorphonuclear neutrophils (PMN) (8). PMN are the most abundant leukocyte in the blood circulation, that migrates quickly to the site on infection. PMN react against foreign pathogens by executing different effector mechanisms, such reactive oxygen species (ROS) production, phagocytosis, release of immunomodulatory molecules [cytokines, chemokines (CXCL1, CXCL8, CXCL10)] (9,10) and release of neutrophil extracellular traps (NETs) (10,11,12). NET formation is an important defense mechanism against a wide range of parasites as *B. besnoiti*, *N. caninum*, *T. cruzi*, *L. infantum*, *D. immitis*, *A. vasorum* and *H. contortus* (10,11,24,37,41,42,58). Nonetheless, molecular determinants of protozoan and metazoan parasites-induced NETs are not fully characterized.

The NETotic process includes well defined steps. Notablythe first correspondsto the decondensation of nuclear chromatin driven by protein arginine deiminase 4 (PAD4)-mediated citrullination of histones (13,14). Then, enzymes that are contained in PMN granules as neutrophil elastase (NE) and myeloperoxidase (MPO) translocate to the nucleus and fuse with the chromatin (15). Finally, the PMN membrane disintegrates as a consequence of the higher ROS concentration and the activity of lytic proteins like gasdermin-D. This enzymatic step produces the formation of pores on the membrane, permitting the NETs extrusion into the extracellular matrix (16,17). Classification of NETs is dependent on different criteria. For example, considering the time and speed involved in the process and the dependency with the

## **2.5 *Trypanosoma brucei brucei*-induced aggregated NETs (*aggNETs*) are dependent on purinergic receptors P2X1 and P2Y6**

---

activation of NOX, they could be categorized as suicidal or vital NETosis (18). Regarding the NETs phenotype, NETs are classified into three phenotypes: (i) spread NETs (*sprNETs*) consisting of an smooth and elongated web-like structure of decondensed chromatin, with a diameter of 15-17  $\mu\text{m}$ , (ii) diffuse NETs (*diffNETs*) which are formed by a complex of extracellular decondensed chromatin decorated with antimicrobial proteins, having a size between 15-20  $\mu\text{m}$  and (iii) aggregated NETs (*aggNETs*), described as a “big ball of yarn” and a size of more than 20  $\mu\text{m}$  (10,19,20).

Interestingly, the first description of *aggNETs* was achieved by the stimulation of PMN with monosodium urate crystals (MSU) (59). MSU crystals drives to a resolution of inflammation in gout, most likely by the degradation of inflammatory cytokines (21,22) and sequestration of inflammatory mediators in the *aggNETs* and thus, modulatinh the recruitment of new leukocytes (21). After co-incubation of PMN with MSU crystals, PMN will try to phagocytose the MSU crystals, then will produce ROS, release granular proteins and produce NETs (11,23,24,60). Notably, MSU crystals induce ETs in neutrophils, eosinophils and basophils, but not in mononuclear cells (61); also, a potential function of MSU-induced NETs in this context is the immobilization of the MSU crystals (62).

A second important aspect of the MSU crystals-induced NETs research is the fact that PMN density present in *aggNETs* plays a critical role in the observed biological effects. In this context, it has been demonstrated that an increase in PMN density is correlated with a rise in the release of NE (22,25). The increase in NE concentration allows the degradation of proteins of the extracellular matrix (26). In addition, it is known that PMN release proteases that have an effect classified as pro- and anti-inflammatory; while in the acute state enzymes trigger a pro-inflammatory/tissue damaging effect, enzymes will have a regulatory function in the resolution of inflammation and stimulation of tissue repair in the chronic inflammation (25). The role of *aggNETs* in the physio-pathological aspects of the Nagana disease in cattle is unknown.

Adenosine nucleotides as ATP and adenosin nucleosides (ADO) are known to have a crucial role in energy metabolism. In addition, these molecules can act as signal molecules associated with danger or tissue damage, modulating the proinflammatory response (27). ATP and ADO activates the purinergic signaling, by interaction with specific purinergic receptors (28). Purinergic signaling is among the most conserved transduction signal in evolution. In humans, proteins and molecules belonging to the purinergic signaling pathway are expressed in all

## **2.5 *Trypanosoma brucei brucei*-induced aggregated NETs (aggNETs) are dependent on purinergic receptors P2X1 and P2Y6**

---

tissues and cell types (28,30). Purinergic receptors are classified in two families: receptors for ATP (P2 receptors) and receptors for ADO (P1 receptors). P2 receptors are sub-classified into ionotropic P2X and metabotropic P2Y (28,29). The P2X receptor is a trimeric ion channel activated exclusively by ATP (28,31). Following the binding of ATP, P2X becomes permeable to Na<sup>+</sup>, K<sup>+</sup> and Ca<sup>++</sup> (28). In the case of P2Y, is a G-protein-coupled receptor and is triggered by ATP, adenosine diphosphate (ADP), and non-ADO nucleotides as uridine triphosphate (UTP) and uridine diphosphate (UDP) (29). In PMN the participation of P2 and P1 (respectively) modulates critical functions such as migration, degranulation, and ROS production (27,28,32). Recent data shows that MSU crystals activate the purinergic receptor P2Y6 in THP1 macrophages and human keratinocytes (33). Also, P2Y6 receptor, that has a high affinity to UDP, modulates IL-8-mediated chemotaxis of leukocytes (34,35). MRS2578, a potent antagonist of P2Y6 receptor, inhibits IL-8 and IL-6 release in human PMN (36). So far, the participation of the purinergic signaling in bovine PMN has been demonstrated for protozoan parasites as *B. besnoiti* and *C. parvum*, since the preincubation of the cells with NF449, an inhibitor of P2X1, reduces the release of DNA and NET formation (20,37). This inhibitory effect is also observed when the cells are activated with non-esterified fatty acids as oleic and linoleic acids (38), indicating a conserved role of the purinergic signaling in bovine PMN. Finally, we observed recently that *T. b. brucei* procyclic trypomastigotes triggers predominantly the formation of the aggNETs phenotype and that NF449 reduces DNA release, nuclear area expansion (NAE) and NET formation, suggesting a pivotal role of P2X1 in *T. b. brucei*-mediated PMN activation.

In the present report, we study the NET formation in bovine PMN induced by the bloodstream metacyclic trypomastigote stage of *T. b. brucei* via scanning electron microscopy (SEM), immunofluorescence analyses and three-dimensional (3D) holotomographic microscopy. As comparison and positive controls, we used ionomycin and MSU crystals, as a known purinergic signaling activator of PMN and P2R-mediated NET release. Also, the influence of time and PMN density was evaluated. In addition, PMN activation was also estimated by Seahorse technology determining the oxygen consumption rate (OCR) and extracellular acidification rate (ECAR). Current data shows that *T. b. brucei*-triggered aggNETs seems to be related as purinergic-dependent process, considering that PMN treatment with the purinergic signaling inhibitors NF449 (P2X1) and MRS2578 (P2Y6) decreases the formation aggNETs and reduce the OCR in bovine PMN confronted with *T. b. brucei*.

## **2.5 *Trypanosoma brucei brucei*-induced aggregated NETs (aggNETs) are dependent on purinergic receptors P2X1 and P2Y6**

---

### **MATERIAL AND METHODS**

#### **Ethics statements**

This study was conducted following the Justus Liebig University Giessen (JLU) Animal Care Committee Guidelines. Protocols were approved by Ethics Commission for Experimental Animal Studies of Federal State of Hesse (Regierungspräsidium Giessen; A9/2012; JLU-No.521\_AZ) and in accordance to European Animal Welfare Legislation: ART13TFEU and current applicable German Animal Protection Laws.

#### ***T. b. brucei* bloodstream metacyclic trypomastigote form culture**

*T. b. brucei* bloodstream metacyclic trypomastigotes (strain Lister 427, antigenic type MITat 1.2 clone 221a) were cultured in HMI-9 medium (PAN-Biotech; Germany) supplemented with 10% heat-inactivated fetal calf serum (FCS) at 37°C and 5% CO<sub>2</sub>, as previously described (39).

#### **Isolation of bovine PMN**

Healthy adult dairy cows served as blood donors. Animals were bled by puncture of jugular vein and 30 ml peripheral blood were collected in 12 ml heparinized sterile plastic tubes (Kabe Labortechnik). Then, 20 ml of heparinized blood were diluted in 20 ml sterile PBS with 0.02% EDTA (Sigma-Aldrich), layered on top of 12 ml Histopaque-1077 separating solution (density = 1.077 g/l; Sigma Aldrich) and centrifuged (800 × g, 45 min). The plasma and the buffy coat were carefully aspirated, and the remaining red blood cells (RBC) and pellet at the bottom of the tube were suspended in Hank's balanced salt solution (HBSS). RBC were removed by a flash hypotonic lysis performed with 1 volume of ice-cold phosphate buffered water solution containing 5.5 mM NaH<sub>2</sub>PO<sub>4</sub>, 8.4 mM HK<sub>2</sub>PO<sub>4</sub> at pH 7.2. After 1 min of RBC lysis, 2 volumes of hypertonic phosphate buffer containing 5.5 mM NaH<sub>2</sub>PO<sub>4</sub>, 0.46 M NaCl and pH 7.2 were added to recover the isotonicity; after this, the tubes were centrifuged at 600 × g for 10 min at 20°C. The neutrophil pellet was washed with HBSS 3 times. After this, PMN were suspended in 5 ml of HBSS and counted in a Neubauer haemocytometer. Finally, freshly isolated bovine PMN were allowed to rest at 37 °C and 5% CO<sub>2</sub> atmosphere for 30 min before experimental use.

## **2.5 *Trypanosoma brucei brucei*-induced aggregated NETs (aggNETs) are dependent on purinergic receptors P2X1 and P2Y6**

---

### **Scanning electron microscopy (SEM) analysis**

Bovine PMN (n = 3) were co-cultured with vital *T. b. brucei* bloodstream metacyclic trypomastigotes (ratio of 1:1,  $1.2 \times 10^6$ ) for 4h on 12-well plates (Greiner) containing 10 mm-coverslips (Thermo Fisher Scientific) pre-coated with 0.01% poly-L-lysine (Sigma-Aldrich) at 37 °C and 5% CO<sub>2</sub>. After incubation, cells were fixed in a medium containing 2.5% glutaraldehyde (Merck), 2.5% paraformaldehyde (Merck) and 300 mM Hepes (Carl Roth), post-fixed in 1% osmium tetroxide (Merck), washed in distilled water, dehydrated, critical point dried by CO<sub>2</sub>-treatment and sputtered with gold particles. Finally, all samples were visualized via a Philips XL30® scanning electron microscope at the Institute of Anatomy and Cell Biology, JLU Giessen, Germany.

### ***T. b. brucei*-triggered NETs visualized by immunofluorescence analysis**

Bovine PMN (n = 3) were co-cultured with vital *T. b. brucei* bloodstream metacyclic trypomastigotes (ratios of 1:1,  $1.2 \times 10^6$ ) for 4 h and 18 h on coverslips (10 mm of diameter; Thermo Fisher Scientific) pre-coated with 0.01% poly-L-lysine (Sigma-Aldrich) at 37°C and 5% CO<sub>2</sub>. After corresponding incubation time, the cells were fixed in 4% paraformaldehyde (Merck) and stored at 4 °C until further use. To visualize NETs structures, DAPI staining (4',6-diamidino-2-phenylindole, Thermo Fisher) was used to stain total DNA, anti-histone (H1, H2A/H2B, H3 and H4, 1:200, Merck #MAB3422) and anti-neutrophil elastase (NE) (1:200, Abcam #ab68672) antibodies were used to detect NET-specific components/proteins. The samples were incubated for 1 h (RT) with blocking buffer, containing 3% bovine serum albumin (BSA; Sigma-Aldrich) and 0.3% Triton X-100 (Thermo Fischer Scientific). Then, the samples were incubated in primary antibody solutions for 3 h at RT followed by three washing steps with sterile PBS, and incubated in secondary antibody solutions (Alexa 594 goat anti-mouse IgG #A110005, Alexa 488 goat anti-rabbit IgG #A11008, 1:500, Invitrogen) for 30 min at RT in darkness. Finally, the samples were washed three times with sterile PBS and mounted upside-down with Fluoromount G (Thermo Fischer Scientific). Visualization of NETs formation was achieved using an inverted IX81 epifluorescence microscope equipped with an XM 10 digital camera (both Olympus).

## **2.5 *Trypanosoma brucei brucei*-induced aggregated NETs (*aggNETs*) are dependent on purinergic receptors P2X1 and P2Y6**

---

### **3D holotomographic microscopy and image analysis**

3D holotomographic images were obtained from coverslips prepared for immunofluorescence, as previously mentioned. Images were obtained by using a 3D Cell Explorer-fluo microscope (Nanolive®) equipped with 60× magnification ( $\lambda = 520$  nm, sample exposure 0.2 mW/mm<sup>2</sup> and a depth of field of 30  $\mu$ m) and a fluorescence unit (CoolLED pE-300ultra) (40). Images were analyzed using STEVE software (Nanolive®) to obtain refractive index-based z-stacks. In addition, the raw data was analyzed using Digital staining of subcellular structures was performed based on generated RI data.

### **Blockage of purinergic signaling in PMN stimulated with *T. b. brucei* bloodstream metacyclic trypomastigotes**

Bovine PMN ( $n = 3$ ) were suspended in sterile HBSS buffer (Sigma-Aldrich) at a final density of  $1.2 \times 10^6$  cells. For NF449 (P2X1 inhibitor, 100 and 10  $\mu$ M, Tocris, #7038) and MRS2578 (P2Y6 inhibitor, 10  $\mu$ M; Biozol) inhibition studies, PMN and the parasite were seeded on 0.01% poly-L-lysine pre-coated coverslips (Greiner). After 4h or 18h of exposure, cells were fixed in 2% paraformaldehyde (Roth) and stained for immunofluorescence analyses, as previously described. After this, five power vision field images were randomly taken for each condition using an inverted epifluorescence IX81® microscope (Olympus) equipped with a XM 10® digital camera (Olympus) for further analysis.

### **Quantification of oxygen consumption rates and extracellular acidification rates in *T. b. brucei* bloodstream metacyclic trypomastigotes-exposed PMN**

Activation of PMN was performed by using Seahorse XFp analyzer (Agilent). Briefly,  $1 \times 10^6$  PMN from three different donors were pelleted (500 x g for 10 min, RT). Then, the supernatant was discarded and cells were suspended in 0.5 ml of RPMI XF assay medium (Agilent), supplemented with 2mM of l-glutamine, 1mM pyruvate and 10mM glucose. Then,  $1 \times 10^5$  cells (50 $\mu$ l of cell solution) were gently placed in each well of an eight-well XFp analyzer plate (Agilent) pre-coated for 30 min with 0.001% poly-L- lysine (Sigma Aldrich). After this, 50  $\mu$ l of XF assay medium (Agilent) were added to blank wells (=no cell-control). Finally, 130  $\mu$ l of XF assay medium (Agilent) was added to all wells (180  $\mu$ l total volume) and cells were

## 2.5 *Trypanosoma brucei brucei*-induced aggregated NETs (*aggNETs*) are dependent on purinergic receptors P2X1 and P2Y6

---

incubated at 37° without CO<sup>2</sup> supplementation for 45 min before Seahorse measurements. When NF449 was used to inhibit the function of the P2X1, a 10 μM solution was used as a pre-treatment of the PMN; when MRS2578 was used to inhibit the function of the purinergic receptor P2Y6, a 10 μM solution was used as a pre-treatment. On the other hand, *T. b. brucei* bloodstream metacyclic trypomastigotes were suspended in RPMI XF assay medium (Agilent, 300.000 parasites/20 μl) and placed in one of the four injection ports of the instrument. For PMN controls, only 20 μl of XF® assay medium (Agilent) was dispensed. The assay included basal measurements of three readings, followed by the injection of the vital *T. b. brucei* bloodstream metacyclic trypomastigotes or medium and 30 reading cycles. The total duration of the assay was 213 min. Background subtraction, determination of oxygen consumption rate (OCR), extracellular acidification rate (ECAR) and area under the curve was performed using Wave® software (Desktop Version, Agilent).

### Analysis of *aggNET* phenotype

For quantification of *aggNETs* phenotype, we followed the description given by (19,20,41,42). Briefly, two PMN (n = 3) densities were used and 1.2 x 10<sup>6</sup> PMN were seeded on 0.01% poly-L-lysine (Sigma-Aldrich) pre-coated coverslips (Thermo Fischer Scientific) and exposed to *T. b. brucei* bloodstream metacyclic trypomastigotes (1:1 ratio, 1.2 x 10<sup>6</sup>) for 4 h and 18 h (37 °C, 5% CO<sup>2</sup>). Considering previous reports (25,43), ionomycin (5μg/mL) and monosodium urate crystals (MSU) (1mg/ml) were used as positive controls for the formation of *aggNETs*. Afterwards, samples were fixed in 2% paraformaldehyde (Merck) and stored at 4 °C until further analysis. The presence of *aggNETs* was quantified by visualization and staining of extracellular DNA with DAPI staining (4',6-diamidino-2-phenylindole, Thermo Fisher), anti-NE (1:200, Abcam #ab68672) and anti-histone (H1, H2A/H2B, H3 and H4, 1:200, Merck #MAB3422) antibodies as previously described (20). For visual quantification, five random power vision pictures were taken from each experimental condition using an inverted IX81® fluorescence microscope equipped with an XM 10® digital camera (both Olympus) and analyzed microscopically based on previously described typical morphological characteristics (20). To quantify PMN forming NETs, *aggNETs* and the number of cells forming the aggregated the images were exported using CellSens® imaging software (Olympus) and analyzed using Image J® software (Fiji version 1.7, NIH). The percentage of cell doing NETs and the percentage of *aggNETs* were calculated.

## **2.5 *Trypanosoma brucei brucei*-induced aggregated NETs (aggNETs) are dependent on purinergic receptors P2X1 and P2Y6**

---

### **Statistical Analysis**

For all experiments in the current study, an  $\alpha=0.05$  was defined to assume a p-value considered significant. The data was analyzed applying non-parametric analyses: Mann-Whitney test when two experimental conditions were compared and Kruskal-Wallis test followed by Dunn's posthoc test for multiple comparisons. Shapiro-Wilk normality test was performed on the data of inhibitors. In this case, differences between treatments were estimated by ANOVA. All graphs (mean  $\pm$  SD), AUC calculations and statistical analyses were performed using Graph Pad® Prism software (v.7.03).

## **2.5 *Trypanosoma brucei brucei*-induced aggregated NETs (*aggNETs*) are dependent on purinergic receptors P2X1 and P2Y6**

---

### **RESULTS**

#### ***T. b. brucei* bloodstream metacyclic trypomastigotes are able to induce NETs and *aggNETs* formation at 4 and 18 h post incubation.**

SEM analysis unveiled that exposure of bovine PMN to *T. b. brucei* bloodstream metacyclic trypomastigotes (Fig. 1) for 4h induced the formation of *aggNET* (arrows Fig. 1B-1E). In addition, co-culture of PMN with ionomycin and MSU crystals was performed as positive control, confirming the formation of this phenotype (Fig. 1C-1D-1F-1G).

By knowing this, immunofluorescence analyses were performed, confirming presence of NETs formation by the co-localization of classical components: extracellular DNA decorated with histones and neutrophil elastase (NE) (Fig. 4, Fig. 5). Here we performed co-culture with two different time points: 4 h and 18 h of incubation, ratio of 1:1 (bovine PMN: parasite). Regarding the differences between both time points, we could see that bovine PMN were able to react against the presence of the stimuli here evaluated, with the consequent activation and formation of *aggNETs* (Fig. 4H, 4L, 4P; Fig. 5H, 5L, 5P).

In addition, pretreatment of bovine PMN was performed by using purinergic inhibitor NF449 (inhibitor of the P2X1 receptor) and MRS2578 (inhibitor of the P2Y6 receptor), that allowed us to unveil a strong decrease on formations of NETs and *aggNETs* in both time points here studied.

#### **3D-holotomographic imaging of *T. b. brucei*-mediated NETs**

Using a 3D-holotomographic cell-based imaging system, we here studied how does the volume of bovine PMN changes after 4h of stimulation with *T. b. brucei* bloodstream metacyclic trypomastigotes. As is depicted in Fig. 2A, classical morphology of bovine PMN can be observed after performing digital staining, revealing round shape of the cell, with multi-lobulated nuclei. After stimulation, Fig. 2A shows the decondensation of the nuclei achieved as consequence of the presence of the parasite, triggering the formation of *aggNETs*. Interestingly, when the analysis of images was performed, we were able to obtain the refractive index (RI) of them. This info is directly related with the size of the nuclei from the cells, allowing us to estimate the volume that control and stimulated cell have. As Fig. 2B shows, we here observed

## **2.5 *Trypanosoma brucei brucei*-induced aggregated NETs (*aggNETs*) are dependent on purinergic receptors P2X1 and P2Y6**

---

that control PMN had an RI with a mean of 4298.7  $\mu\text{m}^3/\text{field}$  compared with the stimulated one having 6587.52  $\mu\text{m}^3/\text{field}$ .

### ***T. b. brucei*-induced PMN activation seems to be dependent on purinergic signaling**

As previously mentioned, we studied the role of the purinergic signaling pathway regarding *T. b. brucei*-triggered NETs release, *aggNETs* formation and bovine PMN activation, knowing that is an energy and ATP-dependent process (28,29). Therefore, NF449 (inhibitor of the P2X1 receptor) and MRS2578 (inhibitor of the receptor P2Y6) were tested evaluating the effect on activation of the cells by using Seahorse XF® analyzer (Agilent). As illustrated in Fig. 5, after obtaining the basal OCR and ECAR of non-stimulated PMN, live bloodstream metacyclic trypomastigotes stage of *T. b. brucei* were injected and able to trigger a sustained increase in time in OCR and ECAR. As Fig. 8 depicts, analysis of the area under the curve (AUC) revealed an increase in OCR in the control group within the three treatments.

Also, a transitory enhancement of ECAR was observed in the treated PMN exposed *T. b. brucei*; as has been previously reported by our group (20). Interestingly, the observed increase in OCR of the stimulated cells was prevented by the pre-treatment with MRS2578 (10  $\mu\text{M}$ ) (Fig. 3A, Fig. 3C), allowing us to suspect an involvement of P2Y6 receptors in the process. As is shown in Fig. 3B and Fig. 3D, area under the curve analysis (AUC) revealed a significant increase ( $p > 0,05$ ) when we compared treated cells against non-treated, in the case of OCR and ECAR.

Surprisingly, when the same conditions were evaluated with the treatment of 10  $\mu\text{M}$  of NF449, inhibitor of P2X1 receptor, results differ. As can be seen in Fig. 3E – Fig. 3G, results shown to us a non-sustained effect in time in OCR and ECAR, situation confirmed with the AUC analysis.

### **Purinergic receptors P2Y6 and P2X1 are involved in *aggNET*-formation**

To complement the results obtained by immunofluorescence microscopy in fixed cells, observer-based quantification of cell number casting NETs and *aggNETs* formation was performed, revealing that bovine PMN were able to react to the presence of the different stages of the parasite and different stimuli, as observed in Fig. 4 and Fig. 5. We here quantified the percentage of bovine PMN performing NETs in the time points previously mentioned, where we observe that with 4h of co-culture, the stimulated cells casted 11.22% of NETs, whereas the

## **2.5 *Trypanosoma brucei brucei*-induced aggregated NETs (*aggNETs*) are dependent on purinergic receptors P2X1 and P2Y6**

---

treated cells with NF449 casted 3.9% and 11.13% (100  $\mu$ M and 10  $\mu$ M, respectively). In the case of MRS2578, the percentage achieved corresponds to 8.53% (Fig. 6A). 18 h of incubation showed to us that 12.35% from the bovine stimulated PMN were forming NETs, alike as our other incubation time. Also, NF449 treatments decreased the NETs formation to 2.83% (100  $\mu$ M), while NF449 and MRS2578 (10  $\mu$ M) remained equal (11.13% and 8.53%, respectively) (Fig. 6C). Finally, the positive controls were also quantified, obtaining a 13.78% for ionomycin and 9.77% for MSU crystals in the 4h time point, against 8.09% and 19.12% at 18h, respectively (Fig. 6B, Fig. 6D).

Fig. 6E and Fig. 6G shows the effect of the purinergic inhibitors in both time points, regarding the formation of *aggNETs*. With co-culture of 4 h, we obtained a total of 24.81% of *aggNETs* formation with the presence of the *T. b. brucei* bloodstream metacyclic trypomastigotes; interestingly with the treatment of NF449 (100  $\mu$ M), this was completely abolished in contrast with the concentration of 10  $\mu$ M of the same inhibitor, where we were able to quantify a total of 18.09% of this phenotype. Interestingly, in the case of MRS2578 (10  $\mu$ M), a 1.66% of *aggNETs* could be measured, unveiling to us the strong effect of this inhibitor in this process (Fig. 6E), when compared with NF449 (10  $\mu$ M). In the condition of 4 h of co-culture, we observe that the amount of *aggNETs* formed by the presence of the parasite was practically alike, showing a total of 22.65% of *aggNETs* formation. Related to the effect of the inhibitors a similar situation occurred by knowing that NF449 (100  $\mu$ M) and MRS2578 (10  $\mu$ M) completely ended the *aggNETs*-formation and, also, NF449 (10  $\mu$ M) decreased the formation of this phenotype to 11.61% (Fig. 6G), when compared with the controls.

Lastly, we quantified the formation of *aggNETs* triggered by ionomycin and MSU crystals at 4h and 18h of incubation, observing similar percentage in both time points with ionomycin (18.49% and 22.87%, respectively) and MSU crystals (17.24% and 18.09%, respectively) (Fig. 6F, Fig. 6H).

## 2.5 *Trypanosoma brucei brucei*-induced aggregated NETs (*aggNETs*) are dependent on purinergic receptors P2X1 and P2Y6

---

### Discussion

In this study, we show that the bloodstream metacyclic trypomastigote stage from the euglenozoan parasite *T. b. brucei* triggers *aggNETs* formation in a process dependent of the purinergic receptors P2X1 and P2Y6. Previous reports have demonstrated and characterized differences between phenotypes of NETs triggered by several types of parasites, such *S. stercoralis*, *H. contortus*, *A. vasorum*, *D. immitis*, *T. brevior*, *B. malayi* and *T. b. brucei* procyclic trypomastigotes (10,19,20,41,42,44,45). In this sense, this work represents first report that confirms *T. b. brucei*-induces *aggNETs* is stage independent (20). Previous study from our group showed that PMN are able to cast a 28.3% of NETs against *T. b. brucei* procyclic trypomastigotes, having *aggNETs* as main phenotype (20). Here we observed that bloodstream metacyclic trypomastigotes cast the formation of *aggNETs* independently of the time point here analyzed (4 h and 18 h). In addition, we report for the first time RI-based acquisitions of *aggNETs* by holotomographic microscopy. This technique allowed us to monitor 3D holotomographic signals to characterize the appearance of the *aggNETs* at 4 h of stimulation. In previous reports, we achieved to perform RI-based digital staining values of cell structures (20,40). Here, applying the same technique, we were able to estimate, for the first time, the volume that *aggNETs* can have after co culture with *T. b. brucei* bloodstream metacyclic trypomastigotes, confirming the loss of normal shape of PMN during the NETs formation (12).

Overall, *aggNETs* can be induced by different molecules such  $\text{Ca}^{++}$  ionophores and crystalized structures (46). Given that, we explored ionomycin and MSU crystals as inductors in bovine PMN, due to the fact that release of NETs will occur by the  $\text{Ca}^{++}$  permeabilization with ionomycin and direct contact between PMN and MSU crystals (25,43,47). In our experimental setting, we observed that ionomycin has stronger effect triggering *aggNETs* at 4 h compared with 18 h. This finding resembles a prior work, where they observed that the formation of *aggNETs* in human PMN, after incubation with MSU crystals, was able to fill the circumference of the well, whereas the aggregated formed by ionomycin were smaller and often dispersed over the well (25). A possible explanation to this could be the fact that  $\text{Ca}^{++}$  mobilizing effect will be already stabilized at 18 h of stimulation. In this sense,  $\text{Ca}^{++}$  ionophores have been considered as triggers for the formation of NETs in PMN (48–51), being ionomycin described as cause *aggNETs* inductor (25,43,47). Additionally, the mechanism underlying MSU-driven NETs formation are possibly linked to the physical contact between both components, which can be imperative to trigger the NET formation (25,43,47). Moreover, to confirm if this was

## **2.5 *Trypanosoma brucei brucei*-induced aggregated NETs (*aggNETs*) are dependent on purinergic receptors P2X1 and P2Y6**

---

also extended to bovine PMN, we here co-cultured freshly isolated PMN with MSU crystal and quantify the formation of NETs and *aggNETs*. Interestingly, here we observed that at 4 h and 18 h was an increase of the *aggNETs*. Nevertheless, it must be highlighted that here we observed bigger accumulation of *aggNETs* at 4 h of incubation. Prior works suggests that, *aggNETs* driven by MSU crystals could be affected by the attraction with surrounding cells generating a swarming-like effect, generating a dynamic process that facilitates the formation of aggregated (25). However, one of the mechanisms that is considered to be related with the process, is the direct effect of the crystal against the membrane of the cell, leading to ion fluxes and the initiation of NET release (33,43). In this context, one alternative mechanism possibly involved on the process of MSU crystal-induced NETs, is the participation of purinergic receptors. NETs formation has been previously described as a process accompanied by the release of ectonucleotides to the cellular environment, being them bended to purinergic receptors and, consequently, regulating the immune signaling and response (43,52). It has been already demonstrated that purinergic signaling plays an important role in PMN functions, that includes ROS, signaling pathways (53) and migration as a consequence of chemotaxis to sites of cell damage (43). In this study we evaluated participation of P2X1 and P2Y6 present in PMN ROS production and NETs formation. Related to ROS production by PMN, it is known that seems to be essential for the release of NETs, being associated with an increase in OCR (16,17), and with an enhancement of the ECAR to fulfill the proper NET formation (20,54). By knowing this, we here demonstrate how OCR and ECAR are strongly enhanced in PMN after the injection of vital and motile *T. b. brucei* bloodstream metacyclic trypomastigotes. More interestingly, after the pre-treatment of PMN with NF449 and MRS2578, independently, we here see how both processes are strongly affected, allowing to confirm the involvement of both. This result may reflect the critical role of extracellular nucleotides and nucleosides as signaling molecules in the activation process of the PMN.

Another interesting aspect of PMN relays in the sensing capacity they have to recognize size and movement of the stimuli, that have been already proved against bacteria and fungi (55,56); nonetheless, little is known regarding the parasite movement. Due to the strong and continue motility that *T. b. brucei* has, activation of PMN after the first contact with this parasite will occur, situation that must be considered as a relevant aspect on the formation of this aggregated, similar to the previously described with MSU crystals. In this context, *T. b. brucei* motility is best described as a dragging movement of the flagellum (57) and due to the location of the parasite in the host, is feasible to presume that endothelial damage caused by NETs will occur,

## **2.5 *Trypanosoma brucei brucei*-induced aggregated NETs (*aggNETs*) are dependent on purinergic receptors P2X1 and P2Y6**

---

as has been reports with other parasites (41,48). Further studies measuring the damage of *aggNETs* in endothelial cells will be performed.

The overall relevance of *aggNETs* accumulation driven by *T. b. brucei*, relies on the role that this phenotype has in the anti-inflammatory stage of inflammation, evidence have proved that it can regulate the process by releasing proteases, playing a fundamental part in the resolution and helping to the stimulation of tissue repair (22,25) being extremely relevant in the case of Nagana, considering the location of the parasite inside of the host. The fundamental role of purinergic-signaling must be addressed in future studies, since as we here demonstrate, they are involved and participate in the *T. b. brucei* NETs and *aggNETs* release.

## **2.5 *Trypanosoma brucei brucei*-induced aggregated NETs (*aggNETs*) are dependent on purinergic receptors P2X1 and P2Y6**

---

### **Author Contributions**

IC conceptualization and supervision. DG investigation (PMN isolation, *T. b. brucei* cell culture, SEM, immunofluorescence and inhibition experiments), formal analyses, data visualization and wrote the original draft. IC carried out investigation (Nanolive) and data visualization. IC, AT and CH reviewed the manuscript. CH, AT funding acquisition.

### **Conflict of Interest Statement**

The authors declare that the research was conducted in the absence of any commercial or financial relationships that could be construed as a potential conflict of interest

### **Funding**

DG is funded by the Chilean Scholarship Program “Doctorado Becas Chile” Number /2019-72200437 from the National Agency for Research and Development (ANID). The publication fees were partially funded by the Open Access Publication Fund from Justus Liebig University of Giessen (JLU).

### **Acknowledgments**

The authors would like to acknowledge Anika Seipp, Institute of Anatomy and Cell Biology, JLU Giessen, Germany, for her technical support in scanning electron microscopy analyses. We further thank all staff members of JLU Giessen teaching and research station Oberer Hardthof.

## 2.5 *Trypanosoma brucei brucei*-induced aggregated NETs (aggNETs) are dependent on purinergic receptors P2X1 and P2Y6

---

### BIBLIOGRAPHY

1. Matthews KR. The developmental cell biology of *Trypanosoma brucei*. *Journal of Cell Science* (2005) 118:283–290. doi: 10.1242/jcs.01649
2. Radwanska M, Vereecke N, Deleeuw V, Pinto J, Magez S. Salivarian Trypanosomosis: A Review of Parasites Involved, Their Global Distribution and Their Interaction With the Innate and Adaptive Mammalian Host Immune System. *Front Immunol* (2018) 9:2253. doi: 10.3389/fimmu.2018.02253
3. Deplazes P., Parasitology in veterinary medicine. (2016).
4. Malvy D, Chappuis F. Sleeping sickness. *Clinical Microbiology and Infection* (2011) 17:986–995. doi: <https://doi.org/10.1111/j.1469-0691.2011.03536.x>
5. Connor RJ. The impact of nagana. *Onderstepoort J Vet Res* (1994) 61:379–383.
6. Uilenberg G Boyt, WP, Food and Agriculture Organization,. A field guide for diagnosis, treatment and prevention of African animal trypanosomosis. Rome: FAO (1998).
7. Stijlemans B, Leng L, Brys L, Sparkes A, Vansintjan L, Caljon G, Raes G, Van Den Abbeele J, Van Ginderachter JA, Beschin A, et al. MIF contributes to *Trypanosoma brucei* associated immunopathogenicity development. *PLoS Pathog* (2014) 10:e1004414. doi: 10.1371/journal.ppat.1004414
8. Innate immunity in vertebrates: an overview. *Immunology* (2016) 148:125–139. <https://onlinelibrary.wiley.com/doi/abs/10.1111/imm.12597>
9. Hermosilla C, Caro TM, Silva LMR, Ruiz A, Taubert A. The intriguing host innate immune response: novel anti-parasitic defence by neutrophil extracellular traps. *Parasitology* (2014) 141:1489–1498. doi: 10.1017/S0031182014000316
10. Muñoz-Caro T, Rubio R MC, Silva LMR, Magdowski G, Gärtner U, McNeilly TN, Taubert A, Hermosilla C. Leucocyte-derived extracellular trap formation significantly contributes to *Haemonchus contortus* larval entrapment. *Parasites & Vectors* (2015) 8:607. doi: 10.1186/s13071-015-1219-1
11. de Buhr N, Bonilla MC, Jimenez-Soto M, von Köckritz-Blickwede M, Dolz G. Extracellular Trap Formation in Response to *Trypanosoma cruzi* Infection in Granulocytes Isolated From Dogs and Common Opossums, Natural Reservoir Hosts. *Front Microbiol* (2018) 9:966. doi: 10.3389/fmicb.2018.00966
12. Brinkmann V, Reichard U, Goosmann C, Fauler B, Uhlemann Y, Weiss DS, Weinrauch Y, Zychlinsky A. Neutrophil extracellular traps kill bacteria. *Science* (2004) 303:1532–1535. doi: 10.1126/science.1092385

## 2.5 *Trypanosoma brucei brucei*-induced aggregated NETs (aggNETs) are dependent on purinergic receptors P2X1 and P2Y6

---

13. Leshner M, Wang S, Lewis C, Zheng H, Chen XA, Santy L, Wang Y. PAD4 mediated histone hypercitrullination induces heterochromatin decondensation and chromatin unfolding to form neutrophil extracellular trap-like structures. *Front Immunol* (2012) 3:307. doi: 10.3389/fimmu.2012.00307
14. Li P, Li M, Lindberg MR, Kennett MJ, Xiong N, Wang Y. PAD4 is essential for antibacterial innate immunity mediated by neutrophil extracellular traps. *Journal of Experimental Medicine* (2010) 207:1853–1862. doi: 10.1084/jem.20100239
15. Papayannopoulos V, Metzler KD, Hakkim A, Zychlinsky A. Neutrophil elastase and myeloperoxidase regulate the formation of neutrophil extracellular traps. *Journal of Cell Biology* (2010) 191:677–691. doi: 10.1083/jcb.201006052
16. Ravindran M, Khan MA, Palaniyar N. Neutrophil Extracellular Trap Formation: Physiology, Pathology, and Pharmacology. *Biomolecules* (2019) 9: doi: 10.3390/biom9080365
17. Fuchs TA, Abed U, Goosmann C, Hurwitz R, Schulze I, Wahn V, Weinrauch Y, Brinkmann V, Zychlinsky A. Novel cell death program leads to neutrophil extracellular traps. *J Cell Biol* (2007) 176:231–241. doi: 10.1083/jcb.200606027
18. Yipp BG, Kubes P. NETosis: how vital is it? *Blood* (2013) 122:2784–2794. doi: 10.1182/blood-2013-04-457671
19. Lange MK, Penagos-Tabares F, Muñoz-Caro T, Gärtner U, Mejer H, Schaper R, Hermosilla C, Taubert A. Gastropod-derived haemocyte extracellular traps entrap metastrongyloid larval stages of *Angiostrongylus vasorum*, *Aelurostrongylus abstrusus* and *Troglostrongylus brevior*. *Parasit Vectors* (2017) 10:50. doi: 10.1186/s13071-016-1961-z
20. Grob D, Conejeros I, Velásquez ZD, Preußner C, Gärtner U, Alarcón P, Burgos RA, Hermosilla C, Taubert A. *Trypanosoma brucei brucei* Induces Polymorphonuclear Neutrophil Activation and Neutrophil Extracellular Traps Release. *Front Immunol* (2020) 11:559561. doi: 10.3389/fimmu.2020.559561
21. Schauer C, Janko C, Munoz LE, Zhao Y, Kienhöfer D, Frey B, Lell M, Manger B, Rech J, Naschberger E, et al. Aggregated neutrophil extracellular traps limit inflammation by degrading cytokines and chemokines. *Nat Med* (2014) 20:511–517. doi: 10.1038/nm.3547
22. Knopf J, Leppkes M, Schett G, Herrmann M, Muñoz LE. Aggregated NETs Sequester and Detoxify Extracellular Histones. *Front Immunol* (2019) 10:2176. doi: 10.3389/fimmu.2019.02176
23. Rosales C. Neutrophil: A Cell with Many Roles in Inflammation or Several Cell Types? *Front Physiol* (2018) 9:113. doi: 10.3389/fphys.2018.00113

## **2.5 *Trypanosoma brucei brucei*-induced aggregated NETs (aggNETs) are dependent on purinergic receptors P2X1 and P2Y6**

---

24. Pereira MA, Alexandre-Pires G, Câmara M, Santos M, Martins C, Rodrigues A, Adriana J, Passero LFD, Pereira da Fonseca I, Santos-Gomes G. Canine neutrophils cooperate with macrophages in the early stages of *Leishmania infantum* in vitro infection. *Parasite Immunol* (2019) 41: e12617. doi: 10.1111/pim.12617
25. Hahn J, Schauer C, Czegley C, Kling L, Petru L, Schmid B, Weidner D, Reinwald C, Biermann MHC, Blunder S, et al. Aggregated neutrophil extracellular traps resolve inflammation by proteolysis of cytokines and chemokines and protection from antiproteases. *FASEB J* (2019) 33:1401–1414. doi: 10.1096/fj.201800752R
26. Shapiro SD. Neutrophil elastase: path clearer, pathogen killer, or just pathologic? *Am J Respir Cell Mol Biol* (2002) 26:266–268. doi: 10.1165/ajrcmb.26.3.f233
27. Antonioli L, Pacher P, Vizi ES, Haskó G. CD39 and CD73 in immunity and inflammation. *Trends Mol Med* (2013) 19:355–367. doi: 10.1016/j.molmed.2013.03.005
28. Wang X, Chen D. Purinergic Regulation of Neutrophil Function. *Front Immunol* (2018) 9:399. doi: 10.3389/fimmu.2018.00399
29. Rubenich DS, de Souza PO, Omizzollo N, Lenz GS, Sevigny J, Braganhol E. Neutrophils: fast and furious-the nucleotide pathway. *Purinergic Signal* (2021) 17:371–383. doi: 10.1007/s11302-021-09786-7
30. Cekic C, Linden J. Purinergic regulation of the immune system. *Nat Rev Immunol* (2016) 16:177–192. doi: 10.1038/nri.2016.4
31. Idzko M, Ferrari D, Eltzschig HK. Nucleotide signalling during inflammation. *Nature* (2014) 509:310–317. doi: 10.1038/nature13085
32. Grassi F. Purinergic control of neutrophil activation. *J Mol Cell Biol* (2010) 2:176–177. doi: 10.1093/jmcb/mjq014
33. Uratsuji H, Tada Y, Kawashima T, Kamata M, Hau CS, Asano Y, Sugaya M, Kadono T, Asahina A, Sato S, et al. P2Y6 receptor signaling pathway mediates inflammatory responses induced by monosodium urate crystals. *J Immunol* (2012) 188:436–444. doi: 10.4049/jimmunol.1003746
34. Hidalgo MA, Carretta MD, Teuber SE, Zárate C, Cárcamo L, Concha II, Burgos RA. fMLP-Induced IL-8 Release Is Dependent on NADPH Oxidase in Human Neutrophils. *J Immunol Res* (2015) 2015:120348. doi: 10.1155/2015/120348
35. von Kügelgen I. Pharmacology of P2Y receptors. *Brain Res Bull* (2019) 151:12–24. doi: 10.1016/j.brainresbull.2019.03.010

## 2.5 *Trypanosoma brucei brucei*-induced aggregated NETs (aggNETs) are dependent on purinergic receptors P2X1 and P2Y6

---

36. Liu G-D, Ding J-Q, Xiao Q, Chen S-D. P2Y6 receptor and immunoinflammation. *Neurosci Bull* (2009) 25:161–164. doi: 10.1007/s12264-009-0120-3
37. Zhou E, Conejeros I, Gärtner U, Mazurek S, Hermosilla C, Taubert A. Metabolic requirements of *Besnoitia besnoiti* tachyzoite-triggered NETosis. *Parasitol Res* (2020) 119:545–557. doi: 10.1007/s00436-019-06543-z
38. Alarcón P, Manosalva C, Quiroga J, Belmar I, Álvarez K, Díaz G, Taubert A, Hermosilla C, Carretta MD, Burgos RA, et al. Oleic and Linoleic Acids Induce the Release of Neutrophil Extracellular Traps via Pannexin 1-Dependent ATP Release and P2X1 Receptor Activation. *Front Vet Sci* (2020) 7:260. doi: 10.3389/fvets.2020.00260
39. Hirumi H, Hirumi K. Continuous cultivation of *Trypanosoma brucei* blood stream forms in a medium containing a low concentration of serum protein without feeder cell layers. *J Parasitol* (1989) 75:985–989.
40. Larrazabal C, Hermosilla C, Taubert A, Conejeros I. 3D holotomographic monitoring of Ca<sup>(++)</sup> dynamics during ionophore-induced *Neospora caninum* tachyzoite egress from primary bovine host endothelial cells. *Parasitol Res* (2022) 121:1169–1177. doi: 10.1007/s00436-021-07260-2
41. Grob D, Conejeros I, López-Osorio S, Velásquez ZD, Segeritz L, Gärtner U, Schaper R, Hermosilla C, Taubert A. Canine *Angiostrongylus vasorum*-Induced Early Innate Immune Reactions Based on NETs Formation and Canine Vascular Endothelial Cell Activation In Vitro. *Biology (Basel)* (2021) 10: doi: 10.3390/biology10050427
42. Muñoz-Caro T, Conejeros I, Zhou E, Pikhovych A, Gärtner U, Hermosilla C, Kulke D, Taubert A. *Dirofilaria immitis* Microfilariae and Third-Stage Larvae Induce Canine NETosis Resulting in Different Types of Neutrophil Extracellular Traps. *Front Immunol* (2018) 9:968. doi: 10.3389/fimmu.2018.00968
43. Sil P, Hayes CP, Reaves BJ, Breen P, Quinn S, Sokolove J, Rada B. P2Y6 Receptor Antagonist MRS2578 Inhibits Neutrophil Activation and Aggregated Neutrophil Extracellular Trap Formation Induced by Gout-Associated Monosodium Urate Crystals. *J Immunol* (2017) 198:428–442. doi: 10.4049/jimmunol.1600766
44. Bonne-Année S, Kerepesi LA, Hess JA, Wesolowski J, Paumet F, Lok JB, Nolan TJ, Abraham D. Extracellular traps are associated with human and mouse neutrophil and macrophage mediated killing of larval *Strongyloides stercoralis*. *Microbes Infect* (2014) 16:502–511. doi: 10.1016/j.micinf.2014.02.012

## 2.5 *Trypanosoma brucei brucei*-induced aggregated NETs (aggNETs) are dependent on purinergic receptors P2X1 and P2Y6

---

45. McCoy CJ, Reaves BJ, Giguère S, Coates R, Rada B, Wolstenholme AJ. Human Leukocytes Kill *Brugia malayi* Microfilariae Independently of DNA-Based Extracellular Trap Release. *PLoS Negl Trop Dis* (2017) 11:e0005279. doi: 10.1371/journal.pntd.0005279
46. Li Y, Cao X, Liu Y, Zhao Y, Herrmann M. Neutrophil Extracellular Traps Formation and Aggregation Orchestrate Induction and Resolution of Sterile Crystal-Mediated Inflammation. *Front Immunol* (2018) 9:1559. doi: 10.3389/fimmu.2018.01559
47. Davidsson L, Dahlstrand Rudin A, Sanchez Klose FP, Buck A, Björkman L, Christenson K, Bylund J. In Vivo Transmigrated Human Neutrophils Are Highly Primed for Intracellular Radical Production Induced by Monosodium Urate Crystals. *Int J Mol Sci* (2020) 21: doi: 10.3390/ijms211113750
48. Conejeros I, Velásquez ZD, Grob D, Zhou E, Salecker H, Hermosilla C, Taubert A. Histone H2A and Bovine Neutrophil Extracellular Traps Induce Damage of *Besnoitia besnoiti*-Infected Host Endothelial Cells but Fail to Affect Total Parasite Proliferation. *Biology (Basel)* (2019) 8: doi: 10.3390/biology8040078
49. Kankaanranta H, Moilanen E. Flufenamic and tolfenamic acids inhibit calcium influx in human polymorphonuclear leukocytes. *Mol Pharmacol* (1995) 47:1006–1013.
50. Burgos RA, Conejeros I, Hidalgo MA, Werling D, Hermosilla C. Calcium influx, a new potential therapeutic target in the control of neutrophil-dependent inflammatory diseases in bovines. *Vet Immunol Immunopathol* (2011) 143:1–10. doi: 10.1016/j.vetimm.2011.05.037
51. Kenny EF, Herzig A, Krüger R, Muth A, Mondal S, Thompson PR, Brinkmann V, Bernuth H von, Zychlinsky A. Diverse stimuli engage different neutrophil extracellular trap pathways. *Elife* (2017) 6:e24437. doi: 10.7554/eLife.24437
52. Dahl G. ATP release through pannexon channels. *Philos Trans R Soc Lond B Biol Sci* (2015) 370: doi: 10.1098/rstb.2014.0191
53. Chen Y, Yao Y, Sumi Y, Li A, To UK, Elkhail A, Inoue Y, Woehrle T, Zhang Q, Hauser C, et al. Purinergic signaling: a fundamental mechanism in neutrophil activation. *Sci Signal* (2010) 3:ra45. doi: 10.1126/scisignal.2000549
54. Azevedo EP, Rochael NC, Guimarães-Costa AB, de Souza-Vieira TS, Ganilho J, Saraiva EM, Palhano FL, Foguel D. A Metabolic Shift toward Pentose Phosphate Pathway Is Necessary for Amyloid Fibril- and Phorbol 12-Myristate 13-Acetate-induced Neutrophil Extracellular Trap (NET) Formation. *J Biol Chem* (2015) 290:22174–22183. doi: 10.1074/jbc.M115.640094

## **2.5 *Trypanosoma brucei brucei*-induced aggregated NETs (aggNETs) are dependent on purinergic receptors P2X1 and P2Y6**

---

55. Floyd M, Winn M, Cullen C, Sil P, Chassaing B, Yoo D-G, Gewirtz AT, Goldberg JB, McCarter LL, Rada B. Swimming Motility Mediates the Formation of Neutrophil Extracellular Traps Induced by Flagellated *Pseudomonas aeruginosa*. *PLoS Pathog* (2016) 12:e1005987. doi: 10.1371/journal.ppat.1005987
56. Branzk N, Lubojemska A, Hardison SE, Wang Q, Gutierrez MG, Brown GD, Papayannopoulos V. Neutrophils sense microbe size and selectively release neutrophil extracellular traps in response to large pathogens. *Nat Immunol* (2014) 15:1017–1025. doi: 10.1038/ni.2987
57. Ooi C-P, Bastin P. More than meets the eye: understanding *Trypanosoma brucei* morphology in the tsetse. *Front Cell Infect Microbiol* (2013) 3:71. doi: 10.3389/fcimb.2013.00071
58. Villagra-Blanco R, Silva LMR, Muñoz-Caro T, et al (2017) Bovine Polymorphonuclear Neutrophils Cast Neutrophil Extracellular Traps against the Abortive Parasite *Neospora caninum*. *Front Immunol* 8:606. <https://doi.org/10.3389/fimmu.2017.00606>
59. Mitroulis I, Kambas K, Chrysanthopoulou A, et al (2011) Neutrophil extracellular trap formation is associated with IL-1 $\beta$  and autophagy-related signaling in gout. *PLoS One* 6:e29318. <https://doi.org/10.1371/journal.pone.0029318>
60. Rada B. Neutrophil Extracellular Traps and Microcrystals. *J Immunol Res*. 2017;2017:2896380. doi:10.1155/2017/2896380
61. Schorn C, Janko C, Krenn V, et al (2012a) Bonding the foe - NETting neutrophils immobilize the pro-inflammatory monosodium urate crystals. *Front Immunol* 3:376. <https://doi.org/10.3389/fimmu.2012.00376>
62. Schorn C, Janko C, Latzko M, et al (2012b) Monosodium urate crystals induce extracellular DNA traps in neutrophils, eosinophils, and basophils but not in mononuclear cells. *Front Immunol* 3:277. <https://doi.org/10.3389/fimmu.2012.00277>

## 2.5 *Trypanosoma brucei brucei*-induced aggregated NETs (*aggNETs*) are dependent on purinergic receptors P2X1 and P2Y6

---

### FIGURES

**Fig. 1. *T. b. brucei* bloodstream metacyclic trypomastigotes are able to induce *aggNETs* formation, analyzed via scanning electron microscopy (SEM).** Bovine polymorphonuclear neutrophils were exposed for 4h to *T. b. brucei* bloodstream metacyclic trypomastigotes and fixed for posterior SEM analyzes. Co-culture reveals *aggNETs* formation indicated by arrows (B - E). Exposure of bovine PMN against ionomycin and MSU crystals resulted in *aggNETs* formation (1C – 1D – 1F – 1G).

**Fig. 2. 3D-holotomographic microscopy of bovine PMN co-incubated with *T. b. brucei* metacyclic bloodstream trypomastigotes.** Refractive index and fluorescent signal-based images of bovine PMN stimulated with *T. b. brucei* bloodstream metacyclic trypomastigotes, were obtained at 4h, bovine PMN alone were used as controls (A). B illustrate the measurements of refractive index volume of the control and stimulated PMN.

**Fig. 3. *T. b. brucei* bloodstream metacyclic trypomastigotes-induced metabolic changes in exposed bovine PMN.** Activation of PMN was monitored by an extracellular flux analyzer (Seahorse) for oxygen consumption rate (OCR) proton efflux rate (PER). PMN were incubated in XF RPMI media for 45 min without CO<sub>2</sub> and pre-treated with MRS2578 (10 $\mu$ M), then alive *T. b. brucei* bloodstream metacyclic trypomastigotes were injected at the time point indicated by arrows. The increase in OCR (A) and PER (C) was monitored for 213 min. The area under the curve (AUC) was calculated for all registries and plotted as mean  $\pm$  SD (B, D; n = 3) showing the increase in both parameters for activated PMN.

**Fig. 4. Immunofluorescence analyses of *T. b. brucei* bloodstream metacyclic trypomastigotes-induced *aggNETs* formation after 4h of co-culture.** Bovine PMN (n = 3) were incubated with *T. b. brucei* bloodstream metacyclic trypomastigotes (1,2 x 10<sup>6</sup>). Presence of DNA (C, G, K, O, S, W, 1; blue), neutrophil elastase (B, F, J, N, R, V, Z; green), and histones (H1, H2A/H2B, H3, H4) (A, E, I, M, Q, U, Y; red) in *T. b. brucei* bloodstream metacyclic trypomastigotes induced NETs. (D, H, L, P, T, X, 2; merge) shows the merge of the three channels.

**Fig. 5. Immunofluorescence analyses of *T. b. brucei* bloodstream metacyclic trypomastigotes-induced *aggNETs* formation after 18h of co-culture.** Bovine PMN (n = 3) were incubated with *T. b. brucei* bloodstream metacyclic trypomastigotes (1,2 x 10<sup>6</sup>). Presence of DNA (C, G, K, O, S, W, 1; blue), neutrophil elastase (B, F, J, N, R, V, Z; green), and histones

## 2.5 *Trypanosoma brucei brucei*-induced aggregated NETs (*aggNETs*) are dependent on purinergic receptors P2X1 and P2Y6

---

(H1, H2A/H2B, H3, H4) (A, E, I, M, Q, U, Y; red) in *T. b. brucei* bloodstream metacyclic trypomastigotes induced NETs. (D, H, L, P, T, X, 2; merge) shows the merge of the three channels.

**Fig. 6. Quantification by percentage of NETs and *aggNETs* formation.** Immunofluorescence pictures were used to manually count the number of cells casting NETs and formation of *aggNETs*. After 4h of incubation, a total of 11,22% of bovine PMN were casting NETs; nevertheless, after treatments with the purinergic inhibitors NF449 (100 and 10 $\mu$ M) and MRS2578 (10 $\mu$ M) the percentage was decreased to 3,9%, 11,13% and 8,53%, respectively (A). Ionomycin was able to trigger 13,78% of the cells and MSU crystals 9,77% (B). Interestingly, at the 18h of incubation, the total amount of cells casting NETs was increased to 12,35% (C). After the previously mentioned treatments, the percentage changed to 2,83%, only in the case of NF449 100 $\mu$ M (C). Variation of ionomycin (8,09%) and MSU crystals (19,12%) was observed (D). Regarding the formation of *aggNETs*, in 4h of co-culture, a total of 24,81% was achieved. Cells treated with NF449 (10 $\mu$ M) were able to cast a 18,09% and with MRS2578 a 1,66%. Ionomycin had a percentage of 18,49 and MSU crystals of 17,24 (E). In the case of 18h of co-culture, the amount of *aggNETs* was 22,65%; with NF449 (10 $\mu$ M) the percentage changed to 11,61. NF449 (100 $\mu$ M) and MRS2578 (10  $\mu$ M) were able to abolish the process in this time point (E, G). Ionomycin and MSU crystals also demonstrated changes (F, G).

## 2.5 *Trypanosoma brucei brucei*-induced aggregated NETs (*aggNETs*) are dependent on purinergic receptors P2X1 and P2Y6

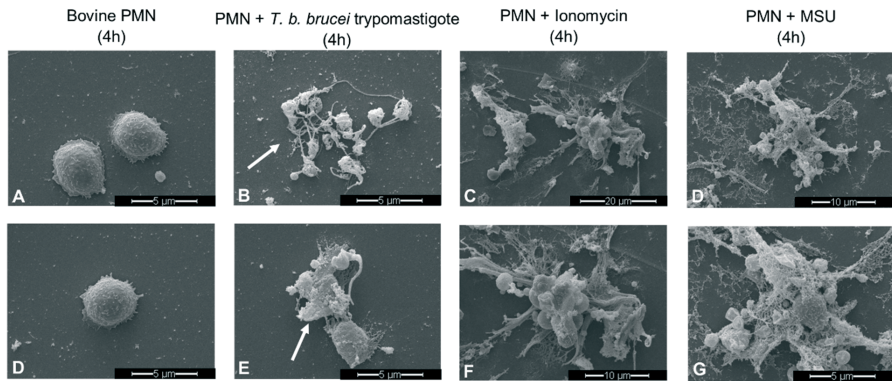
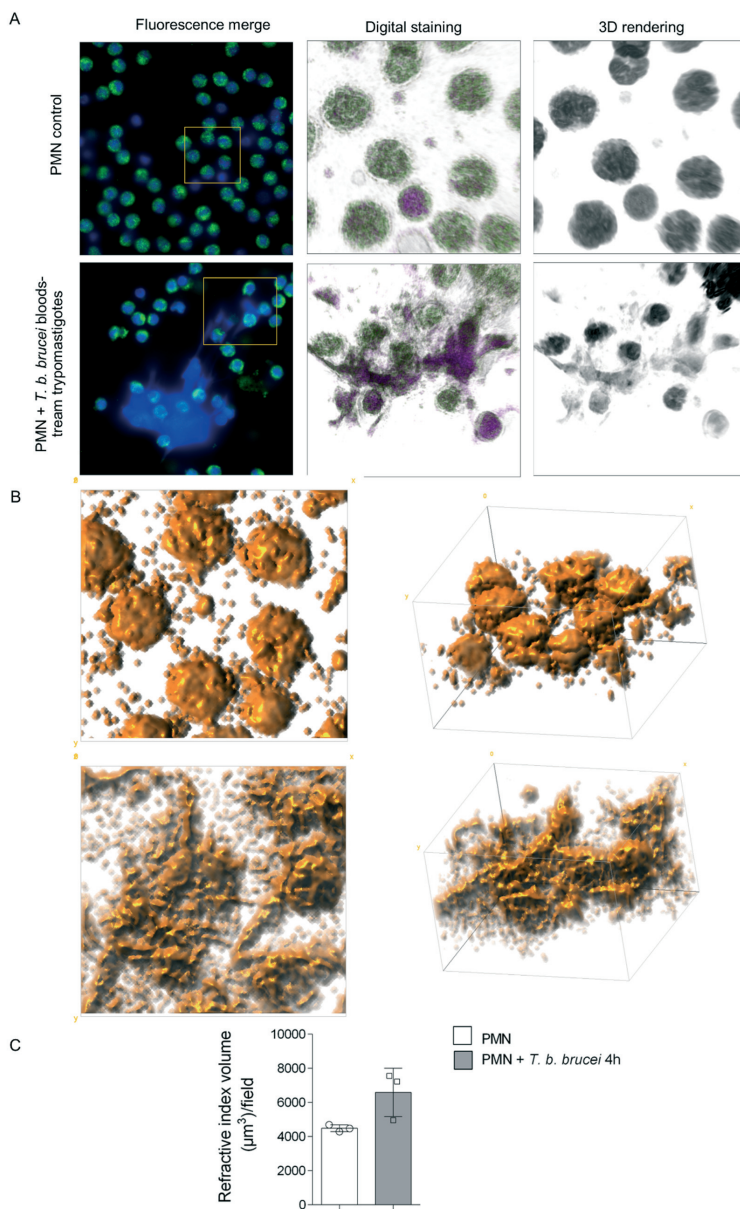


Figure 1

## 2.5 *Trypanosoma brucei brucei*-induced aggregated NETs (*aggNETs*) are dependent on purinergic receptors P2X1 and P2Y6



**Figure 2**

## 2.5 *Trypanosoma brucei brucei*-induced aggregated NETs (aggNETs) are dependent on purinergic receptors P2X1 and P2Y6

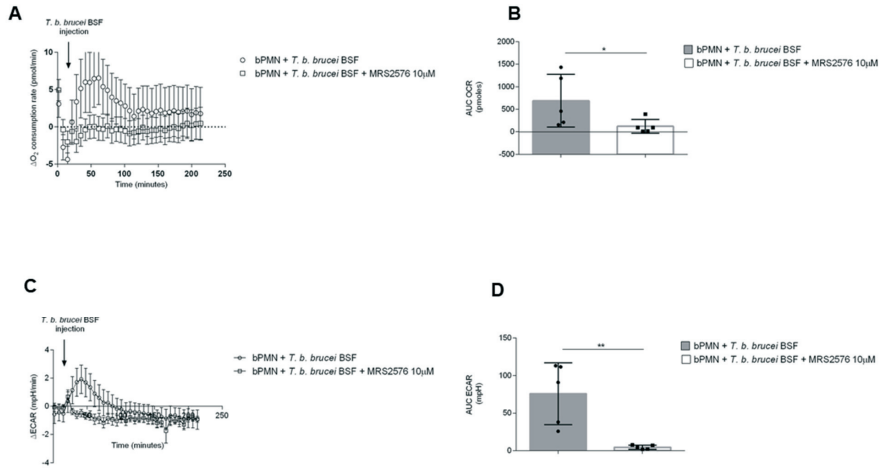


Figure 3

## 2.5 *Trypanosoma brucei brucei*-induced aggregated NETs (aggNETs) are dependent on purinergic receptors P2X1 and P2Y6

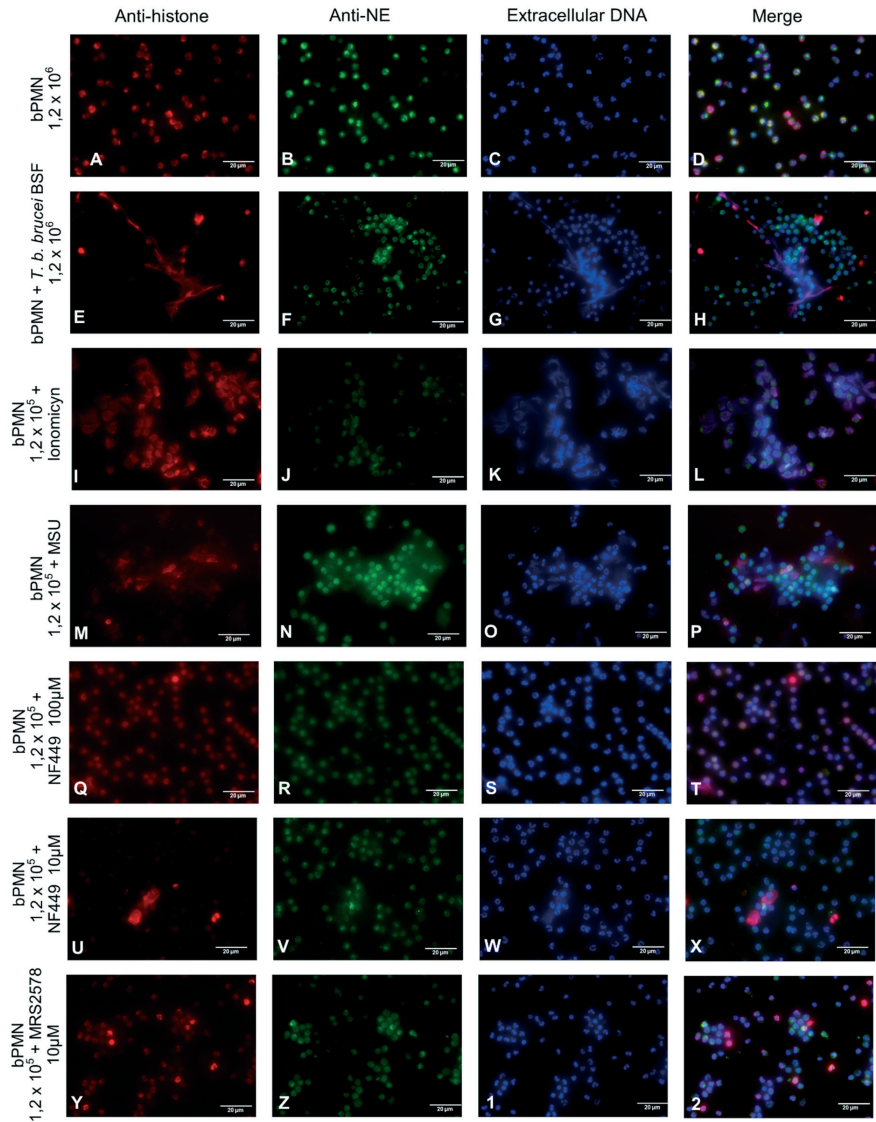


Figure 4

## 2.5 *Trypanosoma brucei brucei*-induced aggregated NETs (*aggNETs*) are dependent on purinergic receptors P2X1 and P2Y6

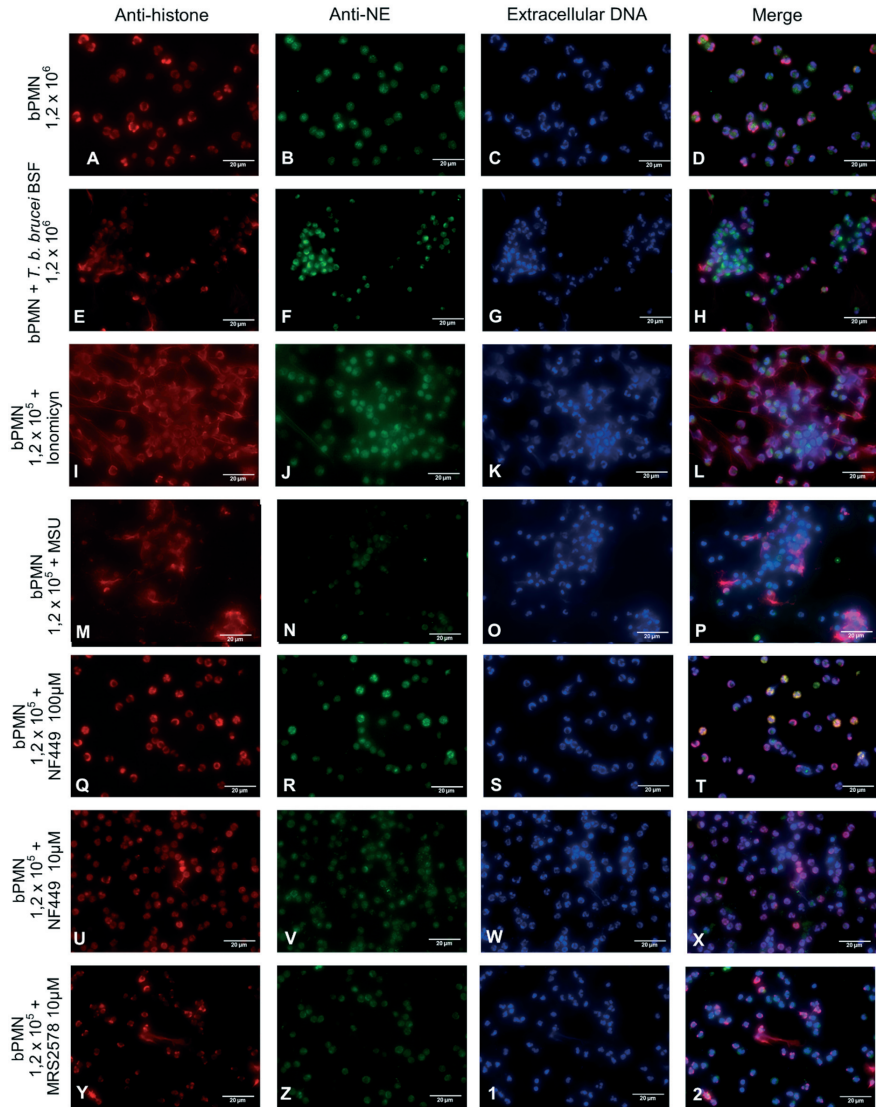


Figure 5

## 2.5 *Trypanosoma brucei brucei*-induced aggregated NETs (aggNETs) are dependent on purinergic receptors P2X1 and P2Y6

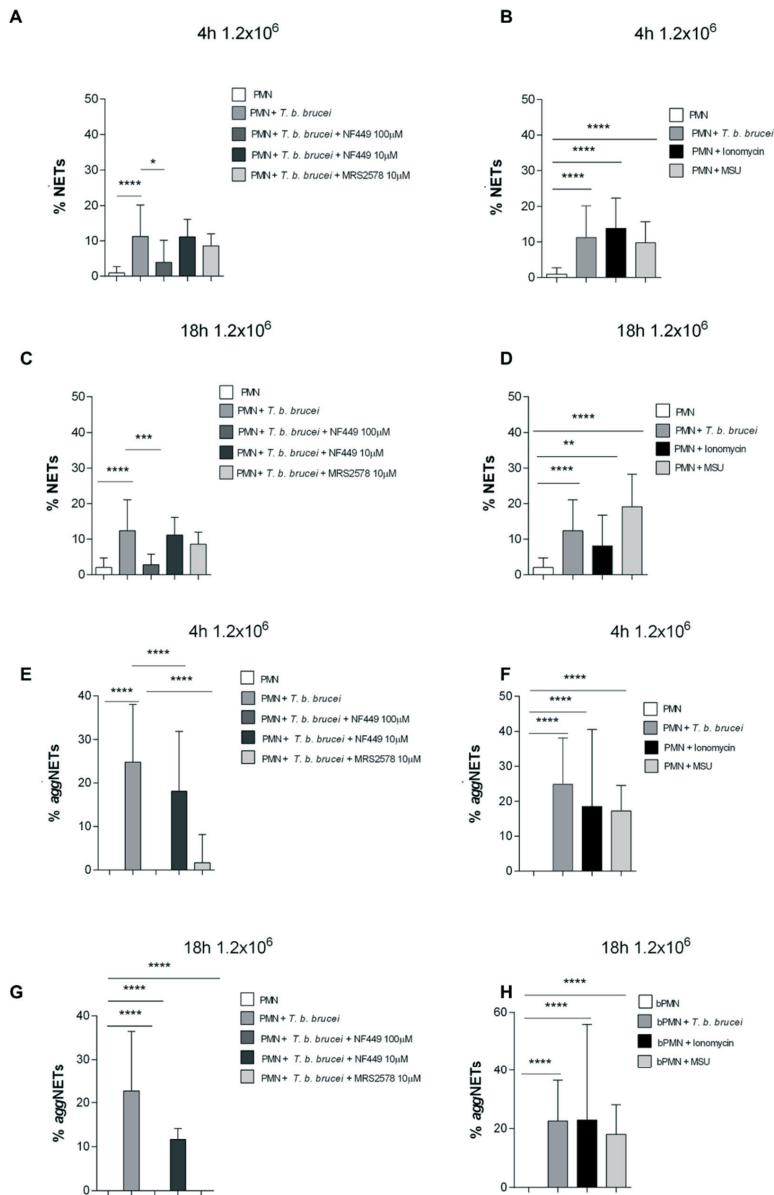


Figure 6

## **2.6. *SARCOPTES SCABIEI* SOLUBLE ANTIGEN INCREASES INTRACELLULAR CALCIUM CONCENTRATION, ROS PRODUCTION AND EVOKES WEAK NET RELEASE IN BOVINE POLYMORPHONUCLEAR NEUTROPHILS**

This chapter is based on the following unpublished paper

Grob, D.; Larrazabal, C.; Conejeros, I.; López-Osorio, S.; Taubert, A.; Hermosilla, C. *Sarcoptes scabiei* soluble antigen increases intracellular calcium concentration, ROS production and evokes weak net release in bovine polymorphonuclear neutrophils (manuscript in preparation)

Eigener Anteil in der Publikation:

Projektplanung	50 %, zusammen mit Ko-Autoren und Betreuern
Durchführung des Versuches	50 %, weitestgehend selbständig
Auswertung der Experimente	70 %, weitestgehend selbständig
Erstellung der Publikation	70 %, weitestgehend selbständig

## **2.6 *Sarcoptes scabiei* soluble antigen increases intracellular calcium concentration, ROS production and evokes weak NET release in bovine polymorphonuclear neutrophils**

---

***Sarcoptes scabiei* soluble antigen increases intracellular calcium concentration, ROS production and evokes weak NET release in bovine polymorphonuclear neutrophils**

<sup>1,\*</sup>Grob D., <sup>1</sup>Larrazabal C., <sup>1</sup>Conejeros I., <sup>1,2</sup>Lopez-Osorio S., <sup>1</sup>Taubert A., <sup>1</sup>Hermosilla, C.

<sup>1</sup>Institute for Parasitology, Justus Liebig University Giessen, Giessen, Germany

<sup>2</sup>Grupo de Investigación CIBAV, Universidad de Antioquia UdeA, Medellín 050034, Colombia

\*Corresponding author: Institute for Parasitology. Biomedical Research Center Seltersberg, Justus Liebig University Giessen, Schubertstr. 81, 35392 Giessen, Germany. e-mail: [daniela.grob@vetmed.uni-giessen.de](mailto:daniela.grob@vetmed.uni-giessen.de) (Daniela Grob)

**Keywords:** *Sarcoptes scabiei*, NET formation, PMN, pH, calcium efflux, cattle

## **2.6 *Sarcoptes scabiei* soluble antigen increases intracellular calcium concentration, ROS production and evokes weak NET release in bovine polymorphonuclear neutrophils**

---

### **ABSTRACT**

*Sarcoptes scabiei* is an astigmatan ectoparasite and the causal agent of the sarcoptic mange in humans and animals. The life cycle of this skin mite has four stages that will develop in the *stratum corneum* of the host. Infections will occur when close contact with an infected host exist. Clinical symptoms of *S. scabiei*-mange include severe dermatitis, pruritus, hyperkeratosis and exudation. Polymorphonuclear neutrophils (PMN) are the most abundant leukocyte population in the bloodstream and being important in most inflammatory conditions of the skin. PMN are able to produce reactive oxygen species (ROS), to conduct degranulation and to cast neutrophil extracellular traps (NETs) as early host innate defense mechanisms. NETs are structures formed by chromatin and enzymes that can capture and kill foreign pathogens. Likewise, during the early activation of the PMN,  $Ca^{++}$  signaling has a pivotal role in PMN functions such reactive oxygen species (ROS) production, chemotaxis and granule secretion. In this report, we analyzed the interaction between bovine PMN against *S. scabiei* mites and the PMN function when stimulated with *S. scabiei* antigen (*ScAg*). Functional parameters that were studied includes NET formation, ROS formation and intracellular  $Ca^{++}$  concentration ( $[Ca^{++}]_i$ ). Current data shows that *S. scabiei* induces a low quantity of NETs but this effect was not observed when the corresponding soluble antigen (*ScAg*) was used as activator. However, *ScAg* induces ROS and increased  $[Ca^{++}]_i$  on bovine PMN.

## **2.6 *Sarcoptes scabiei* soluble antigen increases intracellular calcium concentration, ROS production and evokes weak NET release in bovine polymorphonuclear neutrophils**

---

### **INTRODUCTION**

Sarcoptic mange or scabiosis is an infectious disease skin in mammals, caused by the astigmata mite *Sarcoptes scabiei*. In general, *S. scabiei* has been morphologically characterized by tortoise-like body (idiosoma) with cuticular spines and short legs, which in the case of pair III and IV does not extend the idiosoma representing an feature of the *Sarcoptidae* family (Arlian and Morgan, 2017). Biologically, *S. scabiei* infection is limited to superficial layers of the host skin, where shortly after the host invasion, mites borrow under the stratus corneum, fulfilling its nutrients requirements by host lymph acquisition, finishing thereafter the life cycle after in 15-20 days by laying borrowed eggs (Arlian and Morgan, 2017). Clinically, scabiosis is characterized by a dermatitis accompanied by severe pruritus and a matted hair coat and thickened hyperkeratotic hyperpigmented skin, generating discomfort in the affected animals compromising food conversion and animal welfare (Rentería-Solís et al., 2014). The development of a vaccine against *S. scabiei* faced several difficulties as lack of an in vitro culture system, the inconsistent immune response driven by its antigens, among others (Casais et al., 2016; Shen et al., 2020; Zhang et al., 2012) suggest a complex interaction between the mite infestation and the host immune response.

Clinical manifestations of *S. scabiei* infection occurs after 4-6 weeks of the infection (Arlian and Morgan, 2017). Transcriptomic analysis during the early stage of *S. scabiei* infection in porcine skin shows a down regulation of the chemoattractant CXCL8, Toll-like receptors (TLR) and its downstream signaling proteins during the first week post infection (Bhat et al., 2020). In line, *in vitro* studies have shown that *S. scabiei* antigen (*ScAg*) interferes with the production of pro inflammatory modulators such as IL-8 or G-CSF in human dermal fibroblasts and keratinocytes (Morgan and Arlian, 2010; Mullins et al., 2009). Furthermore, the exposition to *ScAg* down regulate adhesion molecules such ICAM-1 and E-selectin in endothelial cells (Elder et al., 2009). Overall, this represents a divergence from other parasitic mites such *Psoroptes* spp., where clinical evidence of the immune response onset appears shortly after the infection (Chen et al., 2021; Sarre et al., 2015), while pro inflammatory cytokines such CXCL-6, CXCL-8 and TNF- $\alpha$  are up regulated at 24 h post infection (Burgess et al., 2010). Given that, it has been proposed that *S. scabiei* modulates the host-immune response, activating an inflammatory response only after an inflammatory threshold is overpassed (Mounsey et al., 2013). Due to the mite location at the intercellular phase in epidermis, antigenic and vasoactive substances originated by *S. scabiei* as saliva, molting hormones and feces diffuse and interact with

## **2.6 *Sarcoptes scabiei* soluble antigen increases intracellular calcium concentration, ROS production and evokes weak NET release in bovine polymorphonuclear neutrophils**

---

surrounding cells (Arlan and Morgan, 2017). Once the mite population exceed a tolerance threshold, a marked immune response characterized by eosinophilia, and eosinophilic recruitment within the infected area occurs (Bhat et al., 2017). The importance of eosinophil-driven responses to modulate *S. scabiei* infection is unclear (Bhat et al., 2017). In line, the administration of drug Cyclosporine A in ovine reduces *Psoroptes ovis* mite burden is possible that allergic immune responses are indeed necessary for establishment of the parasite into host skin (Huntley et al., 2005). Furthermore, during the clinical stage of scabiosis other immune cells are recruited into the skin (Bhat et al., 2017). This immune recruitment includes different cell types such lymphocytes, eosinophils and polymorphonuclear neutrophils (PMN) (Bhat et al., 2017).

PMN are the most abundant leukocyte in blood and the first ones to arrive to the site of the infection (Brinkmann et al., 2004; Fuchs et al., 2007; Kolaczowska and Kubes, 2013; Papayannopoulos, 2018). Despite the neglected role that this phagocyte has in scabiosis, transcriptomic analyses indicates significant up regulation of chemoattractant substances involved in PMN recruitment at 8 weeks post infection in pigs (Bhat et al., 2020). Likewise, independent reports indicate a PMN accumulation after infection in different host animals (Bhat et al., 2017; Dagleish et al., 2007; Swe et al., 2017). In humans, a retrospective study in skin samples infected with *S. scabiei*, shown that 52% of samples have an increased number of PMN on the skin (Elwood et al., 2015), suggesting an innate immune response during the early stages of *S. scabiei* infection. PMN have different effector mechanisms with microbicidal effect including phagocytosis, degranulation and reactive oxygen species (ROS) production (Fuchs et al., 2007). Interestingly, serine protease paralogs (SMIPPs) and serine protease inhibitors (scabies mite serpins, SMS) from *S. scabiei* are capable interfere with the complement system and opsonisation (Mika et al., 2012). Specifically opsonized *Staphylococcus aureus* phagocytosis by PMN is reduced after SMSB4 treatment, reducing bacterial killing and permitting pyoderma-obtained isolates proliferation *in vitro* (Swe and Fischer, 2014). Notably, bacterial contamination with *S. aureus* represents one of the more significant complications of scabiosis in human and animals (Bhat et al., 2017; Dagleish et al., 2007; Swe et al., 2017), suggesting that the PMN modulation by *S. scabiei* can influence the disease outcome.

Beyond the canonical killing strategies carried out by PMN, cumulated evidence have shown that this granulocyte is capable to release its nuclear DNA content into a fine and delicate extracellular structures named neutrophil extracellular traps (NETs) (Brinkmann et al., 2004).

## **2.6 *Sarcoptes scabiei* soluble antigen increases intracellular calcium concentration, ROS production and evokes weak NET release in bovine polymorphonuclear neutrophils**

---

NETs are composed by decondensed chromatin, decorated with antimicrobial components, which include MPO, neutrophil elastase (NE), lactoferrin, calprotectin, LL37, pentraxin, proteinase 3, cathepsin G, among others (Papayannopoulos et al., 2010; Urban et al., 2009). This composition permits killing of microorganisms by NETs (Brinkmann et al., 2004). NET formation is particularly important as a response against larger pathogens that could not been removed by other antimicrobial responses such phagocytosis (Branzk et al., 2014; Muñoz-Caro et al., 2018, 2015). In this context, PMN are capable to release NETs against parasitic nematodes such as *Haemonchus contortus*, *Strongyloides stercoralis*, *Ostertagia ostertagi*, *Brugia malayi* and *Angiostrongylus vasorum* L3 (Bonne-Année et al., 2014; Grob et al., 2021; McCoy et al., 2017; Mendez et al., 2018; Muñoz-Caro et al., 2018, 2015), while *Fasciola hepatica* juvenile stage and soluble antigen only induced a weak NET release (Peixoto et al., 2021), suggesting that its release can be influenced by the parasite specie. So far, no evidence exist regarding the role of NETs release against parasitic mites.

The aim of this work is to characterize for the first time the response of isolated PMN against the parasitic mite *S. scabiei* and the corresponding antigen *ScAg*.

## **2.6 *Sarcoptes scabiei* soluble antigen increases intracellular calcium concentration, ROS production and evokes weak NET release in bovine polymorphonuclear neutrophils**

---

### **MATERIALS AND METHODS**

#### **Ethic statements**

This study was conducted in accordance to Justus Liebig University Giessen (JLU) Animal Care Committee Guidelines. Protocols were approved by Ethic Commission for Experimental Animal Studies of Federal State of Hesse (Regierungspräsidium Giessen; A9/2012; JLU-No.521\_AZ) and in accordance to European Animal Welfare Legislation: ART13TFEU and current applicable German Animal Protection Laws.

#### **Isolation of bovine PMN**

Healthy adult dairy cows ( $n = 4$ ) served as blood donors. Animals were bled by puncture of the jugular vein and 30 ml peripheral blood were collected in 12 ml heparinized sterile plastic tubes (Kabe Labortechnik). Then, 20 ml of heparinized blood were diluted in 20 ml sterile PBS with 0.02% EDTA (Sigma-Aldrich), layered on top of 12 ml Histopaque<sup>®</sup>-1077 separating solution (density = 1.077 g/l; Sigma Aldrich) and centrifuged ( $800 \times g$ , 45 min). The plasma and the buffy coat were carefully aspirated, and the remaining red blood cells (RBC) and pellet at the bottom of the tube were suspended in Hank's balanced salt solution (HBSS). RBC were removed by a flash hypotonic lysis performed with 1 volume of cold phosphate buffered water solution containing 5.5 mM  $\text{NaH}_2\text{PO}_4$ , 8.4 mM  $\text{HK}_2\text{PO}_4$  at pH 7.2. After 1 min of RBC lysis, 2 volumes of hypertonic phosphate buffer containing 5.5 mM  $\text{NaH}_2\text{PO}_4$ , 0.46 M NaCl and pH 7.2 were added to recover the isotonicity; after this, the tubes were centrifuged at  $600 g$  for 10 min at  $20^\circ\text{C}$ . The neutrophil pellet was washed with HBSS 3 times. PMN were re-suspended in 5 ml of HBSS and counted in a Neubauer haemocytometer. Finally, freshly isolated bovine PMN were allowed to rest at  $37^\circ\text{C}$  and 5%  $\text{CO}_2$  atmosphere for 30 min before experimental use.

#### ***S. scabiei* isolation and soluble antigen (ScAg) preparation**

Samples were obtained from infected cows with clinical symptoms. Hair was clipped on the affected area and scrapping was performed by using a sharp spoon. The collected scraped material was stored in a vessel at  $4^\circ\text{C}$  for further use. Then, the samples were placed in a conical test tube and 6 ml of 10% potassium hydroxide (KOH) solution was added. After this, digestion was performed by boiling the sample with a Bunsen burner for periods of 15 sec each, until the hair structure disappear. Next, the sample was centrifuged at  $600 \times g$  for 3 min (RT). The

## **2.6 *Sarcoptes scabiei* soluble antigen increases intracellular calcium concentration, ROS production and evokes weak NET release in bovine polymorphonuclear neutrophils**

---

supernatant was decanted into a new tube, on which 8 ml of concentrated sugar solution with a density of 1.3 gr/mL (550g of Sugar, 443 ml of Tap-water, 7 ml Formaldehyde 37%) were added and vigorously shaken. Thereafter, samples were centrifuged at 600 x g for 3 min (RT). Finally, two drops of the liquid surface were placed in a cover glass to check and confirm the presence of the parasite. For the ScAg elaboration, *S. scabiei* mites obtained after the digestion were suspended in 300 µl sterile phosphate-buffered saline (PBS) followed by a sonication step consisting of five cycles of 15 sec in an ice bath (Sonorex RK31® bath-type sonicator; Bandelin, Berlin, Germany). The sonicated material was centrifuged at 10.000 x g for 20 min at 4° to separate solid debris from the solution. The protein concentration of the ScAg was determined using the method of Bradford. ScAg solutions were stored at -20°C until further use.

### **Live cell interaction between bovine PMN and digested *S. scabiei***

Freshly isolated bovine PMN ( $2 \times 10^5$ ;  $n = 3$ ) were centrifuged at 300 x g for 10 min RT, cells were thereafter suspended in 1 ml of RPMI 1640 cell culture medium without phenol red (Sigma-Aldrich) with Sytox Green® (1:1000; Thermo Fischer) for the extracellular DNA staining. Three isolated *S. scabiei* mites were allowed to settle down for 10 min to the bottom of a plastic 8 µ-Slide well (Ibidi®) before stained bovine PMN were added to the center of the well. The plate was incubated for 60 min, taking pictures every 10 min using an inverted Olympus IX81® fluorescence microscope. At the end of the experiment, images were exported using CellSens® imaging software (Olympus). The pictures were analyzed using Image J® software (Fiji version 1.7, NIH).

### **Detection of Extracellular DNA and Protein Markers of NETs by Fluorescence Microscopy**

Bovine PMN ( $n = 3$ ,  $2 \times 10^5$ /sample) were co-cultured with *S. scabiei* or with antigen in concentrations ranging from 10µg to 100µg for 120 min (37°C and 5% CO<sub>2</sub> atmosphere) on coverslips (15 mm diameter, Thermo Fischer Scientific) pre-treated with 0.01% poly-L-lysine (Sigma-Aldrich). After the incubation time, cells were fixed in 4% paraformaldehyde (Merck) and stored at 4 °C until further use. To visualize NET structures, DAPI staining (4',6-diamidino-2-phenylindole, Thermo Fisher) was used to stain total DNA. Anti-histone (H1, H2A/H2B, H3 and H4, 1:200, Merck #MAB3422) and anti-neutrophil elastase (NE) (1:200, Abcam #ab68672) antibodies were used to detect NET-specific components/proteins. First, the samples were

## **2.6 *Sarcoptes scabiei* soluble antigen increases intracellular calcium concentration, ROS production and evokes weak NET release in bovine polymorphonuclear neutrophils**

---

incubated for 60 min (RT) with blocking buffer, containing 3% bovine serum albumin (BSA; Sigma-Aldrich) and 0.3% Triton X-100 (Thermo Fischer Scientific). After this, the samples were incubated in primary antibody solutions for 180 min at RT followed by three washing steps with sterile PBS, and incubated in secondary antibody solutions (Alexa 594 goat anti-mouse IgG #A110005, Alexa 488 goat anti-rabbit IgG #A11008, 1:500, Invitrogen) for 30 min at RT in darkness. Finally, the samples were washed three times with sterile PBS and mounted upside-down with Fluoromount G<sup>®</sup> without DAPI (Thermo Fischer Scientific). Visualization of the specimens was achieved using an inverted IX81<sup>®</sup> epifluorescence microscope equipped with an XM 10<sup>®</sup> digital camera (both Olympus) or by applying confocal microscopy (Zeiss LSM 710<sup>®</sup>).

### **Assessment of different phenotypes of NETs**

To perform the quantification of the different phenotypes of NETs [i.e., spread NETs (*spr*NETs), diffuse NETs (*diff*NETs) and aggregated NETs (*agg*NETs)], freshly isolated bovine PMN ( $n = 3, 2 \times 10^5$ /sample) were seeded on 0,01% poly-L-lisine (Sigma Aldrich) pre-treated coverslips (Thermo Fischer Scientific) and exposed to the presence of *ScAg* (10 $\mu$ g and 100 $\mu$ g) for 120 min. After this, samples were fixated in 2% paraformaldehyde (Merck) and stored at 4°C until further analysis. The assessment of the different phenotypes was performed by visualization by immunofluorescence staining, as previously described. For visual quantification, random power vision photos were taken from each experimental condition using an inverted IX81<sup>®</sup> fluorescence microscope, equipped with an XM10<sup>®</sup> camera (Olympus) and analyzed bases on the classical morphology characteristics, as has been already published (Grob et al., 2020; Peixoto et al., 2021).

### **Tracking of intracellular Ca<sup>++</sup> fluxes**

Calcium intracellular concentration was estimated by fluorescence using the Ca<sup>++</sup>-sensitive dye Fluo-4-AM (Invitrogen<sup>®</sup>). Freshly isolated PMNs were loaded with the dye as described elsewhere (Conejeros et al., 2012). Briefly, bovine PMN were incubated 30 min in HBSS at 37 °C with media containing Fluo-4-AM 2.5  $\mu$ M, thereafter dye excess was removed by washing with HBSS. The Ca<sup>++</sup> flux measurement over time was performed in a 96 well plate in a concentration of  $5 \times 10^6$  PMN/ml. Experimental conditions included *ScAg* or A23187 at 5  $\mu$ M (Sigma). The Ca<sup>++</sup> flux over time was estimated by calculation of the area under the curve

## **2.6 *Sarcoptes scabiei* soluble antigen increases intracellular calcium concentration, ROS production and evokes weak NET release in bovine polymorphonuclear neutrophils**

---

(AUC) of the obtained registries, using the first 50 sec prior stimuli exposure as basal line, in a total time of 540s of record.

### **Live holotomographic microscopy**

Intracellular Ca<sup>++</sup> fluxes were visualized by the Ca<sup>++</sup>-sensitive dye fluo-4 AM (Invitrogen) following the manufacturer recommendations. Briefly, 1x10<sup>5</sup> Fluo-4 loaded PMN were seeded in a Ibidi plate and then recorded with a 3D cell-explorer-Fluo microscope (Nanolive®) equipped with a 60x magnification ( $\lambda = 520$  nm, sample exposure 0.2 mW/mm<sup>2</sup> and a depth of field of 30  $\mu$ m) equipped with a fluorescence unit (CoolLED pE-300ultra), as described by (Larrazabal et al., 2021). Images were acquired every 6 sec in both, refractive index (RI) and FITC fluorescence channel. The obtained raw data was analyzed using STEVE software (Nanolive®) to obtain a refractive index (RI)-based z-stack. Using the RI data, digital staining of cellular structures was performed on the PMN during the ScAg induction. Post-processing analysis was achieved by using Image J software (Fiji version 1.7, NIH). Holotomographic z-stacks with the average intensity of the images as a projection output were obtaining using Z Project plugin. Confirmation of Ca<sup>++</sup> flux in PMN exposed to ScAg was performed on Fluo-4 derived fluorescence images represented as pseudo color for better visualization.

### **Estimation of Extracellular and Total Reactive Oxygen Species Production**

To assess the effect ScAg on bovine PMN oxidative response, we used the luminol-chemiluminescence assay, as described previously (Rinaldi et al., 2007). Briefly, 1 × 10<sup>6</sup> PMNs were suspended in HBSS and placed in a 96-well plate at 37°C and then 50  $\mu$ M of luminol (Sigma) was added and gently mixed. The cells were stimulated with ScAg at 10  $\mu$ g/ml. Finally, basal ROS production was during 120 sec prior ScAg exposure followed by an induced ROS production registry over 1900 sec using a Luminoskan microplate reader (Thermo Scientific, MA, USA).

### **Phagocytosis Assay**

Phagocytic activity was determined by cellular uptake of pH-sensitive rhodamine-conjugated *E. coli* particles (pHrodo™ Phagocytosis Particle Labeling Kit for Flow Cytometry, Invitrogen, Carlsbad, CA). Briefly, to 100 $\mu$ l of whole blood 20 $\mu$ l of pHrodo™ dye-labeled *E. coli* was added. in uptake buffer. The samples were incubated at 37°C and 4°C (negative phagocytosis control) for 15 min, following the manufacturer recommendations. The rate of phagocytosis

## **2.6 *Sarcoptes scabiei* soluble antigen increases intracellular calcium concentration, ROS production and evokes weak NET release in bovine polymorphonuclear neutrophils**

---

was determined by flow cytometry at an excitation wavelength of 560 and emission wavelength of 585 nm respectively using a BD Accuri™ C6 Plus flow cytometer (BD Bioscience, Heidelberg, Germany).

### **Statistical analyses**

Statistical analyses were performed in GraphPad® Prism 8 (version 8.4.3) software. Data description was carried out by presenting arithmetic mean ± standard deviation. The non-parametric statistical test Mann-Whitney for comparison of two experimental conditions was applied. In cases of three or more conditions, Kruskal-Wallis test was used. Whenever global comparison by Kruskal-Wallis test indicated significance, post hoc multiple comparison tests were carried out by Dunn tests to compare test with control conditions. Outcomes of statistical tests were considered to indicate significant differences when  $p \leq 0.05$  (significance level).

## **2.6 *Sarcoptes scabiei* soluble antigen increases intracellular calcium concentration, ROS production and evokes weak NET release in bovine polymorphonuclear neutrophils**

---

### **RESULTS**

#### ***S. scabiei* mites and antigen (*ScAg*) are weak inducers of bovine NETosis**

In this study, we intended to analyze whether different parasite stages or *ScAg* are capable of induce an early bovine NETs release. As depicted on **Fig. 1**, *S. scabiei* mites have the capacity to activate bovine PMN after an exposure of 60 min in a co-cultured medium, nevertheless weak NETs formation was observed. After 20 min of co-culture, we were able to discover that some bovine PMN were attached to the surface of *Sarcoptes scabiei* mites, moreover, in the live cell fluorescence imaging we were able to observe that no extracellular filaments extruded from the bovine PMN were released (**Fig. 1A–1C**). Even so, to confirm these observations, same technique was applied with the different stages of the parasite (adult, ninfa and egg), allowing us to corroborate that no NETs release was triggered by the presence of the parasite (**Fig. 1A – 1I**).

Then, immunofluorescence analyses were performed to detect the classical components of NETs (NE, histones and DNA) in *ScAg*-confronted PMN. The isolated bovine PMN were co-cultured with *ScAg* 10 µg and 100 µg. After 2 h of co-culture, *ScAg* is able to induce a weak process of NET release from bovine PMN, but only in the concentration of 10 µg *ScAg* (**Fig. 2E–2L**). This, since in the case of the bovine PMN stimulated with 100 µg *ScAg*, we were able to observe a rather cytotoxic effect from the antigen (**Fig. 2A–2L**). Regarding the generation of different phenotypes of NETs, after 120 min of co-culture of bovine PMN with *ScAg* (10µg and 100 µg), we were able to observe NET formation, mainly *spr*NETs, which consist of a smooth and elongated web-like structures of decondensed chromatin and antimicrobial proteins, having a diameter of 15-17µm (**Fig. 2N–2O**).

#### ***ScAg* induces a fast and sustained Ca<sup>++</sup> flux in bovine PMNs.**

Intracellular Ca<sup>++</sup> flux measurements shows that PMN stimulated with 10 µg of *ScAg* have an increase in the intracellular Ca<sup>++</sup> concentration over time (**Fig. 3A**). Kinetically, the antigen induced Ca<sup>++</sup> flux was constant over time, having an enhancement of its slope after 250 sec post induction (**Fig. 3A**). Quantitatively, the AUC analysis shows that *ScAg* induce a significant increase of the Ca<sup>++</sup> signal over time ( $p= 0.002$ ) (**Fig. 3B**), but 2.2 fold smaller than the generated by A23187 (**Fig. 3B**). The Ca<sup>++</sup> flux induced by *ScAg* was corroborated by live cell holotomographic fluorescence microscopy analysis (**Fig. 3C**). As observed in **Fig. 3C** *ScAg*,

## **2.6 *Sarcoptes scabiei* soluble antigen increases intracellular calcium concentration, ROS production and evokes weak NET release in bovine polymorphonuclear neutrophils**

---

induces an increase in the Ca<sup>++</sup> driven signal, maintaining a high signal during the registry within the PMN cytoplasm, without any evident morphological changes over time (0sec, 6sec, 12sec, 18sec) (**Fig. 3D**).

### ***ScAg* evokes oxidative response in bovine PMN**

*ScAg* at 10 µg/ml induces a fast and sustained increase in the ROS-dependent luminescence, reaching a peak at 240 s post stimulation and slowly declining over time until basal levels after 900-100 s post induction (**Fig. 4A**). The AUC analysis revealed a significant increase ( $p=0.0079$ ) of ROS production over time (**Fig. 4B**).

### ***ScAg* does not affect bovine PMN phagocytosis**

Phagocytic capacity of bovine PMN was assessed by FACS using pHrodo™ labeled bioparticles as suitable for phagocytosis assays. As illustrated in **Fig. 5**, our data shows an average of  $69.2 \pm 15.64\%$  PMN performed phagocytosis, without any observable effect driven by *ScAg* pre-treatment since the percentage on this condition was similar ( $76,52 \pm 15.41\%$ ) .

## **2.6 *Sarcoptes scabiei* soluble antigen increases intracellular calcium concentration, ROS production and evokes weak NET release in bovine polymorphonuclear neutrophils**

---

### **DISCUSSION**

Sarcoptic mange is a globally extended infectious skin disease of mammals caused by the borrowing astigmatid mite infection *S. scabiei*. Given the life cycle of this parasite, a close interaction between the *S. scabiei* stage and the innate immune response will occur during its infestation (Arlan and Morgan, 2017; Bhat et al., 2017). Likewise, other skin related inflammatory processes are characterized by endothelial activation, leading to vascular permeability and rapid flux of PMN to the tissue for control of foreign pathogens (Lin et al., 2011). In the case of *S. scabiei* and other mites infection, an increase of PMN have been reported in blood and tissue in humans and different mammal species (Dagleish et al., 2007; Elwood et al., 2015; Little et al., 1998; Löwenstein et al., 1996; Skerratt, 2003). Furthermore, *S. scabiei* infection is largely associated to immunomodulatory phenomena, clinically mirrored by a late manifestation of infections signs (>4 weeks) (Arlan and Morgan, 2017; Bhat et al., 2017). In this context, we firstly explored the interaction of PMN against *S. scabiei* stages. We found that co-culture of bovine PMN with *S. scabiei* exoskeleton did not induced a significant accumulation of PMN on parasite structure, suggesting that isolated PMN are not capable to recognize or effectively attach to its chitin exoskeleton. Interestingly, histologic skin biopsies shows that PMN infiltrate is mainly localized in the perivascular area of dermic layer during *S. scabiei* infestation (Elwood et al., 2015). The fact that PMN do not migrate nor attach to *S. scabiei* surface suggest that the antigenic composition of the parasite has not been recognized by PMN. This observation resembles a recent study on *F. hepatica* juveniles, were only a limited attachment to live trematode was reported (Peixoto et al., 2021). On the other hand, the skin microenvironment modulates the innate immune response and thus, skin-associated factors could be critical to elicit a different response (Kabashima et al., 2019)

PMN combat pathogen invasion by different strategies (Fuchs et al., 2007; Nathan, 2006). However, in the case of metazoan infection, effector responses such as phagocytosis are limited, since PMN are unable to engulf large pathogens (Grob et al., 2021; Muñoz-Caro et al., 2015). Considering this, nematodes have been confirmed as NET formation inductors in different animal species, such as *Haemonchus contortus*, *Strongyloides stercoralis*, *Ostertagia ostertagi*, *Brugia malayi* and more recently *Angiostrongylus vasorum* L3 (Bonne-Année et al., 2014; Grob et al., 2021; Mendez et al., 2018; Muñoz-Caro et al., 2018, 2015). Our results reveals that *S. scabiei* stages are not capable to effectively induce NET release in bovine PMN. This last is in line with our findings regarding the attachment, and suggest a low reactivity of the PMN against

## **2.6 *Sarcoptes scabiei* soluble antigen increases intracellular calcium concentration, ROS production and evokes weak NET release in bovine polymorphonuclear neutrophils**

---

the presence of *S. scabiei* exoskeleton. Overall, PMN as other immune cells can recognize foreigner structures by PRRs receptors, such as TLR or Dectin 1 (Thomas and Schroder, 2013). Likewise, the participation of PRR as NET inducers have been consistently reported against different pathogens, including parasites (Muñoz-Caro et al., 2021; Thomas and Schroder, 2013). In principle, the large chitin composition in *S. scabiei* exoskeleton can be recognized by the immune system (Elieh Ali Komi et al., 2018). Indeed, a recent report demonstrated that chitinase-like protein present in *S. scabiei* evokes immune reaction and permits protection against scabiosis in rabbits (Shen et al., 2018). However, our results were not conclusive in these terms. To study the immunogenic capacity of *S. scabiei* antigen we also used different concentrations of ScAg to stimulate PMN. In contrast with the “whole mite” results, we found that bovine PMN stimulated with 10µg of ScAg-achieve a weak NET formation. NET identity was confirmed by the co-localization of NE, histones and extracellular DNA. Moreover, ScAg-induced NET formation resulted mainly in one specific NET phenotype, characterized by the presence of *spr*NETs after the exposure to the ScAg. Regarding to the other phenotypes, it has been described that *diff*NETs correspond to a complex of extracellular decondensed chromatin, having a size of 15-20µm. *agg*NETs are defined by having a ball of yarn-like structure, with a size of more than 20µm, which were not able to observe in this study.

Weak NET release was also observed in *F. hepatica* juveniles-confronted PMN (Peixoto et al., 2021), suggesting that parasite specific features can determine the outcome of NET formation. By knowing that species such as *Sarcoptes spp.* feed from lymph of host, the intake of immune components such as antibody or antimicrobial peptides is largely accepted as defense mechanism (Arlan and Morgan, 2017; Bhat et al., 2017; Liu et al., 2014; Shen et al., 2020). It has been suggested that inflammation permits an increase in nutrients delivered to parasites, generating a paradoxical role in terms of immune response (Huntley et al., 2005).

Ca<sup>++</sup> flux is necessary for PMN effector mechanisms, such degranulation, ROS and subsequently NET release (Burgos et al., 2011; Hann et al., 2020), by considering that PMN antimicrobial performance is largely associated to oxidative responses such ROS production capable of protect against pathogens (Nguyen et al., 2017). Accordingly, we evaluated the outcome of ScAg stimulation in bovine PMN Ca<sup>++</sup> homeostasis. Current data shows that ScAg evokes a fast and sustained Ca<sup>++</sup> flux in bovine PMN. Ca<sup>++</sup> fluxes in PMN are evoked by chemoattractant molecules (i.e. CXCL8, PAF or LTB4), adhesion molecules (L-selectin or CD11b) and Fc-receptors (Futosi et al., 2013). In the case of pathogen-derived molecules,

## **2.6 *Sarcoptes scabiei* soluble antigen increases intracellular calcium concentration, ROS production and evokes weak NET release in bovine polymorphonuclear neutrophils**

---

evidence of a  $\text{Ca}^{++}$  dependent activation in PMN is unclear. In this context, human PMN stimulated by zymosan mobilizes intracellular  $\text{Ca}^{++}$  stores (Schwab et al., 1992). While, *Lucilia sericata*-derived excretion/secretion molecules modulate PMN oxidative and non-oxidative responses independently of  $\text{Ca}^{++}$  signaling (van der Plas et al., 2007). Despite that, analysis of different synthetic TLR agonists revealed that only TLR 2/1 chemical activation evokes  $\text{Ca}^{++}$  flux bovine PMN by a store opened  $\text{Ca}^{++}$  entry (Conejeros et al., 2015). This divergent findings indicates that pathogen derived molecules can induce  $\text{Ca}^{++}$  fluxes in PMN by other routes than the canonic PRR activation.

Since, NET formation is downstream signaled by other antimicrobial events such ROS production (Fuchs et al., 2007), we evaluated the capacity of *ScAg* to evoke oxidative burst in bovine PMN. Here, we found that *ScAg* exposure evokes a fast and sustained ROS production, confirming the capacity of *ScAg* as oxidative inductor bovine PMN. In general, ROS production in PMN is linked to NADPH complex activation (Fuchs et al., 2007). This enzymatic complex catalyzes the conversion of  $\text{O}_2$  molecules into superoxide ( $\text{O}_2^-$ ). These molecules will suffer enzymatic dismutation to hydrogen peroxide ( $\text{H}_2\text{O}_2$ ), continuing with the conversion of hydrogen peroxidase into hypochlorous acid (HOCl) thanks to the role of myeloperoxidase (MPO), generating a highly oxidative environment capable of destroy microorganisms (Nguyen et al., 2017). In the case of arthropods-driven innate immune response, this represents the first report regarding oxidative responses of PMN against *S. scabiei*. Interestingly, prior reports showed that *S. scabiei* infected dogs presents a disturbed oxidant/antioxidant balance (Camkerten et al., 2009; Singh et al., 2011). Considering this, is possible to speculate that during *S. scabiei* infection, skin PMN could contribute to oxidative stress in the host.

During *S. scabiei* infection, the immunomodulation driven by the parasite delays the immune response against the infection. Likewise, commensal bacteria like *S. aureus* often colonize the skin during severe cases of scabiosis (Bhat et al., 2017; Dagleish et al., 2007; Swe et al., 2017), indicating a reduced effect of PMN-driven antimicrobial response. Given that, to confirm the effect of *ScAg* on bovine PMN, we evaluated its effect on phagocytic activity. We found that *ScAg* at concentrations capable of trigger bovine PMN responses fail to effectively affect the phagocytic activity of bovine PMN. Overall, this finding disagree with a prior report that shows that the recombinant serpin SMSB4 from *S. scabiei* is capable to interfere with the complement system, reducing the phagocytosis capacity of the PMN (Swe and Fischer, 2014). Intriguingly, the immunomodulatory role of serpins is extended to other parasitic arachnids such as

## **2.6 *Sarcoptes scabiei* soluble antigen increases intracellular calcium concentration, ROS production and evokes weak NET release in bovine polymorphonuclear neutrophils**

---

*Amblyomma americanum*, *Ixodes ricinus* or *Rhipicephalus micropilus*, where the secretion from salivary glands facilitates a delay on the immune response, ensuring the tick feeding (Chlastáková et al., 2021; Coutinho et al., 2020; Tirloni et al., 2019). In that context, is possible to speculate that effect of serpins on PMN phagocytic activity could be limited to complement facilitated phagocytosis, without affecting opsonization independent phagocytosis in isolated PMN.

In summary, we found that *S. scabiei* antigen evokes  $\text{Ca}^{++}$  flux and ROS production and weak NETs release in bovine PMN, without affecting the phagocytic activity. Nevertheless, since *S. scabiei* exoskeleton did not activated isolated PMN, is possible that the antigenic composition of this parasite influence the recognition of PMN.

## **2.6 *Sarcoptes scabiei* soluble antigen increases intracellular calcium concentration, ROS production and evokes weak NET release in bovine polymorphonuclear neutrophils**

---

### **References**

- Arlian, L.G., Morgan, M.S., 2017. A review of *Sarcoptes scabiei*: past, present and future. *Parasit Vectors* 10, 297. <https://doi.org/10.1186/s13071-017-2234-1>
- Bhat, S.A., Mounsey, K.E., Liu, X., Walton, S.F., 2017. Host immune responses to the itch mite, *Sarcoptes scabiei*, in humans. *Parasit Vectors* 10, 385. <https://doi.org/10.1186/s13071-017-2320-4>
- Bhat, S.A., Walton, S.F., Ventura, T., Liu, X., McCarthy, J.S., Burgess, S.T.G., Mounsey, K.E., 2020. Early immune suppression leads to uncontrolled mite proliferation and potent host inflammatory responses in a porcine model of crusted versus ordinary scabies. *PLoS Negl Trop Dis* 14, e0008601. <https://doi.org/10.1371/journal.pntd.0008601>
- Bonne-Année, S., Kerepesi, L.A., Hess, J.A., Wesolowski, J., Paumet, F., Lok, J.B., Nolan, T.J., Abraham, D., 2014. Extracellular traps are associated with human and mouse neutrophil and macrophage mediated killing of larval *Strongyloides stercoralis*. *Microbes Infect* 16, 502–511. <https://doi.org/10.1016/j.micinf.2014.02.012>
- Branzk, N., Lubojemska, A., Hardison, S.E., Wang, Q., Gutierrez, M.G., Brown, G.D., Papayannopoulos, V., 2014. Neutrophils sense microbe size and selectively release neutrophil extracellular traps in response to large pathogens. *Nature Immunology* 15, 1017–1025. <https://doi.org/10.1038/ni.2987>
- Brinkmann, V., Reichard, U., Goosmann, C., Fauler, B., Uhlemann, Y., Weiss, D.S., Weinrauch, Y., Zychlinsky, A., 2004. Neutrophil extracellular traps kill bacteria. *Science* 303, 1532–1535. <https://doi.org/10.1126/science.1092385>
- Burgess, S.T.G., Frew, D., Nunn, F., Watkins, C.A., McNeilly, T.N., Nisbet, A.J., Huntley, J.F., 2010. Transcriptomic analysis of the temporal host response to skin infestation with the ectoparasitic mite *Psoroptes ovis*. *BMC Genomics* 11, 624. <https://doi.org/10.1186/1471-2164-11-624>
- Burgos, R.A., Conejeros, I., Hidalgo, M.A., Werling, D., Hermosilla, C., 2011. Calcium influx, a new potential therapeutic target in the control of neutrophil-dependent inflammatory

## **2.6 *Sarcoptes scabiei* soluble antigen increases intracellular calcium concentration, ROS production and evokes weak NET release in bovine polymorphonuclear neutrophils**

---

- diseases in bovines. *Veterinary Immunology and Immunopathology* 143, 1–10. <https://doi.org/10.1016/j.vetimm.2011.05.037>
- Camkerten, I., Sahin, T., Borazan, G., Gokcen, A., Erel, O., Das, A., 2009. Evaluation of blood oxidant/antioxidant balance in dogs with sarcoptic mange. *Vet Parasitol* 161, 106–109. <https://doi.org/10.1016/j.vetpar.2008.12.019>
- Casais, R., Granda, V., Balseiro, A., Del Cerro, A., Dalton, K.P., González, R., Bravo, P., Prieto, J.M., Montoya, M., 2016. Vaccination of rabbits with immunodominant antigens from *Sarcoptes scabiei* induced high levels of humoral responses and pro-inflammatory cytokines but confers limited protection. *Parasit Vectors* 9, 435. <https://doi.org/10.1186/s13071-016-1717-9>
- Chen, Z., Claerebout, E., Chiers, K., Pas, M., Pardon, B., van Mol, W., Casaert, S., De Wilde, N., Duchateau, L., Geldhof, P., 2021. Dermal immune responses against *Psoroptes ovis* in two cattle breeds and effects of anti-inflammatory dexamethasone treatment on the development of psoroptic mange. *Veterinary Research* 52, 1. <https://doi.org/10.1186/s13567-020-00874-x>
- Chlastáková, A., Kotál, J., Beránková, Z., Kaščáková, B., Martins, L.A., Langhansová, H., Prudnikova, T., Ederová, M., Kutá Smatanová, I., Kotsyfakis, M., Chmelař, J., 2021. Iripin-3, a New Salivary Protein Isolated From *Ixodes ricinus* Ticks, Displays Immunomodulatory and Anti-Hemostatic Properties In Vitro. *Front Immunol* 12, 626200. <https://doi.org/10.3389/fimmu.2021.626200>
- Conejeros, I., Gibson, A.J., Werling, D., Muñoz-Caro, T., Hermosilla, C., Taubert, A., Burgos, R.A., 2015. Effect of the synthetic Toll-like receptor ligands LPS, Pam3CSK4, HKLM and FSL-1 in the function of bovine polymorphonuclear neutrophils. *Dev Comp Immunol* 52, 215–225. <https://doi.org/10.1016/j.dci.2015.05.012>
- Conejeros, I., Jara, E., Carretta, M.D., Alarcón, P., Hidalgo, M.A., Burgos, R.A., 2012. 2-Aminoethoxydiphenyl borate (2-APB) reduces respiratory burst, MMP-9 release and CD11b expression, and increases I-selectin shedding in bovine neutrophils. *Res Vet Sci* 92, 103–110. <https://doi.org/10.1016/j.rvsc.2010.10.005>

## **2.6 *Sarcoptes scabiei* soluble antigen increases intracellular calcium concentration, ROS production and evokes weak NET release in bovine polymorphonuclear neutrophils**

---

- Coutinho, M.L., Bizzarro, B., Tirloni, L., Berger, M., Freire Oliveira, C.J., Sá-Nunes, A., Silva Vaz, I.J., 2020. *Rhipicephalus microplus* serpins interfere with host immune responses by specifically modulating mast cells and lymphocytes. *Ticks Tick Borne Dis* 11, 101425. <https://doi.org/10.1016/j.ttbdis.2020.101425>
- Dagleish, M.P., Ali, Q., Powell, R.K., Butz, D., Woodford, M.H., 2007. Fatal *Sarcoptes scabiei* infection of blue sheep (*Pseudois nayaur*) in Pakistan. *J Wildl Dis* 43, 512–517. <https://doi.org/10.7589/0090-3558-43.3.512>
- Elder, B.L., Arlian, L.G., Morgan, M.S., 2009. Modulation of human dermal microvascular endothelial cells by *Sarcoptes scabiei* in combination with proinflammatory cytokines, histamine, and lipid-derived biologic mediators. *Cytokine* 47, 103–111. <https://doi.org/10.1016/j.cyto.2009.05.008>
- Elieh Ali Komi, D., Sharma, L., Dela Cruz, C.S., 2018. Chitin and Its Effects on Inflammatory and Immune Responses. *Clin Rev Allergy Immunol* 54, 213–223. <https://doi.org/10.1007/s12016-017-8600-0>
- Elwood, H., Berry, R.S., Gardner, J.M., Shalin, S.C., 2015. Superficial fibrin thrombi and other findings: a review of the histopathology of human scabietic infections. *J Cutan Pathol* 42, 346–352. <https://doi.org/10.1111/cup.12482>
- Fuchs, T.A., Abed, U., Goosmann, C., Hurwitz, R., Schulze, I., Wahn, V., Weinrauch, Y., Brinkmann, V., Zychlinsky, A., 2007. Novel cell death program leads to neutrophil extracellular traps. *J Cell Biol* 176, 231–241. <https://doi.org/10.1083/jcb.200606027>
- Futosi, K., Fodor, S., Mócsai, A., 2013. Neutrophil cell surface receptors and their intracellular signal transduction pathways. *Int Immunopharmacol* 17, 638–650. <https://doi.org/10.1016/j.intimp.2013.06.034>
- Grob, D., Conejeros, I., López-Osorio, S., Velásquez, Z.D., Segeritz, L., Gärtner, U., Schaper, R., Hermosilla, C., Taubert, A., 2021. Canine *Angiostrongylus vasorum*-Induced Early Innate Immune Reactions Based on NETs Formation and Canine Vascular Endothelial Cell Activation In Vitro. *Biology (Basel)* 10, 427. <https://doi.org/10.3390/biology10050427>

## **2.6 *Sarcoptes scabiei* soluble antigen increases intracellular calcium concentration, ROS production and evokes weak NET release in bovine polymorphonuclear neutrophils**

---

- Grob, D., Conejeros, I., Velásquez, Z.D., Preußner, C., Gärtner, U., Alarcón, P., Burgos, R.A., Hermosilla, C., Taubert, A., 2020. *Trypanosoma brucei brucei* Induces Polymorphonuclear Neutrophil Activation and Neutrophil Extracellular Traps Release. *Front Immunol* 11, 559561. <https://doi.org/10.3389/fimmu.2020.559561>
- Hann, J., Bueb, J.-L., Tolle, F., Brécard, S., 2020. Calcium signaling and regulation of neutrophil functions: Still a long way to go. *J Leukoc Biol* 107, 285–297. <https://doi.org/10.1002/JLB.3RU0719-241R>
- Huntley, J.F., van den Broek, A., Machell, J., Mackellar, A., Pettit, D., Meikle, L., Barcham, G., Meeusen, E.N.T., Smith, D., 2005. The effect of immunosuppression with cyclosporin A on the development of sheep scab. *Vet Parasitol* 127, 323–332. <https://doi.org/10.1016/j.vetpar.2004.10.021>
- Kabashima, K., Honda, T., Ginhoux, F., Egawa, G., 2019. The immunological anatomy of the skin. *Nature Reviews Immunology* 19, 19. <https://doi.org/10.1038/s41577-018-0084-5>
- Kolaczowska, E., Kuberski, P., 2013. Neutrophil recruitment and function in health and inflammation. *Nat Rev Immunol* 13, 159–175. <https://doi.org/10.1038/nri3399>
- Larrazabal, C., Hermosilla, C., Taubert, A., Conejeros, I., 2021. 3D holotomographic monitoring of Ca(++) dynamics during ionophore-induced *Neospora caninum* tachyzoite egress from primary bovine host endothelial cells. *Parasitol Res.* <https://doi.org/10.1007/s00436-021-07260-2>
- Lin, A.M., Rubin, C.J., Khandpur, R., Wang, J.Y., Riblett, M., Yalavarthi, S., Villanueva, E.C., Shah, P., Kaplan, M.J., Bruce, A.T., 2011. Mast Cells and Neutrophils Release IL-17 through Extracellular Trap Formation in Psoriasis. *J. Immunol.* 187, 490. <https://doi.org/10.4049/jimmunol.1100123>
- Little, S.E., Davidson, W.R., Rakich, P.M., Nixon, T.L., Bounous, D.I., Nettles, V.F., 1998. Responses of red foxes to first and second infection with *Sarcoptes scabiei*. *J Wildl Dis* 34, 600–611. <https://doi.org/10.7589/0090-3558-34.3.600>
- Liu, X., Walton, S., Mounsey, K., 2014. Vaccine against scabies: necessity and possibility. *Parasitology* 141, 725–732. <https://doi.org/10.1017/S0031182013002047>

## **2.6 *Sarcoptes scabiei* soluble antigen increases intracellular calcium concentration, ROS production and evokes weak NET release in bovine polymorphonuclear neutrophils**

---

- Löwenstein, M., Loupal, G., Baumgartner, W., Kutzer, E., 1996. Histology of the skin and determination of blood and serum parameters during the recovery phase of sarcoptic mange in cattle after ivermectin (Ivomec) treatment. *Appl Parasitol* 37, 77–86.
- McCoy, C.J., Reaves, B.J., Giguère, S., Coates, R., Rada, B., Wolstenholme, A.J., 2017. Human Leukocytes Kill *Brugia malayi* Microfilariae Independently of DNA-Based Extracellular Trap Release. *PLoS Negl Trop Dis* 11, e0005279. <https://doi.org/10.1371/journal.pntd.0005279>
- Mendez, J., Sun, D., Tuo, W., Xiao, Z., 2018. Bovine neutrophils form extracellular traps in response to the gastrointestinal parasite *Ostertagia ostertagi*. *Scientific Reports* 8, 17598. <https://doi.org/10.1038/s41598-018-36070-3>
- Mika, A., Reynolds, S.L., Mohlin, F.C., Willis, C., Swe, P.M., Pickering, D.A., Halilovic, V., Wijeyewickrema, L.C., Pike, R.N., Blom, A.M., Kemp, D.J., Fischer, K., 2012. Novel scabies mite serpins inhibit the three pathways of the human complement system. *PLoS One* 7, e40489. <https://doi.org/10.1371/journal.pone.0040489>
- Morgan, M.S., Arlian, L.G., 2010. Response of human skin equivalents to *Sarcoptes scabiei*. *J Med Entomol* 47, 877–883. <https://doi.org/10.1603/me10012>
- Mounsey, K.E., McCarthy, J.S., Walton, S.F., 2013. Scratching the itch: new tools to advance understanding of scabies. *Trends Parasitol* 29, 35–42. <https://doi.org/10.1016/j.pt.2012.09.006>
- Mullins, J.S., Arlian, L.G., Morgan, M.S., 2009. Extracts of *Sarcoptes scabiei* De Geer downmodulate secretion of IL-8 by skin keratinocytes and fibroblasts and of GM-CSF by fibroblasts in the presence of proinflammatory cytokines. *J Med Entomol* 46, 845–851. <https://doi.org/10.1603/033.046.0415>
- Muñoz-Caro, T., Conejeros, I., Zhou, E., Pikhovych, A., Gärtner, U., Hermosilla, C., Kulke, D., Taubert, A., 2018. *Dirofilaria immitis* Microfilariae and Third-Stage Larvae Induce Canine NETosis Resulting in Different Types of Neutrophil Extracellular Traps. *Frontiers in Immunology* 9, 968. <https://doi.org/10.3389/fimmu.2018.00968>

## **2.6 *Sarcoptes scabiei* soluble antigen increases intracellular calcium concentration, ROS production and evokes weak NET release in bovine polymorphonuclear neutrophils**

---

- Muñoz-Caro, T., Gibson, A.J., Conejeros, I., Werling, D., Taubert, A., Hermosilla, C., 2021. The Role of TLR2 and TLR4 in Recognition and Uptake of the Apicomplexan Parasite *Eimeria bovis* and Their Effects on NET Formation. *Pathogens* 10. <https://doi.org/10.3390/pathogens10020118>
- Muñoz-Caro, T., Rubio R, M.C., Silva, L.M.R., Magdowski, G., Gärtner, U., McNeilly, T.N., Taubert, A., Hermosilla, C., 2015. Leucocyte-derived extracellular trap formation significantly contributes to *Haemonchus contortus* larval entrapment. *Parasites & Vectors* 8, 607. <https://doi.org/10.1186/s13071-015-1219-1>
- Nathan, C., 2006. Neutrophils and immunity: challenges and opportunities. *Nature Reviews Immunology* 6, 173–182. <https://doi.org/10.1038/nri1785>
- Nguyen, G.T., Green, E.R., Mecsas, J., 2017. Neutrophils to the ROScUE: Mechanisms of NADPH Oxidase Activation and Bacterial Resistance. *Front Cell Infect Microbiol* 7, 373. <https://doi.org/10.3389/fcimb.2017.00373>
- Papayannopoulos, V., 2018. Neutrophil extracellular traps in immunity and disease. *Nat Rev Immunol* 18, 134–147. <https://doi.org/10.1038/nri.2017.105>
- Papayannopoulos, V., Metzler, K.D., Hakkim, A., Zychlinsky, A., 2010. Neutrophil elastase and myeloperoxidase regulate the formation of neutrophil extracellular traps. *J Cell Biol* 191, 677–691. <https://doi.org/10.1083/jcb.201006052>
- Peixoto, R., Silva, L.M.R., López-Osório, S., Zhou, E., Gärtner, U., Conejeros, I., Taubert, A., Hermosilla, C., 2021. *Fasciola hepatica* induces weak NETosis and low production of intra- and extracellular ROS in exposed bovine polymorphonuclear neutrophils. *Dev Comp Immunol* 114, 103787. <https://doi.org/10.1016/j.dci.2020.103787>
- Rentería-Solís, Z., Min, A.M., Alasaad, S., Müller, K., Michler, F.-U., Schmäschke, R., Wittstatt, U., Rossi, L., Wibbelt, G., 2014. Genetic epidemiology and pathology of raccoon-derived *Sarcoptes* mites from urban areas of Germany. *Med Vet Entomol* 28 Suppl 1, 98–103. <https://doi.org/10.1111/mve.12079>

## **2.6 *Sarcoptes scabiei* soluble antigen increases intracellular calcium concentration, ROS production and evokes weak NET release in bovine polymorphonuclear neutrophils**

---

- Rinaldi, M., Moroni, P., Paape, M.J., Bannerman, D.D., 2007. Evaluation of assays for the measurement of bovine neutrophil reactive oxygen species. *Veterinary Immunology and Immunopathology* 115, 107–125. <https://doi.org/10.1016/j.vetimm.2006.09.009>
- Sarre, C., González-Hernández, A., Van Coppennolle, S., Grit, R., Grauwet, K., Van Meulder, F., Chiers, K., Van den Broeck, W., Geldhof, P., Claerebout, E., 2015. Comparative immune responses against *Psoroptes ovis* in two cattle breeds with different susceptibility to mange. *Vet Res* 46, 131. <https://doi.org/10.1186/s13567-015-0277-x>
- Schwab, J.C., Leong, D.A., Mandell, G.L., 1992. A wave of elevated intracellular free calcium spreads through human neutrophils during phagocytosis of zymosan. *J Leukoc Biol* 51, 437–443. <https://doi.org/10.1002/jlb.51.5.437>
- Shen, N., Wei, W., Chen, Y., Ren, Y., Xiong, L., Tao, Y., Gu, X., Xie, Y., Peng, X., Yang, G., 2020. An Antibody Persistent and Protective Two rSsCLP-Based Subunit Cocktail Vaccine against *Sarcoptes scabiei* in a Rabbit Model. *Vaccines (Basel)* 8. <https://doi.org/10.3390/vaccines8010129>
- Shen, N., Zhang, H., Ren, Y., He, R., Xu, J., Li, C., Lai, W., Gu, X., Xie, Y., Peng, X., Yang, G., 2018. A chitinase-like protein from *Sarcoptes scabiei* as a candidate anti-mite vaccine that contributes to immune protection in rabbits. *Parasit Vectors* 11, 599. <https://doi.org/10.1186/s13071-018-3184-y>
- Singh, S.K., Dimri, U., Sharma, M.C., Swarup, D., Sharma, B., 2011. Determination of oxidative status and apoptosis in peripheral blood of dogs with sarcoptic mange. *Vet Parasitol* 178, 330–338. <https://doi.org/10.1016/j.vetpar.2011.01.036>
- Skerratt, L.F., 2003. Cellular response in the dermis of common wombats (*Vombatus ursinus*) infected with *Sarcoptes scabiei* var. *wombati*. *J Wildl Dis* 39, 193–202. <https://doi.org/10.7589/0090-3558-39.1.193>
- Swe, P.M., Christian, L.D., Lu, H.C., Sriprakash, K.S., Fischer, K., 2017. Complement inhibition by *Sarcoptes scabiei* protects *Streptococcus pyogenes* - An in vitro study to unravel the molecular mechanisms behind the poorly understood predilection of *S.*

## 2.6 *Sarcoptes scabiei* soluble antigen increases intracellular calcium concentration, ROS production and evokes weak NET release in bovine polymorphonuclear neutrophils

---

- pyogenes* to infect mite-induced skin lesions. PLoS Negl Trop Dis 11, e0005437. <https://doi.org/10.1371/journal.pntd.0005437>
- Swe, P.M., Fischer, K., 2014. A scabies mite serpin interferes with complement-mediated neutrophil functions and promotes staphylococcal growth. PLoS Negl Trop Dis 8, e2928. <https://doi.org/10.1371/journal.pntd.0002928>
- Thomas, C.J., Schroder, K., 2013. Pattern recognition receptor function in neutrophils. Trends Immunol 34, 317–328. <https://doi.org/10.1016/j.it.2013.02.008>
- Tirioni, L., Kim, T.K., Berger, M., Termignoni, C., da Silva Vaz, I.J., Mulenga, A., 2019. *Amblyomma americanum* serpin 27 (AAS27) is a tick salivary anti-inflammatory protein secreted into the host during feeding. PLoS Negl Trop Dis 13, e0007660. <https://doi.org/10.1371/journal.pntd.0007660>
- Urban, C.F., Ermert, D., Schmid, M., Abu-Abed, U., Goosmann, C., Nacken, W., Brinkmann, V., Jungblut, P.R., Zychlinsky, A., 2009. Neutrophil Extracellular Traps Contain Calprotectin, a Cytosolic Protein Complex Involved in Host Defense against *Candida albicans*. PLOS Pathogens 5, e1000639. <https://doi.org/10.1371/journal.ppat.1000639>
- van der Plas, M.J.A., van der Does, A.M., Baldry, M., Dogterom-Ballering, H.C.M., van Gulpen, C., van Dissel, J.T., Nibbering, P.H., Jukema, G.N., 2007. Maggot excretions/secretions inhibit multiple neutrophil pro-inflammatory responses. Microbes Infect 9, 507–514. <https://doi.org/10.1016/j.micinf.2007.01.008>
- Zhang, R., Jise, Q., Zheng, W., Ren, Y., Nong, X., Wu, X., Gu, X., Wang, S., Peng, X., Lai, S., Yang, G., 2012. Characterization and evaluation of a *Sarcoptes scabiei* allergen as a candidate vaccine. Parasit Vectors 5, 176. <https://doi.org/10.1186/1756-3305-5-176>

## 2.6 *Sarcoptes scabiei* soluble antigen increases intracellular calcium concentration, ROS production and evokes weak NET release in bovine polymorphonuclear neutrophils

---

### FIGURES

**Fig. 1. PMN adhesion to *S. scabiei* is stage-dependent.** Bovine polymorphonuclear neutrophils (PMN,  $2 \times 10^5$ ) were exposed for 60 min to *S. scabiei* adults, which did not adhere completely to the surface of *S. scabiei* adults (**Fig. 1A – 1C**), visualized by staining extracellular DNA (Sytox Green®), (**Fig. 1B**) Exposure of bovine PMN with *S. scabiei* ninfa (60 min) resulted in weak PMN adhesion, same situation in (**D, E, F**) the co-culture with *S. scabiei* eggs (**G, H, I**).

**Fig. 2. Immunofluorescence analyses of *S. scabiei*-induced weak NET formation.** Bovine PMN ( $n = 3$ ) were incubated with *ScAg* (10 or 100  $\mu\text{g/ml}$ ). Presence of DNA (**A, E, I**; blue), neutrophil elastase (**B, F, J**; green), and histones (H1, H2A/H2B, H3, H4) (**C, G, K**; red) in *ScAg* induced NETs. (**D, H, L**; merge) shows the merge of the three channels. (**M**) reveals the percentage of *ScAg* triggered NETosis. (**N-O**) demonstrate the presence of spread NETs (*spr*NETs).

**Fig. 3. *ScAg*-induced calcium flux.** Bovine neutrophils were loaded with Fluo4-AM (2.5  $\mu\text{M}$ ) in HBSS/ $\text{Ca}^{++}$  buffer and then stimulated with 10  $\mu\text{g}$  *ScAg*. The  $\text{Ca}^{++}$  ionophore A23187 served as a positive control. (**A**) Demonstrate the changes upon the calcium entry. (**B**) Depicts area under the curve (AUC). (**C**) Represents a time-lapse of stained PMN with Fluo4-AM, demonstrating the changes suffered by the stimulated PMN. (**D**) Depicts the concordant frames of figure (**C**), representing the refractive index of this video.

**Fig. 4. ROS production in *ScAg*-exposed bovine PMN.** ROS production evaluated by the use of luminol (**Fig. 4**). Reactive oxygen species were increased during the stimulation of bovine PMN (**Fig. 4A**). AUC was calculated and represented as mean  $\pm$  SD (**Fig. 4B**).

**Fig. 5. PMN phagocytosis of pHrodo-*E. coli* bioparticles is not affected by *ScAg* in bovine PMN.** Bovine PMN were exposed to *E. coli*- bioparticles conjugated with the pH sensitive probe pHrodo. Representative diagrams of the gating strategy and analysis is shown in (**A**). The percentage of phagocytosis in the untreated and *ScAg*-exposed PMN was determined by flow cytometry (**B**). PMN without pHrodo bioparticles served as a negative control.

**2.6 *Sarcoptes scabiei* soluble antigen increases intracellular calcium concentration, ROS production and evokes weak NET release in bovine polymorphonuclear neutrophils**

---

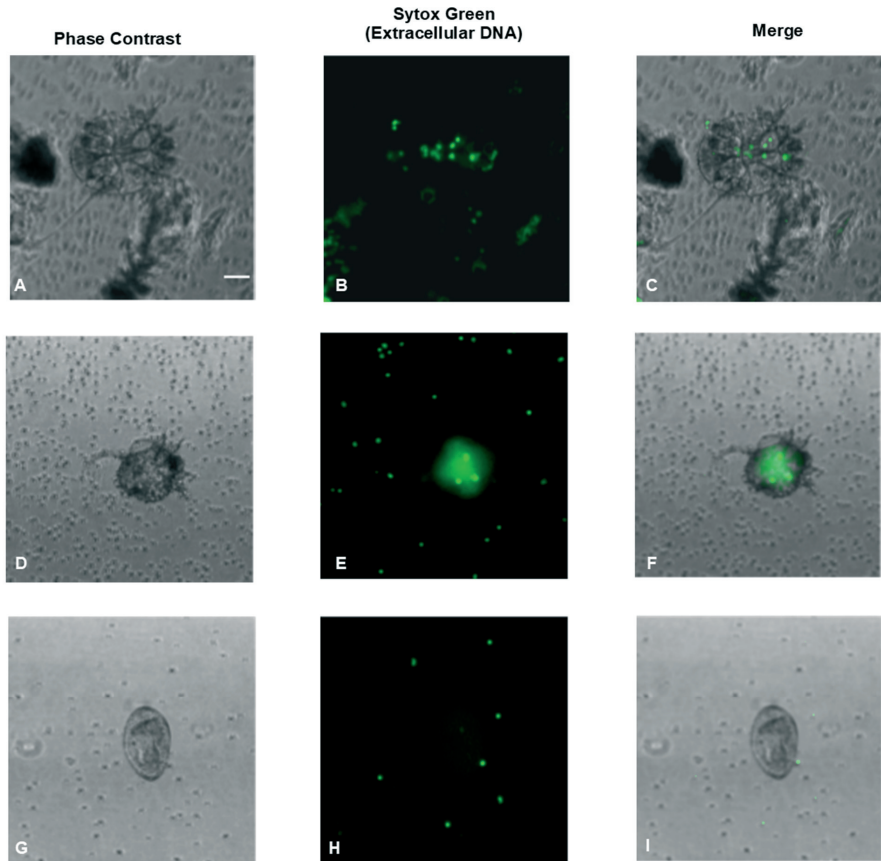


**Figure 1**

## 2.6 *Sarcoptes scabiei* soluble antigen increases intracellular calcium concentration, ROS production and evokes weak NET release in bovine polymorphonuclear neutrophils

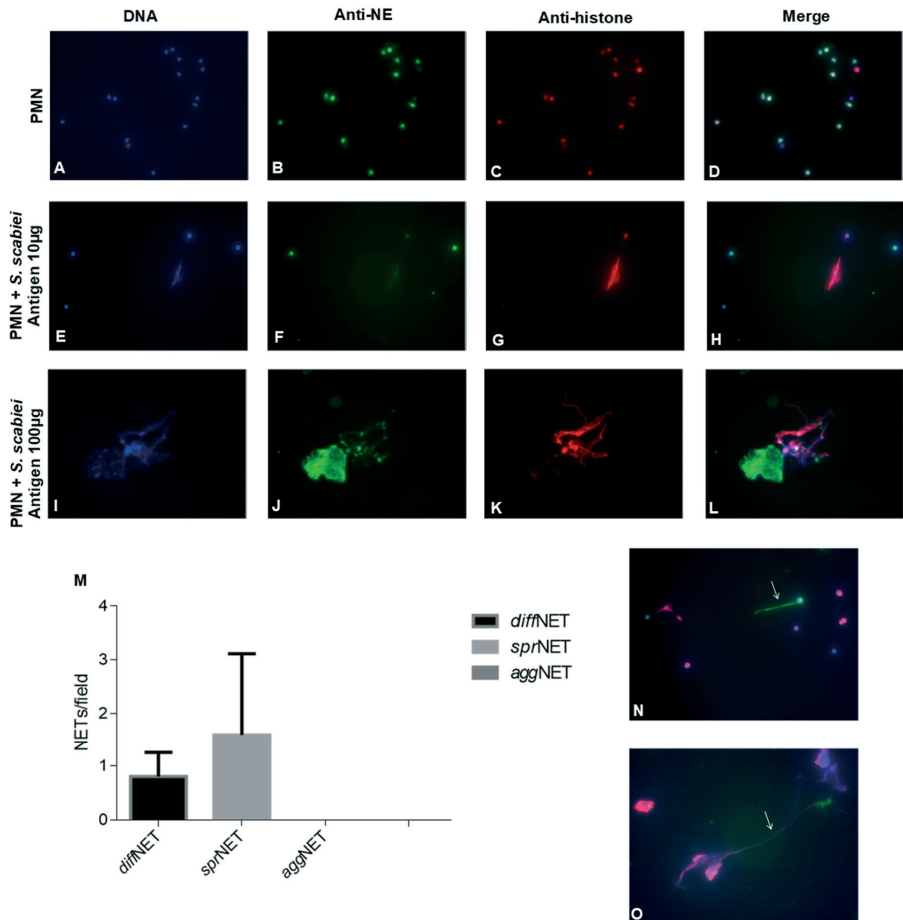


Figure 2

## 2.6 *Sarcoptes scabiei* soluble antigen increases intracellular calcium concentration, ROS production and evokes weak NET release in bovine polymorphonuclear neutrophils

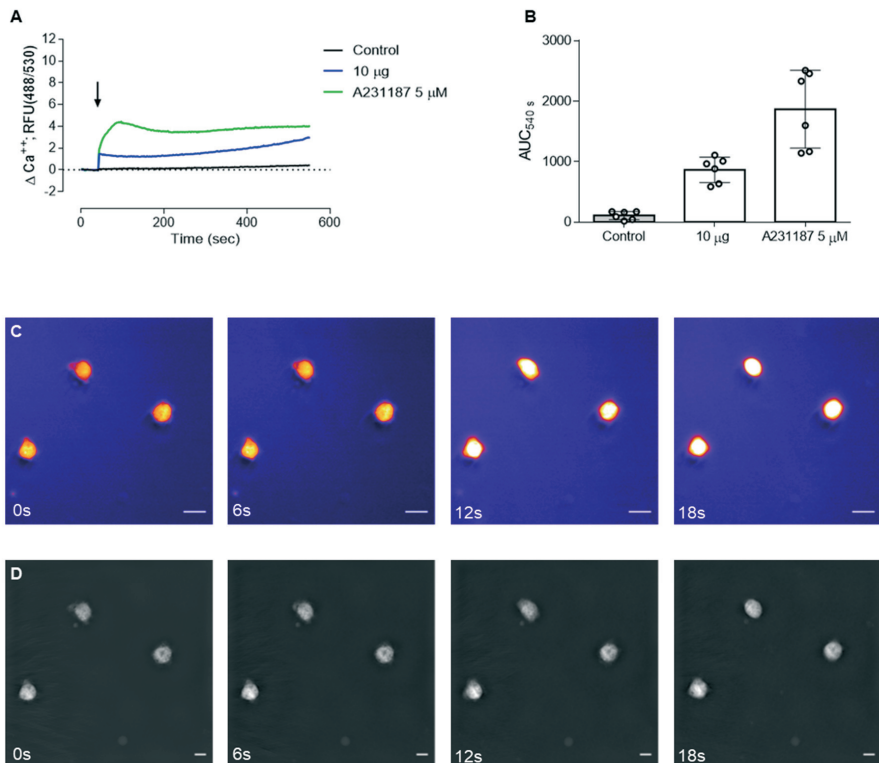


Figure 3

## 2.6 *Sarcoptes scabiei* soluble antigen increases intracellular calcium concentration, ROS production and evokes weak NET release in bovine polymorphonuclear neutrophils

---

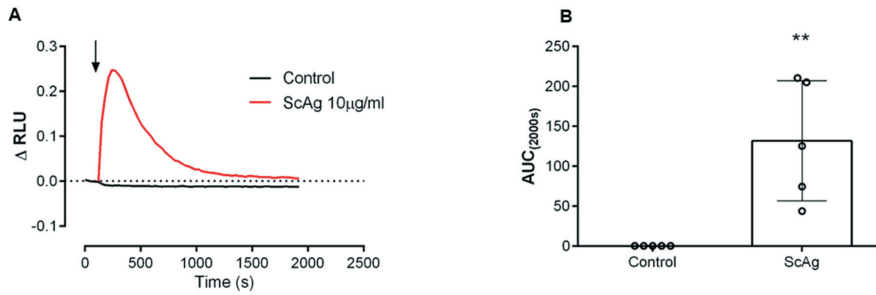


Figure 4

## 2.6 *Sarcoptes scabiei* soluble antigen increases intracellular calcium concentration, ROS production and evokes weak NET release in bovine polymorphonuclear neutrophils

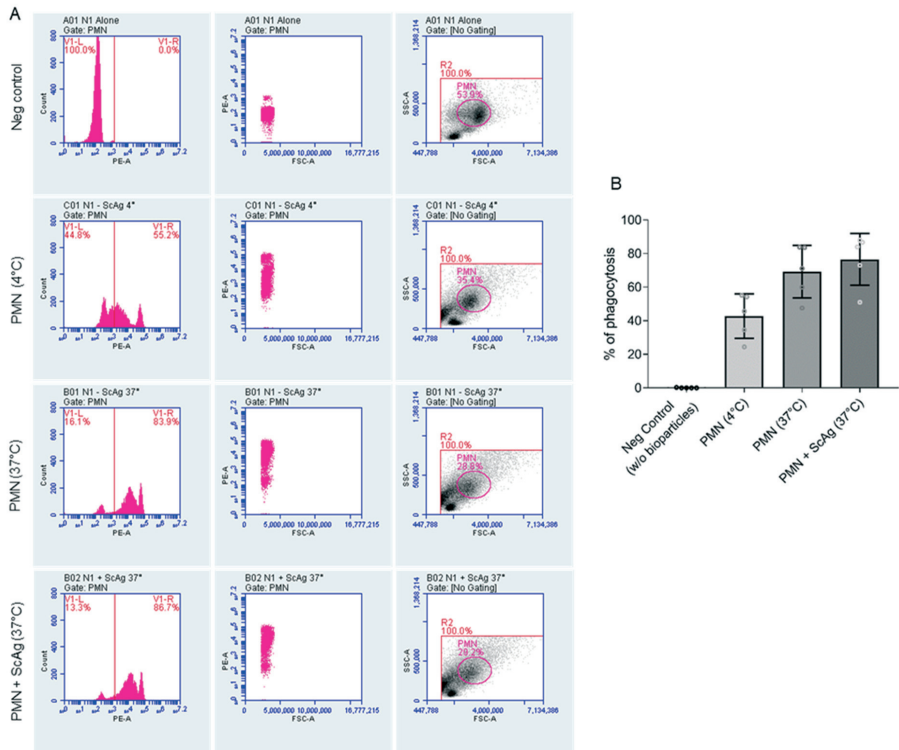


Figure 5

### 3. DISCUSSION

Faced with daily exposure to various pathogens, mammals rely heavily on the innate immune system as a first responder to intruders (Hermoisilla et al., 2014, Silva et al., 2016). PMN are the most abundant and fastest responding innate immune effector cells (Brinkmann et al., 2004, Brinkmann and Zychlinski, 2012). Thus, these leukocytes play a pivotal role in early innate immune reactions by acting when inflammation occurs and then subside. When pathogens invade the mammalian body, PMN kill them through three major strategies, i. e. phagocytosis, degranulation and the extrusion of NETs (Chen et al. 2021).

The current work focuses on PMN-derived NET formation as early host innate effector mechanism against different parasitic stages and species. More specifically spoken, the focus of this doctoral thesis relays on comparative analysis of *T. b. brucei* stages, such as procyclic trypomastigotes (chapter 2.1) and bloodstream stages, such as bloodstream metacyclic trypomastigotes (chapter 2.5) in their capacities as NET-inducers in bovine PMN, which is also the main definitive host in Africa. Additionally, parasite-dependent NETs phenotypes were analyzed in more detail. Consequently, the formation of *aggNETs* induced by *T. b. brucei* was studied in more detail. Likewise, new insights regarding purinergic signaling involved on parasite-triggered NETosis were here analyzed.

Also, we described for the first time the capacity of angiotropic *A. vasorum* as potent inductor of canine-derived NETs as well as activation of primary canine aortic endothelial cells (CAEC) (chapter 2.2). Finally, the response of bovine PMN including oxidative activity and calcium signaling against *S. scabiei* stages and antigens were also analyzed (chapter 2.6). Overall, the content of this work permits a more complete understanding of how innate immune system interact with extracellular/intracellular protozoan-, nematode- and arthropod parasites located in different tissues such as endothelium, blood and skin and providing novel insights into signaling pathways.

NETs release is a conserved phenomenon within animal kingdom (Villagra-Blanco et al. 2019). For instance, NET formation has been described so far in humans, mice, dolphins, seals, horses, donkeys, felids and canids among others (Baker et al. 2008; Abi Abdallah et al. 2012; Reichel et al. 2013; Muñoz-Caro et al. 2015; Imlau et al. 2020; Yáñez-Ortiz et al. 2021; Li et al. 2022). In ruminants, NET formation has been observed in goats, sheep and bovines (Behrendt et al. 2010; Muñoz Caro et al. 2014; Silva et al. 2014; Muñoz-Caro et al. 2015b, c, 2016; Villagra-Blanco et al. 2017b; Worku et al. 2021). This effector mechanism is not only limited

### 3. Discussion

---

to vertebrates, since innate immune cells from invertebrates such as earthworms and insects, can also release NET-like structures (Homa et al. 2016; Carrau et al. 2021). Similarly, gastropod-derived haemocytes have also been demonstrated to cast extracellular-like structures against the lungworm *Angiostrongylus vasorum* (Lange et al., 2017). These gastropod-derived ETs, abbreviated nowadays as invertebrate extracellular phagocyte traps (InEPTs) resulted in different phenotypes (*spr*InEPTs and *agg*InEPTs) against larvae of *A. vasorum* as reported for canine NETosis (chapter 2.2), evidencing an extended and conserved innate immune mechanism between invertebrate and vertebrate species (Lange et al. 2017; Penagos-Tabares et al. 2018; Villagra-Blanco et al. 2019). It is expected that the list of species which are able to cast ETs will increase in the following years.

Regarding the capacity of euglenozoan parasite *T. b. brucei* as NET inducer, current data shows that both stages, procyclic trypomastigotes and metacyclic (bloodstream) trypomastigotes induce NETs in a stage-independent manner and producing as a result different NETs phenotype (chapter 2.1 and 2.5). Interestingly, the magnitude of the response was similar despite of the stages and strains used in these experiments. During its life cycle, *T. b. brucei* deeply changes its phenotype over time and the parasite stage might influence the response of the host immune system. Regarding NET formation dynamics, we found that procyclic- and bloodstream metacyclic trypomastigotes are capable to evoke NET release in bovine PMN at different time points of confrontation. In detail, our studies revealed that 28.3% of exposed bovine PMN released NETs upon procyclic trypomastigote stimulation after 2 h (chapter 2.1). Similar observations were obtained using bloodstream metacyclic trypomastigotes, since when *T. b. brucei*-confronted PMN were analyzed at 4 h and 18 h, the magnitude of the response was similar, i. e. 11.22% and 12.35% of NET formation, for procyclic- and for bloodstream trypomastigote stages, respectively, indicating that NETs induced by *T. b. brucei* occurred before 4 h (chapter 2.5). These results must be interpreted in the context of the *in vivo* infection route of *T. b. brucei*. Here, firstly *T. b. brucei* procyclic trypomastigotes must migrate from the *Glossina* salivary glands into the insect proboscis and from there, after skin penetration and deposition, into skin-draining lymph nodes and finally into bloodstream vessels. This migration implies morphological and metabolic changes from procyclic- into metacyclic trypomastigotes stages (Van Den Abbeele et al. 2010; Alfituri et al. 2020).

One of the most characteristic features of euglenozoan *T. b. brucei* trypomastigotes is its ability to effectively evade adaptive host immune response via continuous changes of VSG (Pinger et al. 2017). This VSG switching starts very early during host infection permitting an effective

### 3. Discussion

---

evasion of protective adaptive host immune response. Scientific evidence shows that full VSG coat replacement requires only ~4.5 days in *T. b. brucei*; nonetheless, switched cells are able to reach 7.6% and 1.3% initial VSG levels after 17.1 and 28.8 h, respectively (Pinger et al. 2017). Taking this into account, it seems possible to speculate that humoral response is a less effective defense mechanism to control *T. b. brucei* infections not only due to constant antigen variation, but also due to late appearance of neutralizing antibodies (Tizard 2013). This might suggest that early host innate immune responses conducted by PMN could represent fast and reliable reactions for parasitaemia reduction. In this sense, differential immune performance has been reported between trypanotolerant and trypanosusceptible breeds, where specifically rustic trypanotolerant N'Dama and the short horn Baoulé and Lagune breeds shows a higher tolerance not only against *T. b. brucei* infections when compared with Zebu, but also to helminthes and ectoparasites (Mattioli et al. 2000), indicating a relevant genetic component in terms of innate immune response. Trypanotolerance corresponds to the heritable ability of the host to suffer less or no harm despite the infection. So far, this phenomenon is unclear; nonetheless, studies have demonstrated pivotal of higher PRR expression, such as Toll/interleukin-1 receptor and CXCR4 in these trypanotolerant cattle breeds and all data pointing on stronger innate immune reactions when compared to susceptible breeds (Berthier et al. 2016).

One of the main cell types involved in early host innate immune responses are circulating PMN. The overall microbicidal role of PMN relays on the control and removal of foreign pathogens, through different effector mechanisms including generation of ROS (Segal and Levi 1973, Segal 2005, Nguyen et al. 2017). This process relies on the protein complex NADPHOX or NOX. Accumulated evidence of PMN physiology have consistently shown the crucial participation of NOX as early signal for the NETotic process (Rinaldi et al. 2007; Nguyen et al. 2017). Consequently, NOX-driven NET formation is one of the main effector mechanisms against a wide range of intracellular apicomplexan parasites, including *E. bovis*, *E. arloingi*, *E. ninokohlyakimovae*, *B. besnoiti*, *N. caninum* and *C. parvum* (Behrendt et al. 2008; Muñoz Caro et al. 2014; Silva et al. 2014; Muñoz-Caro et al. 2014; Villagra-Blanco et al. 2017; Zhou et al. 2019; Pérez et al. 2021; Hasheminasab et al. 2022). Thus, present work on *T. b. brucei*-induced NETosis adds valuable information for comparative purposes to apicomplexan-triggered NETosis as a euglenozoan extracellular dwelling parasite. We showed that *T. b. brucei* procyclic trypomastigotes triggered a fast and sustained oxidative response in exposed bovine PMN (chapter 2.1). ROS production is directly linked with an increase in mitochondrial oxygen consumption rates (OCR) and extracellular acidification rates (ECAR) (Fink et al. 2012). Because of dramatic increase of OCR in this process it is also described as “respiratory burst”

### 3. Discussion

---

(Segal 2005; Nathan 2006). OCR and ECAR permit to analyze the bioenergetics signature of activated PMN, allowing to unveil the energetic source by sequential inhibition of different cellular metabolic pathways as well as metabolites and enzymes (Fink et al. 2012; Shah-Simpson et al. 2016). Notably, in PMN it seems possible to use this metabolic technology to evaluate the activation of NOX due to the increased OCR (Pelletier et al. 2014). Live *T. b. brucei* procyclic trypomastigotes and bloodstream metacyclic trypomastigotes are able to induce a fast and sustained increase in mitochondrial OCR and ECAR in bovine PMN (chapter 2.1 and 2.5), suggesting that ROS production and induction of PMN-derived metabolic activities are elicited as anti-parasitic responses. This finding does not correlate with the observation on *C. parvum*-induced NETs, where the addition of live parasites did not result in changes of OCR and ECAR values (Hasheminasab et al. 2022). Interestingly, when PMN were pretreated with rotenone/antimycin A and stimulated later on with live *T. b. brucei* procyclic trypomastigotes, *T. b. brucei* triggered-NET formation was partially inhibited (chapter 2.1). Regarding mitochondrial activity, when phenylhydrazine (FCCP, disruptor of mitochondrial membrane potential) was evaluated, a reduction in NET formation was also observed (chapter 2.1). The participation of ROS during NETs formation permits to classify this process as suicidal or vital NETosis (Yipp and Kubes 2013). Suicidal NETosis is a ROS-related mechanism, concluding with NET release by plasma membrane rupture and cell lysis, not allowing PMN to continue with their normal functions (Takei et al. 1996; Yipp and Kubes 2013). In contrast, vital NETosis has been recognized as a mechanism where NETs release and normal function of PMN can coexist, being initiated without NOX activation and being faster than suicidal NETosis (120 - 180 min) (Pilszczek et al. 2010; Yipp et al. 2012; Villagra-Blanco et al. 2019). Apicomplexan parasites such as *T. gondii*, *N. caninum*, *B. besnoiti* and *C. parvum* have been proved as suicidal NETs triggers (Villagra-Blanco et al. 2019; Zhou et al. 2020b; Hasheminasab et al. 2022). These results are inconsistent with the ones from Zhou et al., where bovine PMN cast rapid vital NETosis after stimulation for 30 min with *B. besnoiti*-bradyzoites (Zhou et al. 2020b), showing that these processes are not mutually exclusive. Current data show that bovine PMN cast suicidal NETs against *T. b. brucei* procyclic trypomastigotes (chapter 2.1). This observation is based on SEM analyses that show an evident compromise of PMN membrane structure. This is accompanied by increased ROS production. Indeed, pharmacological blockage of NOX with diphenyleneiodonium (DPI) was not able to inhibit this enzyme indicating that NOX activation is a landmark event of *T. b. brucei*-driven PMN activation (chapter 2.1).

### 3. Discussion

---

There are several techniques and methods to analyze NET formation based on scanning electron microscopy (SEM)- and fluorescence microscopy image-based analyses, flow cytometry (FACS), ELISA and extracellular DNA quantification (Brinkmann et al. 2012; Gonzalez et al. 2014; Mohanty et al. 2017; Rebernick et al. 2018). From a critical point of view, several techniques must be used in parallel in order to study NET formation properly. In this study, NET structures were visualized with several microscopy techniques such as SEM, laser scanning confocal microscopy- (LSCM), and live cell 3D-holotomographic microscopy-analyses. NETs were assessed as fine networks of grosser and thinner strands of DNA origin, able to attach to *T. b. brucei* stages unveiled in SEM- and LSCM analyses (chapters 2.1 and 2.5). These findings are in line with previous euglenozoan-triggered NETs release (Hermosilla et al. 2014; Villagra-Blanco et al. 2017a, 2019; Pereira et al. 2019). Immunofluorescence analyses of classical NETs-components were also performed, observing co-localization of pan histones (i. e. H1, H2A/H2B, H3, H4), NE and MPO in *T. b. brucei*-triggered NETs (chapter 2.1 and chapter 2.5). In addition, recent studies have analyzed the host cell parasite interaction by live-cell 3D holotomographic microscopy (Larrazabal et al. 2021c, a, b; Conejeros et al. 2022; Lopez-Osorio et al. 2022), allowing a technical approach by generation of 3D renders and digital staining based on the refractive index (RI) of cellular components. This technique showed to be useful to visualize classical components of bovine PMN such as cytoplasmic granules, multi-lobulated nuclei and pseudopod formation (Larrazabal et al. 2021c, a, b; Conejeros et al. 2022; Zhou et al., 2020b).

During early NET formation, ROS production and mediators evokes morphological changes in PMN, as the expansion of nuclear area (NAE) driven by chromatin decondensation (Papayannopoulos et al. 2010). Co-culture of bovine PMN with procyclic trypomastigotes caused an increase in the nuclear area of stimulated cells after 2 h of co-culture, unveiling a strong NETotic process (chapter 2.1). Additionally, detection of nuclear degeneration of bovine PMN was achieved, indicating a late NETotic process after 3 h of parasite-exposure (Papayannopoulos et al. 2010). Analysis of fluorescence microscopy-derived images permits semi-automatic quantification of NET formation, requiring one or two fluorescent markers (Brinkmann et al. 2012; Gonzalez et al. 2014; Mohanty et al. 2017; Rebernick et al. 2018). Nonetheless, all protocols have been established for human/mice models, limiting the use of PMN originating from other species. In the case of 'DNA area and NETosis analysis' (i. e. DANA), this method showed capability to perform a suitable quantification of the total amount of PMN and NAE in bovine- and canine-derived PMN (chapter 2.1 and 2.2) (Rebernick et al. 2018). By using the default threshold of 90  $\mu\text{m}^2$  for NAE, detection of a significant increase in

### 3. Discussion

---

the percentage of *T. b. brucei* procyclic trypomastigote-triggered NET formation was detected. As described in chapter 2.5, when bovine PMN were stimulated with *T. b. brucei* bloodstream metacyclic trypomastigotes, the presence of PMN-derived NETs aggregation (i. e. *aggNETs*) against these parasitic stages was also observed. On this regard, the aggregation limited the usefulness of the software package, being necessary to explore other methodological approaches to investigate in more detail *T. b. brucei*-triggered *aggNETs*.

NETs phenotype categorization was also possible to achieve. As already stated, NETs can be classified in three categories: *i) sprNETs ii) diffNETs and iii) aggNETs* (Schauer et al. 2014; Muñoz-Caro et al. 2015c, 2018; Lange et al. 2017; Zhou et al., 2020b). These phenotypes have been reported to occur in PMN of different mammalian species such as humans, mice, bovines, canines, dolphins and notably also in terrestrial gastropods (i. e. snails and slugs) (Schauer et al. 2014; Lange et al. 2017; Muñoz-Caro et al. 2018; Villagra-Blanco et al., 2019; Hahn et al. 2019; Hasheminasab et al. 2022).

In the case of *T. b. brucei*, procyclic- and metacyclic trypomastigotes triggered *aggNETs* formation at 2, 4 and 18 h and at different PMN : parasite ratios (chapter 2.1 and 2.5). The specific role of *aggNETs* in parasite infection is not fully understood; nevertheless, they have become an interesting research topic due to the role they play in controlling inflammatory diseases like human gout (Schauer et al. 2014; Sil et al. 2017; Hahn et al. 2019). Human gout is an aseptic inflammatory disease that affects the joints, caused by strong immune responses against MSU crystals deposition within the synovial space. Due to the chemical identity and the microscopically pointed shape they exhibit, MSU crystals cause mechanical damage by shearing and tearing surrounding tissues causing macroscopic lesions, thereby alerting and activating surrounding PMN (Schauer et al. 2014; Sil et al. 2017; Li et al. 2018). Recent studies have found that PMN ingest MSU crystals and that these crystals accumulate inside the cell as high-density structures (Hahn et al., 2019). Interestingly, MSU crystals are well-known to induce strong *aggNETs* (Schauer et al., 2014), with a concomitant release of cytokines and chemokines such as TNF- $\alpha$ , IL-6, IL-8. Regarding other chemicals capable to trigger strong *aggNETs*, ionomycin, a calcium ionophore, has also been described (Hahn et al. 2019). Mechanisms involved in MSU crystal-triggered *aggNETs* remains unclear and the same holds true for *H. contortus*- and *D. immitis*-induced *aggNETs*. A possible mechanism is the formation of pores within PMN membrane, as a consequence of MSU crystals shapes, causing ion fluxes and subsequent enhanced NET formation (Dalbeth et al. 2016). It has also been suggested that physical contact between PMN and MSU crystals is mandatory for NETs and *aggNET*

### 3. Discussion

---

formation. (Hahn et al. 2019). Bovine PMN are able to trigger as well *aggNETs* when stimulated with MSU crystals and ionomycin, proving that both stimuli have the same outcome in a different species (chapter 2.5). Direct contact between bovine PMN and MSU crystals resulted in *aggNETs* formation, after 4 h and 18 h of co-culture, suggesting similar mechanisms as reported for human PMN (chapter 2.5). In this sense, *aggNETs* could have a fundamental anti-inflammatory role in Nagana but further studies are needed to clarify this point.

Considering the inflammatory microenvironment, PMN are exposed to multiple and heterogeneous molecules that modulate their directed antimicrobial responses. The capacity of PMN to react in the presence of extracellular nucleotides and nucleosides, such as ATP and ADO, is largely associated to the activation of P2 and P1 purinergic receptors, respectively (Rubenich et al. 2021). In bovines, the role of purinergic signaling in PMN activation has been clearly demonstrated (Alarcón et al. 2020). In this sense, the current study found that both NF449, a purinergic inhibitor of P2X1 receptor, and MRS2578, an inhibitor of P2Y6 receptor, played a fundamental role in activation of bovine PMN and *aggNETs* induced by procyclic trypomastigotes and bloodstream metacyclic trypomastigotes (chapter 2.1 and 2.5). Previous reports have demonstrated decreased NET formation, after treatment with 100  $\mu\text{M}$  of NF449 with other parasites, including apicomplexan *N. caninum*, *C. parvum* and *B. besnoiti*, without specific effects on parasite-induced NETs phenotypes (Villagra-Blanco et al. 2017b; Zhou et al. 2020a; Hasheminasab et al. 2022). Equal concentration of NF449 was able to decrease formation of NETs and *aggNETs* in bovine PMN confronted to vital *T. b. brucei* (chapter 2.1 and 2.5). This data must be interpreted with caution, considering that the high concentration of NF449 does not permit to exclude an influence of other G-protein-coupled receptors, in comparison to others reports in bovine PMN (Alarcón et al. 2020). Therefore, it is not possible to exclude other off target pharmacological effects in experiments developed with procyclic trypomastigotes (chapter 2.1). This last aspect was studied further using NF449 at 100  $\mu\text{M}$  and 10  $\mu\text{M}$ , showing that even at lower concentrations the inhibitory effect was achieved indicating a specific -at least for the pharmacological data- and crucial role P2X1 in *T. b. brucei*-mediated NETosis (chapter 2.5). Regarding the role of P2Y6 receptor, MRS2578 inhibited *aggNETs* formation (chapter 2.5). The mechanisms by which MRS2578 blocks purinergic receptor P2Y6 has not been elicited yet but suspecting to be related with regulation of IL-8-mediated signaling in case of human PMN (Jacob et al. 2013; Sil et al. 2017).

Beyond extended knowledge regarding NET release against unicellular pathogens, major knowledge gaps are still present in favor of this transversal innate immune response against

### 3. Discussion

---

more complex metazoan parasites. Large-sized metazoan parasites such as *S. japonicum*, *S. stercoralis*, *H. contortus*, *A. vasorum*, *D. immitis*, *Troglostrongylus brevior*, *Brugia malayi* have been described as potent NETs inducers, showing that this defense mechanism could be extended to *A. vasorum* L<sub>3</sub> and even to zoonotic-relevant mite *S. scabiei* (chapter 2.2 and 2.6 respectively) (Bonne-Année et al. 2014; Muñoz-Caro et al. 2015c; McCoy et al. 2017; Lange et al. 2017; Muñoz-Caro et al. 2018; Peixoto et al., 2021; Wang et al. 2022). Conversely, only weak NETosis, OCR and ROS production were reported for *Fasciola hepatica*-stimulated bovine PMN (Peixoto et al., 2021). Former authors showed that neither metacercariae, newly excysted juveniles (NEJ) nor soluble antigens of *F. hepatica* induced strong PMN reactions (Peixoto et al., 2021).

Following infection of the canid definitive host, *A. vasorum* is constantly exposed to components of the innate immune system, including cell barriers and cells of the innate immune system. Previous studies showed that metazoan parasites triggered NET, InEPT and EET formation (Muñoz-Caro et al. 2015c, 2018; Lange et al. 2017; Penagos-Tabares et al. 2018). When canine PMN were confronted with vital *A. vasorum* L<sub>3</sub>, NET formation of exposed canine PMN was achieved after 3 h (chapter 2.2). This was further confirmed by labeling NETs-canonical components, analyzed with SEM- and IF-imaging, confirming *A. vasorum*-induced NETs (Lange et al. 2017; Muñoz-Caro et al. 2018; Penagos-Tabares et al. 2018). In this case, DANA default threshold of 90  $\mu\text{m}^2$  for NAE was also tested in canine PMN, showing an expansion of NAE values (chapter 2.2). Regarding *A. vasorum*-triggered phenotypes, *spr*NETs were the most abundant ones (chapter 2.2). This is in concordance with previous reports of canine PMN co-cultured with *D. immitis* microfilariae and vital L<sub>3</sub> (Muñoz-Caro et al. 2018) thereby showing parasite species- and stage-independent NETs release.

Endothelial cells of blood and lymph vessels play a relevant role in host defense against foreign microorganisms, creating a mechanical barrier that separates vascular space from other tissues. They have been established as highly immune-reactive, producing adhesion molecules, cytokines/chemokines and initiating pro-inflammatory responses (DiStasi and Ley 2009). More importantly, a clear link between inflammation, innate immunity, endothelium and NETs has been established for the pathogenesis of numerous diseases, including autoimmune and metabolic disorders. Patients with type 1 and 2 diabetes tend to release NETs, affecting directly endothelial cells (Wong et al. 2015). Under diabetic conditions, PMN are able to produce an increased amount of cytokines and superoxide components which then activate endothelium thereby facilitating vascular microenvironments which supports more NETs release. Western

### 3. Discussion

---

blotting revealed an upregulation of PAD4 in PMN from individuals with diabetes when compared to healthy controls, supporting chromatin decondensation (Wong et al. 2015). NETs have also been detected in atherosclerotic lesions and arterial thrombi (Döring et al. 2017). In pathogenesis of atherosclerosis lipid-driven inflammatory disease of endothelial arteries has been demonstrated, where once again endothelial cell activation facilitates the retention of proteins that will cause endothelial damage and triggering recruitment of leukocytes, specifically PMN, leading to vessel occlusion and consequent ischemia and/or thrombosis (Döring et al. 2017). Vascular-derived activation of PMN might also be participating in certain parasitoses where endothelium is parasitized (i. e. sarcocystiosis and besnoitiosis). *B. besnoiti* infects *in vivo* host endothelial cells during acute phase of bovine besnoitiosis, replicating fast intracellularly within lymph/blood endothelium up-regulating expression of adhesion molecules on the surface of these cells. Consistently, primary bovine umbilical vein endothelial cells (BUVEC) are directly affected by *B. besnoiti*-tachyzoites during intracellular replication, causing endothelial cell activation and damage and up-regulation of adhesion molecules, such P-selectin, E-selectin, VCAM-1 and ICAM-1 after 12 and 24 h p. i.. These molecules are responsible of triggering the recruitment cascade of PMN within vessels (Kolaczowska and Kubes 2013). In order to assess NETs release by activated endothelium, BUVEC monolayers were infected *B. besnoiti* tachyzoites. *B. besnoiti*-BUVEC monolayers were tested in static and dynamic conditions for spontaneous release of NETs as reported elsewhere (Maksimov et al. 2017). Similarly, VCAM-1, P-selectin, ICAM-1 and E-selectin were shown to be increased in *B. besnoiti*-infected BUVEC at 12 h p. i., followed by PMN adhesion and NET release under physiological flow conditions (chapter 2.3). These findings confirmed prior reports of *B. besnoiti* up-regulating P-selectin and ICAM-1 *in vitro*, where a significant increase of PMN adhesion on to *B. besnoiti*-infected BUVEC monolayers were observed (Maksimov et al. 2017). In general, expression of adhesion molecules is related with the migration process of leukocytes to the site of inflammation, where they will support development of an effective immune response (Maksimov et al. 2016). Moreover, similar up-regulation patterns occurred during other coccidian *in vitro* infections, where specifically *T. gondii*, *N. caninum* and *E. bovis* exhibited an effective chemoattractant endothelial activation, thereby enhancing the migration of PMN into the infection site, indicating that endothelial cells were involved in early innate defense against coccidian infections (Taubert et al. 2006; Hermosilla et al., 2006; Maksimov et al. 2016). Interestingly, endothelial activation could represent a relevant feature in other parasitic infections. In the case of canine angiostrongylosis a close interaction between the aortic, heart and pulmonary endothelial cells and adult nematodes is implicit due to their

### 3. Discussion

---

location within the canine host (Schnyder et al. 2017). Given that, *A. vasorum* soluble antigen *AvAg* released by the parasite are in close contact with endothelial cells of the host, pro-inflammation of vessels are commonly reported in naturally *A. vasorum*-infected animals (Rinaldi et al. 2014). Overall, after stimulation with *A. vasorum* L<sub>3</sub> and *AvAg*, activation of canine aortic endothelial cells (CAEC) was achieved (chapter 2.2), specifically showing classical adhesion molecule expression, such P-selectin, E-selectin, VCAM-1 and ICAM-1. However, inter donor variations were observed in these *in vitro* CAEC assays, and which might indicate an individual susceptibility to the clinical disease (chapter 2.2). This last, takes special relevance since high variability in clinical manifestations and intensity between infected animals is the rule in clinical set up (Chapman et al. 2004).

In addition to Maksimov et al. (2017), for the first time *B. besnoiti* tachyzoite-triggered NETs were investigated on their capacities to induce endothelial cell damage and subsequently influence intracellular proliferation of tachyzoites in BUVEC monolayers (chapter 2.3). In more detail, we evaluated host endothelial cell damage triggered by H2A and *B. besnoiti* tachyzoite-triggered NET preparations and estimated effects of non-attached PMN over *B. besnoiti*-infected BUVEC-monolayers under physiological flow conditions (chapter 2.3). Overall, all treatments (H2A, *B. besnoiti*-triggered NETs and floating PMN) induced damage of endothelium. Nonetheless, host endothelial cell damage fail to significantly influence the intracellular parasite replication in terms of PV diameter and abundance of intracellular parasites. Therefore, these findings deny any direct adverse effects of NETs on intracellular *B. besnoiti* replication (chapter 2.3), suggesting the independency of NETs as immune strategy against intracellular stages of *B. besnoiti*.

Within the same mammalian species, namely domestic dogs, for the first time in literature colostrum-derived PMN were exposed to *N. caninum* tachyzoites and thereafter assessed on NETs release and phagocytic activities (chapter 2.4). Herein, we reported that canine colostrum PMN cast NETs against vital and dead tachyzoites of *N. caninum*. These findings show the relevance of colostrum uptake for the health status of neonates and suggesting that intestinal absorbed colostrum PMN will display anti-parasitic functions within neonates body (chapter 2.4). Isolation of canine colostrum-derived PMN differs strongly when compared to PMN isolation from peripheral blood. Main limitations of proper isolation are for instance the colostrum volume and the very high fat content of this milk (Segawa et al. 2011). This last trait could explain different reactions of canine colostrum PMN when compared to previous results of peripheral blood-derived PMN (chapter 2.2). Phenotypes of NETs were also assessed in

### 3. Discussion

---

canine colostrum-derived PMN, but in contrast to previous studies, no clear tendencies towards a specific type were detected. In detail, *N. caninum*-triggered colostrum *agg*NETs and *diff*NETs demonstrated almost equal occurrences, and *spr*NETs being almost not present (chapter 2.4). This differs with previous reports, in which *spr*NETs were classified as the most abundant phenotype of canine PMN stimulated with large and motile *A. vasorum* L<sub>3</sub> (chapter 2.2) as well as *D. immitis* microfilaria/larvae (Muñoz-Caro et al. 2018). Some colostrum PMN did not lose their integrity after *N. caninum*-tachyzoite stimulation thereby indicating vital NETosis as already reported to closely-related *B. besnoiti* (Zhou et al. 2020). In summary, first investigations on canine colostrum PMN support the relevance of these cells in neonates, adding new insights in newborn immunological mechanisms of defense (chapter 2.4). Lastly, phagocytosis was also evaluated, observing that colostrum PMN are able to perform their phagocytic function in neonates (chapter 2.4), confirming the conserved efficiency of all these ancient effector mechanisms.

Beyond the canonical response that endoparasites triggers in innate immune cells, the interaction between ectoparasites and PMN have largely been neglected. This last, takes special relevance in mites infestation in mammals since the close interaction with the parasite and the epidermal tissue is characterized by the trigger of massive migration of immune cells into the different components of the dermis (Hoffmann and Enk 2016). Overall, sarcoptic mange is a relevant zoonotic dermal disease caused by obligate parasitic *S. scabiei* mites (Roncalli 1987). In general, *S. scabiei*-infestations are delimited to superficial layers of the host skin. After infestation, migration of mites to the *stratum corneum* will occur in order to fulfill their nutrient requirements (Arlian and Morgan 2017). Epithelial cells act not only as mechanical barrier against infections/infestations but also as innate immune cells (Hoffmann and Enk 2016). *In vitro* studies have proved that *S. scabiei* antigens (*ScAg*) in human keratinocytes are able to interfere with production of IL-8 and G-CSF, both important pro-inflammatory modulators (Morgan and Arlian 2010). Here, for the first time stimulation of isolated bovine PMN with either *S. scabiei* stages (adults, nymphs, larvae and eggs) and soluble *ScAg* were performed. After co-culture, slight attachment of PMN to the exoskeleton of *S. scabiei* was observed; nonetheless, stimulation with 10  $\mu$ M *ScAg* resulted in weak NETs production (chapter 2.6). Similar findings were recently described after stimulation of bovine PMN with *F. hepatica* juvenile stages (NEJ), metacercariae and eggs (Peixoto et al. 2021). Assessment of *S. scabiei*-induced NETs phenotypes was performed and *spr*NETs were the most abundant ones to be extruded against different mite stages. Effector mechanisms activated by *ScAg* were also tested thereby confirming that *ScAg* is not capable of affect the phagocytic capacity of bovine PMN.

### 3. Discussion

---

Nonetheless, stimulation with 10  $\mu\text{M}$  *ScAg* evokes a fast and sustained  $\text{Ca}^{++}$  flux in bovine PMN most likely indicating participation of store-operated calcium entry (SOCE) as previously shown for various apicomplexan protozoa-induced NETosis, including the species *E. bovis* (Muñoz-Caro et al., 2015) and *C. parvum* (Muñoz-Caro et al., 2016) (chapter 2.6).

The contents presented in this doctoral thesis provides a better understanding of PMN activation during NETotic process, novel insights into NETs phenotypes and purinergic signaling pathways involved in *T. b. brucei*-induced NETosis. Additionally, new knowledge regarding parasite-host interactions and consequences related with endothelium activation were here achieved, leading to better understanding of parasite adverse effects in the hosts. Despite the promising results here shown, questions regarding the specific mechanisms underlying parasite recognition, parasite antigens inducing NET formation and the modulatory capacity of all these parasites to either stimulate, modulate or even to hamper PMN activities as seen for *S. scabiei*, are still unclear and demanding more investigations. Likewise, the interaction of endothelial system as component of the innate immune system and released NETs with pro-inflammatory molecules, must be assessed in further studies. Particularly, the role of ‘anchored NETs’ and/or ‘cell-free NETs’ on endothelium activation should be continued in the near future. As such, activation of endothelial pro-MMP2 and impairment in vasorelaxation by NETs through externalization of PMN-derived MMP9 have been reported (Fernandez-Patron et al. 2001; Alves-Filho et al. 2021).

Overall, the realization of this doctoral thesis allowed to generate new knowledge regarding immune responses against two *T. b. brucei* stages in the bovine system and *A. vasorum* stages in canine immune system, being extremely relevant to the immense economic consequences that AAT has in African cattle industry and canine angiostrongylosis for domestic and wild canids. The data here presented will also be a starting point for further studies on host pathogen recognition, PMN-leukocyte (e. g. monocytes, eosinophils) interactions and the role of NETosis and endothelium in the onset of protective host innate immune responses against intracellular, extracellular as well as metazoan parasites.

#### 4. ZUSAMMENFASSUNG

Polymorphkernige Neutrophile (PMN) sind die am häufigsten vorkommenden Leukozyten in Lymphe sowie im Blut. Sie werden schnell aus dem Blutkreislauf an Infektionsstellen rekrutiert, um dort Krankheitserreger zu bekämpfen. So reagieren PMN auf protozoäre und metazoische Parasiten durch folgende Effektormechanismen: Freisetzung von immunmodulatorischen Molekülen (d. h. Zytokinen und Chemokinen), Phagozytose, Produktion von reaktiven Sauerstoffspezies (ROS) und der Freisetzung von neutrophilen extrazellulären Traps (NETs). NETs wurden als feine extrazelluläre Strukturen beschrieben, die aus dekondensiertem Chromatin bestehen und mit antimikrobiellen Komponenten wie Myeloperoxidase (MPO), Neutrophiler Elastase (NE), Lactoferrin, Calprotein, LL37, Pentraxin, Proteinase 3 oder Cathepsin G versehen sind. Es wurden bereits mehrere Parasitenarten als Induktoren von NETs beschrieben, darunter unter anderem *Besnoitia besnoiti*, *Neospora caninum* und *Dirofilaria immitis*. Die vorliegende Dissertation thematisiert weitere relevante Parasiten, wie z.B. die Blutstromparasiten *Trypanosoma brucei brucei* und *Angiostrongylus vasorum*. Dabei sind folgende Ergebnisse besonders hervorzuheben:

Die Kokultur von Rinder-PMN mit *T. b. brucei*-Stadien, d.h. prozyklische Trypomastigoten und metazyklische Blutkreislauf-Trypomastigoten, führten zu einer starken NET-Freisetzung und PMN-Aktivierung. Dieser Prozess war unabhängig von Zeitpunkt und Parasitenstadium. Bei Konfrontation von vitalen *T. b. brucei*-Stadien mit Rinder-PMN wurde eine schnelle und anhaltende Erhöhung der Sauerstoffverbrauchsrate (OCR) und der extrazellulären Ansäuerungsrate (ECAR) erreicht, was auf eine Produktion von ROS als Reaktion auf den Parasiten hindeutet. Des Weiteren wurden NET-Strukturen durch SEM-Bilder, konfokale Laserscanmikroskopie und holotomographische 3D-Mikroskopie-Analysen lebender Zellen visualisiert. Diese zeigen die Ko-Lokalisierung von DNA mit antimikrobiellen Molekülen, die im PMN-Kern und -Granula vorhanden sind. Dabei konnten Histone (H1, H2A/H2B, H3, H4) und Neutrophile Elastase als klassische Komponenten der extrazellulären Abwehrstrukturen dargestellt werden. Darüber hinaus wurden morphologische Veränderungen in der Ausdehnung des Kernbereichs von Rinder-PMN als Folge der Chromatin-Dekondensation beobachtet. Hier wurde eine Analyse von Fluoreszenzmikroskopie-Bildern durchgeführt, wobei eine halbautomatische Quantifizierung der NETs-Bildung angewendet wurde, die als „DNA-Bereichs- und NETosis-Analyse“ (DANA) bezeichnet wird.

Darüber hinaus wurde eine Bewertung verschiedener Phänotypen von NETs durchgeführt, die zeigte, dass die Bildung von *aggNETs* der am häufigsten vorkommende Phänotyp war, wenn

## 4. Zusammenfassung

---

Rinder-PMN mit *T. b. brucei* prozyklische Trypomastigoten und metazyklische Trypomastigoten konfrontiert wurden. Dieses Ergebnis war unabhängig vom Zeitpunkt und von dem PMN/Parasiten-Verhältnis.

Um die Beteiligung purinerner Rezeptoren an der Aktivierung von Rinder-PMN und an der Bildung von *aggNETs* zu untersuchen, wurden die purinergen Inhibitoren NF449 (Antagonist des P2X1-Rezeptors) und MRS2578 (Antagonist des P2Y6-Rezeptors) getestet. In diesem Zusammenhang enthüllte NF449 bei 100  $\mu\text{M}$  und 10  $\mu\text{M}$  eine inhibitorische Wirkung, was die spezifische Rolle von P2X1 in *T. b. brucei*-vermittelter NETose widerspiegelt. Die Wirkung von MRS2578 wurde bei 10  $\mu\text{M}$  bestätigt, was eine Rolle von P2Y6 in diesem Prozess beweist. Diese Ergebnisse wurden erzielt, indem die Hemmung der Bildung von *aggNETs* mit Bildanalysen und OCR-Messungen in Rinder-PMN untersucht wurde.

Hunde-PMN wurden mit vitalen *A. vasorum*-L<sub>3</sub> stimuliert und die Veränderungen in der NAE der Zellen und der NET-Bildung analysiert. Dabei war *sprNETs* der am häufigsten vorkommende Phänotyp. Nach der Stimulation von Endothelzellen der Aorta des Hundes (CAEC) durch lösliches Antigen von *A. vasorum* (*AvAg*) wurde deren Aktivierung durch Messungen klassischer Adhäsionsmoleküle, einschließlich P-Selectin, E-Selectin, VCAM-1 und ICAM-1, bestätigt.

Zusätzlich konnte eine Endothelzellschädigung beim Wirt nachgewiesen werden, die durch NETs und H2A durch Aktivierung von *B. besnoiti*-Tachyzoiten, ausgelöst wurde. Dies bestätigt die von NETs stammenden schädlichen Wirkungen auf mit *B. besnoiti* infizierte BUVEC-Monolayer unter physiologischen Bedingungen.

Es wurden hier Experimente mit Kolostrum-PMN von Hündinnen durchgeführt, wobei beobachtet wurde, dass Hunde-Kolostral-PMN in der Lage sind, NETs gegen vitale sowie tote *N. caninum*-Tachyzoiten zu bilden. Des Weiteren konnte die phagozytische Funktion von Kolostral-PMN bei Neugeborenen gezeigt werden.

Schließlich wurden Experimente mit Rinder-PMN gegen *S. scabiei*-Stadien (Adulte, Nymphen, Larven und Eier) sowie lösliches *S. scabiei*-Antigen (*ScAg*) durchgeführt. Dabei konnte eine leichte Anheftung von PMN an das Exoskelett von *S. scabiei*-Stadien beobachtet werden. Es wurde jedoch nach Stimulation von Rinder-PMN mit 10  $\mu\text{M}$  *ScAg* nur eine schwache NET-Produktion erreicht. Phagozytose, ROS-Produktion und Ca<sup>++</sup>-Flüsse konnten nach der Stimulierung mit 10  $\mu\text{M}$  *ScAg* beobachtet werden. Insgesamt belegen die präsentierten Daten, dass nicht alle Parasiten NETose in gleicher Art und Weise induzieren können, weshalb

## **4. Zusammenfassung**

---

zukünftige Arbeiten im Bereich Modulations- sowie Evasionsstrategien des angeborenen Immunsystems auf Parasiten erforderlich sind.

## 5. SUMMARY

Polymorphonuclear neutrophils (PMN) have been described as the most abundant leukocyte in lymph and bloodstream, being rapidly recruited from circulation to sites of infection to fight against foreign pathogens. PMN reacts against protozoan and metazoan parasites by different effector mechanisms, including the release of immunomodulatory molecules (i. e. cytokines and chemokines), phagocytosis, production of reactive oxygen species (ROS), and release of neutrophil extracellular traps (NETs). NETs have been described as a delicate extracellular structure formed by decondensed chromatin and adorned with antimicrobial components, such as myeloperoxidase (MPO), neutrophil elastase (NE), lactoferrin, calprotectin, LL37, pentraxin, proteinase 3 or cathepsin G. In this sense, several protozoan and metazoan parasite species have been described as inducers of NETs, including *Besnoitia besnoiti*, *Neospora caninum* and *Dirofilaria immitis*, among others. A close interaction between members of these groups were here studied, specifically in the case of the bloodstream parasites *Trypanosoma brucei brucei* and *Angiostrongylus vasorum*. In this sense, the main findings in the current work are:

Co-culture of bovine PMN with *T. b. brucei* stages, i. e. procyclic trypomastigotes and bloodstream metacyclic trypomastigotes, resulted in strong NETs release and PMN activation, independent of the time-point and parasitic stage. A fast and sustained increase in time of oxygen consumption rates (OCR) and extracellular acidification rates (ECAR) was achieved, when live *T. b. brucei* stages were confronted with bovine PMN, suggesting that ROS production might be caused as a response against the parasite. NET structures were visualized by SEM pictures, laser scanning confocal microscopy and live cell 3D-holotomographic microscopy analyzes, unveiling the co-localization of DNA with antimicrobial molecules present in PMN nucleus and granules, such as histones (H1, H2A/H2B, H3, H4) and neutrophil elastase, confirming the classical components of these extracellular defense structures. Moreover, morphological changes in expansion of nuclear area from bovine PMN were observed, as a consequence of chromatin decondensation. Analysis of fluorescence microscopy-derived images was here performed, applying a semi-automatic quantification of NETs formation called 'DNA area and NETosis analysis' (DANA).

Assessment of different phenotypes of NETs was performed, proving that the formation of *aggNETs* was the most abundant phenotype present, when bovine PMN were stimulated with *T. b. brucei* procyclic trypomastigotes and metacyclic trypomastigotes, independent of the time-point and PMN : parasite ratio.

## 5. Summary

---

Regarding the participation of purinergic receptors in activation of bovine PMN and *aggNETs* formation, the purinergic inhibitors NF449 (antagonist of P2X1 receptor) and MRS2578 (antagonist of P2Y6 receptor) were tested. In this context, NF449 at 100  $\mu$ M and 10  $\mu$ M unveiled the inhibitory effect, proving a specific role for the P2X1 in *T. b. brucei*-mediated NETosis. Thus, the effect of MRS2578 at 10  $\mu$ M was confirmed, verifying a role of the P2Y6 in this process. These results were achieved by confirming the inhibition of *aggNETs* formation with images analyzes and measurements of OCR in bovine PMN.

Canine PMN were stimulated with vital *A. vasorum* L3, observing changes in the NAE of the cells and NETs formation, being *sprNETs* the most abundant phenotype. Interestingly, after stimulation with *A. vasorum* soluble antigen (*AvAg*), activation of canine aortic endothelial cells (CAEC) was confirmed, by measurements of classical adhesion molecules, including P-selectin, E-selectin, VCAM-1 and ICAM-1. In this line, host endothelial cell damage triggered by *B. besnoiti* tachyzoites isolated NETs and H2A was demonstrated, confirming NETs-derived adverse effects against BUVEC-monolayers infected with *B. besnoiti*, under physiological flow conditions.

Remarkably, experiments with colostrum PMN from bitches were here performed, observing that canine colostrum PMN are able to cast NET against vital and dead *N. caninum* tachyzoites. Even so, the ability of colostrum PMN to perform its phagocytic function in neonates was also here achieved.

Lastly, experiments of bovine PMN against *S. scabiei* stages (adults, nymphs, larvae and eggs) and soluble *S. scabiei* antigen (*ScAg*) were performed, proving a slight attachment of PMN to the exoskeleton of *S. scabiei* stages. However, after stimulation of bovine PMN with 10  $\mu$ M *ScAg*, a weak NETs production was achieved. Notably, phagocytosis, ROS production and  $Ca^{++}$  fluxes were observed, after stimulation with 10  $\mu$ M *ScAg*. Overall, presented data evidence that not all parasites can induce NETosis and therefore demanding future work on modulation or evasion strategies of this innate effector process by parasites.

## 6. REFERENCES

- Abi Abdallah DS, Lin C, Ball CJ, et al (2012) *Toxoplasma gondii* triggers release of human and mouse neutrophil extracellular traps. *Infect Immun* 80:768–777. <https://doi.org/10.1128/IAI.05730-11>
- Alarcón P, Manosalva C, Quiroga J, et al (2020) Oleic and Linoleic Acids Induce the Release of Neutrophil Extracellular Traps via Pannexin 1-Dependent ATP Release and P2X1 Receptor Activation. *Front Vet Sci* 7:260. <https://doi.org/10.3389/fvets.2020.00260>
- Alkayed F, Kashimata M, Koyama N, et al (2012) P2Y11 purinoceptor mediates the ATP-enhanced chemotactic response of rat neutrophils. *J Pharmacol Sci* 120:288–295. <https://doi.org/10.1254/jphs.12173fp>
- Almería S (2013) *Neospora caninum* and Wildlife. *ISRN Parasitol* 2013:947347. <https://doi.org/10.5402/2013/947347>
- Alsán M (2015) The Effect of the TseTse Fly on African Development. *American Economic Review* 105:382–410. <https://doi.org/10.1257/aer.20130604>
- Alvarez-García G, Frey CF, Mora LMO, Schares G (2013) A century of bovine besnoitiosis: an unknown disease re-emerging in Europe. *Trends Parasitol* 29:407–415. <https://doi.org/10.1016/j.pt.2013.06.002>
- Alves-Filho JC, Marcel Silva Melo B, Ryffel B (2021) MMP-9 Mediates Cross-Talk between Neutrophils and Endothelial Cells in Psoriasis. *J Invest Dermatol* 141:716–718. <https://doi.org/10.1016/j.jid.2020.09.006>
- Antonioli L, Pacher P, Vizi ES, Haskó G (2013) CD39 and CD73 in immunity and inflammation. *Trends Mol Med* 19:355–367. <https://doi.org/10.1016/j.molmed.2013.03.005>
- Baker VS, Imade GE, Molta NB, et al (2008) Cytokine-associated neutrophil extracellular traps and antinuclear antibodies in *Plasmodium falciparum* infected children under six years of age. *Malar J* 7:41. <https://doi.org/10.1186/1475-2875-7-41>
- Bassel LL, Caswell JL (2018) Bovine neutrophils in health and disease. *Cell and Tissue Research* 371:617–637. <https://doi.org/10.1007/s00441-018-2789-y>
- Basso W, Schares G, Gollnick NS, et al (2011) Exploring the life cycle of *Besnoitia besnoiti* - experimental infection of putative definitive and intermediate host species. *Vet Parasitol* 178:223–234. <https://doi.org/10.1016/j.vetpar.2011.01.027>

## 6. References

---

- Bauer B, Amsler-Delafosse S, Clausen PH, et al (1995) Successful application of deltamethrin pour on to cattle in a campaign against tsetse flies (*Glossina* spp.) in the pastoral zone of Samorogouan, Burkina Faso. *Trop Med Parasitol* 46:183–189
- Behrendt JH, Ruiz A, Zahner H, et al (2010) Neutrophil extracellular trap formation as innate immune reactions against the apicomplexan parasite *Eimeria bovis*. *Vet Immunol Immunopathol* 133:1–8. <https://doi.org/10.1016/j.vetimm.2009.06.012>
- Benavides J, González-Warleta M, Arteché-Villasol N, et al (2022) Ovine Neosporosis: The Current Global Situation. *Animals (Basel)* 12:. <https://doi.org/10.3390/ani12162074>
- Berthier D, Brenière SF, Bras-Gonçalves R, et al (2016) Tolerance to Trypanosomatids: A Threat, or a Key for Disease Elimination? *Trends Parasitol* 32:157–168. <https://doi.org/10.1016/j.pt.2015.11.001>
- Black MW, Boothroyd JC (2000) Lytic cycle of *Toxoplasma gondii*. *Microbiol Mol Biol Rev* 64:607–623. <https://doi.org/10.1128/MMBR.64.3.607-623.2000>
- Bolt G, Monrad J, Koch J, Jensen AL (1994) Canine angiostrongylosis: a review. *Vet Rec* 135:447–452. <https://doi.org/10.1136/vr.135.19.447>
- Bonne-Année S, Kerepesi LA, Hess JA, et al (2014) Extracellular traps are associated with human and mouse neutrophil and macrophage mediated killing of larval *Strongyloides stercoralis*. *Microbes Infect* 16:502–511. <https://doi.org/10.1016/j.micinf.2014.02.012>
- Branzk N, Papayannopoulos V (2013) Molecular mechanisms regulating NETosis in infection and disease. *Seminars in Immunopathology* 35:513–530. <https://doi.org/10.1007/s00281-013-0384-6>
- Brazil JC, Louis NA, Parkos CA (2013) The role of polymorphonuclear leukocyte trafficking in the perpetuation of inflammation during inflammatory bowel disease. *Inflamm Bowel Dis* 19:1556–1565. <https://doi.org/10.1097/MIB.0b013e318281f54e>
- Brinkmann V, Goosmann C, Kühn LI, Zychlinsky A (2012) Automatic quantification of in vitro NET formation. *Front Immunol* 3:413. <https://doi.org/10.3389/fimmu.2012.00413>
- Brinkmann V, Reichard U, Goosmann C, et al (2004) Neutrophil extracellular traps kill bacteria. *Science* 303:1532–1535. <https://doi.org/10.1126/science.1092385>
- Brinkmann V, Zychlinsky A (2007) Beneficial suicide: why neutrophils die to make NETs. *Nature Reviews Microbiology* 5:577–582. <https://doi.org/10.1038/nrmicro1710>

## 6. References

---

- Brinkmann V, Zychlinsky A (2012) Neutrophil extracellular traps: is immunity the second function of chromatin? *J Cell Biol* 198:773–783. <https://doi.org/10.1083/jcb.201203170>
- Brinkmann Volker, Reichard Ulrike, Goosmann Christian, et al (2004) Neutrophil Extracellular Traps Kill Bacteria. *Science* 303:1532–1535. <https://doi.org/10.1126/science.1092385>
- Brun R, Blum J, Chappuis F, Burri C (2010) Human African trypanosomiasis. *Lancet* 375:148–159. [https://doi.org/10.1016/S0140-6736\(09\)60829-1](https://doi.org/10.1016/S0140-6736(09)60829-1)
- Bukachi SA, Wandibba S, Nyamongo IK (2017) The socio-economic burden of human African trypanosomiasis and the coping strategies of households in the South Western Kenya foci. *PLoS Negl Trop Dis* 11:e0006002. <https://doi.org/10.1371/journal.pntd.0006002>
- Carrau T, Thümecke S, Silva LMR, et al (2021) The Cellular Innate Immune Response of the Invasive Pest Insect *Drosophila suzukii* against *Pseudomonas entomophila* Involves the Release of Extracellular Traps. *Cells* 10:. <https://doi.org/10.3390/cells10123320>
- Cavalcanti DP, de Souza W (2018) The Kinetoplast of Trypanosomatids: From Early Studies of Electron Microscopy to Recent Advances in Atomic Force Microscopy. *Scanning* 2018:9603051. <https://doi.org/10.1155/2018/9603051>
- Chapman PS, Boag AK, Guitian J, Boswood A (2004) *Angiostrongylus vasorum* infection in 23 dogs (1999–2002). *J Small Anim Pract* 45:435–440. <https://doi.org/10.1111/j.1748-5827.2004.tb00261.x>
- Chen R, Zhang X, Gu L, et al (2021) New Insight Into Neutrophils: A Potential Therapeutic Target for Cerebral Ischemia. *Front Immunol* 12:692061. <https://doi.org/10.3389/fimmu.2021.692061>
- Chen Y, Corriden R, Inoue Y, et al (2006) ATP release guides neutrophil chemotaxis via P2Y2 and A3 receptors. *Science* 314:1792–1795. <https://doi.org/10.1126/science.1132559>
- Chen Y, Yao Y, Sumi Y, et al (2010) Purinergic signaling: a fundamental mechanism in neutrophil activation. *Sci Signal* 3:ra45. <https://doi.org/10.1126/scisignal.2000549>
- Choudhury SR, Babes L, Rahn JJ, et al (2019) Dipeptidase-1 Is an Adhesion Receptor for Neutrophil Recruitment in Lungs and Liver. *Cell* 178:1205–1221.e17. <https://doi.org/10.1016/j.cell.2019.07.017>

## 6. References

---

- Clark SR, Ma AC, Tavener SA, et al (2007) Platelet TLR4 activates neutrophil extracellular traps to ensnare bacteria in septic blood. *Nature Medicine* 13:463–469. <https://doi.org/10.1038/nm1565>
- Conejeros I, López-Osorio S, Zhou E, et al (2022) Glycolysis, monocarboxylate transport, and purinergic signaling are key events in *Eimeria bovis*-induced NETosis. *Front Immunol* 13:842482. <https://doi.org/10.3389/fimmu.2022.842482>
- Conejeros I, Velásquez ZD, Grob D, et al (2019) Histone H2A and Bovine Neutrophil Extracellular Traps Induce Damage of *Besnoitia besnoiti*-Infected Host Endothelial Cells but Fail to Affect Total Parasite Proliferation. *Biology (Basel)* 8. <https://doi.org/10.3390/biology8040078>
- Cortes H, Leitão A, Gottstein B, Hemphill A (2014) A review on bovine besnoitiosis: a disease with economic impact in herd health management, caused by *Besnoitia besnoiti* (Franco and Borges). *Parasitology* 141:1406–1417. <https://doi.org/10.1017/S0031182014000262>
- da Silva RC, Langoni H (2009) *Toxoplasma gondii*: host-parasite interaction and behavior manipulation. *Parasitol Res* 105:893–898. <https://doi.org/10.1007/s00436-009-1526-6>
- Dalbeth N, Merriman TR, Stamp LK (2016) Gout. *Lancet* 388:2039–2052. [https://doi.org/10.1016/S0140-6736\(16\)00346-9](https://doi.org/10.1016/S0140-6736(16)00346-9)
- de Buhr N, Bonilla MC, Jimenez-Soto M, et al (2018) Extracellular Trap Formation in Response to *Trypanosoma cruzi* Infection in Granulocytes Isolated From Dogs and Common Opossums, Natural Reservoir Hosts. *Front Microbiol* 9:966. <https://doi.org/10.3389/fmicb.2018.00966>
- Dehghani T, Panitch A (2020) Endothelial cells, neutrophils and platelets: getting to the bottom of an inflammatory triangle. *Open Biol* 10:200161. <https://doi.org/10.1098/rsob.200161>
- Demattio L, Conejeros I, Grob D, et al (2022) *Neospora caninum*-induced NETosis in canine colostral polymorphonuclear neutrophils. *J Reprod Immunol* 154:103749. <https://doi.org/10.1016/j.jri.2022.103749>
- Demirbas-Uzel G (2018) Improving Sterile Insect Technique for tsetse flies through research on their symbiont and pathogens
- Desquesnes M, Gonzatti M, Sazmand A, et al (2022) A review on the diagnosis of animal trypanosomoses. *Parasites & Vectors* 15:64. <https://doi.org/10.1186/s13071-022-05190-1>

## 6. References

---

- DiStasi MR, Ley K (2009) Opening the flood-gates: how neutrophil-endothelial interactions regulate permeability. *Trends Immunol* 30:547–556. <https://doi.org/10.1016/j.it.2009.07.012>
- Döring Y, Soehnlein O, Weber C (2017) Neutrophil Extracellular Traps in Atherosclerosis and Atherothrombosis. *Circ Res* 120:736–743. <https://doi.org/10.1161/CIRCRESAHA.116.309692>
- Dorris M, De Ley P, Blaxter ML (1999) Molecular analysis of nematode diversity and the evolution of parasitism. *Parasitol Today* 15:188–193. [https://doi.org/10.1016/s0169-4758\(99\)01439-8](https://doi.org/10.1016/s0169-4758(99)01439-8)
- Dosch M, Gerber J, Jebbawi F, Beldi G (2018) Mechanisms of ATP Release by Inflammatory Cells. *Int J Mol Sci* 19:. <https://doi.org/10.3390/ijms19041222>
- Dubey JP (2003) Review of *Neospora caninum* and neosporosis in animals. *Korean J Parasitol* 41:1–16. <https://doi.org/10.3347/kjp.2003.41.1.1>
- Dubey JP (2008) The history of *Toxoplasma gondii*--the first 100 years. *J Eukaryot Microbiol* 55:467–475. <https://doi.org/10.1111/j.1550-7408.2008.00345.x>
- Dubey JP, Carpenter JL, Speer CA, et al (1988) Newly recognized fatal protozoan disease of dogs. *J Am Vet Med Assoc* 192:1269–1285
- Engstler M, Pfohl T, Herminghaus S, et al (2007) Hydrodynamic flow-mediated protein sorting on the cell surface of trypanosomes. *Cell* 131:505–515. <https://doi.org/10.1016/j.cell.2007.08.046>
- Ferdushy T, Hasan MT (2010) *Angiostrongylus vasorum*: the “French Heartworm”. *Parasitol Res* 107:765–771. <https://doi.org/10.1007/s00436-010-2026-4>
- Fernandez-Patron C, Zouki C, Whittal R, et al (2001) Matrix metalloproteinases regulate neutrophil-endothelial cell adhesion through generation of endothelin-1[1-32]. *FASEB J* 15:2230–2240. <https://doi.org/10.1096/fj.01-0178com>
- Fink BD, Herlein JA, O'Malley Y, Sivitz WI (2012) Endothelial Cell and Platelet Bioenergetics: Effect of Glucose and Nutrient Composition. *PLOS ONE* 7:e39430. <https://doi.org/10.1371/journal.pone.0039430>
- Fuchs TA, Abed U, Goosmann C, et al (2007) Novel cell death program leads to neutrophil extracellular traps. *J Cell Biol* 176:231–241. <https://doi.org/10.1083/jcb.200606027>

## 6. References

---

- Gabriel C, McMaster WR, Girard D, Descoteaux A (2010) *Leishmania donovani* promastigotes evade the antimicrobial activity of neutrophil extracellular traps. *J Immunol* 185:4319–4327. <https://doi.org/10.4049/jimmunol.1000893>
- Glaus T, Schnyder M, Dennler M, et al (2010) [Natural infection with *Angiostrongylus vasorum*: characterisation of 3 dogs with pulmonary hypertension]. *Schweiz Arch Tierheilkd* 152:331–338. <https://doi.org/10.1024/0036-7281/a000076>
- Gonzalez AS, Bardoel BW, Harbort CJ, Zychlinsky A (2014) Induction and quantification of neutrophil extracellular traps. *Methods Mol Biol* 1124:307–318. [https://doi.org/10.1007/978-1-62703-845-4\\_20](https://doi.org/10.1007/978-1-62703-845-4_20)
- Gonzalez DD, Dus Santos MJ (2017) Bovine colostrum cells—the often forgotten component of colostrum. *J Am Vet Med Assoc* 250:998–1005. <https://doi.org/10.2460/javma.250.9.998>
- Guimarães-Costa AB, Nascimento MTC, Froment GS, et al (2009) *Leishmania amazonensis* promastigotes induce and are killed by neutrophil extracellular traps. *Proc Natl Acad Sci U S A* 106:6748–6753. <https://doi.org/10.1073/pnas.0900226106>
- Hahn J, Schauer C, Czegley C, et al (2019) Aggregated neutrophil extracellular traps resolve inflammation by proteolysis of cytokines and chemokines and protection from antiproteases. *FASEB J* 33:1401–1414. <https://doi.org/10.1096/fj.201800752R>
- Hahn S, Giaglis S, Chowdhury CS, et al (2013) Modulation of neutrophil NETosis: interplay between infectious agents and underlying host physiology. *Semin Immunopathol* 35:439–453. <https://doi.org/10.1007/s00281-013-0380-x>
- Hampton M, Kettle A, Winterbourn C (1998) Inside the Neutrophil Phagosome: Oxidants, Myeloperoxidase, and Bacterial Killing. *Blood* 92:3007–17. [https://doi.org/10.1182/blood.V92.9.3007.421k47\\_3007\\_3017](https://doi.org/10.1182/blood.V92.9.3007.421k47_3007_3017)
- Hasheminasab SS, Conejeros I, D. Velásquez Z, et al (2022) ATP Purinergic Receptor P2X1-Dependent Suicidal NETosis Induced by *Cryptosporidium parvum* under Physioxia Conditions. *Biology* 11:.. <https://doi.org/10.3390/biology11030442>
- Hassanali A, McDowell PG, Owaga MLA, Saini RK (1986) Identification of Tsetse Attractants from Excretory Products of a Wild Host Animal, *Syncerus caffer*. *International Journal of Tropical Insect Science* 7:5–9. <https://doi.org/10.1017/S1742758400003027>

## 6. References

---

- Health (ed) (2021) Manual of diagnostic tests and vaccines for terrestrial animals 2021: OIE Terrestrial manual 2021. In: Manual of diagnostic tests and vaccines for terrestrial animals. OIE, [www.oie.int](http://www.oie.int)
- Helm J, Roberts L, Jefferies R, et al (2015) Epidemiological survey of *Angiostrongylus vasorum* in dogs and slugs around a new endemic focus in Scotland. *Veterinary Record* 177:46–46. <https://doi.org/10.1136/vr.103006>
- Hermosilla C, Caro TM, Silva LMR, et al (2014) The intriguing host innate immune response: novel anti-parasitic defence by neutrophil extracellular traps. *Parasitology* 141:1489–1498. <https://doi.org/10.1017/S0031182014000316>
- Hermosilla C, Ruiz A, Taubert A (2012) *Eimeria bovis*: an update on parasite-host cell interactions. *Int J Med Microbiol* 302:210–215. <https://doi.org/10.1016/j.ijmm.2012.07.002>
- Hermosilla C, Zahner H, Taubert A (2006) *Eimeria bovis* modulates adhesion molecule gene transcription in and PMN adhesion to infected bovine endothelial cells. *Int J Parasitol* 36:423–431. <https://doi.org/10.1016/j.ijpara.2006.01.001>
- Hidalgo AI, Carretta MD, Alarcón P, et al (2019) Pro-inflammatory mediators and neutrophils are increased in synovial fluid from heifers with acute ruminal acidosis. *BMC Vet Res* 15:225. <https://doi.org/10.1186/s12917-019-1974-x>
- Hoare CA (1973) Letter: “*Trypanosoma brucei*-subgroup”. *Trans R Soc Trop Med Hyg* 67:421–422. [https://doi.org/10.1016/0035-9203\(73\)90126-0](https://doi.org/10.1016/0035-9203(73)90126-0)
- Hoffmann JHO, Enk AH (2016) Neutrophil extracellular traps in dermatology: Caught in the NET. *J Dermatol Sci* 84:3–10. <https://doi.org/10.1016/j.jdermsci.2016.07.001>
- Homa J, Ortmann W, Kolaczowska E (2016) Conservative Mechanisms of Extracellular Trap Formation by *Annelida Eisenia andrei*: Serine Protease Activity Requirement. *PLOS ONE* 11:e0159031. <https://doi.org/10.1371/journal.pone.0159031>
- Hope-Rapp E, Moussa Coulibaly O, Klement E, et al (2009) [Double trypanosomal chancre revealing West African trypanosomiasis in a Frenchman living in Gabon]. *Ann Dermatol Venereol* 136:341–345. <https://doi.org/10.1016/j.annder.2008.09.023>
- Idzko M, Ferrari D, Eltzschig HK (2014) Nucleotide signalling during inflammation. *Nature* 509:310–317. <https://doi.org/10.1038/nature13085>

## 6. References

---

- Imlau M, Conejeros I, Muñoz-Caro T, et al (2020) Dolphin-derived NETosis results in rapid *Toxoplasma gondii* tachyzoite ensnarement and different phenotypes of NETs. *Dev Comp Immunol* 103:103527. <https://doi.org/10.1016/j.dci.2019.103527>
- Inoue R, Tsukahara T (2021) Composition and physiological functions of the porcine colostrum. *Anim Sci J* 92:e13618. <https://doi.org/10.1111/asj.13618>
- Jacob F, Pérez Novo C, Bachert C, Van Crombruggen K (2013) Purinergic signaling in inflammatory cells: P2 receptor expression, functional effects, and modulation of inflammatory responses. *Purinergic Signal* 9:285–306. <https://doi.org/10.1007/s11302-013-9357-4>
- Keating J, Yukich JO, Sutherland CS, et al (2015) Human African trypanosomiasis prevention, treatment and control costs: a systematic review. *Acta Trop* 150:4–13. <https://doi.org/10.1016/j.actatropica.2015.06.003>
- Kennedy PGE (2006) Human African trypanosomiasis–neurological aspects. *Journal of Neurology* 253:411–416. <https://doi.org/10.1007/s00415-006-0093-3>
- Knopf J, Leppkes M, Schett G, et al (2019) Aggregated NETs Sequester and Detoxify Extracellular Histones. *Front Immunol* 10:2176. <https://doi.org/10.3389/fimmu.2019.02176>
- Kobayashi SD, Malachowa N, DeLeo FR (2017) Influence of Microbes on Neutrophil Life and Death. *Front Cell Infect Microbiol* 7:159. <https://doi.org/10.3389/fcimb.2017.00159>
- Kolaczowska E, Kubes P (2013) Neutrophil recruitment and function in health and inflammation. *Nature Reviews Immunology* 13:159–175. <https://doi.org/10.1038/nri3399>
- Krafsur ES, Maudlin I (2018) Tsetse fly evolution, genetics and the trypanosomiasis - A review. *Infect Genet Evol* 64:185–206. <https://doi.org/10.1016/j.meegid.2018.05.033>
- Kramer L, Grandi G, Passeri B, et al (2011) Evaluation of lung pathology in *Dirofilaria immitis*-experimentally infected dogs treated with doxycycline or a combination of doxycycline and ivermectin before administration of melarsomine dihydrochloride. *Veterinary Parasitology* 176:357–360. <https://doi.org/10.1016/j.vetpar.2011.01.021>
- Krüger T, Engstler M (2018) The Fantastic Voyage of the Trypanosome: A Protean Micromachine Perfected during 500 Million Years of Engineering. *Micromachines (Basel)* 9. <https://doi.org/10.3390/mi9020063>

## 6. References

---

- Kukulski F, Ben Yebdri F, Lefebvre J, et al (2007) Extracellular nucleotides mediate LPS-induced neutrophil migration in vitro and in vivo. *J Leukoc Biol* 81:1269–1275. <https://doi.org/10.1189/jlb.1206758>
- Lange MK, Penagos-Tabares F, Muñoz-Caro T, et al (2017) Gastropod-derived haemocyte extracellular traps entrap metastrongyloid larval stages of *Angiostrongylus vasorum*, *Aelurostrongylus abstrusus* and *Troglostrongylus brevior*. *Parasites & Vectors* 10:50. <https://doi.org/10.1186/s13071-016-1961-z>
- Larrazabal C, Hermosilla C, Taubert A, Conejeros I (2022) 3D holotomographic monitoring of Ca<sup>(++)</sup> dynamics during ionophore-induced *Neospora caninum* tachyzoite egress from primary bovine host endothelial cells. *Parasitol Res* 121:1169–1177. <https://doi.org/10.1007/s00436-021-07260-2>
- Larrazabal C, López-Osorio S, Velásquez ZD, et al (2021a) Thiosemicarbazone Copper Chelator BLT-1 Blocks Apicomplexan Parasite Replication by Selective Inhibition of Scavenger Receptor B Type 1 (SR-BI). *Microorganisms* 9:. <https://doi.org/10.3390/microorganisms9112372>
- Larrazabal C, Silva LMR, Hermosilla C, Taubert A (2021b) Ezetimibe blocks *Toxoplasma gondii*-, *Neospora caninum*- and *Besnoitia besnoiti*-tachyzoite infectivity and replication in primary bovine endothelial host cells. *Parasitology* 148:1107–1115. <https://doi.org/10.1017/S0031182021000822>
- Latif AA, Ntantiso L, De Beer C (2019) African animal trypanosomosis (nagana) in northern KwaZulu-Natal, South Africa: Strategic treatment of cattle on a farm in endemic area. *Onderstepoort J Vet Res* 86:e1–e6. <https://doi.org/10.4102/ojvr.v86i1.1639>
- Lee CS, Outteridge PM (1981) Leucocytes of sheep colostrum, milk and involution secretion, with particular reference to ultrastructure and lymphocyte sub-populations. *J Dairy Res* 48:225–237. <https://doi.org/10.1017/s0022029900021646>
- Li RH, Nguyen N, Stern JA, Duler LM (2022) Neutrophil extracellular traps in feline cardiogenic arterial thrombi: a pilot study. *J Feline Med Surg* 24:580–586. <https://doi.org/10.1177/1098612X211044986>
- Li Y, Cao X, Liu Y, et al (2018) Neutrophil Extracellular Traps Formation and Aggregation Orchestrate Induction and Resolution of Sterile Crystal-Mediated Inflammation. *Front Immunol* 9:1559. <https://doi.org/10.3389/fimmu.2018.01559>

## 6. References

---

- Lindsay DS, Dubey JP (2020) Neosporosis, Toxoplasmosis, and Sarcocystosis in Ruminants: An Update. *Vet Clin North Am Food Anim Pract* 36:205–222. <https://doi.org/10.1016/j.cvfa.2019.11.004>
- Lindsay DS, Ritter DM, Brake D (2001) Oocyst excretion in dogs fed mouse brains containing tissue cysts of a cloned line of *Neospora caninum*. *J Parasitol* 87:909–911. [https://doi.org/10.1645/0022-3395\(2001\)087\[0909:OEIDFM\]2.0.CO;2](https://doi.org/10.1645/0022-3395(2001)087[0909:OEIDFM]2.0.CO;2)
- Lopez-Orsorio S, Velasquez ZD, Conejeros I, et al (2022) Morphometric analysis of aerobic *Eimeria bovis* sporogony using live cell 3D holotomographic microscopy imaging. *Parasitology Research* 121:1179–1189. <https://doi.org/10.1007/s00436-021-07338-x>
- Lunn J, LEE R, MARTIN P, MALIK R (2003) Antemortem diagnosis of canine neural angiostrongylosis using ELISA. *Australian Veterinary Journal* 81:128–131. <https://doi.org/10.1111/j.1751-0813.2003.tb11071.x>
- MacLean L, Myburgh E, Rodgers J, Price HP (2013) Imaging African trypanosomes. *Parasite Immunol* 35:283–294. <https://doi.org/10.1111/pim.12046>
- Mahajan A, Grüneboom A, Petru L, et al (2019) Frontline Science: Aggregated neutrophil extracellular traps prevent inflammation on the neutrophil-rich ocular surface. *Journal of Leukocyte Biology* 105:1087–1098. <https://doi.org/10.1002/JLB.HI0718-249RR>
- Maksimov P, Hermosilla C, Kleinertz S, et al (2016) *Besnoitia besnoiti* infections activate primary bovine endothelial cells and promote PMN adhesion and NET formation under physiological flow condition. *Parasitol Res* 115:1991–2001. <https://doi.org/10.1007/s00436-016-4941-5>
- Maksimov P, Hermosilla C, Taubert A, et al (2017) GIS-supported epidemiological analysis on canine *Angiostrongylus vasorum* and *Crenosoma vulpis* infections in Germany. *Parasit Vectors* 10:108. <https://doi.org/10.1186/s13071-017-2054-3>
- Malvy D, Chappuis F (2011) Sleeping sickness. *Clin Microbiol Infect* 17:986–995. <https://doi.org/10.1111/j.1469-0691.2011.03536.x>
- Masiga DK, McNamara JJ, Laveissière C, et al (1996) A high prevalence of mixed trypanosome infections in tsetse flies in Sinfra, Côte d’Ivoire, detected by DNA amplification. *Parasitology* 112 ( Pt 1):75–80. <https://doi.org/10.1017/s0031182000065094>

## 6. References

---

- Masuda S, Nakazawa D, Shida H, et al (2016) NETosis markers: Quest for specific, objective, and quantitative markers. *Clin Chim Acta* 459:89–93. <https://doi.org/10.1016/j.cca.2016.05.029>
- Mattioli RC, Pandey VS, Murray M, Fitzpatrick JL (2000) Immunogenetic influences on tick resistance in African cattle with particular reference to trypanotolerant N'Dama (*Bos taurus*) and trypanosusceptible Gobra zebu (*Bos indicus*) cattle. *Acta Trop* 75:263–277. [https://doi.org/10.1016/s0001-706x\(00\)00063-2](https://doi.org/10.1016/s0001-706x(00)00063-2)
- Maudlin I (2006) African trypanosomiasis. *null* 100:679–701. <https://doi.org/10.1179/136485906X112211>
- McCoy CJ, Reaves BJ, Giguère S, et al (2017) Human Leukocytes Kill *Brugia malayi* Microfilariae Independently of DNA-Based Extracellular Trap Release. *PLoS Negl Trop Dis* 11:e0005279. <https://doi.org/10.1371/journal.pntd.0005279>
- Mendez J, Sun D, Tuo W, Xiao Z (2018) Bovine neutrophils form extracellular traps in response to the gastrointestinal parasite *Ostertagia ostertagi*. *Sci Rep* 8:17598. <https://doi.org/10.1038/s41598-018-36070-3>
- Metzemaekers M, Gouwy M, Proost P (2020) Neutrophil chemoattractant receptors in health and disease: double-edged swords. *Cellular & Molecular Immunology* 17:433–450. <https://doi.org/10.1038/s41423-020-0412-0>
- Moghadam ZM, Henneke P, Kolter J (2021) From Flies to Men: ROS and the NADPH Oxidase in Phagocytes. *Front Cell Dev Biol* 9:628991. <https://doi.org/10.3389/fcell.2021.628991>
- Mohanty T, Sørensen OE, Nordenfelt P (2017) NETQUANT: Automated Quantification of Neutrophil Extracellular Traps. *Front Immunol* 8:1999. <https://doi.org/10.3389/fimmu.2017.01999>
- Molinari J, Moreno SA (2018) *Trypanosoma brucei* Plimmer & Bradford, 1899 is a synonym of *T. evansi* (Steel, 1885) according to current knowledge and by application of nomenclature rules. *Syst Parasitol* 95:249–256. <https://doi.org/10.1007/s11230-018-9779-z>
- Moreno CJG, Temporão A, Torres T, Sousa Silva M (2019) *Trypanosoma brucei* Interaction with Host: Mechanism of VSG Release as Target for Drug Discovery for African Trypanosomiasis. *International Journal of Molecular Sciences* 20. <https://doi.org/10.3390/ijms20061484>

## 6. References

---

- Morgan ER, Shaw SE, Brennan SF, et al (2005) *Angiostrongylus vasorum*: a real heartbreaker. Trends in Parasitology 21:49–51. <https://doi.org/10.1016/j.pt.2004.11.006>
- Moxon CA, Chisala NV, Wassmer SC, et al (2014) Persistent endothelial activation and inflammation after *Plasmodium falciparum* Infection in Malawian children. J Infect Dis 209:610–615. <https://doi.org/10.1093/infdis/jit419>
- Mozzini C, Girelli D (2020) The role of Neutrophil Extracellular Traps in Covid-19: Only an hypothesis or a potential new field of research? Thromb Res 191:26–27. <https://doi.org/10.1016/j.thromres.2020.04.031>
- Mugnier MR, Stebbins CE, Papavasiliou FN (2016) Masters of Disguise: Antigenic Variation and the VSG Coat in *Trypanosoma brucei*. PLOS Pathogens 12:e1005784. <https://doi.org/10.1371/journal.ppat.1005784>
- Muñoz Caro T, Hermosilla C, Silva LMR, et al (2014) Neutrophil extracellular traps as innate immune reaction against the emerging apicomplexan parasite *Besnoitia besnoiti*. PLoS One 9:e91415. <https://doi.org/10.1371/journal.pone.0091415>
- Muñoz-Caro T, Conejeros I, Zhou E, et al (2018) *Dirofilaria immitis* Microfilariae and Third-Stage Larvae Induce Canine NETosis Resulting in Different Types of Neutrophil Extracellular Traps. Front Immunol 9:968. <https://doi.org/10.3389/fimmu.2018.00968>
- Muñoz-Caro T, Mena Huertas SJ, Conejeros I, et al (2015a) *Eimeria bovis*-triggered neutrophil extracellular trap formation is CD11b-, ERK 1/2-, p38 MAP kinase- and SOCE-dependent. Vet Res 46:23. <https://doi.org/10.1186/s13567-015-0155-6>
- Muñoz-Caro T, Rubio R MC, Silva LMR, et al (2015b) Leucocyte-derived extracellular trap formation significantly contributes to *Haemonchus contortus* larval entrapment. Parasit Vectors 8:607. <https://doi.org/10.1186/s13071-015-1219-1>
- Mupanomunda M, Williams JF, Mackenzie CD, Kaiser L (1997) *Dirofilaria immitis*: heartworm infection alters pulmonary artery endothelial cell behavior. Journal of Applied Physiology 82:389–398. <https://doi.org/10.1152/jappl.1997.82.2.389>
- Murray M, Murray PK, McIntyre WI (1977) An improved parasitological technique for the diagnosis of African trypanosomiasis. Trans R Soc Trop Med Hyg 71:325–326. [https://doi.org/10.1016/0035-9203\(77\)90110-9](https://doi.org/10.1016/0035-9203(77)90110-9)

## 6. References

---

- Nathan C (2006) Neutrophils and immunity: challenges and opportunities. *Nature Reviews Immunology* 6:173–182. <https://doi.org/10.1038/nri1785>
- Nauseef WM (2004) Assembly of the phagocyte NADPH oxidase. *Histochemistry and Cell Biology* 122:277–291. <https://doi.org/10.1007/s00418-004-0679-8>
- N’Djetchi MK, Ilboudo H, Koffi M, et al (2017) The study of trypanosome species circulating in domestic animals in two human African trypanosomiasis foci of Côte d’Ivoire identifies pigs and cattle as potential reservoirs of *Trypanosoma brucei gambiense*. *PLoS Negl Trop Dis* 11:e0005993. <https://doi.org/10.1371/journal.pntd.0005993>
- Nguyen GT, Green ER, Mecsas J (2017) Neutrophils to the ROScue: Mechanisms of NADPH Oxidase Activation and Bacterial Resistance. *Front Cell Infect Microbiol* 7:373. <https://doi.org/10.3389/fcimb.2017.00373>
- Organization WH, Control WEC on the, Surveillance of Human African Trypanosomiasis (2013: Geneva S (2013) Control and surveillance of human African trypanosomiasis: report of a WHO expert committee
- Paape MJ, Bannerman DD, Zhao X, Lee J-W (2003) The bovine neutrophil: Structure and function in blood and milk. *Vet Res* 34:597–627. <https://doi.org/10.1051/vetres:2003024>
- Papayannopoulos V (2018) Neutrophil extracellular traps in immunity and disease. *Nat Rev Immunol* 18:134–147. <https://doi.org/10.1038/nri.2017.105>
- Peixoto R, Silva LMR, López-Osório S, et al (2021) *Fasciola hepatica* induces weak NETosis and low production of intra- and extracellular ROS in exposed bovine polymorphonuclear neutrophils. *Dev Comp Immunol* 114:103787. <https://doi.org/10.1016/j.dci.2020.103787>
- Pelletier M, Billingham LK, Ramaswamy M, Siegel RM (2014) Chapter Seven - Extracellular Flux Analysis to Monitor Glycolytic Rates and Mitochondrial Oxygen Consumption. In: Galluzzi L, Kroemer G (eds) *Methods in Enzymology*. Academic Press, pp 125–149
- Penagos-Tabares F, Lange MK, Chaparro-Gutiérrez JJ, et al (2018a) *Angiostrongylus vasorum* and *Aelurostrongylus abstrusus*: Neglected and underestimated parasites in South America. *Parasit Vectors* 11:208. <https://doi.org/10.1186/s13071-018-2765-0>
- Penagos-Tabares F, Lange MK, Seipp A, et al (2018b) Novel approach to study gastropod-mediated innate immune reactions against metastrongyloid parasites. *Parasitol Res* 117:1211–1224. <https://doi.org/10.1007/s00436-018-5803-0>

## 6. References

---

- Pereira MA, Alexandre-Pires G, Câmara M, et al (2019) Canine neutrophils cooperate with macrophages in the early stages of *Leishmania infantum* in vitro infection. *Parasite Immunology* 41:e12617. <https://doi.org/10.1111/pim.12617>
- Pérez D, Muñoz-Caro T, Silva LMR, et al (2021) *Eimeria ninakohlyakimovae* casts NOX-independent NETosis and induces enhanced IL-12, TNF- $\alpha$ , IL-6, CCL2 and iNOS gene transcription in caprine PMN. *Exp Parasitol* 220:108034. <https://doi.org/10.1016/j.exppara.2020.108034>
- Pérez-Figueroa E, Álvarez-Carrasco P, Ortega E, Maldonado-Bernal C (2021) Neutrophils: Many Ways to Die. *Front Immunol* 12:631821. <https://doi.org/10.3389/fimmu.2021.631821>
- Perkins JS Ramberg, L, University of Botswana, Harry Oppenheimer Okavango Research Centre, (2004) Environmental recovery monitoring of tsetse fly spraying impacts in the Okavango Delta - 2003 : final report. Harry Oppenheimer Okavango Research Centre, University of Botswana, Maun, Botswana
- Phillipson M, Heit B, Colarusso P, et al (2006) Intraluminal crawling of neutrophils to emigration sites: a molecularly distinct process from adhesion in the recruitment cascade. *J Exp Med* 203:2569–2575. <https://doi.org/10.1084/jem.20060925>
- Phillipson M, Kaur J, Colarusso P, et al (2008) Endothelial domes encapsulate adherent neutrophils and minimize increases in vascular permeability in paracellular and transcellular emigration. *PLoS One* 3:e1649. <https://doi.org/10.1371/journal.pone.0001649>
- Pilszczek FH, Salina D, Poon KKH, et al (2010) A novel mechanism of rapid nuclear neutrophil extracellular trap formation in response to *Staphylococcus aureus*. *J Immunol* 185:7413–7425. <https://doi.org/10.4049/jimmunol.1000675>
- Pinger J, Chowdhury S, Papavasiliou FN (2017) Variant surface glycoprotein density defines an immune evasion threshold for African trypanosomes undergoing antigenic variation. *Nature Communications* 8:828. <https://doi.org/10.1038/s41467-017-00959-w>
- Ponte-Sucre A (2016) An Overview of *Trypanosoma brucei* Infections: An Intense Host-Parasite Interaction. *Front Microbiol* 7:2126. <https://doi.org/10.3389/fmicb.2016.02126>
- Poulin R (2014) Parasite biodiversity revisited: frontiers and constraints. *Int J Parasitol* 44:581–589. <https://doi.org/10.1016/j.ijpara.2014.02.003>

## 6. References

---

- Radwanska M, Vereecke N, Deleeuw V, et al (2018) Salivarian Trypanosomosis: A Review of Parasites Involved, Their Global Distribution and Their Interaction With the Innate and Adaptive Mammalian Host Immune System. *Front Immunol* 9:2253. <https://doi.org/10.3389/fimmu.2018.02253>
- Rebernick R, Fahmy L, Glover C, et al (2018) DNA Area and NETosis Analysis (DANA): a High-Throughput Method to Quantify Neutrophil Extracellular Traps in Fluorescent Microscope Images. *Biol Proced Online* 20:7. <https://doi.org/10.1186/s12575-018-0072-y>
- Rinaldi L, Cortese L, Meomartino L, et al (2014) *Angiostrongylus vasorum*: epidemiological, clinical and histopathological insights. *BMC Veterinary Research* 10:236. <https://doi.org/10.1186/s12917-014-0236-1>
- Rinaldi M, Moroni P, Paape MJ, Bannerman DD (2007) Evaluation of assays for the measurement of bovine neutrophil reactive oxygen species. *Vet Immunol Immunopathol* 115:107–125. <https://doi.org/10.1016/j.vetimm.2006.09.009>
- Roncagli RA (1987) The history of scabies in veterinary and human medicine from biblical to modern times. *Vet Parasitol* 25:193–198. [https://doi.org/10.1016/0304-4017\(87\)90104-x](https://doi.org/10.1016/0304-4017(87)90104-x)
- Rosales C (2018) Neutrophil: A Cell with Many Roles in Inflammation or Several Cell Types? *Front Physiol* 9:113. <https://doi.org/10.3389/fphys.2018.00113>
- Rotureau B, Van Den Abbeele J (2013) Through the dark continent: African trypanosome development in the tsetse fly. *Front Cell Infect Microbiol* 3:53. <https://doi.org/10.3389/fcimb.2013.00053>
- Rubenich DS, de Souza PO, Omizzollo N, et al (2021) Neutrophils: fast and furious-the nucleotide pathway. *Purinergic Signal* 17:371–383. <https://doi.org/10.1007/s11302-021-09786-7>
- Schauer C, Janko C, Munoz LE, et al (2014) Aggregated neutrophil extracellular traps limit inflammation by degrading cytokines and chemokines. *Nature Medicine* 20:511–517. <https://doi.org/10.1038/nm.3547>
- Schmidt J (1998) Effects of benzimidazole anthelmintics as microtubule-active drugs on the synthesis and transport of surface glycoconjugates in *Hymenolepis microstoma*, *Echinostoma caproni*, and *Schistosoma mansoni*. *Parasitology Research* 84:362–368. <https://doi.org/10.1007/s004360050411>

## 6. References

---

- Schnyder M, Bilbrough G, Hafner C, Schaper R (2017) *Angiostrongylus vasorum*, “The French Heartworm”: a Serological Survey in Dogs from France Introduced by a Brief Historical Review. *Parasitol Res* 116:31–40. <https://doi.org/10.1007/s00436-017-5489-8>
- Schnyder M, Fahrion A, Riond B, et al (2010) Clinical, laboratory and pathological findings in dogs experimentally infected with *Angiostrongylus vasorum*. *Parasitol Res* 107:1471–1480. <https://doi.org/10.1007/s00436-010-2021-9>
- Schug K, Krämer F, Schaper R, et al (2018) Prevalence survey on lungworm (*Angiostrongylus vasorum*, *Crenosoma vulpis*, *Eucoleus aerophilus*) infections of wild red foxes (*Vulpes vulpes*) in central Germany. *Parasites & Vectors* 11:85. <https://doi.org/10.1186/s13071-018-2672-4>
- Seangseerattanukulchai K, Piratae S (2021) Drug resistance in blood parasitic infections in cattle: a review. *Ann Parasitol* 67:583–590. <https://doi.org/10.17420/ap6704.374>
- Seesao Y, Gay M, Merlin S, et al (2017) A review of methods for nematode identification. *J Microbiol Methods* 138:37–49. <https://doi.org/10.1016/j.mimet.2016.05.030>
- Segal AW (2005) HOW NEUTROPHILS KILL MICROBES. *Annu Rev Immunol* 23:197–223. <https://doi.org/10.1146/annurev.immunol.23.021704.115653>
- Segal AW, Levi AJ (1973) The Mechanism of the Entry of Dye into Neutrophils in the Nitroblue Tetrazolium (NBT) Test. *Clinical Science and Molecular Medicine* 45:817–826. <https://doi.org/10.1042/cs0450817>
- Segawa T, Itou T, Suzuki M, et al (2011) Hematopoietic cell populations in dolphin bone marrow: Analysis of colony formation and differentiation. *Results Immunol* 1:1–5. <https://doi.org/10.1016/j.rinim.2011.05.004>
- Shah-Simpson S, Pereira CFA, Dumoulin PC, et al (2016) Bioenergetic profiling of *Trypanosoma cruzi* life stages using Seahorse extracellular flux technology. *Molecular and Biochemical Parasitology* 208:91–95. <https://doi.org/10.1016/j.molbiopara.2016.07.001>
- Sheshachalam A, Srivastava N, Mitchell T, et al (2014) Granule protein processing and regulated secretion in neutrophils. *Front Immunol* 5:448. <https://doi.org/10.3389/fimmu.2014.00448>
- Sil P, Hayes CP, Reaves BJ, et al (2017) P2Y6 Receptor Antagonist MRS2578 Inhibits Neutrophil Activation and Aggregated Neutrophil Extracellular Trap Formation Induced by

## 6. References

---

- Gout-Associated Monosodium Urate Crystals. *J Immunol* 198:428–442. <https://doi.org/10.4049/jimmunol.1600766>
- Silva LMR, Hindenberg S, Balzhäuser L, et al (2021) Pneumothorax in a persistent canine *Angiostrongylus vasorum* infection. *Vet Parasitol Reg Stud Reports* 26:100650. <https://doi.org/10.1016/j.vprsr.2021.100650>
- Silva LMR, Muñoz Caro T, Gerstberger R, et al (2014) The apicomplexan parasite *Eimeria arloingi* induces caprine neutrophil extracellular traps. *Parasitology Research* 113:2797–2807. <https://doi.org/10.1007/s00436-014-3939-0>
- Silva LMR, Muñoz-Caro T, Burgos RA, et al (2016) Far beyond Phagocytosis: Phagocyte-Derived Extracellular Traps Act Efficiently against Protozoan Parasites In Vitro and In Vivo. *Mediators Inflamm* 2016:5898074. <https://doi.org/10.1155/2016/5898074>
- Silva LMR, Velásquez ZD, López-Osorio S, et al (2022) Novel Insights Into Sterol Uptake and Intracellular Cholesterol Trafficking During *Eimeria bovis* Macromeront Formation. *Front Cell Infect Microbiol* 12:809606. <https://doi.org/10.3389/fcimb.2022.809606>
- Silvester E, McWilliam KR, Matthews KR (2017) The Cytological Events and Molecular Control of Life Cycle Development of *Trypanosoma brucei* in the Mammalian Bloodstream. *Pathogens* 6:. <https://doi.org/10.3390/pathogens6030029>
- Simarro PP, Diarra A, Ruiz Postigo JA, et al (2011) The human African trypanosomiasis control and surveillance programme of the World Health Organization 2000-2009: the way forward. *PLoS Negl Trop Dis* 5:e1007. <https://doi.org/10.1371/journal.pntd.0001007>
- Šlapeta J (2013) Cryptosporidiosis and Cryptosporidium species in animals and humans: a thirty colour rainbow? *Int J Parasitol* 43:957–970. <https://doi.org/10.1016/j.ijpara.2013.07.005>
- Sousa-Rocha D, Thomaz-Tobias M, Diniz LFA, et al (2015) *Trypanosoma cruzi* and Its Soluble Antigens Induce NET Release by Stimulating Toll-Like Receptors. *PLoS One* 10:e0139569. <https://doi.org/10.1371/journal.pone.0139569>
- Steinberg Benjamin E., Grinstein Sergio (2007) Unconventional Roles of the NADPH Oxidase: Signaling, Ion Homeostasis, and Cell Death. *Science's STKE* 2007:pe11–pe11. <https://doi.org/10.1126/stke.3792007pe11>
- Steverding D (2008) The history of African trypanosomiasis. *Parasit Vectors* 1:3. <https://doi.org/10.1186/1756-3305-1-3>

## 6. References

---

- Szturmowicz M, Demkow U (2021) Neutrophil Extracellular Traps (NETs) in Severe SARS-CoV-2 Lung Disease. *Int J Mol Sci* 22:.. <https://doi.org/10.3390/ijms22168854>
- Takei H, Araki A, Watanabe H, et al (1996) Rapid killing of human neutrophils by the potent activator phorbol 12-myristate 13-acetate (PMA) accompanied by changes different from typical apoptosis or necrosis. *J Leukoc Biol* 59:229–240. <https://doi.org/10.1002/jlb.59.2.229>
- Taubert A, Krüll M, Zahner H, Hermosilla C (2006) *Toxoplasma gondii* and *Neospora caninum* infections of bovine endothelial cells induce endothelial adhesion molecule gene transcription and subsequent PMN adhesion. *Vet Immunol Immunopathol* 112:272–283. <https://doi.org/10.1016/j.vetimm.2006.03.017>
- Taubert A, Wimmers K, Ponsuksili S, et al (2010) Microarray-based transcriptional profiling of *Eimeria bovis*-infected bovine endothelial host cells. *Vet Res* 41:70. <https://doi.org/10.1051/vetres/2010041>
- Tenter AM, Heckeroth AR, Weiss LM (2000) *Toxoplasma gondii*: from animals to humans. *Int J Parasitol* 30:1217–1258. [https://doi.org/10.1016/s0020-7519\(00\)00124-7](https://doi.org/10.1016/s0020-7519(00)00124-7)
- Thomson S, Hamilton CA, Hope JC, et al (2017) Bovine cryptosporidiosis: impact, host-parasite interaction and control strategies. *Vet Res* 48:42. <https://doi.org/10.1186/s13567-017-0447-0>
- Tobe SS (1978) Reproductive physiology of *Glossina*. *Annu Rev Entomol* 23:283–307. <https://doi.org/10.1146/annurev.en.23.010178.001435>
- Tomasina R, Francia ME (2020) The Structural and Molecular Underpinnings of Gametogenesis in *Toxoplasma gondii*. *Front Cell Infect Microbiol* 10:608291. <https://doi.org/10.3389/fcimb.2020.608291>
- Torr SJ, MAUDLIN I, VALE GA (2007) Less is more: restricted application of insecticide to cattle to improve the cost and efficacy of tsetse control. *Medical and Veterinary Entomology* 21:53–64. <https://doi.org/10.1111/j.1365-2915.2006.00657.x>
- Tyler KM, Matthews KR, Gull K (1997) The bloodstream differentiation-division of *Trypanosoma brucei* studied using mitochondrial markers. *Proc Biol Sci* 264:1481–1490. <https://doi.org/10.1098/rspb.1997.0205>

## 6. References

---

- Velásquez ZD, López-Osorio S, Waiger D, et al (2021) *Eimeria bovis* infections induce G(1) cell cycle arrest and a senescence-like phenotype in endothelial host cells. *Parasitology* 148:341–353. <https://doi.org/10.1017/S0031182020002097>
- Villagra-Blanco R, Silva LMR, Conejeros I, et al (2019) Pinniped- and Cetacean-Derived ETosis Contributes to Combating Emerging Apicomplexan Parasites (*Toxoplasma gondii*, *Neospora caninum*) Circulating in Marine Environments. *Biology* 8:. <https://doi.org/10.3390/biology8010012>
- Villagra-Blanco R, Silva LMR, Gärtner U, et al (2017a) Molecular analyses on *Neospora caninum*-triggered NETosis in the caprine system. *Dev Comp Immunol* 72:119–127. <https://doi.org/10.1016/j.dci.2017.02.020>
- Villagra-Blanco R, Silva LMR, Muñoz-Caro T, et al (2017b) Bovine Polymorphonuclear Neutrophils Cast Neutrophil Extracellular Traps against the Abortive Parasite *Neospora caninum*. *Front Immunol* 8:606. <https://doi.org/10.3389/fimmu.2017.00606>
- Votýpka J, Modrý D, Oborník M, et al (2017) Apicomplexa. *Handbook of the Protists* 1–58
- Wang L, Zhu Z, Liao Y, et al (2022) Host liver-derived extracellular vesicles deliver miR-142a-3p induces neutrophil extracellular traps via targeting WASL to block the development of *Schistosoma japonicum*. *Mol Ther* 30:2092–2107. <https://doi.org/10.1016/j.ymthe.2022.03.016>
- Wang X, Chen D (2018) Purinergic Regulation of Neutrophil Function. *Front Immunol* 9:399. <https://doi.org/10.3389/fimmu.2018.00399>
- Wang X, Qin W, Xu X, et al (2017) Endotoxin-induced autocrine ATP signaling inhibits neutrophil chemotaxis through enhancing myosin light chain phosphorylation. *Proc Natl Acad Sci U S A* 114:4483–4488. <https://doi.org/10.1073/pnas.1616752114>
- Wei Z, Hermosilla C, Taubert A, et al (2016) Canine Neutrophil Extracellular Traps Release Induced by the Apicomplexan Parasite *Neospora caninum* In Vitro. *Front Immunol* 7:436. <https://doi.org/10.3389/fimmu.2016.00436>
- Williams PP (1993) Immunomodulating effects of intestinal absorbed maternal colostral leukocytes by neonatal pigs. *Can J Vet Res* 57:1–8
- Wong SL, Demers M, Martinod K, et al (2015) Diabetes primes neutrophils to undergo NETosis, which impairs wound healing. *Nat Med* 21:815–819. <https://doi.org/10.1038/nm.3887>
- Woo PT (1970) The haematocrit centrifuge technique for the diagnosis of African trypanosomiasis. *Acta Trop* 27:384–386

## 6. References

---

- Woodfin A, Voisin M-B, Beyrau M, et al (2011) The junctional adhesion molecule JAM-C regulates polarized transendothelial migration of neutrophils in vivo. *Nature Immunology* 12:761–769. <https://doi.org/10.1038/ni.2062>
- Worku M, Rehrah D, Ismail HD, et al (2021) A Review of the Neutrophil Extracellular Traps (NETs) from Cow, Sheep and Goat Models. *International Journal of Molecular Sciences* 22. <https://doi.org/10.3390/ijms22158046>
- Yáñez-Ortiz I, Catalán J, Mateo-Otero Y, et al (2021) Extracellular Reactive Oxygen Species (ROS) Production in Fresh Donkey Sperm Exposed to Reductive Stress, Oxidative Stress and NETosis. *Antioxidants (Basel)* 10. <https://doi.org/10.3390/antiox10091367>
- Yipp BG, Kubes P (2013) NETosis: how vital is it? *Blood* 122:2784–2794. <https://doi.org/10.1182/blood-2013-04-457671>
- Yipp BG, Petri B, Salina D, et al (2012) Infection-induced NETosis is a dynamic process involving neutrophil multitasking in vivo. *Nat Med* 18:1386–1393. <https://doi.org/10.1038/nm.2847>
- Yousefi S, Gold JA, Andina N, et al (2008) Catapult-like release of mitochondrial DNA by eosinophils contributes to antibacterial defense. *Nat Med* 14:949–953. <https://doi.org/10.1038/nm.1855>
- Zambrano F, Melo A, Rivera-Concha R, et al (2022) High Presence of NETotic Cells and Neutrophil Extracellular Traps in Vaginal Discharges of Women with Vaginitis: An Exploratory Study. *Cells* 11. <https://doi.org/10.3390/cells11203185>
- Zhou E, Conejeros I, Gärtner U, et al (2020a) Metabolic requirements of *Besnoitia besnoiti* tachyzoite-triggered NETosis. *Parasitol Res* 119:545–557. <https://doi.org/10.1007/s00436-019-06543-z>
- Zhou E, Conejeros I, Velásquez ZD, et al (2019) Simultaneous and Positively Correlated NET Formation and Autophagy in *Besnoitia besnoiti* Tachyzoite-Exposed Bovine Polymorphonuclear Neutrophils. *Front Immunol* 10:1131. <https://doi.org/10.3389/fimmu.2019.01131>
- Zhou E, Silva LMR, Conejeros I, et al (2020b) *Besnoitia besnoiti* bradyzoite stages induce suicidal and rapid vital-NETosis. *Parasitology* 147:401–409. <https://doi.org/10.1017/S0031182019001707>
- (1998) Control and surveillance of African trypanosomiasis. Report of a WHO Expert Committee. Switzerland

## 7. ACKNOWLEDGMENTS

I would like to give my deepest gratitude and appreciations to Prof. Dr. Carlos Hermosilla for the trust in me and giving me a chance in the Institute, regardless everything.

To Prof. Dr Carlos Hermosilla and Prof. Dr. Anja Taubert, for supervising my doctoral thesis and the opportunity to form part of the Institute of Parasitology of the JLU.

As well, I would like to give my special regards and appreciations to the post-doctoral researchers from the Institute. To Dr. Iván Conejeros, who assisted and supported me during the complete process. Also, to Dr. Zahady Velásquez and Dr. Liliana Silva, for the constant help during my doctoral studies. The group of post-doctoral researchers from the Institute contributed to the complete development of the present doctoral work and formation as new researcher.

In this line, I must thank to other doctoral students from the Institute: Lisa Segeritz, Lisbeth Rojas and Gabriel Espinosa, with whom I had the joy of share as a doctoral student and as a friend during the development of my doctoral studies.

I would like to also express my gratitude to Dr. Christin Ritter, Hannah Salecker, the technical assistants from our group who always where there to help me on my daily work over all these years.

To Dr. Ulrich Gärtner and Anika Seipp from the Institute of Anatomy, for always helping us with the beautiful SEM pictures of our samples. In this line, many thanks to Prof. Dr. Janzen from the University of Wurzburg, for the support with the Trypanosome culture. To Dr. Roland Schaper for the help and access that made the *A. vasorum* paper possible.

I would like to thank to all the team of the dairy farm Oberer Hardthof of the University, for always receiving us with a smile, even when it was cold or they were overwhelmed with work. The healthy state of the animals allowed us to always obtain the samples without problems.

To my parents, Mónica Guerra and Luis Alberto Grob, who were there every day encouraging me to overcome myself every day. In this sense, also to my sister, Victoria Grob, who was constantly listening to me and celebrating my victories during these years.

Lastly, I must say my deepest gratitude to my beloved partner, husband and college Camilo Larrazabal. Without him, I would never be able to face and overcome the huge challenge that was doing doctoral studies, bringing me every day love, happiness and support.

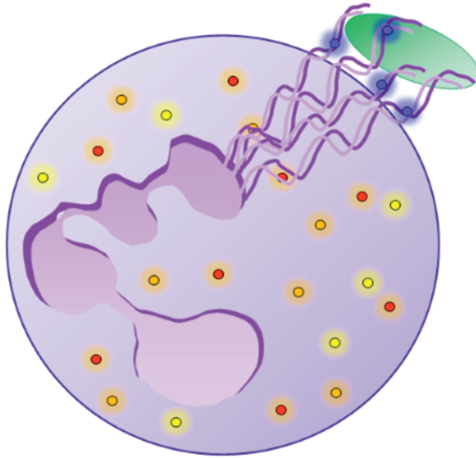
## **8. DECLARATION**

Here I declare that I have completed the submitted doctoral thesis, independently and with any unauthorized outside help; only with financial support here mentioned on this work. All the analyzes conducted in the present doctoral thesis, were made under the principles of good scientific practice, as is stated in the statute of the Justus-Liebig University Giessen for ensuring good scientific practices. All the texts that have been here quoted verbatim or by analogy from published and non-published writings, all the corresponding details are based on verba information have been identified as such

## **9. FUNDING**

The present study was funded by the Institute of Parasitology, pf the Justus-Liebig University Gießen (Germany). In this sense, selected experiments were supported by Elanco Animal Health GmbH (40789 Monheim, Germany).

Finally, studies and life expenses in Germany were founded by a PhD fellowship of the National Agency for Research and Development (ANID), DOCTORADO BECAS CHILE Number/2019-72200437.



*édition scientifique*  
**VVB LAUFERSWEILER VERLAG**

VVB LAUFERSWEILER VERLAG  
STAUFENBERGRING 15  
D-35396 GIESSEN

Tel: 0641-5599888 Fax: -5599890  
redaktion@doktorverlag.de  
www.doktorverlag.de

ISBN: 978-3-8359-7105-9



9 783835 197105 9